Identification of essential and virulence genes in *Mycoplasma pneumoniae*

Dissertation

for the award of the degree

"*Doctor rerum naturalium*"

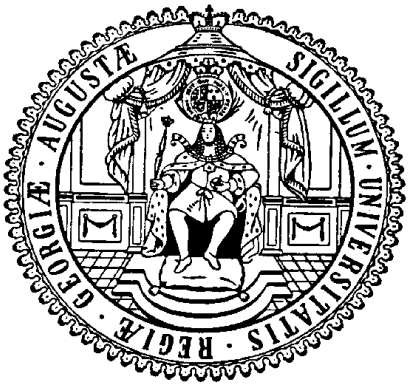

of the Georg-August-Universität Göttingen

within the doctoral program "Microbiology & Biochemistry"

of the Georg-August-University School of Science (GAUSS)

submitted by

Cedric Blötz

from Northeim

Göttingen 2019

THESIS COMMITTEE

Prof. Dr. Jörg Stülke (Supervisor and 1st Reviewer)
Institute of Microbiology and Genetics
Department of General Microbiology, University of Göttingen

Prof. Dr. Carsten Lüder (2nd Reviewer)
Institute for Medical Microbiology
Department for Medical Microbiology, University Medical Center of Göttingen

PD Dr. Michael Hoppert (3rd Reviewer)
Institute of Microbiology and Genetics
Department of General Microbiology, University of Göttingen

Further Members of the Examination Board

Prof. Dr. Stefanie Pöggeler
Institute of Microbiology and Genetics
Department of Genetics of Eukaryotic Microorganism

Prof. Dr. Fabian M. Commichau
Institute of Microbiology and Genetics
Department of General Microbiology, University of Göttingen

Prof. Dr. Henning Urlaub
Max-Planck-Institute for Biophysical Chemistry
Bioanalytical Mass Spectrometry Group, Göttingen

Date of oral examination: 02.04.2019

STATEMENT OF AUTHORSHIP

I hereby declare that the doctoral thesis entitled, “Identification of essential and virulence genes in *Mycoplasma pneumoniae*” has been written independently and with no other sources and aids than quoted.

Cedric Blötz

DANKSAGUNG

Lieber Jörg, gute 20.000 km haben wir mal mehr mal weniger stressfrei bereist. Unglaublich, wie viel ich dank dir und der Arbeit reisen konnte. Ich bin dir für all die Möglichkeiten und Freiheiten, die du mir gegeben hast wirklich dankbar. Schon als Bachelorstudent und auch im Master hatte ich das Gefühl, dass du ein Professor/ Doktorvater bist, dem seine Studenten und Doktoranden und auch ihre Themen wichtig sind. Ich find es toll, dass ich sogut wie immer zu dir konnte, um mir wissenschaftlichen, organisatorischen oder persönlichen Rat zu holen. Darüber hinaus ist es großartig, einen Chef zu haben, mit dem man bei Bier und Sektflöten immer Spaß haben kann.

Christina, ohne dich wäre ich im Labor-"handwerklichen" wie auch in meiner Ideenvielfalt was Versuche betrifft, heute nicht da wo ich bin. Was hätte ich ohne deine Weisheiten aus der Tageszeitung manchmal nur getan. Es schmerzt mich nicht mehr dein Student und Kollege zu sein. Wie gern habe ich mit dir gelacht. Auch dir Katrin möchte ich an dieser Stelle danken. Wie so viele habe ich unglaublich viel von dir gelernt und durch unsere Zusammenarbeit, Diskussionen und Anregungen profitiert. Wie aus euch beiden Lehrmeister, Kollegen und schließlich Freunde wurden ist wunderbar.

Freunde. Anika - Larissa, das seid ihr, tolle Freundinnen. Anika, unglaublich wie die Zeit angefangen hat zu rasen seit wir uns im Bachelor kennengelernt haben. Wie oft du mich unterstützt hast. Wie oft ich dich mit Fragen und meiner „Überorganisation" genervt habe. Wie oft wir zusammen Tränen gelacht haben. Larissa, du warst wohl die beste Studentin, die ich hatte und je haben konnte. Was haben wir gelacht, was hatten wir für Spaß. Du bist immer da, bei allem. Vielen Dank!

Hannes du warst ein toller Labornachbar und Kollege. Danke, für so viele anregende Diskussionen und überdachte Versuchsplanungen, toll wie oft wir uns gegenseitig geholfen haben. Es war eine schöne Zeit.

Auch allen anderen Kollegen und meinen Studenten (Neil, Alex, Erik, Anika, Tenzin) möchte ich hier danken. Ihr habt mir hier seit 2010 (Bachelor bis Doktor) die Arbeit zu einer unvergesslichen Zeit gemacht. Besonders betonen möchte ich die unermüdliche Arbeit und wirklich immer erquickende Art von Silvia, die nicht nur für mich, sondern für dieser Abteilung eine große Bereicherung ist.

Miri, was soll ich sagen? Ich wurde aufgenommen, fast rausgeworfen und doch haben wir in den letzten 4 Jahren unglaubliche Momente erlebt. Eine unglaubliche Zeit endet, aber das ist kein Ende! Mit dir kann man Pferde stehlen, Weinkeltereien eröffnen oder HAIdefinition-Filme gucken. Es ist schön wie wir für einander da sind. Danke für alles. Vielen Dank dass du meine Arbeit so gründlich gelesen hast. „*s*"! Auf viele weitere schöne Momente!

HoMaMaDa oder auch Mama, Papa, Marc, Darleen - selbst wenn ihr fachlich weniger zu der Arbeit beigetragen habt, hätte ich all das nicht ohne euer Zutun geschafft. Ihr habt mir so viel Mut, Stärke und Liebe gegeben und mich immer unterstützt und oft mehr an mich geglaubt als ich selbst. Vielen Dank Marc, dass du meine Launen und meine fehlende Zeit einfach weggesteckt hast und immer zu mir stehst. Es ist schön eine solch unglaublich tolle Familie zu haben.

An dieser Stelle möchte ich mich auch bei meinen Prüfern Carsten und Michael bedanken, die immer ein offenes Ohr hatten. Danke auch dir Fabian für immer volle Sektgläser und interessante Diskussionen. Ein Dank gilt auch den weiteren Mitgliedern meines Prüfungskomitees, Prof. Pöggeler und Prof. Urlaub.

Vielen Dank auch all den tollen Kooperationspartnern in fast der ganzen Welt - Francis, Ludwig, Juri, Carole, Dan, Carlos, Roger, Maria, und Luis.

From a few peaks rising above the fog we try to imagine what the hidden landscape underneath might look like.

Pieter W. Postma
BIOCHEMIST

LIST OF PUBLICATIONS

Publications part of the dissertation:

Blötz, C., Treffon, K., Kaever, V., Schwede, F., Hammer, E., and Stülke, J. (2017) Identification of the components involved in cyclic di-AMP signaling in *Mycoplasma pneumoniae*. *Front Microbiol* **8:** 1328.

Blötz, C., Lartigue, C., Valverde Timana, Y., Ruiz, E., Paetzold, B., Busse, J., and Stülke, J. (2018) Development of a replicating plasmid based on the native *oriC* in *Mycoplasma pneumoniae*. *Microbiology* **164**: 1372–1382.

Blötz, C., Krüger, L., Kahle, A., Singh, N., Dickmanns, A., Stülke, J., (2019) How to get rid of peroxides? The detoxification system and its regulation in *Mycoplasma pneumoniae.* (unpublished)

Blötz, C., Singh, N., Dumbke, R., Stülke, J., (2019) Characterization of the immunoglobulin binding protein (IbpM) from *Mycoplasma pneumoniae.* (unpublished)

Other publications:

Blötz, C., and Stülke, J. (2017) Glycerol metabolism and its implication in virulence in Mycoplasma. *FEMS Microbiol Rev* **41**: 640–652.

Yus, E., Lloréns-Rico. V., Martínez, S., Gallo, C., Eilers, H., **Blötz, C**., Stülke, J., Lluch-Senar, M., Serrano, L. (2019) Reconstruction of regulatory network in a minimal bacterium reveals extensive non-transcription factor dependent regulation. (submitted)

O'Reilly, F., Sinn, L., **Blötz, C.**, Liang, X., Lenz, S., Mahamid, J., Stülke, J., and Rappsilber, J. (2019) *In situ* structural analysis reveals NusA as a physical link between transcription and translation in *Mycoplasma pneumoniae.* (unpublished)

Other contribution:

Bingyao, Z., **Blötz, C.**, and Stülke, J. (2017) *Myco*Wiki-database: mycowiki.uni-goettingen.de

TABLE OF CONTENT

LIST OF ABBREVIATIONS

ABC	ATP binding cassette
ADCC	antibody-dependent cellular cytotoxicity
ADP	adenosine diphosphate
Ala	alanine
amp	ampicillin
AMP	adenosine monophosphate
AP	alkaline phosphatase
ATP	adenosine triphosphate
BACTH	bacterial two-hybrid assay
BLAST	basic local alignment search tool
bp	base pairs
BSA	bovine serum albumin
cAMP	cyclic AMP
CARDS	Community-Acquired Respiratory Distress Syndrome
cat	chloramphenicol
CBPP	contagious bovine pleuropneumonia
c-di-AMP	cyclic adenosine monophosphate
c-di-GMP	cyclic diguanosine monophosphate
CoA	coenzyme A
Cys	cystein
DAC	diadenylate cyclase
DH	dehydrogenase
DHAP	dihydroxyacetone phosphate
DIG	digoxigenin
DNA	deoxyribonucleic acid
DUF	domain of unknown function
E	essential
e.g.	for example (Latin)
EDTA	ethylenediaminetetraacetic acid
ELISA	enzyme linked immunosorbent assay
et al.	and other (Lain)
F	fitness
Fig.	figure
FOX	ferrous ion oxidation with xylenol orange
Fur	ferric uptake regulator
fwd	forward
G3P	glycerol 3-phosphate
glc	glucose
glyc	glycerol
GPC	glycerophosphocholine
H_2O	water
H_2O_2	hydrogen peroxide
HBEC	human bronchial epithelial cells
HEPES	4-(2-hydroxyethyl)-1-piperazine-ethanesulfonic acid (buffer)
HMW	high molecular weight
i.e.	that is to say (Latin)
IBP	immunoglobulin binding protein
IFN-β	beta-interferon
Ig	immunoglobulin
IPTG	isopropyl-β-D-thiogalactopyranosid
ITC	isothermal titration calorimetry
JCVI	J. Craig Venter Institute
kan	kanamycin
kb	kilobase pairs
LB	lysogeny broth
LC-MS	liquid chromatography-mass spectrometry
LFH	long flanking homology
LRR	leucine-rich repeat
MG	*Mycoplasma genitalium*
MIB	*M. mycoides* IG binding protein
MIP	*M. mycoides* IG protease
MPN	*Mycoplasma pneumoniae*
mRNA	messenger RNA
NE	non-essential
O_2	molecular oxygen
OD_{nm}	optical density, λ at nm
OHP	organic hydro peroxide
ORF	open reading frame
ori	origin of replication
PBS	phosphate buffered saline
PCR	polymerase chain reaction
PDE	phosphodiesterases
PDHC	pyruvate dehydrogenase complex
PEG	polyethylene glycol
pH	power of hydrogen
pNPP	*para*-nitrophenol phosphate
ppGpp	guanosin-3′,5′-bispyrophosphat
Prx	peroxiredoxins
psi	pounds per square inch
puro	puromycin
PVDF	polyvinylidene difluoride
qRT	quantitative real-time
RECON	reductase controlling NF-kB
rev	reverse
RNA	ribonucleic acid
RNase	ribonuclease
ROS	reactive oxygen species
rpm	rounds per minute
RT	room temperature
SDS	sodium dodecyl sulfate
SOD	superoxide dismutase
spec	spectinomycin
STING	stimulator of interferon genes
Tab	table
tBP	*tert*-butyl hydroperoxide
TC	transcription
tet	tetracycline
TF	transcription factor
TL	translation
TM	transmembrane
Tn	transposon
Tris	tris(hydroxymethyl)-aminometha
Trp	tryptophan
U	units
WT	wild type
zeo	zeocin

Units	
°C	degree Celsius
λ	Lamda
bp	base pairs
g	gram
g	standard gravity
h	hour
l	liter
m	meter
min	minute
mol	mol
M	molar
Pa	Pascal
s	seconds
V	volt

Prefixes	
M	mega
k	kilo
m	milli
µ	micro
n	nano
p	pico

Nucleotides	
A	adenosine
C	cytosine
G	huanosin
T	thymine
U	uracil

SUMMARY

The bacterial group of Firmicutes includes many pathogenic bacteria, as *Mycoplasma pneumoniae.* The Gram-positive, but cel wall-less bacterium is characterized by a minimal genome with only 694 genes. Elucidating the function of all genes encoded in *M. pneumoniae* would allow the understanding of a cell in its entire complexity. Unfortunately, these bacteria grow very slowly and are hard to manipulate genetically. Only a few techniques and tools are available for the manipulation of *M. pneumoniae*. In this work, we extended the toolbox for *M. pneumoniae* with the first self-replicating plasmid pGP2756. It enabled for the first-time plasmid-based protein overexpression, expression of fusion proteins and complementation assays in *Mycoplasma,* to analyze unknown virulence factors contributing to mycoplasmal pathogenicity. Even if *Mycoplasmas* contain only down to 482 genes, one-third thereof is of unknown function and has no homology to any available nucleotide sequence so far. For instance, they lack common detoxification enzymes, such as catalase or superoxide dismutase, but many *Mycoplasmas* use hydrogen peroxide as a virulence factor. Accordingly, we investigated how they can tolerate high peroxide concentrations. Recently, peroxiredoxins were identified in the genomes of *Mycoplasmas*, which act as antioxidant enzymes. We identified and characterized two similar genes *mpn625* and *mpn668* to have specific detoxification activities for hydrogen peroxide and organic peroxide, respectively. Analyzing their specific regulation in *M. pneumoniae*, which has in general only a few transcription factors, revealed that the trigger enzyme GlpQ and the protein kinase C are involved in peroxide stress response. Strikingly, GlpQ and the protein kinase C have a strong influence on each other's expression. In addition, we identified, *mpn329* encoding a zinc responsive regulator (Zur) rather a ferrous iron regulator (Fur), which could alter gene expression in response to the intracellular ion homeostasis and peroxide concentration. For effective pathogenicity, *M. pneumoniae* needs to escape the host immune system using immunoglobulin binding proteins. In this work, the novel immunoglobulin binding protein of *M. pneumoniae* IbpM was identified. Our experiments show that IbpM is a multi-binding protein with high affinity for human immunoglobulins, plasminogen and fibronectin. IbpM represents a new surface protein of *M. pneumoniae* likely responsible for the efficient immune evasion properties of this bacterium often leading to chronic infections. Pathogenicity was shown to be strongly connected to c-di-AMP metabolism in many Firmicutes. Our results show that this essential messenger is present even in the near-minimal bacterium *M. pneumoniae*, controlling potassium homeostasis by binding to the potassium uptake protein KtrC and might contribute to mycoplasmal pathogenicity.

With this work we have shown that even if *M. pneumoniae* contains only 694 genes, there is more controlled gene expression, second messenger-regulated protein functions and undiscovered virulence mechanisms as ever thought of.

CHAPTER 1 | Introduction

***Mycoplasma pneumoniae* - taxonomy, classification and cell biology**

Gram-positive bacteria occur mainly in two phyla, *Firmicutes* and *Actinobacteria*. Further, *Firmicutes* can be divided into *Bacilli*, *Clostridia* and *Mollicutes* (Wolf *et al.*, 2004). The *Mollicutes* probably derived from the *Streptococcus* branch of *Bacilli* (Maniloff *et al.*, 1996), but have lost many characteristics of their ancestors during extensive genome minimization. While *Bacilli* and *Actinobacteria* possess a rigid cell-wall, structured by internal cytoskeleton, and many can form resistant endospores, the *Mollicutes* have lost the required genes (Balish and Krause, 2006; Dandekar *et al.*, 2002). So far, *Mollicutes* including *Ureaplasma*, *Spiroplasma* and *Mycoplasmas* are cell free-living bacteria with the smallest genomes able to self-replicate. Their name is derived from the Latin words *mollis* and *cutis* meaning soft and skin, respectively. They form pleomorphic cells, from pear-shaped *Mycoplasmas* (see Fig. 1.1) to helical *Spiroplasmas*, which also differ in their way of movement, gliding or twisting, respectively. By now, there are 132 species described in the genus of *Mycoplasma* (http://www.bacterio.cict.fr/index.html). *Mycoplasmas* are found widespread as parasites in nature, *i.e.* plants, fish, reptiles, mammals and humans. The average cell size is about 1 µm, which is remarkably small in comparison to *Bacilli* that can grow up to 10 µm in cell length. Moreover, not only their cell size mirrors the degenerative evolution, but also the genome size. In average *Mollicutes* contain a single circular chromosome from 0.58 to 2.2 mega base pairs with a relative low GC content of 23 - 40%. Two major species *Mycoplasma pneumoniae* and *Mycoplasma genitalium* are extensively used for research in systems and synthetic biology. Both species are opportunistic human pathogens. While *M. pneumoniae* infects the upper respiratory tract (Waites and Talkington, 2004), *M. genitalium* infects mainly the ciliated epithelia of the urogenital tract (Tully *et al.*, 1981). *M. genitalium* and *M. pneumoniae* have chromosomes containing 482 and 688 protein-coding genes, respectively (Dandekar *et al.*, 2000; Fraser *et al.*, 1995). In comparison the *Bacillus subtilis* chromosome contains 4100 protein-coding genes (Barbe *et al.*, 2009).

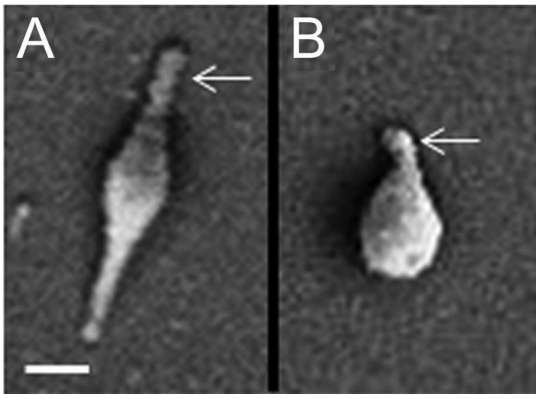

Figure 1.1 | Scanning electron micrographs of (A) *M. pneumoniae* and (B) *M. genitalium* from Balish, 2014; Arrows, indicate the attachment organelle. Scale bar, 200 nm.

Mycoplasma pneumoniae - carbon metabolism and regulation

Due to the enormous genome reduction in *M. pneumoniae* and *M. genitalium* both organisms strongly rely on the nutrient acquisition from the host tissue. This is due to the absence of *de novo* synthesis of purines and pyrimidines, absence of the citric acid cycle, fatty acid synthesis and an incomplete electron transport chain (Pollack, 2002; Waites and Talkington, 2004). Additionally, there is a special feature concerning the genetic code; the standard stop codon UGA encodes for tryptophan (Inamine *et al.*, 1990). However, the loss of many biosynthetic pathways requires growth on complex medium for *in vitro* growth and even the addition of serum for the incorporation of sterols into the triple-layered cell membrane (Halbedel *et al.*, 2007; Miles, 1992). The uptake of the required nutrients is exemplified by the presence of many genes coding for transport systems that make up 17% of all genes of *M. pneumoniae* (Großhennig *et al.*, 2013). Generation of energy is most efficiently done with glucose as carbon source which allows also the best growth for *M. pneumoniae*. Additionally, fructose, mannose, glycerophosphocholine (GPC) and probably glycerol-3-phosphate and ascorbate can be used for energy generation via glycolysis (Halbedel *et al.*, 2004; Halbedel *et al.*, 2007; Yus *et al.*, 2009). Interestingly, mannitol cannot be used as sole carbon source even though *M. pneumoniae* is equipped with the genes for its uptake and utilization (Halbedel *et al.*, 2004; Yus *et al.*, 2009). For the generation of ATP not only the substrate level phosphorylation in glycolysis can be used, further pyruvate can be oxidized to acetyl-CoA, which is converted into acetate and ATP by additional substrate level phosphorylation. In addition, pyruvate can be reduced to lactate, which is secreted similar as acetate and leads to typical acidification of the growth medium (Cordwell *et al.*, 1997; Halbedel *et al.*, 2007; Miles, 1992). Due to the constant habitat on the human lung epithelial cells, *M. pneumoniae* does not require complex regulatory networks controlling gene expression for adaptation to environmental changes, as *B. subtilis* does. *B. subtilis* needs fast adaptation to changing environmental conditions for survival, maintained by tight regulation of gene expression, translation and protein activity. However, even if *M. pneumoniae* is an extracellular human pathogen, under so far unknown conditions and mechanisms, the bacteria can penetrate cells, survive, and replicate (Dallo and Baseman, 2000).

The concept of minimal organisms and synthetic life

It was suggested that *Mycoplasmas* do not regulate their metabolism at all, instead they would underlie random gene expression, “transcriptional noise”. This noise can be interpreted as up and down fluctuations of expression in a random manner. Now, regulatory proteins besides the sigma factor were identified, *e.g.* the heat shock control protein HrcA (Himmelreich *et al.*, 1996; Madsen *et al.*, 1996). In comparison to other bacteria,

M. pneumoniae still encodes a small number of transcription factors (TFs). However, they can properly respond to environmental perturbations (Güell *et al.*, 2009). Several studies showed evidence for the regulation by phosphorylation or acetylation and post-transcriptional regulation (Chen *et al.*, 2016; Halbedel *et al.*, 2004; Schmidl *et al.*, 2010a; van Noort *et al.*, 2012). Moreover, non-TFs seem to be an additional layer of regulation, such as moonlighting proteins, as well as DNA topology, genomic organization and response regulation mediated via riboswitches (Barrick and Breaker, 2007; Junier *et al.*, 2016; reviewed for *Mycoplasmas* by Miravet-Verde *et al.*, 2017; Schmidl *et al.*, 2011; Travers and Muskhelishvili, 2005). Moreover, the set of genes with an unknown function could comprise hitherto undiscovered TFs.

The reduction of metabolic pathways and the presence of a minimal set of TFs to regulate gene expression clearly shows the degenerative evolution of minimal organisms. In addition to *Mollicutes*, naturally minimal genomes exist throughout all kingdoms. The prokaryotic symbiont *Nasuia deltocephalinicola* is the bacterium with the smallest genome, which is known so far (112 kb) (Bennett and Moran, 2013). Other representatives for small and sequenced genomes are the archeum *Nanoarchaeum equitans* (460 kb), the parasitic *M. genitalium* (580 kb), and the aquatic bacterium *Pelagibacter ubique* (1309 kb) which is free-living (Fraser *et al.*, 1995; Giovannoni *et al.*, 2005; Waters *et al.*, 2003). The most discussed example of genome minimization is of course the symbiogenesis which suggests the origin of eukaryotic organelles in intracellular bacteria (Aanen and Eggleton, 2017; López-García *et al.*, 2017). With this theory in mind, it is unclear if minimal prokaryotic symbionts and parasites are still living organisms or rather organelles. Recently, the formation of organelle-like structures was shown, when the genome from *Mycoplasmas* were introduced into yeast cells (Karas *et al.*, 2019). However, the minimal organisms *M. pneumoniae* and *M. genitalium* are capable of independent life when cultivated in complex medium, which attracted the research interest in past decades to study the minimal set of genes required for life. The question “What is life?” is as old as humanity, philosophers and scientists of the past 5000 years tried to find the answer.

Nowadays, scientists want to answer this question by creating artificial cells containing only the minimal set of genes required for survival and reproduction (Glass *et al.*, 2017). For this purpose, *Mycoplasmas* seem to be the ideal target as they are natural near-minimal cells. The genome comparison between the first whole-genome sequenced organisms, *M. genitalium* and *Haemophilus influenzae,* showed a core set of 250 essential genes (Fleischmann *et al.*, 1995; Fraser *et al.*, 1995). These genes were suggested as the minimal set for life. Afterwards, the gene essentiality in *M. genitalium* was addressed with knockout experiments revealing that up to 55% of the genes can be interrupted by transposons individually without lethal effect and so-called non-essential (Hutchison III *et*

al., 1999). Later, also the essentiality of genes in *M. pneumoniae* was evaluated and three categories were assigned (see Fig. 1.2): (i) essential, (ii) fitness, and (iii) non-essential genes (Christen *et al.*, 2011; Lluch-Senar *et al.*, 2015). The assigned genes consist of 342 essential plus 93 fitness genes, while 259 of 694 ORFs were identified as non-essential (Lluch-Senar *et al.*, 2015). These data also confirmed the essential protein machinery from all *Mollicutes*, that consisted of 104 essential proteins (Grosjean *et al.*, 2014). Beyond the gene essentiality, for *M. pneumoniae* detailed annotations and information are available at the genomic, proteomic, metabolomic levels and for global transcription and regulation (Güell *et al.*, 2009; Kühner *et al.*, 2009; Lluch-Senar *et al.*, 2013; Maier *et al.*, 2011; Schmidl *et al.*, 2010b; Yus *et al.*, 2009; Yus *et al.*, 2012; Yus *et al.*, 2017). Overall, these data form the basis for the creation of an artificial cell.

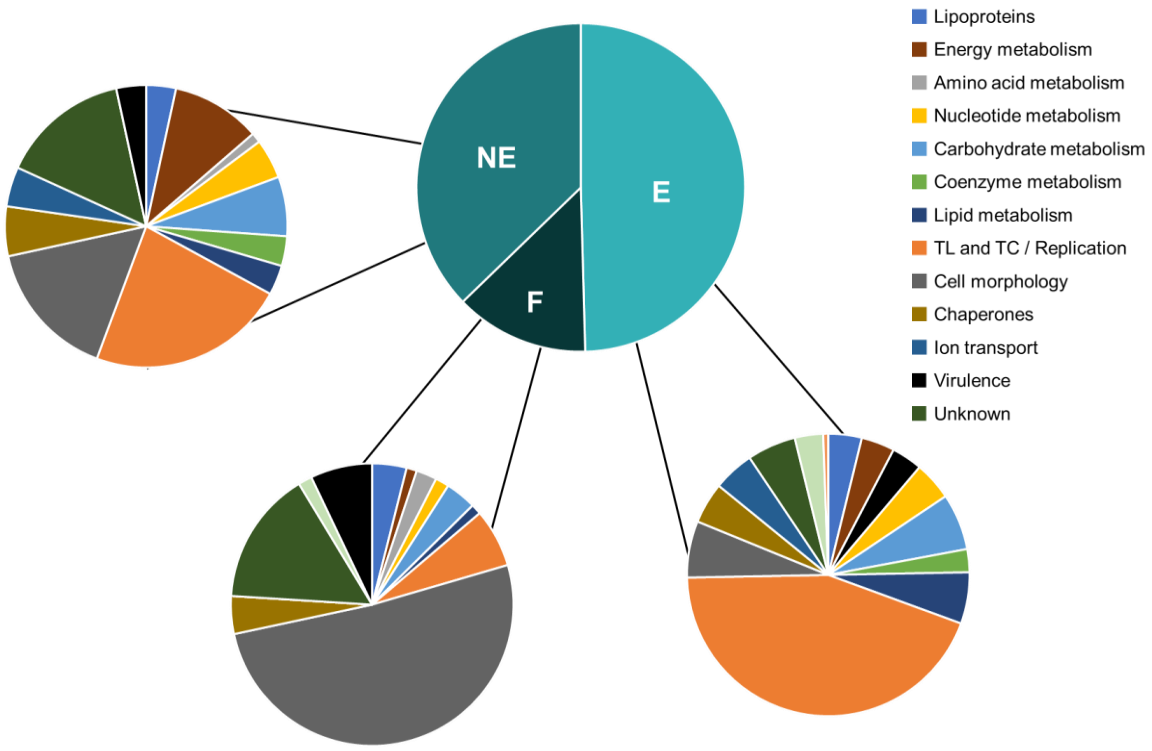

Figure 1.2 | Essentiality of genes in *M. pneumoniae* according to data from Lluch-Senar *et al.*, 2015. The 694 identified ORFs were assigned into categories: essential (E; 342 genes), fitness (F; 93 genes), and non-essential (NE; 259 genes) genes. The categories were further split into categories according to their biological functions in the legend. TL, translation; TC, transcription.

Two major approaches were started to create a cell reduced to the minimal gene set required for life: The top-down and the bottom-up approach. The top-down approach uses the genome of an organism and sequentially reduces its size by extensive deletion of non-essential genes. This approach often leads to dead-ends since these stepwise reductions alter the possibilities to manipulate the reduced genome further, resulting *e.g.* in loss of competence, temperature sensitivity, *etc*. (Hashimoto *et al.*, 2005; Reuss, Chapter 5, 2017).

Moreover, available techniques and selection markers reduce the possible amount of deletions or make the process fastidious. The top-down approach was used to reduce the genomes of several organisms, *e.g. B. subtilis* (Kobayashi *et al.*, 2003; Reuß *et al.*, 2017), *Escherichia coli* (Baba *et al.*, 2006; Gerdes *et al.*, 2003; Hashimoto *et al.*, 2005) or *Saccharomyces cerevisiae* (Giaever *et al.*, 2002). The second route of building a minimal organism called “bottom-up” describes the design and construction of a chromosome from scratch, which is synthesized and subsequently transplanted into a cell envelope. The bottom-up approach needs careful evaluation of a certain cell function or a required metabolite as essential or non-essential. For essential metabolites one must decide if the cells must create it *de novo* or simply take it up. For instance, amino acids can be synthesized from simple precursors or transported into the cell. Amino acid synthesis or uptake is essential for any cell, but none of the genes of the synthesis or the uptake must be essential alone. The same is true for gene homologs, from a single point of view, all can be non-essential, but at least one must be maintained to sustain the cell functionally. This is exemplified by the essential second messenger cyclic di-AMP in *B. subtilis*, that can be produced by three cyclases. Each cyclase can be deleted without any impact, but the second messenger must be produced at least from one cyclase to sustain cell viability (Commichau *et al.*, 2015). However, if the growth conditions are modified also these genes are non-essential and therefore belong to a class of fitness genes, that are only essential under certain conditions or for robust growth. Therefore, individual essentiality is only true for selected conditions, exemplified by the *MiniBacillus* project. Within this project the reduced strains must double in less than 60 min, at 37°C in LB-glucose medium (Reuß *et al.*, 2016). This shows that the estimation of core essential genes of all organisms is hard to predict. The essentiality depends always on the growth conditions and more important, on processes that can be achieved on different routes to maintain cellular functions. However, optimal tools for such an enormous project were not at a working stage. After the development of the required techniques that allowed the chemical synthesis of a whole genome and further the transplantation into a cell envelope the main obstacles were solved to minimize a genome and create artificial life (Gibson *et al.*, 2008; Lartigue *et al.*, 2007). For these experiments different *Mycoplasma* species were used. The combination of developed techniques allowed the synthesis of a watermarked *Mycoplasma mycoides* genome and the subsequent transplantation into the empty cell envelope of *Mycoplasma capricolum* (Gibson *et al.*, 2010). After in-depth analysis of the created cell and reevaluation of essential genes in combination with a new transposon study, the synthetic organism JCVI-syn3.0 was born (531 kb; 438 proteins and 35 RNAs; Hutchison III, 2016). JCVI-syn3.0 is smaller than *M. genitalium* and represents the best approximation of a minimal cell so far. Interestingly, JCVI-syn3.0 still contains 149 genes with an unknown biological

function and in a follow up 48 more genes could be inactivated by transposon mutagenesis. However, the overall goal would be an organism without the requirement of a recipient cell, rather an artificial envelope as well.

Bacterial virulence and pathometabolism

The unknown biological functions of proteins in JCVI-syn3.0 reflect also the open questions in *M. genitalium* and *M. pneumoniae*. Many of the genes do not have homologs in other species or their specific function is unknown. A limited toolkit for the manipulation of species from the *pneumoniae* clade heavily slowed down research with these species. For the routine work plasmids, knock-out techniques, protein expression systems are missing. However, the investigation of unknown genes and proteins in *M. pneumoniae* could shed light on many interesting questions. Revealing the biological function of unknown genes and proteins could lead to the identification of new targets for drugs against pathogenic bacteria and even to the goal of a synthetic minimal cell (Gallagher *et al.*, 2007). For *M. pneumoniae* and other pathogenic *Mycoplasmas*, this is of increasing importance since the mechanisms of virulence and their (patho)metabolism are not completely understood. Many *Mycoplasmas* cause severe illness and economic losses, such as *M. pneumoniae* and *M. mycoides* (Bajantri *et al.*, 2018; Shifrine *et al.*, 1972). *M. pneumoniae* infects the human lung and leads to atypical pneumoniae, fever, encephalitis and often chronic manifestation (Smith, 2010). *M. mycoides* as the causative agent of contagious bovine pleuropneumonia (CBPP) (Vilei *et al.*, 2000), is responsible for severe losses in livestock production and in consequence for serious socio-economic impacts in Africa (Onono *et al.*, 2014; Tambi *et al.*, 2006).

Bacteria use many different strategies to successfully colonize host tissues. In general, bacteria use virulence factors for host invasion, causing disease and evade the host defenses. These virulence factors can be sorted into functional groups: (i) adherence factors, (ii) invasion factors, (iii) evasion/capsules, and (iv) endo-/exotoxins. For several bacterial pathogens adhesion to host cells is the pre-requisite for host infection. It is well established that many Gram-positive bacteria such as *Mycobacterium tuberculosis* or group B *Streptococci* use pili to attach to epithelial cells (Alteri *et al.*, 2007; Telford *et al.*, 2006; Lauer *et al.*, 2005). Similarly, *Mycoplasmas* attach to epithelial cells, but their mechanism of attachment is different. They are not using pili but rather their electron dense tip structures. For *M. pneumoniae* and *M. genitalium* recent studies showed detailed insights into the gliding and attachment mechanisms of the apical tip (Krause *et al.*, 2018; Prince *et al.*, 2014; Seybert *et al.*, 2018). In *M. pneumoniae* the major adhesin P1 is re-organized after human cell contact from whole-cell distribution to the apical tip and hydrolyzed to the major P1 protein (Chourasia *et al.*, 2014; Waldo and Krause, 2006). Besides P1 the high

molecular weight (HMW) proteins 1 - 3 and several auxiliary lipoproteins directs and form the intricate network at the tip (reviewed by Chaudhry *et al.*, 2007; Page and Krause, 2013; Willby *et al.*, 2004). In addition, cytoplasmic proteins such as elongation factor Tu, the chaperones GroEL and the glyceraldehyde-3-phosphate dehydrogenase (GAP-DH) were shown to be surface located and responsible for host cell contact (Grimmer and Dumke, 2019; Hagemann *et al.*, 2017; Widjaja *et al.*, 2017). These protein-protein interactions emphasize the dynamic and complexity of celladhesion to the human host by *M. pneumoniae.* After adhesion, *M. pneumoniae* strongly relies on the nutrient acquisition from host cells (Waites and Talkington, 2004). *M. pneumoniae* is mainly regarded as extracellular obligate pathogen that lyse and destroy human cells for the subsequent uptake of amino and fatty acids, cofactors, and sugars from the host. For this purpose, they use metabolites such as hydrogen peroxide (H_2O_2) or hydrogen sulfide (H_2S) and nucleases for host cell lysis (Großhennig *et al.*, 2016; Halbedel *et al.*, 2007; Li *et al.*, 2018; Somerson *et al.*, 1965; Sudha *et al.*, 2010; Yamamoto *et al.*, 2016). Besides metabolite derived virulence factors, *M. pneumoniae* is discussed to induce several cytopathic effects through the community-acquired respiratory distress syndrome (CARDS) toxin with ADP-ribosyl transferase activity (Hardy *et al.*, 2009; Kannan and Baseman, 2006). Recombinant CARDS induces vacuoles in mammalian cells and ADP-ribosylates target proteins, but the toxin is barely expressed *in vitro* (Hardy *et al.*, 2009; Kannan and Baseman, 2006; Kannan *et al.*, 2010). Expression analysis with *M. pneumoniae* in contact with human cells indicate the regulation of the *cards* gene (Kannan *et al.*, 2010), but the mechanism is still elusive. Such regulatory mechanism could be thermally controlled, as the major virulence regulator PrfA in *Listeria monocytogenes* (Johansson *et al.*, 2002), or secondary mRNA structures (riboswitches) sensing ions or metabolites (Barrick and Breaker, 2007; Kim *et al.*, 2007). Interestingly, the genome sequence of *Mycoplasma iowae* contains two copies of the *cards* toxin (Wei *et al.*, 2012). *Mycoplasma* species cause rather chronic infections instead of killing their hosts, except for *Mycoplasma alligatoris* which causes a lethal invasive disease in alligators and caimans (Brown *et al.*, 2004). Therefore, it is thought that these bacteria can modulate and escape the host immune defenses very efficiently. A reason for the long-term survival in host tissue is exemplified by the antigenic variation of *M. genitalium.* This is facilitated by recombination and modification of MgPa (encoded by *mgpABC*; P1 homolog of *M. pneumoniae*), that seems to be an efficient strategy of host adaptation and evading host immune system by antigenic variation, but the genetic mechanisms are not clear (Ma *et al.*, 2007). These genome rearrangements are well described for other *Mycoplasma* species, *e.g*. *Mycoplasma agalactiae, Mycoplasma pulmonis and Mycoplasma bovis* (Bhugra *et al.*, 1995; Chopra-Dewasthaly *et al.*, 2008; reviewed by Citti *et al.*, 2010; Lysnyansky *et al.*, 1999; Lysnyansky *et al.*, 2001). In these species the adhesion proteins

VPMA, VSA and VSP, respectively, create nearly unlimited variation by the site-directed recombination. Recently, another peculiarity to evade host defense mechanisms, using capsular polysaccharides, was proven for *Mycoplasma mycoides in vivo* which was postulated already 40 years ago (Buttery *et al.*, 1976; Jores *et al.*, 2019). Furthermore, the exopolysaccharide capsule of *Mycoplasma gallisepticum* seems to be involved in virulence and adhesion, while in *Mycoplasma pulmonis* the capsule is protective against the host complement system (Bolland *et al.*, 2012; Tajima *et al.*, 1982). However, no capsule production or its relation for virulence was investigated in *M. pneumoniae* so far.

In addition to the machinery for host defense survival, many *Mycoplasmas* must cope with high concentrations of hydrogen peroxide. This is produced in their own metabolism or sequestered from host cells as defense metabolite. Higher amounts are mainly toxic for host cells and other bacteria, competing in the same niche, while *Mycoplasma* far better tolerate peroxide stress. However, peroxides and superoxide anions are harmful for proteins, lipids, and the DNA when not detoxified rapidly (Gusarov and Nudler, 2005). Many aerobic bacteria developed various strategies, sensing and responding the oxidative stress in their habitat (Mongkolsuk and Helmann, 2002). Surprisingly *Mycoplasmas* can tolerate these toxic concentrations of reactive oxygen species (ROS) very well, even lacking most of these strategies. The oxidative stress response of *B. subtilis* is well-studied and here exemplified. *B. subtilis* contains multiple defense proteins against H_2O_2, organic peroxides and hydroxyl radicals, such as catalases (KatA, KatX, KatE), superoxide dismutases (SodA, SodF), alkyl hydroperoxide reductases (AhpCF, AhpAT), and organic hydroperoxide reductases (OhrA, OhrB) (Antelmann *et al.*, 1996; Bsat *et al.*, 1996; Chen *et al.*, 1995; Engelmann and Hecker, 1996; Fuangthong *et al.*, 2001; Inaoka *et al.*, 1999). All these enzymes contribute to the detoxification of ROS. The expression of these enzymes in response to oxidative stress is regulated by different transcription factors, *i.e.* PerR, OhrR, and σ^B (Helmann *et al.*, 2003). In other bacteria, such as *E. coli* or *Salmonella* spp., the regulatory mechanism is controlled by another class of transcription factors, like OxyR and SoxR (Christman *et al.*, 1985; reviewed in Marinho *et al.*, 2014). Additionally, ROS resistance is influenced by the regulators Fur and Spx, which control iron/manganese homeostasis and general oxidative stress, respectively (Pi and Helmann, 2017; Schäfer *et al.*, 2019). However, it was supposed that the genomes of *Mollicutes* do not contain genes for catalase and superoxide dismutase (Baumann, 1989; Fraser *et al.*, 1995; Tryon and Baseman 1992). These two are the common detoxifying enzymes in most bacteria. Interestingly, as the only exceptions so far, *M. iowae* contains an active catalase and *Mycoplasma hyopneumoniae* contains an active superoxide dismutase (Chen *et al.*, 2000; Pritchard *et al.*, 2014). However, this is most likely due to horizontal gene transfer from anaerobic bacteria. Irrespectively of the rare examples, such

as catalase or SOD, nothing of the ROS resistance mechanisms in *M. pneumoniae* is known. In several bacterial species the organic hydroperoxide resistance proteins (Ohr) and osmotically inducible protein C homologs (OsmC) degrade organic peroxide (Lesniak *et al.*, 2003; Mongkolsuk *et al.*, 1998). This superfamily of peroxiredoxins is also found in different *Mycoplasmas* but OsmC proteins seem to be restricted to the pneumoniae cluster. Interestingly, *Mycoplasmas* seem to control the gene expression of *ohr* and *osmC* homologs specifically when exposed to diffrerent ROS or physical stresses. This is also true in other bacteria, *e.g*. *Xanthomonas campestris* and *Pseudomonas aeruginosa* (Atichartpongkul *et al.*, 2001; Mongkolsuk *et al.*, 1998). In *M. gallisepticum* and *M. genitalium* the Ohr homologs are proven to degrade peroxides and both favour organic peroxides over hydrogen peroxide (Jenkins *et al.*, 2008; Zhang and Baseman, 2014). The detoxification of ROS is suggested to play a significant role in mycoplasmal virulence (Lynch and Cole, 1980; Ben-Menachem *et al.*, 1998).

Tools for genetic manipulation of *Mycoplasmas*

To address biological questions experimentally, it is an indispensable requirement to manipulate the organisms of interest. For many organisms, Gram-positive and Gram-negative exemplified by *B. subtilis* and *E. coli*, respectively, the toolbox is relatively large and continuously extended. These bacteria can be transformed easily with plasmids, chromosomal DNA or linear DNA fragments (Sambrook *et al.*, 1989; Dubnau *et al.*, 1991). Beside their relative slow growth this is the first technical bottleneck when working with *Mycoplasmas,* that lack natural systems for competence and DNA uptake (Dybvig, 1990 Dybvig and Voelker, 1996). However, it is possible to transfer DNA by electroporation into the target cells. The insertion of plasmids into research organisms for ectopic protein expression, complementation, reporter analysis, etc. is important. First in *M. mycoides* naturally occurring plasmids were identified and modified for research interests (Bergemann and Finch, 1988; Dybvig and Khaled, 1990). More recently, for several *Mycoplasmas* species replicating plasmids that are not incorporated into the genome were developed (Cordova *et al.* 2002; Chopra-Dewasthaly *et al.*, 2005; Janis *et al.*, 2005; Lartigue *et al.*, 2003). So far, no existing plasmid was replicative and stable in *M. pneumoniae* or *M. genitalium*. To investigate constructed parts *in vivo* the introduction into the *M. pneumoniae* genome was necessary. This is only possible after single genome integration via transposons, which occurs randomly (Halbedel and Stülke, 2007). Furthermore, targeted gene deletion is complicated since *M. pneumoniae* is not expressing the required recombination machinery. Only in a few examples homologous recombination was observed for *Mycoplasmas*, *i.e. M. genitalium, M. gallisepticum or M. pulmonis* (Cao *et al.*, 1994; Cordova *et al.*, 2002; Dhandayuthapani *et al.*, 1999). Interestingly, the

combination of in-yeast genome modification using the CRISPR/Cas9 editing tool, with the genome transplantation technique facilitate the creation of modified *Mycoplasmas* (Lartigue *et al.*, 2007; Tsarmpopoulos *et al.*, 2016). Unfortunately, neither using the genome of *M. pneumoniae* nor the cell envelope for transplantation were successful. Recently, our collaborators developed a technique for *M. pneumoniae* enabling the targeted gene deletion with the possibility of resistance cassette removal (Piñero-Lambea *et al.*, unpublished). Overall, the biology of *Mycoplasmas* in the *pneumoniae* cluster with highly reduced genomes seem to be different from other Mollicutes. New techniques pave the way for the research with *Mycoplasmas*, for *in vivo* and *in vitro* characterization of many unknown genes in these organisms.

AIM OF THE THESIS

The decreased growth rate of the near-minimal bacteria *M. genitalium* and *M. pneumoniae* slow down the work progress of research. Furthermore, missing methods for adequate manipulation of *M. pneumoniae* hamper the research with this bacterium as well. More knowledge about *Mycoplasmas* could answer interesting questions concerning essential genes and virulence in bacteria. Since we are interested in the minimal set of genes required for a cell to sustain life, we will work with the naturally genome-reduced bacterium *M. pneumoniae.* Using *M. pneumoniae* we will directly overcome bottlenecks, *i.e*. backups or redundant enzyme functions are not present, that could influence our minimization approach. Furthermore, many "-omic" data are already collected.

In the first place, we will focus on the development of a plasmid able to replicate within the cells. This plasmid will extend the limited toolbox available for *M. pneumoniae*. This plasmid will be useful for several approaches, *e.g*. for *in vivo* gene expression or complementation. Moreover, the development of an efficient deletion technique, that allows multiple targeted deletions in one genome, is an important issue. With a new deletion system, we intend to characterize essential genes and gene sets in *M. pneumoniae.* The characterization of unknown genes is the prerequisite for the genome reduction, ultimately leading to a *mini*CELL that will be used in medical therapy (www.minicell.org). This cell should be deficient in virulence, but able to target specific host cells. Leading to our second main goal, the construction of a safe cell chassis. Therefore, we must identify hidden virulence factors and erase them from the genome. We will analyze *M. pneumoniae* mutants and characterize their phenotypes, according to attachment, growth, and virulence. Specific protein functions will be analyzed *in vitro* and *in vivo,* with recombinant enzymes produced in *E. coli* or overproduction in *M. pneumoniae* cells, respectively. Further, we can test specific protein functions in complementation assays using *B. subtilis* mutants.

As we are specifically interested in the essential set of genes, we want to investigate the essential second messenger c-di-AMP, its homeostasis and potential interactions partners. For *B. subtilis* the production, degradation and regulatory mechanisms are well described but not for *Mollicutes* at all. The essentiality of genes required for c-di-AMP metabolism and putative binding proteins will be addressed. The results will shed light on second messenger metabolism in a near-minimal organism, beside the essential gene set of *M. pneumoniae*.

CHAPTER 2 | Cyclic di-AMP in a minimal organism

Results described in chapter 2 were published in *Frontiers in Microbiology*:

Identification of the Components Involved in Cyclic Di-AMP Signaling in *Mycoplasma pneumoniae*

Cedric Blötz[1†], Katrin Treffon[1†], Volkhard Kaever[2], Frank Schwede[3], Elke Hammer[4] and Jörg Stülke[1]

[1]Department of General Microbiology, University of Göttingen, Germany
[2]Research Core Unit Metabolomics, Hannover Medical School, Germany
[3]Biolog Life Science Institute, Bremen, Germany
[4]Department of Functional Genomics, University Medicine Greifswald, Germany

[†]These authors have contributed equally to this work.

AUTHOR CONTRIBUTION

CB, KT, and JS designed the study. CB and KT cultivated *Mycoplasma* cells. KT performed cloning and protein test expression. KT cultivated *E. coli* producing CdaM and CB cultivated *Mycoplasmas* for *in vivo* c-di-AMP determination. VK determined intracellular c-di-AMP levels. CB and KT screened for transposon mutants. CB overproduced and purified phosphodiesterases. CB performed enzyme assays. FS prepared the c-di-AMP coupled agarose. CB and KT performed c-di-AMP pull-down experiments. EH performed MS analysis. CB designed the Figures. CB and JS wrote the manuscript.

ABSTRACT

Bacteria often use cyclic dinucleotides as second messengers for signal transduction. While the classical molecule c-di-GMP is involved in lifestyle selection, the functions of the more recently discovered signaling nucleotide cyclic di-AMP are less defined. For many Gram-positive bacteria, c-di-AMP is essential for growth suggesting its involvement in a key cellular function. We have analyzed c-di-AMP signaling in the genome-reduced pathogenic bacterium *Mycoplasma pneumoniae*. Our results demonstrate that these bacteria produce c-di-AMP, and we could identify the diadenylate cyclase CdaM (MPN244). This enzyme is the founding member of a novel family of diadenylate cyclases. Of two potential c-di-AMP degrading phosphodiesterases, only PdeM (MPN549) is active in c-di-AMP degradation, whereas NrnA (MPN140) was reported to degrade short oligoribonucleotides. As observed in other bacteria, both the c-di-AMP synthesizing and the degrading enzymes are essential for *M. pneumoniae* suggesting control of a major homeostatic process. To obtain more insights into the nature of this process, we have identified a c-di-AMP-binding protein from *M. pneumoniae*, KtrC. KtrC is the cytoplasmic regulatory subunit of the low affinity potassium transporter KtrCD. It is established that binding of c-di-AMP inhibits the KtrCD activity resulting in a limitation of potassium uptake. Our results suggest that the control of potassium homeostasis is the essential function of c-di-AMP in *M. pneumoniae*.

INTRODUCTION

To respond to changes in their environment, bacteria have evolved a large set of signal detection and transduction systems. Such signals can be directly sensed by proteins, they may feed into complex networks that control gene expression via transcription factors, or they are first converted to so-called second messengers which in turn provoke a response. Many bacteria use dedicated nucleotides as second messengers, among them cyclic AMP, (p)ppGpp and the cyclic dinucleotides c-di-AMP and c-di-GMP (Gomelsky, 2011).

cAMP is the paradigmatic second messenger, and this nucleotide is involved in coordinating carbon and nitrogen metabolism and in carbon catabolite repression in *Escherichia coli* and related bacteria (Görke and Stülke, 2008; You *et al.*, 2013). (p)ppGpp is formed upon starvation and triggers a reduction of cellular house-keeping activities (Steinchen and Bange, 2016). Cyclic di-GMP is in many bacteria involved in the choice between sessile and motile lifestyles (Hengge, 2009). While these second messengers have been intensively studied in a large number of different bacteria, cyclic di-AMP has been discovered only less than a decade ago (Witte *et al.*, 2008).

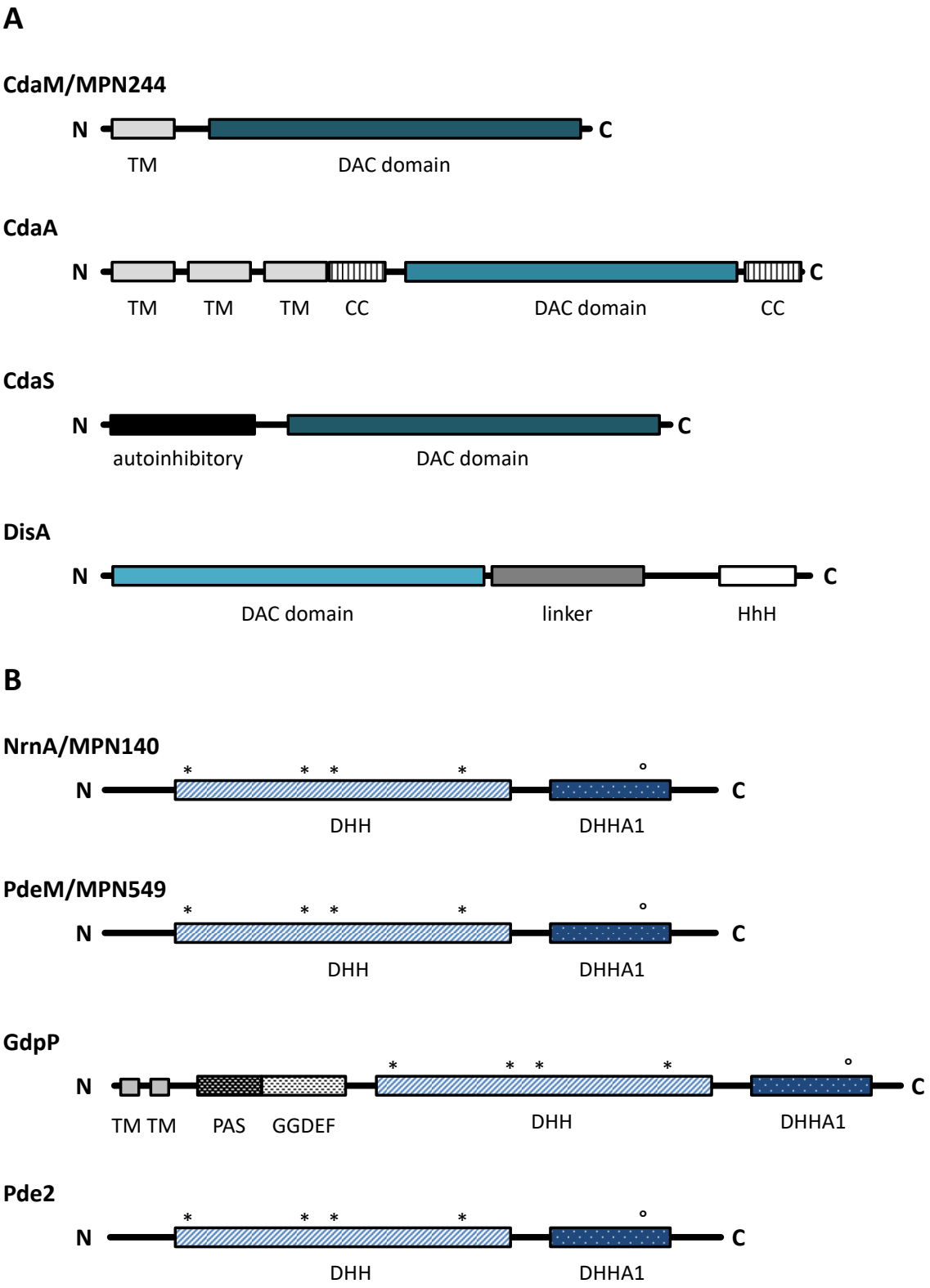

Figure 2.1 | Domain architecture of c-di-AMP related enzymes. Black lines indicate protein sequences and the boxes represent domains. (A) The four classes of c-di-AMP producing DACs. Intensity of the blue color indicates differences in the DAC domain. (B) Phosphodiesterases specific for c-di-AMP degradation. Conserved residues in the DHH and DHHA1 motifs are indicated with asterisks and circle, respectively. DAC, di-adenylate

cyclase; TM, transmembrane domain; CC, coiled-coil domain; HhH, Helix-hairpin-Helix; PAS, Per-Arnt-Sim sensor domain; DHH/DHHA/GGDEF, Asp-His-His/ Asp-His-His-Ala/ Gly-Gly-Asp-Glu-Phe.

This nucleotide was found in the crystal structure of the so-called DNA integrity scanning protein DisA, which exhibits diadenylate cyclase activity (Witte *et al.*, 2008). C-di-AMP is formed in a variety of both Gram-positive and Gram-negative bacteria with the notable exception of the gamma-proteobacteria including the enterobacteria. Several studies have revealed that this second messenger is essential for many Gram-positive bacteria with a low genomic GC content (the *Firmicutes*). This has been shown for *Bacillus subtilis*, *Staphylococcus aureus*, *Listeria monocytogenes*, and many other species (Luo and Helmann, 2012; Corrigan and Gründling, 2013; Commichau *et al.*, 2015). Moreover, the accumulation of c-di-AMP has also been shown to cause severe problems for the cells (Mehne *et al.*, 2013; Gundlach *et al.*, 2015b). To control the intracellular levels of c-di-AMP, the bacteria that produce cyclic di-AMP do also possess phosphodiesterases to degrade this molecule (Rao *et al.*, 2010; Corrigan *et al.*, 2011; Commichau *et al.*, 2015; Huynh and Woodward, 2016).

All known diadenylate cyclases share a conserved domain, the so-called DAC domain (Römling, 2008; Commichau *et al.*, 2015; Rosenberg *et al.*, 2015). However, the DAC domain can be found in different arrangements with other domains. Based on the domain organization, three classes of diadenylate cyclases have been studied so far (see Figure 2.1). The proteins of the CdaA class are membrane proteins with three transmembrane domains at the N-terminus (Gundlach *et al.*, 2015b). This class of diadenylate cyclases is the most widespread, and it is ubiquitous in most *Firmicutes*. CdaS is a cyclase that is only found in *B. subtilis* and closely related spore formers. This cyclase consists of an N-terminal autoinhibitory domain and the DAC domain (Mehne *et al.*, 2014). Finally, the enzymes of the DisA class are found in spore-forming *Firmicutes* (*Bacillus* spp., *Clostridium* spp.) and in the Actinobacteria. These octameric enzymes have their DAC domain at the N-terminus and bind DNA via a C-terminal helix-hairpin-helix domain (Witte *et al.*, 2008; Commichau *et al.*, 2015). While most bacterial species contain one diadenylate cyclase, *B. subtilis* encodes three enzymes, one of each class (Mehne *et al.*, 2013). Two principal classes of c-di-AMP-degrading phosphodiesterases have been described: The proteins of the first class possess a domain called DHH-DHHA1 with a catalytic Asp-His-His motif. The DHH-DHHA1 domain can either be part of a larger protein as in *B. subtilis* GdpP or exert the enzymatic activity without any additional domains as described for *Streptococcus pneumoniae* Pde2 (see Figure 2.1, Rao *et al.*, 2010; Bai *et al.*, 2013). The enzymes of the second class possess a so-called HD domain with a His-Asp catalytic motif (Huynh *et al.*, 2015).

While the functions of cAMP, (p)ppGpp, and c-di-GMP are well understood, this is not the case for c-di-AMP. Earlier studies have implicated c-di-AMP in the control of cell wall homeostasis (Corrigan *et al.*, 2011; Luo and Helmann, 2012; Mehne *et al.*, 2013). Moreover, c-di-AMP formation by DisA was suggested to be important for integrity control, repair and recombination of DNA (Oppenheimer-Shaanan *et al.*, 2011; Campos *et al.*, 2014). The isolation of c-di-AMP binding proteins has identified the small signal transduction protein DarA (c-di-AMP receptor A), the pyruvate carboxylase, subunits of potassium transporters, and ATP-binding subunits of osmoprotectant ABC transporters (Corrigan *et al.*, 2013; Sureka *et al.*, 2014; Gundlach *et al.*, 2015a; Huynh *et al.*, 2016; Schuster *et al.*, 2016). Moreover, c-di-AMP binds and inhibits the KdpD sensor kinase that controls the expression of a high affinity potassium transporter in *S. aureus* (Moscoso *et al.*, 2016). Finally, c-di-AMP binds an RNA molecule, i.e., the riboswitch that controls the expression of the potassium transporters KimA and KtrAB in *B. subtilis* (Nelson *et al.*, 2013; Gundlach *et al.*, 2017). Binding to both KtrA and the riboswitch controlling its expression makes c-di-AMP the only second messenger that controls a biological process (potassium uptake) by binding both to a protein and to the corresponding mRNA molecule (Commichau *et al.*, 2015). Among all identified targets of c-di-AMP, not a single one is essential. Only recently, c-di-AMP essentiality could be traced back to the control of potassium homeostasis in *B. subtilis* (Gundlach *et al.*, 2017). We are interested in signal transduction in the strongly genome-reduced pathogenic bacterium *Mycoplasma pneumoniae*. This bacterium encodes only 694 proteins (Lluch-Senar *et al.*, 2015), reflecting its adaptation to rather constant environmental conditions in the natural habitat, human lung epithelia. Accordingly, *M. pneumoniae* possesses only three putative transcription factors to control gene expression. However, the mechanisms of transcriptional regulation in *M. pneumoniae* are still poorly understood (Güell *et al.*, 2009). In addition, the second messenger ppGpp is likely formed by *M. pneumoniae* as deduced from the presence of a ppGpp synthetase-encoding gene (Eilers, 2010). In this study, we have analyzed the presence of components involved in c-di-AMP signaling in *M. pneumoniae*. We demonstrate that this second messenger is formed by this bacterium and have identified the enzymes responsible for its synthesis and degradation. Moreover, we have discovered that c-di-AMP binds to the *M. pneumoniae* KtrC protein, indicating a function in the control of potassium uptake.

MATERIALS AND METHODS

Bacterial strains and growth conditions. *Mycoplasma pneumoniae* was handled under L2 laboratory safety conditions. The *M. pneumoniae* strain used in this study was *M. pneumoniae* M129 (ATCC 29342). *M. pneumoniae* was grown at 37°C in 175 cm^2 tissue culture flasks containing 100 ml of modified Hayflick medium as described previously

(Halbedel *et al.*, 2004). Carbon sources were added to a final concentration of 1% (w/v). *Escherichia coli* XL1blue and BL21(DE3)/pLysS (Sambrook *et al.*, 1989) were used as host for cloning and recombinant protein expression, respectively. *E. coli* strains were cultivated in Luria Bertani broth (Sambrook *et al.*, 1989) containing ampicillin 100 mg ml^{-1}. *Bacillus subtilis* 168 was used to extract chromosomal DNA.

DNA manipulation and plasmid construction. Chromosomal DNA from *B. subtilis* and *M. pneumoniae* was isolated using the Blood and Tissue Kit according to the manufacturer's instructions (Qiagen, Hilden, Germany). Transformation of *E. coli* and plasmid DNA extraction was performed using standard procedures (Sambrook *et al.*, 1989). Plasmids for the overexpression and purification of the enzymes potentially involved in c-di-AMP metabolism from *M. pneumoniae* were constructed as follows. The coding sequence of each gene was amplified by PCR with gene specific primers (listed in Supplementary Table S2.1) using chromosomal DNA of *M. pneumoniae* M129 as the template. As the *M. pneumoniae* genes contain TGA codons that code for tryptophan in *M. pneumoniae* but for an opal stop codon in *E. coli*, the PCR fragments were used as templates for mutagenesis by the multiple mutation reaction (Hames *et al.*, 2005) using the amplification primers and 50-phosphorylated mutagenic primers (listed in Supplementary Table S2.1) to introduce TGA to TGG transitions. The cytoplasmic portion of the *B. subtilis gdpP* gene ($GdpP^{84-659}$) was amplified from *B. subtilis* chromosomal DNA. The PCR products of genes potentially encoding phosphodiesterases were digested with BamHI and NdeI and cloned into the expression vector pGP574 (Schilling *et al.*, 2006). This plasmid allows the expression of enzymes carrying a C-terminal Strep-tag. The resulting plasmids are pGP2717 (*mpn140*), pGP2718 (*mpn549*), and pGP2720 (*gdpP*). The PCR product for the potential diadenylate cyclase-encoding gene *mpn244* was cleaved with NdeI and BamHI and cloned into the vector pET3c (Novagene, Darmstadt, Germany). The resulting plasmid was pGP2036. All plasmid inserts were verified by DNA sequencing.

Protein overexpression and purification. The Strep-tagged proteins were overexpressed in *E. coli* BL21(DE3). Expression (1 l culture, 37°C, 200 rpm, baffled flasks) was induced by the addition of 1 mM IPTG to exponentially growing cultures (OD_{600} of 0.6 to 0.8). After expression for 3 hours, the cells were pelleted at 4°C for 20 min at 4 000 rpm and washed once with 20 ml PDE buffer (100 mM Tris-HCl pH8.3, 150 mM NaCl, 1 mM EDTA, 5% glycerol). Cells were lysed using a French press (18 000 p.s.i., 138 000 kPa, three passes, SLM Aminco, United States). After lysis, the crude extracts were centrifuged at 35 000 r.p.m for 30 min. The crude extract was then passed over a StrepTactin column (IBA, Göttingen, Germany). The recombinant proteins were eluted with desthiobiotin (IBA, final concentration

2.5 mM). After elution, the fractions were tested for the desired protein using 12% SDS-PAGE. Only fractions which contained the desired protein in apparent homogeneity (content of the specific protein >95%) were used for further purification by running the proteins over a 10 ml HiTrap Heparin HP column (GE Healthcare) using the ÄKTA prime plus system (GE Healthcare, flow rate 2 ml/min). With 1 M NaCl in the PDE buffer, proteins were eluted from the column. Fractions containing pure protein were concentrated and dialyzed to 1.5 ml without NaCl in PDE buffer using VivaspinR Turbo15 ultrafiltration spin columns (MW 5 000 Da; Sartorius, Göttingen, Germany). Protein concentrations were determined using the Bio-Rad dye-binding assay where bovine serum albumin served as the standard. Aliquots of the proteins were frozen in liquid nitrogen and stored at -80°C prior to further experiments.

Enzyme assays. The assays for phosphatase and phosphordiesterase activities of Strep-tagged proteins were performed as described previously (Diethmaier *et al.*, 2014). Phosphatase activity against para-nitrophenol phosphate (pNPP) was assayed in a buffer containing 100 mM Tris-HCl pH8.3, 10 mM NaCl, 0.1 mM $MnCl_2$, 25 mM pNPP and different amounts of purified protein in a total volume of 100 µl. Phosphodiesterase activity against bis-pNPP was assayed in a buffer containing 100 mM Tris-HCl pH8.3, 10 mM NaCl, 0.1 mM $MnCl_2$, or $MgCl_2$, 1 - 7.5 mM bis-pNPP and purified protein in a total volume of 100 µl. The reactions were initiated by the addition of the protein, and the reaction mixture was incubated at 37°C for 4 h. Relative substrate cleavage was quantified by measuring the OD_{410} using a microplate reader (EPOCH| 2, BioTek, Winooski, United States).

Phosphodiesterase activity with cyclic dinucleotides was measured using a quantitative assay based on the interaction of c-di-AMP with the fluorescent dye coralyne (Zhou *et al.*, 2014). Briefly, reaction mixtures (150 µl) consisted of 100 mM Tris-HCl pH8.3, 10 mM NaCl, 0.1 mM $MnCl_2$, and 100 µM c-di-AMP. The reaction was initiated by addition 100 nM enzyme (for MPN549 additionally 50 and 10 nM), and the reaction mixture was incubated at 37°C for 4 h. At different time points the reactions were stopped by addition of 1 µl EDTA (0.5 M), shock-freezing and subsequent boiling for 10 min. To quantify the remaining c-di-AMP, the samples were spun to remove protein precipitate. KBr and coralyne were added to the sample to final concentrations of 250 mM and 10 µM, respectively. After 20 min of incubation at 37°C in the dark, relative c-di-AMP cleavage was determined as described (Zhou *et al.*, 2014) by measuring the fluorescence emission at 475 nm using a microplate reader (SYNERGY Mx, BioTek, Winooski, United States).

In all kinetic experiments, Km and Vmax were determined by nonlinear curve fitting from Lineweaver-Burk plots.

C-di-AMP extraction. The concentrations of c-di-AMP in *E. coli* and in *M. pneumoniae* cells were determined by a liquid chromatography tandem MS (LC-MS/MS) method, essentially as described previously (Mehne *et al.*, 2013; Gundlach *et al.*, 2015b). Briefly, *E. coli* or *M. pneumoniae* cells were grown in LB (20 ml) or MP (100 ml) medium, respectively. For *E. coli* two additional aliquots (1 ml each) of each sample were harvested for total protein determination. For *M. pneumoniae*, the wet weight of each sample was determined. The pellets were resuspended in 300 µl extraction mixture (acetonitrile/methanol/water 40/40/20 v/v/v) and shock-frozen in liquid nitrogen, followed by boiling for 10 min. The boiled samples were centrifuged for 10 min at 4°C and 20 800 g. The supernatants were stored on ice, and the remaining pellets were used for two more extraction steps with 200 µl extraction mixture. For this purpose, the samples were mixed, incubated on ice for 15 min, and centrifuged again. The obtained supernatants were pooled. The samples were incubated at -20°C over night, and centrifuged again (20 min, 4°C, 20 800 g). Then, the supernatant was transferred to a fresh reaction tube, and dried in a speed vac at 50°C for 2 h and resuspended in 200 µl of water. After repeated centrifugation and addition of the internal standard ([^{13}C,^{15}N]c-di-AMP), part of the extract was analyzed by LC-MS/MS.

Quantification of c-di-AMP by MS/MS. Chromatographic separation was performed on a series 200 high-pressure liquid chromatography (HPLC) system (PerkinElmer Life Sciences) as described previously (Mehne *et al.*, 2013). The analyte detection was performed on an PI4000 triple-quadrupole mass spectrometer equipped with an electrospray ionization source (AB Sciex), using selected reaction monitoring (SRM) analysis in positive ionization mode. The SRM transitions labeled “quantifier” were used to quantify the compound of interest, whereas “identifier” SRM transitions were monitored as confirmatory signals. The quantifier SRM transitions were most intense and were therefore used for quantification.

Pull down of c-di-AMP binding proteins via c-di-AMP coupled agarose. To isolate c-di-AMP-binding proteins from *M. pneumoniae*, we made use of immobilized c-di-AMP (2′-O-(6-aminohexylcarbamoyl)-cyclic diadenosine monophosphate on agarose (2′-AHC-c-di-AMP-agarose; BIOLOG, Bremen, Germany). We prepared *M. pneumoniae* crude cell extracts from 150 mg cells per assay. The cells were lysed in pulldown buffer (100 mM Tris-HCl pH7.5, 100 mM KCl, 150 mM NaCl, 5 mM $MgCl_2$, 0.5 mM DTT, 0.1% (v/v) Tween-20, and 1x cOmpleteTM protease inhibitor (Roche Diagnostics, Mannheim, Germany)). Cells were lysed in a tissue lyser with 0.1 mm glass beads (2 × 2.5 min, 30 Hz, cooled block) followed by ultracentrifugation for 30 min at 35 000 rpm and 4°C. To prepare the matrix, 500 µl 2′-AHC-c-di-AMP agarose or ethanolamine-coupled agarose (negative control) were

equilibrated three times with 1 ml of pulldown buffer. After equilibration, the cell lysate and the agarose matrix were incubated rotating over night at 4°C. The supernatant was discarded, and the matrix was washed three times (1 ml 1x PBS; 137 mM NaCl, 2.7 mM KCl, 10 mM Na_2HPO_4, 1.76 mM KH_2PO_4, pH7.4). Elution of binding proteins was performed with 200 µl of 1x PBS, pH7.4 containing 1 mM c-di-AMP and 15 min incubation at RT and 1 400 rpm. The eluted proteins were concentrated using acetone precipitation (1:1 sample:acetone) over night at -20°C. The precipitate was centrifuged 1 h at 14 800 rpm and 4°C. The remaining supernatant was discarded, and the sample dried for 10 min at RT. The remaining pellet was solved in 40 µl 1x PBS and analyzed by SDS-PAGE. Proteins of interest were identified by mass spectrometry as described previously (Meyer *et al.*, 2011). Briefly, after destaining of gel slices, proteins underwent in-gel digestion with trypsin (10 ng/µl trypsin in 20 mM ammonium bicarbonate). Peptides were separated by C18 reverse phase liquid chromatography (nanoAcquity UPLC system, 10 cm, Waters, Manchester, United Kingdom) in a linear gradient of 0.1% acetic acid in acetonitrile from 5% up to 25% within 65 min (flow rate: 400 nl/min). MS analysis was performed on a LTQ-Orbitrap Velos hybrid mass spectrometer (Thermo Electron, Bremen, Germany) operated in data-dependent MS/MS mode. Proteins were identified by searching all MS/MS spectra against a *M. pneumoniae* M129 protein database (687 entries, extracted from Uniprot rel. 05-2014) using Sequest algorithm on a SorcererTM software platform. Initial mass tolerance for peptide identification on MS and MS/MS peaks were 10 ppm and 1 Da, respectively. Up to two missed tryptic cleavages were allowed. Methionine oxidation (+15.99492 Da) and propionamide modification on cysteine (+71.037109 Da) were set as variable modifications. Protein identification results were evaluated by determination of probability for peptide and protein assignments provided by PeptideProphet and ProteinProphet (ISI Seattle, WA, United States) incorporated in the Scaffold software package rel. 4.3.2 (Proteome Software, Portland, OR, United States). Proteins were identified by at least two peptides with peptide probability >90% reflecting protein probability of >99%.

Assay for *M. pneumoniae* mutants. For the isolation of *M. pneumoniae* mutants, we used an ordered collection of strains carrying insertions of transposon Tn*4001* (Halbedel *et al.*, 2006). The presence of the desired mutant was assayed by a PCR screen using one primer that hybridizes to the transposon (directed outward), and a second primer specific for the gene of interest (see Supplementary Table S2.1).

RESULTS

***M. pneumoniae* proteins potentially involved in c-di-AMP metabolism.** All *Firmicutes* studied so far produce c-di-AMP, and in most of them, this second messenger is essential for the growth of these bacteria (Commichau *et al.*, 2015). However, the presence of this signaling nucleotide has never been analyzed in representatives of the Mollicutes. To address this question for *M. pneumoniae*, we cultivated cells, extracted nucleotides, and analyzed these extracts for the presence of c-di-AMP. The total amount of c-di-AMP (nM) extracted from the pellet was divided by the total cell volume (mg) to yield the c-di-AMP concentration per mg cells. In three independent biological experiments (with three technical replicates each), we determined concentrations of 489 ± 107 nM, 958 ± 153 nM, and 859 ± 81 nM. Such differences among biological replicates are not unusual when assaying c-di-AMP concentrations (Gundlach *et al.*, 2015b). Importantly, our results demonstrate that *M. pneumoniae* does possess c-di-AMP and imply the existence of enzymes that synthesize and degrade this second messenger.

To identify candidate genes involved in *M. pneumoniae* c-di-AMP metabolism, we analyzed the genome for genes encoding proteins possessing a c-di-AMP synthesizing DAC domain as well as for proteins containing c-di-AMP degrading DHH-DHHA1 and HD domains. A single protein containing a DAC domain was found. The DAC domain of this protein, MPN244, is most similar to the domain of the *B. subtilis* sporulation-specific cyclase CdaS. However, the N-terminal domain of this protein is not similar to any domains found in other characterized diadenylate cyclases. According to the UniProt database, the amino acids 6 to 26 form a transmembrane helix. Thus, if MPN244 is endowed with diadenylate cyclase activity, this protein would represent a novel class of diadenylate cyclases. A comparison of the domain arrangement of the different classes of diadenylate cyclases is shown in Figure 2.1A.

An analysis of potential c-di-AMP degrading phosphodiesterases in *M. pneumoniae* failed to identify a protein containing a HD domain similar to that of the *B. subtilis* phosphodiesterase PgpH (Huynh *et al.*, 2015). In contrast, the search for proteins containing a DHH–DHHA1 domain resulted in the identification of two proteins, MPN140 and MPN549. These proteins have been annotated as nano-RNase (NrnA) and probable single-stranded-DNA-specific exonuclease (RecJ) (Postic *et al.*, 2012; Wodke *et al.*, 2015), respectively. Two classes of c-di-AMP specific DHH-DHHA1 phosphodiesterases have been identified: a class of large membrane-bound proteins, as exemplified by *B. subtilis* GdpP. This protein contains an N-terminal transmembrane domain, a PAS domain, and a degenerate GGDEF domain possibly involved in c-di-GMP sensing in addition to the DHH-DHHA1 domain. In contrast, the second class, represented by Pde2 of *Streptococcus pneumoniae*, consists only of the DHH-DHHA1 domain (Bai *et al.*, 2013). Both potential

phosphodiesterases of *M. pneumoniae* are similar to Pde2 rather than to GdpP (see Figure 2.1B for domain organization).

CdaM (MPN244) is a diadenylate cyclase. In order to test whether MPN244 does indeed exhibit diadenylate cyclase activity, we took advantage of the inability of *E. coli* to produce c-di-AMP (Corrigan *et al.*, 2011). The *mpn244* gene was cloned into the expression vector pET3c, and the amounts of c-di-AMP produced in *E. coli* BL21(DE3) carrying the corresponding plasmid pGP2036, were compared to those of the same strain carrying the empty vector pET3c. As observed previously (Mehne *et al.*, 2013), no c-di-AMP was present in the strain with the empty vector. In contrast, the expression of MPN244 resulted in the detection of 47.3 ± 11.8 pmol of c-di-AMP/mg of protein. This result provides unequivocal evidence for the diadenylate cyclase activity of MPN244, and we renamed the protein accordingly CdaM (c-di-AMP synthase of *Mycoplasma*), and the gene *cdaM*.

As c-di-AMP is essential in many Gram-positive bacteria, we wondered whether this is also the case in *M. pneumoniae*. To address this question, we attempted the isolation of a *cdaM* mutant from our transposon mutant library. This library contains 2 976 independent individual transposon mutants, and the probability to find mutants for any non-essential gene is as high as 99.999% (Halbedel *et al.*, 2006). In agreement with previous results (Lluch-Senar *et al.*, 2015), no mutant could be isolated suggesting that the *cdaM* gene and thus c-di-AMP is essential in *M. pneumoniae*.

Phosphodiesterases involved in the degradation of c-di-AMP. As mentioned above, two potential c-di-AMP degrading phosphodiesterases, MPN140 and MPN549, are encoded in the genome of *M. pneumoniae*. To assess their activity, we expressed and purified these enzymes carrying a C-terminal Strep-tag. Initially, we determined the phosphatase and phosphodiesterase activities of both enzymes.

Table 2.1 | Michaelis-Menten-kinetics for phosphodiesterase activity on *bis*-pNPP.

Protein	K_m [mM]		V_{max} [µmol min^{-1} mmol^{-1}]	
	+ $MnCl_2$	+ $MgCl_2$	+ $MnCl_2$	+ $MgCl_2$
MPN140	1.60	2.90	0.22	0.19
MPN549	0.60	0.55	0.04	0.04
GdpP	1.45	1.64	0.02	0.02

To determine phosphatase activities, we used pNPP, a synthetic phosphatase substrate, and the *M. pneumoniae* protein phosphatase PrpC (Halbedel *et al.*, 2006; Schmidl *et al.*, 2010a) as a positive control. While PrpC exhibited a strong phosphatase activity, only negligible activity was detected for MPN140 and MPN549 (data not shown).

Phosphodiesterase activity was assayed against bis-pNPP as the substrate, and the *B. subtilis* phosphodiesterase GdpP served as the control. As shown in Table 2.1, all three enzymes exhibited phosphodiesterase activity against this non-specific substrate.

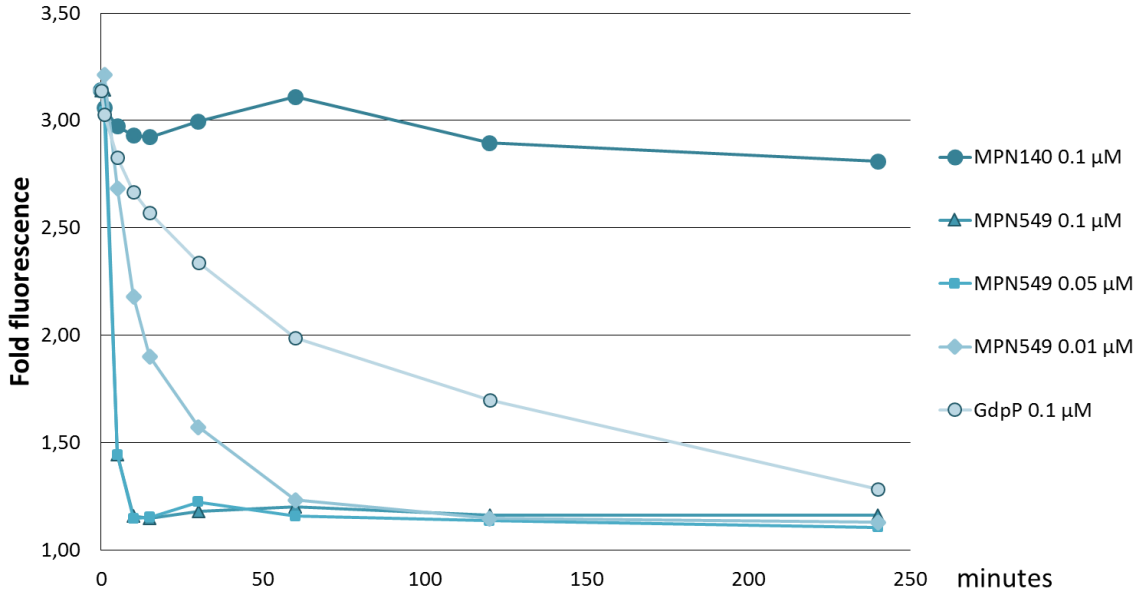

Figure 2.2 | Specific activity of phosphodiesterases toward c-di-AMP. Phosphodiesterases (MPN140, MPN549, GdpP: 100 nM, in addition 50 and 10 nM for MPN549) were added to 100 µM c-di-AMP in 100 mM Tris-HCl pH8.3, 10 mM NaCl, 0.1 mM MnCl2 at 37°C. Reactions were stopped at 0, 5, 10, 15, 30, 60, 120, and 240 min. Upon addition of KBr and coralyne and excitation at 420 nm, fluorescence at 475 nm was measured. The ratio of c-di-AMP-mediated emission vs. a standard without c-di-AMP is shown. Results from a typical experiment are shown. The replicates showed similar results.

Thus, MPN140 and MPN549 are specifically active against phosphodiesters. In order to explore the activity of these enzymes against c-di-AMP, we determined c-di-AMP degradation using binding of c-di-AMP to the fluorescence dye coralyne as an assay. As shown in Figure 2.2, *B. subtilis* GdpP was capable of degrading the nucleotide. For MPN140, no activity against c-di-AMP was observed. In contrast, MPN549 exhibited high activity against c-di-AMP. As little as 10% of the enzyme amount used in the assay with GdpP degraded the nucleotide more rapidly than GdpP. To conclude, our results clearly demonstrate that MPN140 is a phosphodiesterase, but with a substrate distinct from c-di-AMP whereas MPN549 is the c-di-AMP-degrading phosphodiesterase in *M. pneumoniae*. Thus, MPN549 was renamed PdeM (phosphodiesterase of *M. pneumoniae*), and the gene accordingly *pdeM*.

In *B. subtilis*, c-di-AMP is not only essential but also toxic in the absence of the phosphodiesterases that degrade the nucleotide (Gundlach *et al.*, 2015b). Thus, we tested whether a *pdeM* mutant could be isolated from our transposon mutant collection. As

observed in a global transposon mutant study (Lluch-Senar *et al.*, 2015), no mutant could be isolated indicating that the *pdeM* gene is essential in *M. pneumoniae*.

Identification of the c-di-AMP target protein KtrC (MPN461). Our results indicate that c-di-AMP is synthesized in *M. pneumoniae*, and that this second messenger is essential for the growth of the bacteria. This suggests an important physiological function of c-di-AMP. To identify this function, we decided to isolate c-di-AMP-binding proteins, which are excellent candidates for c-di-AMP-mediated regulation. For this purpose, we used c-di-AMP immobilized via a linker to agarose and incubated it with a protein extract of *M. pneumoniae*. As a control, we used agarose containing ethanolamine immobilized via the same linker. After extensive washing (see Materials and Methods), c-di-AMP-binding proteins were eluted with free c-di-AMP. The proteins were analyzed by SDS-PAGE (see Figure 2.3), and a band exhibiting increased intensity in the binding assay identified by mass spectrometry as MPN461.

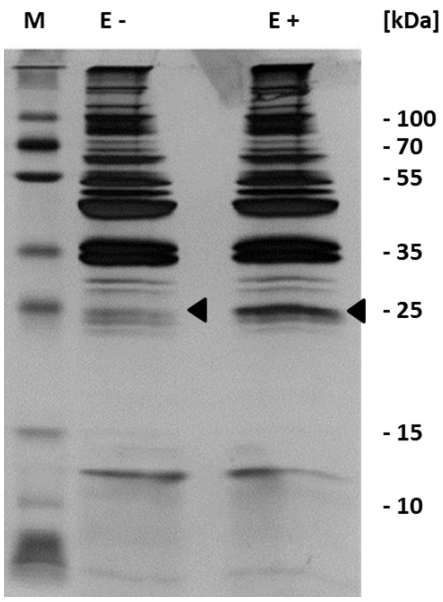

◄ Figure 2.3 | Identification of c-di-AMP binding proteins. Detection of in vitro c-di-AMP binding was performed with c-di-AMP immobilized to an agarose matrix. This was incubated with cell extract from *M. pneumoniae*. The c-di-AMP bound proteins were eluted with free c-di-AMP and analyzed by SDS-polyacrylamide gel electrophoresis and visualized by silver staining. Proteins were identified by mass spectrometry. Arrows show mass spectrometry analyzed bands. E, elution fraction; +, agarose coupled with c-di-AMP; -, agarose coupled with ethanolamine.

This protein is similar to the *B. subtilis* low affinity potassium transporter regulatory subunit KtrC (Holtmann *et al.*, 2003). The *mpn461* gene forms a gene cluster with the upstream gene *mpn460*, which encodes a protein most similar to the integral membrane subunit KtrD of the KtrC-KtrD potassium channel. An alignment of the c-di-AMP-binding region of *S aureus* (Kim *et al.*, 2015) with the relevant residues of *M. pneumoniae* and related proteins from other bacteria indicates that the amino acids interacting with c-di-AMP are

conserved in the *M. pneumoniae* protein (see Figure 2.4). Taken together, these results suggest that c-di-AMP controls potassium transport in *M. pneumoniae*.

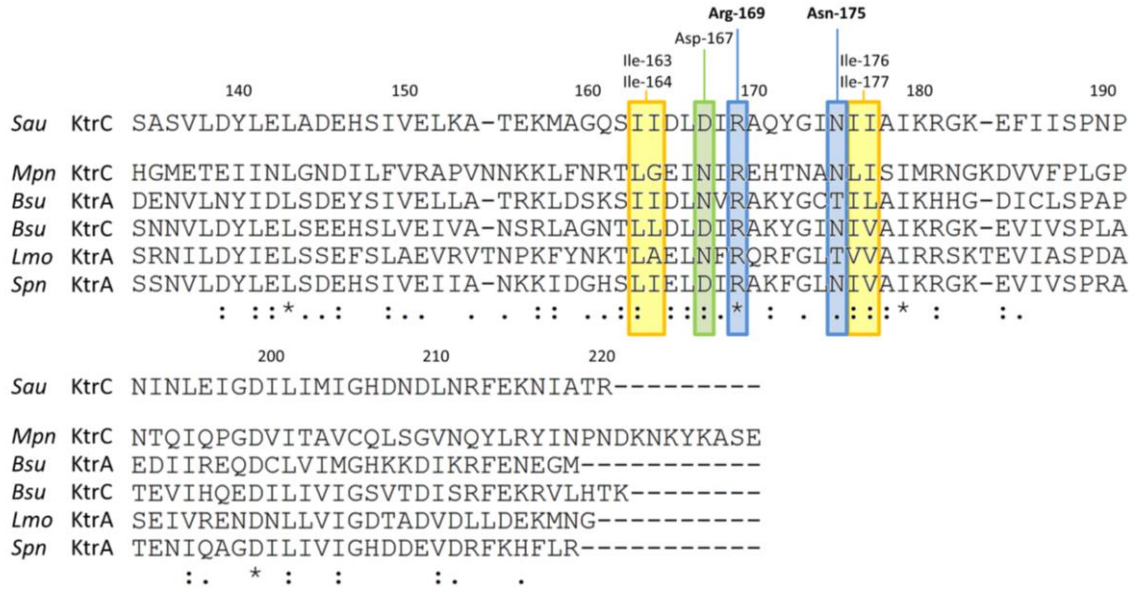

Figure 2.4 | Alignment of the c-di-AMP-binding regions in RCK_C domains of potassium uptake proteins. The C-terminal parts of different KtrC/ KtrA proteins were aligned to the experimentally identified c-di-AMP binding site of *Staphylococcus aureus* (Sau) KtrC (Kim *et al.*, 2015). Residues responsible for c-di-AMP binding are highlighted: Arg-169 and Asn-175 (blue), which directly interact with c-di-AMP are conserved in *M. pneumoniae* KtrC; Asp-167 (green), which also forms a direct hydrogen bond with c-di-AMP is replaced by Asn which is also known to form hydrogen bonds, Ile-163/Ile-164 and Ile-176/Ile-177 (in yellow), which form the hydrophobic patch are well conserved in bacteria. *Mpn Mycoplasma pneumoniae*, *Bsu Bacillus subtilis*, *Spn Streptococcus pneumoniae*, *Lmo Listeria monocytogenes*. * identical amino acids, **:** similar amino acids.

DISCUSSION

In this work, we provide the first analysis of c-di-AMP signaling in the genome-reduced bacterium *M. pneumoniae*. We have identified the diadenylate cyclase CdaM as well as the c-di-AMP degrading phosphodiesterase PdeM. Moreover, we have demonstrated binding of c-di-AMP to KtrC, the regulatory subunit of a potassium transporter.

So far, three distinct classes of diadenylate cyclases have been characterized. The *M. pneumoniae* CdaM protein is the prototype of a fourth class that is specific to the genome-reduced members of the genus *Mycoplasma*. The domains present in the diadenylate cyclases in addition to the enzymatically active DAC domain are thought to be required for signal recognition by the cyclases and thereby to control the activity of the enzymes (Mehne *et al.*, 2014; Commichau *et al.*, 2015). Thus, it is tempting to speculate that the single transmembrane domain associated with CdaM reflects the specific lifestyle of the highly host-dependent and host-adapted *Mycoplasma* cells. Taking into account the

highly peculiar physiology and cell biology of the *Mycoplasmas*, it seems likely that the organization of CdaM is an adaptation to this particular biology.

The phosphodiesterase PdeM consists of a single DHH-DHHA1 domain. This type of c-di-AMP-specific phosphodiesterases has been found in other pathogenic bacteria, including *S. pneumoniae*, *Borrelia burgdorferi*, and *Mycobacterium tuberculosis*. While *S. pneumoniae* encodes both a classical phosphodiesterase (similar to GdpP, see Figure 2.1), the latter bacteria possess only the one-domain proteins, as observed in *M. pneumoniae* (Bai *et al.*, 2013; Manikandan *et al.*, 2014; Ye *et al.*, 2014). In addition to PdeM, *M. pneumoniae* possesses a very similar protein, NrnA (MPN140). The two proteins share 29% identity, which is indicative of functional specialization. Indeed, while both proteins exhibit phosphodiesterase activity toward a generic substrate, only PdeM is able to degrade c-di-AMP. This is in good agreement with the reported activity of NrnA toward short oligoribonucleotides (Postic *et al.*, 2012). Based on the results obtained with other cytoplasmic c-di-AMP specific phosphodiesterases (Bai *et al.*, 2013; Manikandan *et al.*, 2014; Ye *et al.*, 2014), it is tempting to speculate that PdeM may degrade c-di-AMP to pApA, which is in turn degraded to AMP by the activity of NrnA. It is interesting to note that the presence of closely related proteins of which only one has the suspected biochemical activity is not unprecedented in *M. pneumoniae*: of the two potential glycerophosphate phosphodiesterases, only one protein (GlpQ) has the corresponding enzymatic activity, whereas no function has so far been identified for the second protein (MPN566) (Schmidl *et al.*, 2011).

While the reason for c-di-AMP essentiality has long been enigmatic, recent research has suggested that the control of potassium homeostasis is the essential function (Gundlach *et al.*, 2017). Three lines of evidence support this idea: (i) c-di-AMP controls potassium uptake in *B. subtilis*, *L. monocytogenes*, and *S. aureus* both at the level of transporter activity and transporter expression, and it does so by binding very different classes of proteins and even RNA. (ii) In *B. subtilis*, c-di-AMP becomes non-essential if the bacteria are cultivated at low potassium concentrations. (iii) The control of potassium uptake is the common denominator of c-di-AMP signaling in all organisms that have been studied in this respect. The demonstration that even in the genome-reduced bacterium *M. pneumoniae* c-di-AMP binds to the regulatory subunit of the KtrCD potassium transporter is in strong support for a general involvement of c-di-AMP in the control of potassium homeostasis. Moreover, the essentiality of both the diadenylate cyclase CdaM and the phosphodiesterase PdeM indicates that essentiality is not derived from the control of a single protein, but that it is rather related to a homeostatic process that is essential for the cell but that needs to be limited. This reflects the nature of potassium which is essential for

any living cell but which becomes toxic if it accumulates in the cell to non-physiological concentrations (Nissen *et al.*, 2000; Gundlach *et al.*, 2017).

The essentiality of c-di-AMP synthesizing and degrading enzymes and the absence of c-di-AMP and c-di-AMP metabolizing enzymes from human cells makes these proteins excellent candidates for the development of novel antimicrobial drugs. Our work clearly suggests an important function for cyclic di-AMP in *M. pneumoniae*, but further work will be required to understand the molecular mechanisms by which the activity of CdaM is controlled as well as the regulation of KtrC activity by c-di-AMP.

SUPPLEMENTAL MATERIAL

Table S2.1 | Oligonucleotides used in the study of chapter 2.

Acknowledgments. We are grateful to Julia Busse and Annette Garbe for excellent technical assistance and to Tobias Krammer for the help with the characterization of phosphodiesterases. We wish to thank Hinnerk Eilers and Arne Schmeisky for having initiated this project. Achim Dickmanns and Katrin Gunka are acknowledged for helpful discussions.

Funding. This research received funding from the Federal Ministry of Education and Research MiniCell network (Grant 031L0012). Katrin Treffon was supported by a Dorothea-Schlözer stipend from the Georg-August-University of Göttingen.

CHAPTER 3 | New tools for genetic manipulation of *Mycoplasmas*

Results described in chapter 3 were published in *Microbiology*:

Development of a Replicating Plasmid Based on the Native *oriC* in *Mycoplasma pneumoniae*

Cedric Blötz[1], Carole Lartigue[2,3], Yanina Valverde Timana[2,3], Estelle Ruiz[2,3], Bernhard Paetzold[4,†], Julia Busse[1], Jörg Stülke[1]

[1]Department of General Microbiology, University of Göttingen, Germany
[2]INRA, Villenave d'Ornon, France
[3]University of Bordeaux, Villenave d'Ornon, France
[4] Centre for Genomic Regulation (CRG), Barcelona, Spain
[†]Present address: S-Biomedic N.V., Beerse, Belgium

AUTHOR CONTRIBUTION

CB and CL designed the study. CB performed the experiments with MPN and MGE, including plasmid construction, transformation and verification. CB performed MPN Southern hybridization. CB determined the hydrogen peroxide concentration. CB performed stability tests of plasmids. CB analyzed *in silico oriC* regions. YVT and ER performed experiments in other *Mycoplasma* species. JB performed qRT-PCR analysis and cultivated strains. BP provided ideas and corrected the manuscript. CB and JS wrote the manuscript.

ABSRTACT

Bacteria of the genus *Mycoplasma* have recently attracted considerable interest as model organisms in synthetic and systems biology. In particular *Mycoplasma pneumoniae* is one of the most intensively studied organisms in the field of systems biology. However, the genetic manipulation of these bacteria is often difficult due to the lack of efficient genetic systems and some intrinsic peculiarities such as an aberrant genetic code. One major disadvantage in the work with *M. pneumoniae* is the lack of replicating plasmids that can be used for the complementation of mutants and the expression of proteins. In this study, we have analyzed the genomic region around the gene encoding the replication initiation protein, DnaA, and detected putative binding sites for DnaA (DnaA boxes) that are, however, less conserved than in other bacteria. The construction of several plasmids encompassing this region allowed the selection of plasmid pGP2756 that is stably inherited and that can be used for genetic experiments as shown by the complementation assays with the *glpQ* gene encoding the glycerophosphoryl diester phosphodiesterase. Plasmid-borne complementation of the *glpQ* mutant restored the formation of hydrogen peroxide if the bacteria were cultivated in the presence of glycerol phosphocholine. Interestingly, the replicating plasmid can also be used in the close relative, *Mycoplasma genitalium* but not in more distantly related members of the genus Mycoplasma. Thus, plasmid pGP2756 is a valuable tool for the genetic analysis of *M. pneumoniae* and *M. genitalium*.

INTRODUCTION

Bacteria of the genus *Mycoplasma* have recently come under the focus of scientific interest and investigation. This interest results in particular from the extreme genome reduction of these bacteria which makes some of their representatives among organisms with the smallest genome capable of independent life (Waites and Talkington, 2004). In particular, *Mycoplasma* species such as *M. pneumoniae*, *M. genitalium*, *M. capricolum* subsp. *capricolum* and *M. mycoides* subsp. *capri* have been central to the development of the scientific disciplines of systems and synthetic biology, and some of the major breakthroughs in these fields have been achieved with these bacteria. *M. pneumoniae*, with its small 816 kb genome, is one of the most studied organisms in systems biology. A large number of omics-driven studies have been conducted in this organism, including genomics, epigenomics, global transcription, protein-protein interactions, post-translational modifications, DNA modification, identification of essential genomic regions, and metabolomics (Güell *et al.*, 2009; Kühner *et al.*, 2009; Lluch-Senar *et al.*, 2013; Lluch-Senar *et al.*, 2015; Maier *et al.*, 2011; van Noort *et al.*, 2012; Schmidl *et al.*, 2010b; Yus *et al.*, 2009; Yus *et al.*, 2012; Yus *et al.*, 2017). The generated datasets are currently being used

to build a *M. pneumoniae* whole-cell model accounting for the integrated function of every gene in the cell (Goldberg *et al.*, 2017). In contrast, *M. mycoides* and *M. capricolum* are model organisms in the field of synthetic biology. These bacteria were used to create the first bacterial cells with synthetic (minimal) genomes. This represents a key step towards the creation of synthetic life and has left a mark in the nascent field of synthetic biology (Gibson *et al.*, 2010; Hutchison *et al.*, 2016; Lartigue *et al.*, 2009).

Aside from their relevance as minimal cells, *Mycoplasma* species are also important pathogens of both man and a wide range of animals. *M. pneumoniae*, the aetiological agent of primary atypical pneumonia, is a well-established pathogen of the respiratory tract in humans (Atkinson *et al.*, 2008; Smith, 2010; Watanabe *et al.*, 2014). *M. mycoides* and *M. capricolum* cause respiratory diseases in cattle and goats, which have a severe impact on the agricultural sector in developing countries (Houshaymi *et al.*, 1997). Despite the importance of *Mycoplasma* species in research and medicine, their investigation suffers from difficulty in cultivating them in vitro, the use of a modified genetic code in most *Mycoplasma* species (Hames *et al.*, 2005) and, more importantly, the lack of efficient experimental tools for their genetic manipulation, at least for some species of interest such as *M. pneumoniae* (Halbedel and Stülke, 2007). For this latter species, the only existing tools are transposons, which allow random mutagenesis. Targeted chromosomal knock-outs have previously been reported (Krishnakumar *et al.*, 2010), but the efficiency of the method is poor, and it is not applicable for large-scale functional genomics studies. As a consequence, large transposon libraries are required for the isolation of specific mutants (Halbedel *et al.*, 2006). In recent decades, replicating plasmids, also known as ori (origin of replication) plasmids, have been constructed for several *Mycoplasma* species including *M. pulmonis*, *M. capricolum*, *M. bovis*, *M. agalactiae*, *M. synoviae*, *M. hyorhinis*, *M. hyopneumoniae*, *M. gallisepticum*, *M. imitans* and *Mesoplasma florum* (Cordova *et al.*, 2002; Ishag *et al.*, 2017; Janis *et al.*, 2005; Lartigue *et al.*, 2003; Lee *et al.*, 2008; Maglennon *et al.*, 2013; Matteau *et al.*, 2017; Shahid *et al.*, 2014; Sharma *et al.*, 2015). *OriC* plasmids proved useful genetic tools for gene inactivation and also for gene complementation studies and the expression of heterologous proteins. Surprisingly, however, no *oriC* plasmids have been described for the workhorse of systems biology, *M. pneumoniae*. The development of *oriC* plasmids is generally straightforward, requiring the insertion of one or the other intergenic regions surrounding the *dnaA* gene (both, in certain cases), with or without the *dnaA* gene, into an *Escherichia coli* shuttle vector containing an antibiotic marker for *Mycoplasma* species. In Gram-positive bacteria, as well as in *Mycoplasmas*, which have evolved from Gram-positive bacteria, the formation of the DNA replication initiation complex preceding the initiation of the chromosomal replication relies on the binding of the DnaA

proteins to 9-mers sequences known as DnaA boxes, which are found in the intergenic regions flanking the *dnaA* gene (*E. coli* consensus *dnaA* boxes TTATCCACA) (Speck *et al.*, 1997). This was confirmed for all the aforementioned *Mycoplasma* species (Cordova *et al.*, 2002; Ishag *et al.*, 2017; Janis *et al.*, 2005; Lartigue *et al.*, 2003; Maglennon *et al.*, 2013; Shahid *et al.*, 2014; Sharma *et al.*, 2015) except *M. gallisepticum*, for which the DnaA boxes were not found in the short intergenic sequences flanking the *dnaA* gene, but a few kilobases away, in the 1.8 kb intergenic region localized between the *soj* and *dnaN* genes (Lee *et al.*, 2008).

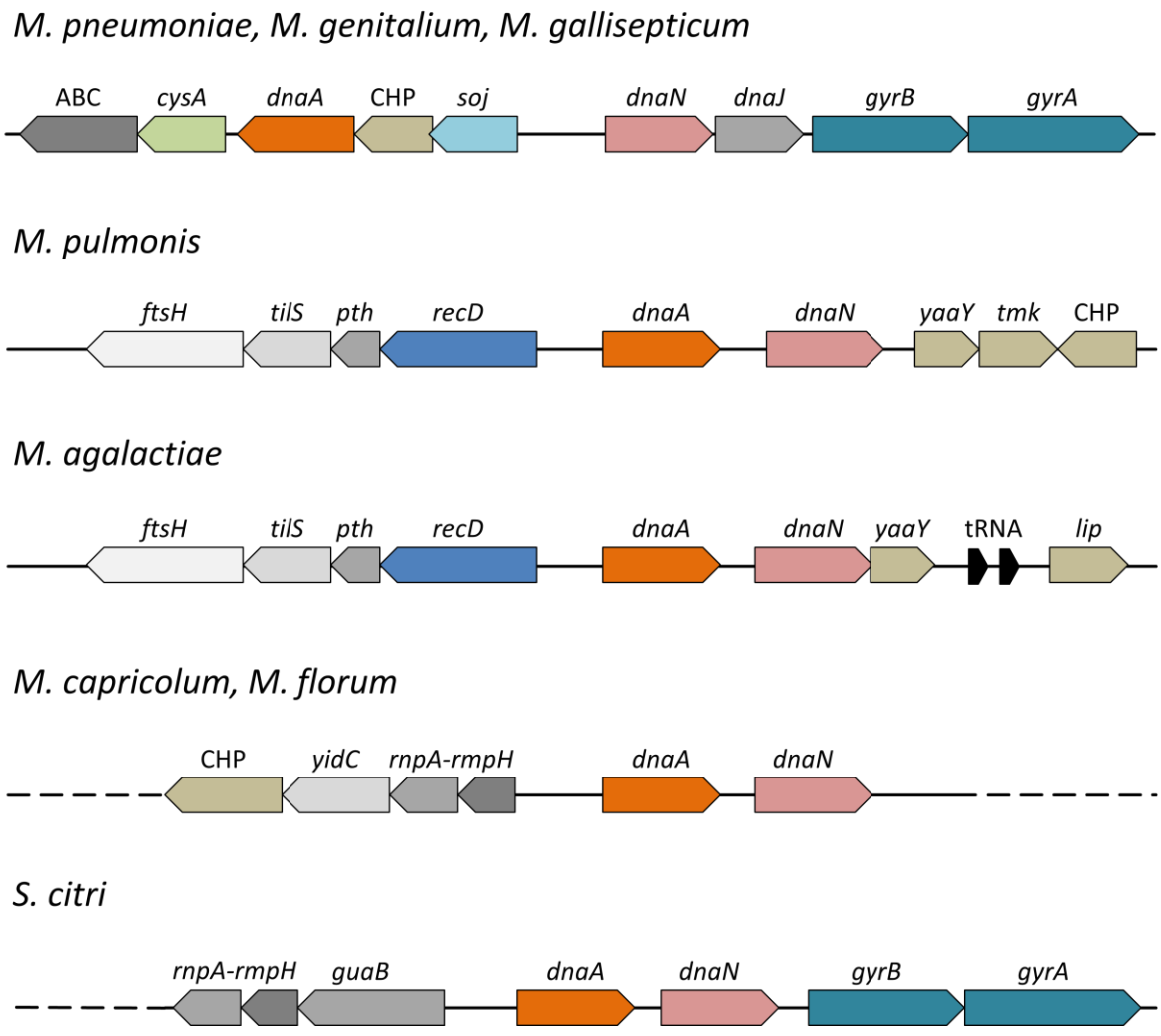

Figure 3.1 | Genetic organization of the *oriC* region in different Mollicutes. The gene orientation is indicated by arrows. Genes are drawn to scale. ABC, ABC transporter permease; CHP, conserved hypothetical protein.

Interestingly, *M. pneumoniae* and *M. gallisepticum* belongs to the same phylogenetic group and genome comparison analysis showed that the organization of their *oriC* regions was very similar (Fig. 3.1), suggesting that the *oriC* of the *M. pneumoniae* genome could be located in a similar position to that of *M. gallisepticum*. In this work, we addressed the lack

of replicating plasmids in *M. pneumoniae*. We created a replicative plasmid, which can serve as a novel tool for the genetic analysis of this human pathogen. Our studies indicate that the *oriC* in *M. pneumoniae* is organized differently as compared with other model bacteria and allowed us to construct a *M. pneumoniae* - *E. coli* shuttle vector that can be used for both the expression of proteins and complementation analyses. We provide evidence for the functionality of the plasmid pGP2756 by complementing a *M. pneumoniae glpQ* mutant lacking the phosphodiesterase responsible for phospholipid utilization, the major carbon source of *M. pneumoniae* in its natural environment, the respiratory epithelium (Schmidl *et al.*, 2011).

MATERIALS AND METHODS

Bacterial strains, transformation and growth conditions. The *M. pneumoniae* strains used in this study were M129 (ATCC 29342) and its isogenic mutant derivatives GPM81 (*glpQ* :: mini-Tn, Gm^R) (Schmidl *et al.*, 2011), GPM118 (pGP2496, Tet^R), GPM119 (*glpQ* :: mini-Tn, pGP2496, Gm^R, Tet^R), GPM120 (M129, pGP2756, Tet^R) and GPM121 (*glpQ* :: mini-Tn, pGP2756, Gm^R, Tet^R). These are listed in Table 3.1. *M. pneumoniae* was grown at 37°C in 175 cm^2 tissue culture flasks containing 100 ml of modified Hayflick medium, as described previously (Halbedel *et al.*, 2004). Carbon sources were added to a final concentration of 1% (w/v). M. genitalium G37 was grown at 37°C in 175 cm^2 tissue culture flasks containing 100 ml of SP-4 medium (Tully *et al.*, 1983). Surface-attached mycoplasmas were washed four times with phosphate-buffered saline (pH7.2). Strains harboring transposon insertions or plasmids were cultivated in the presence of 80 mg ml^{-1} gentamicin and/or 2.5 mg ml^{-1} tetracycline. Plasmids were introduced into *M. pneumoniae* and *M. genitalium* by electroporation using a Gene Pulser (Bio-Rad, Hercules, CA) and the transformants were selected by incubation at 37°C on agar plates containing appropriate antibiotics (Halbedel *et al.*, 2004; Pich *et al.*, 2006). *Mycoplasma capricolum* subsp. *capricolum* (strain California Kid) was grown in SP5-rich medium (Labroussaa *et al.*, 2016) and transformed using the polyethylene glycol (PEG) method with 5% (Lartigue *et al.*, 2009; King and Dybvig, 1991; King and Dybvig, 1994). *Mycoplasma gallisepticum* (strain S6) was grown in Hayflick medium and transformed in the presence of 40% PEG (Cao *et al.*, 1994). For molecular cloning, *E. coli* strain XL1-Blue (Stratagene, San Diego) and DH10B (Grant *et al.*, 1990) were grown at 37°C in lysogeny broth (LB) medium containing the appropriate antibiotics (100 mg ml^{-1} ampicillin, 5 mg ml^{-1} tetracycline).

Plasmid construction. The sequences of the oligonucleotides used in this study are listed in Table S3.1, while the plasmids are listed in Table S3.2. The different *oriC* fragments were amplified from chromosomal DNA of *M. pneumoniae* with restriction overhangs (EcoRI and

XbaI). These were ligated to the pET3c plasmid backbone (XbaI and BamHI) and the *tetM* resistance gene derived from plasmid pMTntetM438 (Pich *et al.*, 2006) (EcoRI and BamHI) in a three-fragment ligation.

Table 3.1 | *Mycoplasma* strains used in the study of chapter 3.

Name	Description	Construction	Reference
Mycoplasma pneumoniae M129			
GPM81	*glpQ*::Tn	pMT85 → M129	Schmidl, 2010
GPM93	chromosomal *tetM*	pMTnTetM438 → GPM81	Schmidl *et al.*, 2011
GPM118	Expression of GlpQ	pGP2496 → M129	This study
GPM119	Expression of GlpQ	pGP2496 → GPM81	This study
GPM120	Empty vector control	pGP2756 → M129	This study
GPM121	Empty vector control	pGP2756 → GPM81	This study
GPM123	*oriC* region *soj-oriC*	pGP2732 → M129	This study
GPM124	*oriC* region *dnaN-oriC*	pGP2733 → M129	This study
Mycoplasma capricolum subsp. *capricolum* California Kid			
Mycoplasma genitalium G37			
Mycoplasma gallisepticum, strain S6			

We constructed a full-length *oriC* plasmid (pGP2756) using the oligonucleotides CB55 and CB56. Additionally, we created two shorter versions splitting the *oriC* region, one with a part of the *oriC* region close to the *soj* gene (pGP2732) and a second one with the *oriC* region close to the *dnaN* gene (pGP2733) using the oligonucleotides CB55/CB103 and CB56/104, respectively. As a control, the resistance cassette was cloned between the EcoRI and BamHI sites of the plasmid backbone, resulting in plasmid pGP2777. For complementation studies, the first two genes of the *glpQ* operon were amplified (*cglT* and *glpQ*) with their native promoter (P_{nat}) and cloned between the AatII and EcoRV sites of the plasmid pGP2756, resulting in pGP2496. To construct plasmid pMPNOriC1, the *oriC* fragment, including the intergenic region (747 nucleotides) and the first 337 nucleotides of the *dnaN* gene, was amplified from *M. pneumoniae* M129 genomic DNA using the primers oriMpneu-F1 and oriMpneu-R1 carrying the restriction sites for BamHI (Table S3.1) and ligated into the BamHI site of plasmid pSRT2, which contained a tetracycline resistance marker (Lartigue *et al.*, 2003). To construct plasmid pMPNOriC2, the *oriC* fragment, including the region between *dnaA* and the first 337 nucleotides of the *dnaN* gene, was amplified using primers oriMpneu-F3 and oriMpneu-R2 and ligated into the EcoRI site of pSRT2.

DNA isolation. Preparation of chromosomal and plasmid DNA from *M. pneumoniae* was performed with pellets from 100 ml cultures. A modified phenol:chloroform extraction was used. Briefly, pellets were resuspended in 400 µl TES buffer (10 mM Tris-HCl pH8.0, 1 mM EDTA, 0.5 M NaCl) and 40 µl lysozyme (20 mg/ml). After incubation for 60 min at 37°C and 800 rpm, the cells were disrupted by adding 80 µl SDS (10%). The nucleic acids were then purified by multiple rounds of phenol:chloroform:iso-amylalcohol and chloroform extraction. The DNA was precipitated with pure ethanol. The pellet obtained after washing with 70% ethanol was dried at room temperature and dissolved in 100 µl sterile water.

Southern hybridization. A 5 µg sample of DNA was pre-incubated with RNase A (1 µl, 20 mg/ml), and digested with NcoI. DNA was separated by electrophoresis on 1% agarose gels, transferred onto a positively charged nylon membrane (Roche Diagnostics, Munich) (Sambrook *et al.*, 1989), and probed with Digoxigenin labeled riboprobes obtained by *in vitro* transcription with T7 RNA polymerase (Roche Diagnostics, Munich) using PCR-generated fragments as templates. Primer pair CB75/76 was used for the amplification of the *oriC* fragment (Table S3.1). The reverse primers contained a T7 RNA polymerase binding sequence. *In vitro* RNA labeling, hybridization and signal detection were carried out according to the manufacturer's instructions (DIG RNA labeling Kit and detection chemicals; Roche Diagnostics).

Determination of *in vivo* hydrogen peroxide production. The hydrogen peroxide production in *M. pneumoniae* was assayed using the MQuant™ peroxide test stripes (Merck, Darmstadt, Germany), as previously described (Hames *et al.*, 2009). Briefly, growing cells were resuspended in 1 ml assay buffer (67.6 mM HEPES (pH7.3), 140 mM NaCl, and 7 mM $MgCl_2$) to OD_{550} = 1, incubated for 1 h at 37°C, and glucose or glycerol phosphocholine (final concentration 100 µM) were added to one aliquot. An aliquot without any added carbon source served as the negative control. After incubation for 0, 1, and 2 hours the test stripes were dipped into the suspensions for 1 second and subsequently read.

Sequence analysis of putative *oriC* regions of *M. pneumoniae.* The origin of replication was searched, within the genome of *M. pneumoniae* (Himmelreich *et al.*, 1996) using Ori-Finder (Gao and Zhang, 2008). The DnaA box motif (TTWTCMACA; W = A or T, M = A or C) was searched allowing not more than two mismatches with respect to the *E. coli* DnaA box (TTATCCACA). Twelve regions in the chromosome include these sequences. Of these regions, that between the *dnaN* and *soj* genes seemed to be best candidate *oriC* location, because of its immediate proximity to the *dnaA* gene and the presence of putative DnaA boxes. The consensus of these sequences (Table 3.2) is shown in Fig. 3.2.

Table 3.2 | Putative DnaA binding boxes in *M. pneumoniae*.

Box number	Sequence	Start position upstream of *dnaA*	End position upstream of *dnaA*	Direction	Matching "perfect" *E. coli* consensus
Box 1*	TTATTAACA	1,529	1,537	+	7/9
Box 2	TTTTCCATT	1,705	1,713	-	6/9
Box 3*	TTCTCTATA	1,759	1,767	-	6/9
Box 4	TTATCTATA	1,877	1,885	+	7/9
Box 5	TTATTCAAA	1,985	1,997	+	7/9
Box 6	TTTTCTTCA	2,064	2,072	-	6/9
Box 7*	TTATATATA	2,141	2,149	+	6/9
Box 8*	TTATATATA	2,142	2,150	-	6/9
Box 9	TTATTAACA	2,216	2,224	+	7/9
Box 10*	TTATTAATA	2,402	2,410	+	6/9

*identified manually with ≥2 mismatches

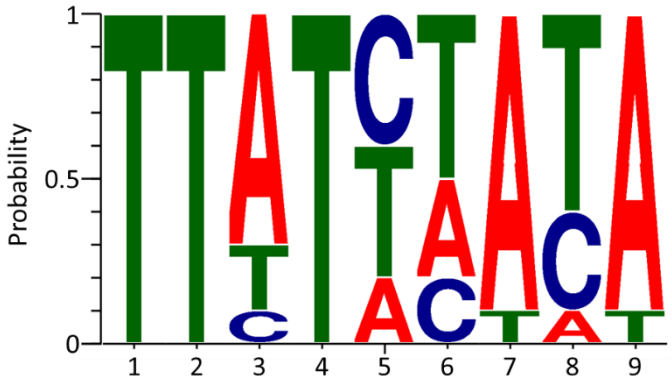

Figure 3.2 | Consensus sequence of the 10 putative DnaA binding boxes between the *soj* and *dnaN* genes. The consensus motif was prepared with the online tool MEME.

Quantification of *oriC* plasmids copy number. Isolated DNA from *M. pneumoniae* M129 containing the pGP2756 *oriC* plasmid at different passages (P2-P5), as well as from the wild type and the reference strain GPM93 (Tn-*tetM*, Schmidl *et al.*, 2011), was used in quantitative PCR (qPCR) assays to determine the copy number of the *tetM* gene. The analyses were performed using the RT oligonucleotides CB158/CB159 and CB160/CB161, targeting *tetM* and *rpoB* respectively (Table S3.1) in iQ SYBR Green Supermix (Bio-Rad). The relative abundance of the *tetM* gene was calculated using the Δ-ΔCt method (Livak and Schmittgen, 2001) normalized to the *rpoB* housekeeping gene. The qPCR amplifications were performed in triplicates using the following conditions: (i) 2 min at 95°C; (ii) 40 cycles of 5 sec at 95°C and 10 sec at 60°C. The copy number of the plasmid in *M. pneumoniae*

cells from different passages (P2 to P5) was determined by comparing the relative abundance of the *tetM* gene to the single copy of the reference strain GPM93.

Accession. A plasmid map and the nucleotide sequence of pGP2756 have been deposited in the *Myco*Wiki database (http://mycowiki.uni-goettingen.de/v1/wiki/view/pGP2756).

RESULTS

Identification of *oriC* in *M. pneumoniae* genome. In contrast to many other mollicutes, no replicative plasmid is yet available for *M. pneumoniae*. Moreover, the origin of replication in *M. pneumoniae* has not been determined experimentally. However, we assumed that the *oriC* was located in the immediate vicinity of the *dnaA* gene, as with most Gram-positive bacteria. In the intergenic region located between the *cysA* and *dnaA* genes (67 nucleotides, see Fig. 3.1), no putative DnaA binding boxes could be identified (Hilbert *et al.*, 1996). Compared to the *oriC* regions of other *Firmicutes* (Briggs *et al.*, 2012), the gene order and G+C content of the *dnaA* region are unique in the closely related species *M. pneumoniae*, *M. genitalium* and *M. gallisepticum* (Lee *et al.*, 2008), Hilbert *et al.*, 1996, Ogasawara and Yoshikawa, 1992; Himmelreich *et al.*, 1997) (see Fig. 3.1). We hypothesized that the *oriC* might be located in the intergenic region between the *soj* and *dnaN* genes, as has been shown for *M. gallisepticum* and *M. imitans* (Lee *et al.*, 2008), and thus, not directly coupled to the immediate surroundings of the *dnaA* gene as in most bacteria. In addition, several DnaA binding boxes were predicted in the 747-nucleotide intergenic region between the *soj* and *dnaN* genes (Hilbert *et al.*, 1996), although the experimental evidence was still missing. To test the earlier prediction, the whole-genome sequence of *M. pneumoniae* was analyzed using the online tool OriFinder (http://tubic.tju.edu.cn/Ori-Finder/) (Gao and Zhang, 2008) and screened for putative DnaA binding boxes. The tool screened for regions containing more than three putative binding boxes with the 'perfect' consensus of either *E. coli* (TTATCCACA) or the consensus sequence for mollicutes (TTWTCMACA; W=A or T, M=A or C) (Cordova *et al.*, 2002), allowing no more than two mismatches. The search returned nine and 12 potential binding regions by applying the *E. coli* or mollicute consensus sequences, respectively. These potential regions were scattered over the whole chromosome and contained three to seven putative binding boxes each. One region was identified as the intergenic region between the *soj* and *dnaN* genes, upstream of the *dnaA* gene. In this area, three more putative boxes could be identified manually. Overall 10 putative binding boxes for DnaA were identified (see Table 3.2, Fig. 3.2 for a consensus). Three of the identified boxes had high similarity

(2 mismatches) to the ‘perfect’ binding box of *E. coli*, while two potential boxes were more flexible at position 3 and another five boxes differed in more than three positions.

Functional analysis of the presumptive *M. pneumoniae oriC* region for plasmid replication. To develop functional *oriC*-based vectors for *M. pneumoniae* and potentially other *Mycoplasma* species, we constructed a series of six plasmids containing various fragments of the putative *M. pneumoniae oriC* region (see Fig. 3.3). The first plasmid (pMPNOriC2) contained a large ~4 kb fragment covering the entire region from the *dnaN* to *dnaA* genes (Fig. 3.3A). The rationale behind this construction was to take into account both the aforementioned analysis of putative DnaA boxes which suggested that the *soj-dnaN* intergenic region drives the initiation of replication in *M. pneumoniae*, and the fact that in Gram-positive bacteria, the *oriC* region is generally located in the vicinity of the *dnaA* gene (Wolański *et al.*, 2015). All other constructions contained the unique *soj-dnaN* intergenic region (complete or partial) identified as containing potential DnaA boxes. The main difference between the two plasmids was their backbone (pBluescript for pMPNOriC1 and pET3c for pGP2756). Plasmids pGP2756 (Fig. 3.3B) and pMPNOriC1 (Fig. 3.3A) contain the entire *soj-dnaN* intergenic region as well as short stretches of the flanking regions (extending 53 and 96 bp into *soj* and *dnaN*, respectively, for pGP2756 and extending 337 bp into *dnaN* for pMPNOriC1). The *soj-dnaN* intergenic region was then split up and two smaller plasmids were created. The plasmid pGP2732 contained the 351 bp upstream of the *soj* gene (extending 53 bp into the *soj* gene), whereas plasmid pGP2733 carried the 435 bp upstream of *dnaN* (extending 96 bp into the *dnaN* gene).

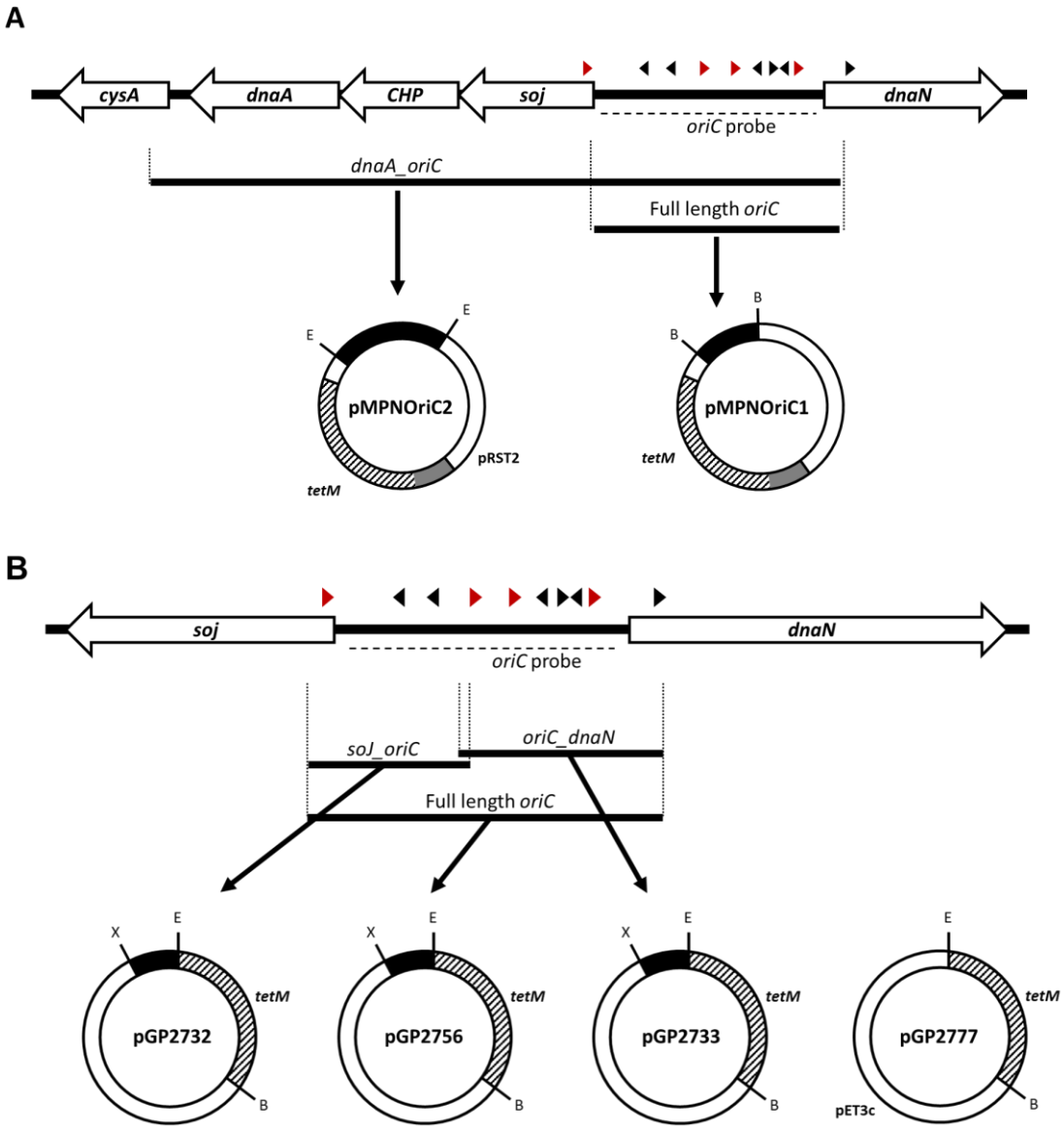

Figure 3.3 | Localization of putative DnaA binding boxes and the constructed plasmids. The putative DnaA binding boxes and their orientation are indicated by black (low similarity to the 'perfect' sequence) and red (high similarity to the 'perfect' sequence) triangles above the intergenic regions. The resistance marker tetM is indicated by grey dashed lines (plus promoter P_{MGE438} grey area). The inserted DNA fragments are denoted by filled black areas. Dashed lines indicate the target region of DNA probes for Southern blotting. (A) Construction of pMPNOriC1 and pMPNOriC2 using the vector pSRT2 for cloning. The plasmid pMPNOriC1 was obtained by ligating the inter- genic region (747 nucleotides) and 337 first nucleotides of the dnaN gene (full length *oriC*) with pSRT2. The plasmid pMPNOriC2 was ligated with the same DNA sequence as pMPNOriC1, but additionally the *dnaA* gene and the intergenic region close to the *cysA* gene (*dnaA-oriC*). (B) Construction of pGP2732, pGP2756, pGP2732 and pGP2777. The plasmids were obtained by ligating the fragments *soj-oriC*, *oriC-dnaA*, full-length *oriC* region into the indicated restriction sites of the vector pET3c. B, BamHI; E, EcoRI; X, XbaI.

In addition, a similar plasmid without the *oriC* region (pGP2777) was created as a control for transformation experiments (see Fig. 3.3B for an overview of these plasmids). *M. pneumoniae* cells were transformed with all plasmids and transformants were selected

for tetracycline resistance. Bacteria transformed with the plasmids pGP2777 (no *oriC* region), pGP2732 (*soj-oriC*) and pGP2733 (*oriC-dnaN*) failed to grow in liquid medium. In contrast, transformation with pGP2756 and pMPNOriC1, both carrying the *soj-dnaN* intergenic region, as well as with pMPNOriC2, covering the entire region (4 kb), yielded viable resistant transformants. The successful transformation of several clones was confirmed by PCR for all three plasmids (data not shown) and Southern blot hybridization for pGP2756 (see Fig. 3.4).

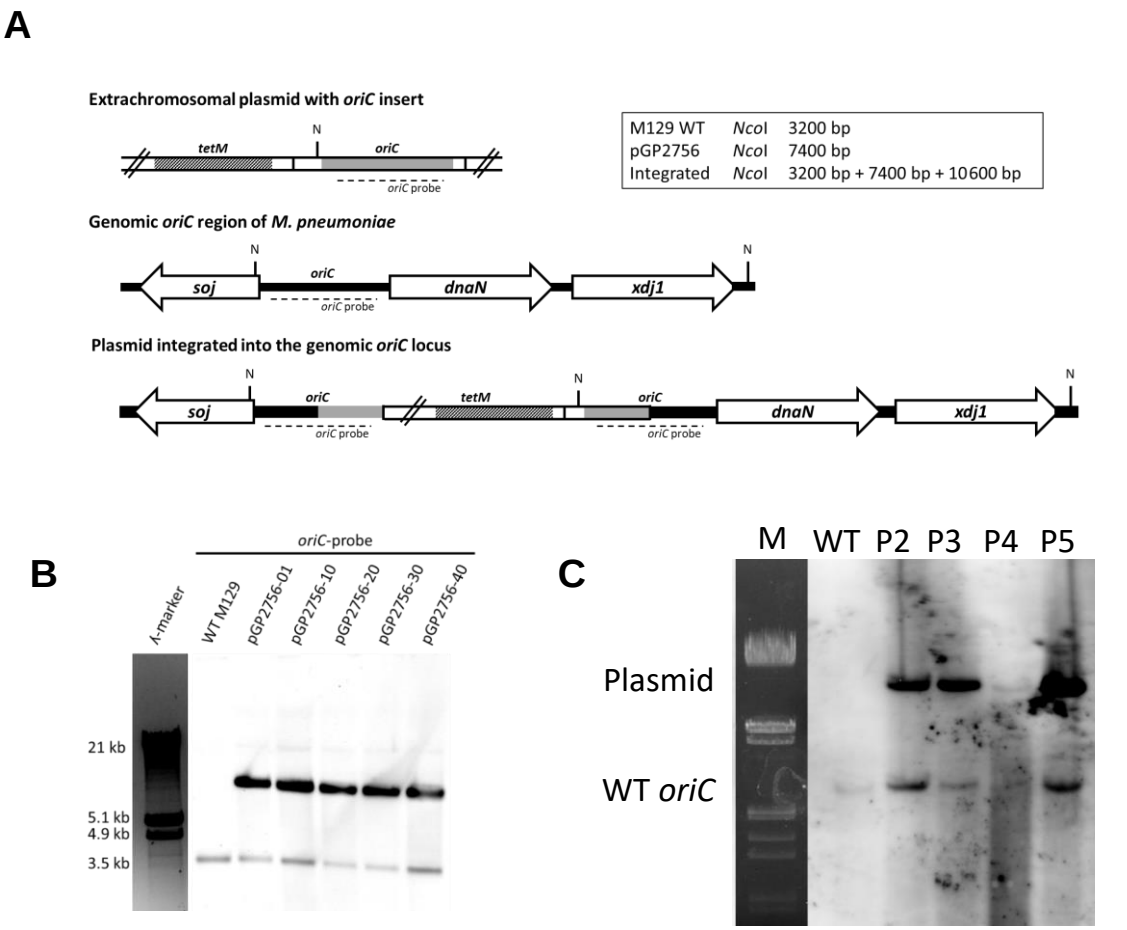

Figure 3.4 | Stability of the plasmid pGP2756 in *M. pneumoniae*. (A) Schematic representation of the expected digestion pattern of the free plasmid, the native genomic area (M129 WT) and the possible genomic area after plasmid integration. The sizes of NcoI (N) DNA fragments detected by an *oriC* probe (dashed line) are noted in the box. (B, C) Southern blot analysis of plasmid and *M. pneumoniae* DNA. The isolated DNA (5 µg) was digested with NcoI prior to electrophoresis. A probe detecting *M. pneumoniae oriC* was used. Lambda-marker (EcoRI/HindIII) was used as size standard detected under UV light. (B) Southern blot of total DNA of a plasmid-free strain (M129) compared to DNA from five *M. pneumoniae* clones transformed with pGP2756 (GPM120). (C) Southern blot of wild type DNA compared to DNA from *M. pneumoniae* transformed with pGP2756 after 2 (P2), 3 (P3), 4 (P4) or 5 (P5) passages in liquid medium.

At this stage, we decided to select pGP2756 for further characterization. We discarded pMPNOriC2 from the study because our goal was to precisely localize the *oriC* region in the

M. pneumoniae genome, and because pMPNOriC1 carries an *oriC* fragment very smilar to that present in pGP2756. All DNA samples were digested with NcoI and separated by gel electrophoresis, blotted and hybridized with an appropriate *oriC*-specific riboprobe. As a control, we isolated chromosomal DNA from wild-type cells. After digestion with NcoI we expected a band of 3.2 kb for chromosomal *oriC*, a band at 7.4 kb for extrachromosomal free plasmid and an additional band at 10.6 kb if the plasmid had integrated into the chromosome (Fig. 3.4A, B). The presence of both the *tetM* resistance gene (detected by PCR) and the *oriC* locus (detected by Southern blot) was verified for all clones tested. The probe detected a single band at 3.2 kb in the untransformed wildtype strain and both a 3.2 and a 7.4 kb band in the transformants (Fig. 3.4A, B). To investigate the possible integration of the plasmid into the native *oriC* locus we performed PCR analysis. No PCR products resulting from possible integration could be detected after passaging the bacteria two times, indicating extra-chromosomal establishment of the plasmid (see Fig. S3.1).

Stability and copy number of the replicative plasmid. The stability of plasmid pGP2756 was investigated by Southern blot hybridization after repeated subcultivation of clones harboring the replicative plasmid (passages P2–P5). The DNA was isolated and analyzed as described above. Southern blot analysis revealed that all clones investigated (P2–P5) still harbored the free plasmid pGP2756 after at least five rounds of cultivation (see Fig. 3.4C). To detect the copy number of the replicative plasmid in the cells, we performed quantitative real-time PCR on the *tetM* gene with DNA of plasmid carrying cells and the reference strain GPM93 that harbors one chromosomally integrated copy of the *tetM* gene. We used the reference value of GPM93 as a fold change of one. In comparison with the housekeeping gene *rpoB*, we calculated that the cells contained an average number of two to three plasmid copies per cell.

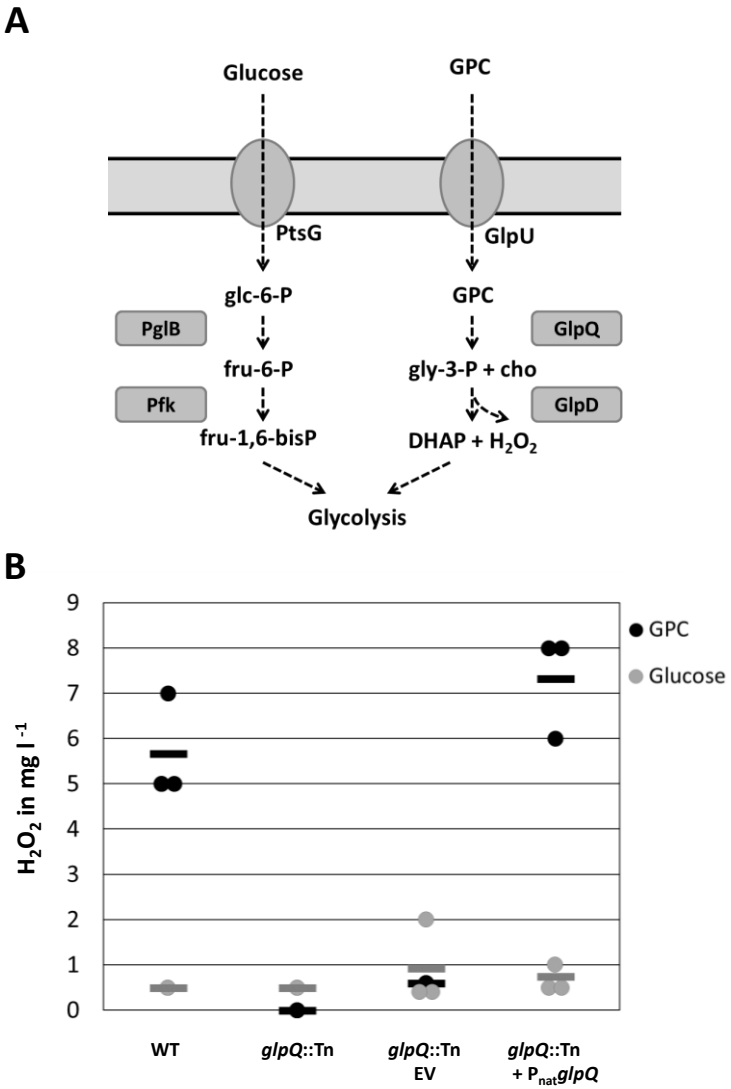

Figure 3.5 | Complementation analysis with pGP2756 of a *glpQ*-mutant (GPM81) impaired in hydrogen peroxide production. (A) General carbon metabolism of *M. pneumoniae* with respect to two different carbon sources, glucose and glycerol phosphocholine (GPC). GlpQ converts glycerol phosphocholine (GPC) into glycerol 3-phosphate and choline (Cho). Subsequently, glycerol 3-phosphate is converted by GlpD into hydrogen peroxide (H_2O_2) and dihydroxyacetone phosphate (DHAP). The GlpQ-deficient strain (GPM81) cannot provide the substrate for GlpD and produces significantly less hydrogen peroxide. Cells grown with glucose produce nearly no hydrogen peroxide due to the different route of substrates. (B) Measurement of hydrogen peroxide levels with glucose (grey) or GPC (black). The different strains were grown in MP medium, collected and washed two times with phosphate-buffered saline. An equal number of cells was supplied with either glucose or GPC, and after 1 h the amount of H_2O_2 yielded was measured with a test stripe and detected by colour changes. Three independent replicates are indicated with points and the average level with a bar. WT, wild type; Tn, mini-Transposon, EV, empty vector.

Use of the recombinant *oriC*-based plasmid pGP2756 as complementation vector. To provide unequivocal evidence that the replicative plasmid is functional, we decided to perform a complementation assay For this purpose, we made use of the phenotype of a *glpQ*::Tn mutant (GPM81), which cannot produce hydrogen peroxide when grown with

glycerol phosphocholine (GPC). For this purpose, we cloned the *glpQ* gene with its native promoter into the replicative plasmid, resulting in pGP2496 (for details, see Methods). We then transformed the *glpQ* mutant GPM81 with this plasmid as well as with the empty vector pGP2756. The resulting complemented or non-complemented strains, as well as the wild-type strain, were analyzed for hydrogen peroxide formation when grown with glucose or GPC. As shown in Fig. 3.5, plasmid-borne expression of the *glpQ* gene in the mutant strain restored the wild-type phenotype, *i.e*. the formation of hydrogen peroxide in the presence of GPC. In conclusion, the complementation of the *glpQ* mutant shows that gene expression from the replicative plasmid pGP2756 is functional in *M. pneumoniae*.

Use of plasmid pGP2756 in other *Mycoplasma* species. To test whether plasmid pGP2756 can also be used in other *Mycoplasma* species, we first attempted to transform the species most closely related to *M. pneumoniae*, *M. genitalium* and *M. gallisepticum*. We expected that this plasmid might behave as it did in *M. pneumoniae*, as the genomes of the three organisms share a similar organization of their *oriC* region (Fig. 3.1). A comparison of the DnaA proteins of the three species revealed high similarity between *M. pneumoniae* and *M. genitalium* (79 % identity). On the other hand, the DnaA protein of *M. gallisepticum* is only distantly related to its counterparts from *M. pneumoniae* and *M. genitalium* (30.6 and 31.9 % identity, respectively). Transformation of *M. genitalium* with pGP2756 yielded viable resistant transformants that could be cultivated in liquid culture. The presence of the replicating plasmid was verified by PCR, indicating that the plasmid does indeed function in *M. genitalium*. *M. gallisepticum* was transformed with the plasmid pGP2756 using a PEG-mediated protocol (Cao *et al.*, 1994). While the positive control, plasmid pMgalloriC, yielded transformants, the plasmid pGP2756 yielded only very few transformants that could not be subcultured, suggesting that the colonies had resulted from spontaneous acquisition of spontaneous resistance. Thus, in good agreement with the conservation of the replication initiation machinery, plasmid pGP2756 was able to replicate in *M. genitalium* but not in *M. gallisepticum.* Given the results obtained with M. genitalium and *M. gallisepticum*, we wondered whether pGP2756 could also replicate in a more distant species such as *M. capricolum*. This latter species was thus transformed with pGP2756 using the PEG protocol (Lartigue *et al.*, 2009). After transformation, the positive control (pMCO3, the *M. capricolum oriC* plasmid) yielded colonies while pGP2756 yielded no more than 10 colonies, as did the negative control pSRT2, *i.e*. less than 0.01% of the colonies obtained with the positive control. Thus, we conclude that the *oriC* from *M. pneumoniae* cannot support plasmid replication in *M. capricolum.*

DISCUSSION

The availability of replicative plasmids is a prerequisite for efficient genetic analysis and manipulation of any bacterium. While *M. pneumoniae* is a model organism for systems biology, tools for the efficient introduction of genes into the bacterium have been limited and there is an urgent need for replicable plasmids (Halbedel and Stülke, 2007; Renaudin, 2002). Thus far, mutants have only been able to be complemented by introducing a gene of interest into the genome using a transposon to facilitate integration (Schmidl *et al.*, 2011, Großhennig *et al.*, 2013). However, this may result in integration into chromosomal regions that interfere with growth, gene expression or protein activity. In this study, we demonstrated the construction and functional verification of the first replicable plasmid for *M. pneumoniae*. Chromosomal *oriC* regions that can be used for plasmid construction are usually located next to the *dnaA* gene in Gram-positive bacteria, and this is also the case for bacteria that are derived from Gram-positive ancestors such as *Mycoplasma* species (Cordova *et al.*, 2002; Janis *et al.*, 2005; Maglennon *et al.*, 2013; Shahid *et al.*, 2014). Interestingly, *M. pneumoniae*, *M. genitalium* and their close relatives *M. gallisepticum* and *M. imitans* are distinct from other bacteria and even other mollicutes with respect to their gene arrangement in this region. While *dnaA* and *dnaN* form a conserved pair of immediately adjacent genes in most organisms, this is not the case in *M. pneumoniae* and its relatives. In mycoplasmas, the soj gene, encoding an ATPase that controls DnaA activity and chromosome partitioning, is located between *dnaN* and *dnaA*. Moreover, the *dnaN* and *dnaA* are oriented divergently in *M. pneumoniae* (Fig. 3.1). Our computational analysis suggested that in

M. pneumoniae the *oriC* might be located between *dnaN* and *soj*, rather than being directly linked to the *dnaA* gene (see Fig. 3.3). Based on the poor sequence conservation of the DnaA proteins of different *Mycoplasma* species, it has been proposed that the requirements for replication initiation might be much more relaxed for *Mycoplasma* spp. than in other bacteria (Lee, Browning and Markham, 2008). This prediction was confirmed by the identification of the putative *M. pneumoniae* DnaA boxes, the consensus of which seem to be rather relaxed (see Fig. 3.2).

Our results also indicated that the poor conservation of replication initiation determinants among the different Mycoplasma species may be the limiting factor for broader use of these plasmids, even in closely related species. Indeed, pGP2756 could be used in *M. genitalium* but not in *M. gallisepticum*, even though both species belong to the *M. pneumoniae* phylogenetic group. Not surprisingly, the plasmid was not able to replicate in *M. capricolum*, a species of the *M. mycoides* group. Similarly, plasmids constructed using the *oriC* region of *M. capricolum*, *M. mycoides* and even *Spiroplasma citri* were used for transformation of *M. capricolum* (all three species belong to the *Spiroplasma* phylogenetic

group) (Lartigue *et al.*, 2003), but not for *M. pneumoniae* or *M. genitalium* (data not shown). Similarly, all attempts to introduce the *M. gallisepticum oriC* plasmid into *M. pneumoniae* failed (Lee *et al.*, 2008). With the construction of a replicative plasmid for the use in *M. pneumoniae*, we have made an important addition to the toolbox that will facilitate the genetic analysis of these bacteria. In the future, the development of novel techniques to construct *M. pneumoniae*-targeted deletion mutants would be a major breakthrough in the genetic study of this minimal pathogen and model organism.

SUPPLEMENTAL METERIAL

Figure S3.1 | Verification of the possible integration of pGP2756 in the *M. pneumoniae* chromosome.

Table S3.1 | Oligonucleotides used in the study of chapter 3.

Table S3.2 | Plasmids used in the study of chapter 3.

Acknowledgments. We are grateful to Katrin Gunka (University of Göttingen), Maria Lluch-Senar and Luis Serrano Pubull (CRG Barcelona) for helpful discussion.

Funding. This was performed within the framework of the ERASynBio 2nd Joint Call for Transnational Research Projects: Building Synthetic Biology Capacity Through Innovative Transnational Projects, with funding from the Federal Ministry of Education and Research MiniCell network (Grant 031L0012).

CHAPTER 4 | Immunoglobulin binding protein IbpM

Characterization of the Immunoglobulin Binding Protein (IbpM) from *Mycoplasma pneumoniae*

Cedric Blötz[1], Neil Singh[1], Roger Dumke[2], and Jörg Stülke[1]*

[1]Department of General Microbiology, University of Göttingen, Germany
[2]Medical Faculty Carl Gustav Carus, Institute of Medical Microbiology and Hygiene, Technical University Dresden, Germany

AUTHOR CONTRIBUTION

CB, RD, and JS designed the study. CB performed cloning and protein expression. CB and NS performed ELISA experiments. RD produced antibodies and performed localization experiments for wily type cells. CB screened and isolated a transposon mutant. CB characterized the *mpn400*::Tn mutant. CB performed colony blot for the mutant. CB and NS investigated protease functions. CB and JS wrote the manuscript.

ABSTRACT

Bacteria evolved many ways to invade, colonize and survive in the host tissue. These complex infection strategies of other bacteria are not present in the Gram-positive but cell-wall less *Mycoplasmas*. They have strongly reduced genomes, equipped with a minimal metabolism and a condensed but highly effective virulence mechanism. *Mycoplasma pneumoniae* is an obligate pathogenic bacterium using its minimal virulence repertoire very efficient, infecting the human lung. *M. pneumoniae* can cause a variety of clinical symptoms including fever, inflammation, atypical pneumoniae and even death. Due to its strongly reduced metabolism, *M. pneumoniae* is dependent on the host nutrition and aims to persist as long as possible, resulting in chronic diseases. *Mycoplasmas* evolved strategies to ideally subvert the host immune system. To manipulate the hosts immune system, proteins fending off host derived immunoglobulins (Igs) are crucial. In this study, we investigated the role of MPN400 as the putative protein responsible for Ig-binding and host immune evasion. We found, that the overall domain architecture and the surface localization corroborated the idea of MPN400 being an Ig-binding protein. The most important finding of this study was the strong binding ability of MPN400 to the human IgG and reduced binding to human IgA and IgM, showing the distinct interaction of MPN400 from *M. pneumoniae* with Igs. We therefore named the protein MPN400 immunoglobulin binding protein of *Mycoplasma* (IbpM). A C-terminal truncated version was still able to bind all Igs but showed decreased affinities compared to the full-length protein. Furthermore, we confirmed the ability of IbpM to bind also to plasminogen and fibronectin. Our study indicates that *M. pneumoniae* uses a refined mechanism for immune evasion, hence IbpM is an ideal candidate for vaccine development and promising target for industrial research.

INTRODUCTION

The cell-wall less bacteria of the genus *Mycoplasma* are commensal, opportunistic or pathogenic bacteria colonizing diverse hosts including plants, animals and humans (Parrott *et al.*, 2016). *Mycoplasmas* belong to the group of Mollicutes, characterized by their strongly reduced genomes (688 ORFs; Dandekar *et al.*, 2000), which is responsible for the restricted metabolic capabilities of these bacteria. The reduction in metabolic pathways is caused by adaptation to their hosts, resulting in the strong dependency on the acquisition of nutrients (Waites and Talkington, 2004; Halbedel *et al.*, 2007). Due to their reduced genome *Mycoplasma pneumoniae* and *Mycoplasma genitalium* are model organisms for systems and synthetic biology, respectively. Furthermore, both are important pathogens in medical research due to their virulence in host tissue, the human lung epithelium and the urogenital tract. *Mycoplasma* species can cause a broad range of symptoms in various hosts, *e.g.*

fever, inflammation, autoimmune responses or atypical pneumoniae (Citti and Blanchard, 2013), followed more often by a chronic disease state rather than killing the host (Atkinson *et al.*, 2008). The strong dependency on the host's survival is a good explanation for the occurrence of chronical diseases caused by mycoplasmal infections. Despite their reduced genomes and consequently the restricted metabolism *Mycoplasmas* can infect efficiently their hosts. Remarkably, only a few virulence factors for *Mycoplasma* are known or well described. For *M. pneumoniae* only the community acquired respiratory distress syndrome (CARDS) toxin is described as a typical toxin representative (Becker *et al.*, 2014; Kannan and Baseman, 2006; Kannan *et al.*, 2016; Johnson *et al.*, 2011). Hydrogen peroxide produced during glycerol utilization is the major virulence factor for *M. pneumoniae* and other *Mycoplasmas* (Blötz and Stülke, 2017; Halbedel *et al.*, 2004; Yus *et al.* 2009). In addition, hydrogen sulfide was also identified to play a significant role in the cytotoxicity of *M. pneumoniae* (Großhennig *et al.*, 2016). Moreover, in some *Mycoplasma* species, e.g. *Mycoplasma fermentans, M. genitalium* or *M. pneumoniae,* immunomodulatory proteins could be identified (Campos *et al.*, 2018; Into *et al.*, 2004; Into *et al.*, 2007; Mühlradt *et al.*, 1997; Okusawa *et al.*, 2004). In Gram-positive and Gram-negative bacteria, such as *Yersinia* spp., *Listeria* spp., *Salmonella* spp., or enterohaemorrhagic *Escherichia* spp. many different mechanisms which influence the host immune response are well-described (Bhavsar *et al.*, 2007). Overall, the cytoadherence or attachment to host cells is a prerequisite for the growth of pathogenic bacteria and a concomitant infection (Rottem *et al.*, 2003; Catrein *et al.*, 2004). The link between attachment and virulence is exemplified by non-adherent *Mycoplasma* mutants which are nearly non-pathogenic (Mudahi-Orenstein *et al.*, 2003; Waldo *et al.*, 2005.; for review: Chaudhry *et al.*, 2007). *M. pneumoniae* and *M. genitalium* encode a very complex protein network, the attachment organelle, which is responsible for their gliding motility and attachment to human epithelial cells (Balish and Krause, 2002; Chaudhry *et al.*, 2016; Krause *et al.*, 2018; Seybert *et al.*, 2018; Kenri *et al.*, 2018). Proteins encoding subunits of this tip seem to be responsible for enhanced survival of *M. genitalium* by antigenic and phase variation, a strategy described for many bacteria (Burgos *et al.*, 2018; van der Woude and Bäumler, 2004). Furthermore, in several bacterial species (mainly Gram-positive) surface proteins are known to bind to human surface proteins. One important class of such binding proteins are immunoglobulin binding proteins (IBPs) (Boyle *et al.*, 1990; Sidorin and Solov'eva, 2010). The IBPs can bind to different immunoglobulins (Igs) without the requirement of antigen-binding sites. This non-immune binding mechanism is thought to protect bacteria from the action of the complement system. This system is responsible for phagocyte independent immune defense in vertebrates, decreasing phagocytosis and finally promote the evasion from the hosts immune system. IBPs are classified into functional groups according to their ability to bind to human or animal

Igs. The most studied IBPs are Protein A (*Staphylococcus aureus*), Protein G (group C *Streptococci*) and the M-protein (group A *Streptococci*) binding to the Fc region (crystallizable fragment of Igs) (Fischetti, 1989; Graille *et al.*, 2000; Sjöbring *et al.*, 1991), and the Protein L (*Finegoldia magna*) which binds the light chain of Igs (Akerström and Björck, 1989; Graille *et al.*, 2002). Interestingly, the M-protein not only binds to Igs, in addition, it is able to bind factor H in serum, thereby blocking the innate immune response (Horstmann *et al.*, 1988). Recently, IBPs were identified in *M. genitalium* (Protein M) and *Mycoplasma mycoides* subsp*. capri* (MIB) (Arfi *et al.*, 2016; Grover *et al.*, 2014). Interestingly, the 50 kDa IBP from *M. genitalium* differs in its tertiary architecture from all available structures in the Protein Data Bank (PDB). Moreover, its structure is different compared to well-known IBPs (Grover *et al.*, 2014). Protein M and homologs of IBPs from other *Mycoplasmas*, not to be confused with the M-protein from *Streptococci*, seem to have evolved convergently. Such a convergent origin of bacterial IBPs was first postulated by Frick and colleagues (Frick *et al.*, 1992). Regarding the reduced genomes of *Mycoplasmas*, the evolution of a putative immune evasion system is striking. Even more striking is the fact that *M. mycoides* possesses multiple copies of a system binding Igs (via MIB) and, proteolytically cleaving off the variable heavy chain (via MIP). Furthermore, in *Ureaplasma ueralyticum* an immunoglobulin A (IgA) specific protease was identified and characterized (Robertson *et al.*, 1984; Spooner *et al.*, 1992). Similar, in *Mycoplasma synoviae* and *Mycoplasma gallisepticum* an IgG protease was identified (Cizelj *et al.*, 2011). However, the MIB-MIP system and Protein M homologs, seem to be conserved mutually exclusive. Both Ig binding proteins do not appear in one genome at the same time. Furthermore, the MIB-MIP system is present in *Mycoplasmas* infecting animals and humans, but not in plant pathogens (Arfi *et al.*, 2016).

In this work we addressed the localization and function of a putative IBP from *M. pneumoniae*, encoded by *mpn400.* Furthermore, we identified putative proteases and investigated their activity to cleave Igs. Our results demonstrate the surface localization of MPN400, that allows in principle the interaction with external factors. Moreover, we produced recombinant MPN400 in *E. coli* and showed via ELISA experiments that purified rMPN400 can bind different Igs. Further, several putative proteases were analyzed for the reactivity towards Igs and possible interactions with MPN400. Screening in a transposon library revealed a *mpn400*-mutant that was isolated, which is used for further *in vivo* characterization. These experiments involve animal models and cytotoxicity assays.

MATERIALS AND METHODS

Bacterial strains, transformation, and growth conditions. The *M. pneumoniae* strains used in this study were *M. pneumoniae* M129 (ATCC 29342) and its isogenic mutant derivative GPM113 (*mpn400*::Tn*4001*, pMT85 transformed into M129).

Plasmid construction. Plasmids for the overexpression and purification of MPN400, MPN400 without C-terminus (A446STOP), and MPN641 (negative control) were constructed as follows. The gene of interest was amplified by PCR from M129 *M. pneumoniae* wild type genomic DNA using oligonucleotides listed in Table S4.1. The vectors pBSKII(-) (Stratagene) and pGP172 (Merzbacher *et al.*, 2004) were digested with KpnI/BamHI for *mpn400* as well as its mutated version and SacI/BamHI for *mpn641*, respectively. The genes *mpn400* was ligated into pBSKII, resulting in pGP2743. The plasmid pGP2743 served as template for the multiple mutation reaction (Hames *et al.*, 2005) to replace TGA (opal stop codon in *E. coli*) by TGG (tryptophan) codons. The codon optimized *mpn400* was amplified from pGP2743 without trans-membrane domain and ligated into pGP172 for expression (pGP3215) or a truncated mpn400 was ligated in the same backbone (pGP3217). The control *mpn641* was ligated into pGP172 (pGP3235). Plasmids were control digested and sequenced. The used and constructed plasmids are listed in Table S4.2.

Production of guinea pig polyclonal antibodies. Polyclonal antisera were produced in guinea pigs (Charles River). The animal experiments were approved by the ethical board of Landesdirektion Sachsen, Dresden, Germany (permit no. 24-9168.25-1/2011/1). Primary subcutaneous immunization of animals with recombinant proteins, booster immunizations and serum collection were performed as reported (Thomas *et al.*, 2013).

Localization of MPN400. Colony blotting was used to specify the localization of MPN400 as described earlier (Thomas *et al.*, 2013). Briefly, diluted *M. pneumoniae* cells were grown for 10 days on PPLO agar plates and colonies were covered with a nitrocellulose membrane for 5 min. The membrane was dried for 10 min at RT, washed and blocked three times (for 10 min, 10 % FCS in PBS/Tween). The reactivity of the blotted proteins was tested either with α-MPN400, α-Nox, and α-P14 (1:250 each). The NADH-oxidase (Nox; Pollack *et al.*, 1997; Hagemann *et al.*, 2017) and the C-terminal part of the main P1 adhesin (P14; Schurwanz *et al.*, 2009) were used as cytosolic and surface-localized reference proteins, respectively.

As a further method, mild surface proteolysis of *M. pneumoniae* cells was carried out. *Mycoplasma* cells were grown as described above, harvested, and the protein concentration was adjusted to 200 µg ml^{-1}. The cells were centrifuged for 5 minutes at

13 000 g and subsequently incubated with 10 µg ml^{-1}, 40 µg ml^{-1}, and 100 µg ml^{-1} or without trypsin (Sigma) in PBS for 30 min at 37°C. The samples were centrifuged (13 000 g, 10 min) and pellets resuspended in 100 µl protein sample buffer followed by 10 min boiling (95°C) and separation by SDS-PAGE. Subsequently, proteins were blotted onto nitrocellulose membranes by standard procedure. The blots were incubated with α-MPN400, α-Nox, and α-P14 (1:250 each). α-guinea pig IgG (Dako; 1:1 000) was used to detect the proteins.

Additionally, the localization was investigated with fluorescence microscopy as described (Thomas *et al.*, 2013). Briefly, fixed *Mycoplasma* cells in chamber slides (Nunc) were incubated with a mixture of corresponding guinea pig antiserum (1:250) and rabbit antiserum to the TX-100-insoluble protein fraction of *M. pneumoniae* proteins (cell staining control; 1:250). After a washing step, cells were treated with FITC-labeled α-guinea pig and TRITC-labeled α-rabbit antibodies (Sigma; 1:500).

Isolation of mutant strains. For the isolation of *M. pneumoniae* mutants, we used an *M. pneumoniae* transposon library carrying insertions of Tn*4001* (Halbedel *et al.*, 2006). The presence of the desired mutant was assayed by a PCR screen using one oligonucleotide that hybridizes to the transposon (directed outward), and a second oligonucleotide specific for the gene of interest (see Supplementary Table S4.1).

Clean-deletion of *M. pneumoniae* genes. To delete *mpn400* we amplified 500 bp on both sited, upstream and downstream of each gene and fused them to the chloramphenicol resistance cassette, encoded on the plasmid pGP2727, flanked by *lox* sites. The resulting plasmid (pGP2729) was used to amplify double stranded DNA with CB212 and CB213, where the two strands were tagged differently. One strand must be protected (for further transformation into *Mycoplasma*) and the second one is tagged with biotin. The biotin tag allows the separation of the two strands with magnetic beads under basic conditions. The protected ssDNA is purified, dried and re-suspended in electroporation buffer. The ssDNA was transformation substrate for the gene deletion strain GPM116 (harboring GP35 recombinase (*mpn560*)-*arcA*::GP35-$Puro^R$). Method adapted from Piñero-Lambea *et al.*, unpublished.

Southern Blot Analysis. Chromosomal DNA was isolated according to the manufacturer's instructions using the Bacterial DNA Kit (PEQLAB, Erlangen). For both strains, M129 and GPM113, cells were grown in T75-flasks and harvested for DNA isolation. 2 µg of each DNA sample was pre-incubated with RNase A (1 µl; 20 mg ml^{-1}) and digested with 3 µl SacI for at least 5 hours at 37°C. Digests were separated by agarose gel electrophoresis (1%), transferred onto positively charged nylon membranes (Roche, Munich) and probed with

digoxigenin-labelled riboprobes as described earlier (Halbedel *et al.*, 2006; Sambrook *et al.*, 1989).

Western blotting. For Western blotting, *M. pneumoniae* GPM113 and the wild type were grown till 95% confluency. Cells were collected and once washed with PBS. Cells were lysed in a tissue lyser with 0.1 mm glass beads (2 × 2.5 min, 30 Hz, cooled block) followed by centrifugation for 10 min at 14000 rpm and 4°C. The protein content of the supernatant was measured using Nanodrop. From each sample 20 µg total protein was mixed with SDS-loading buffer, boiled for 10 min at 95°C and separated in 12% SDS-PAGE. After electrophoresis, the proteins were transferred to a polyvinylidene difluoride (PVDF) membrane (Bio-Rad) by electroblotting (80 mA/membrane, 1 hour). Proteins were detected using antibodies recognizing MPN400 (1:250). The blots were developed with α-guinea pig IgG (Dako; 1:1000) and visualized with a Lumi Imager.

Expression and purification of recombinant proteins. The Strep-tagged proteins were overexpressed in *E. coli* BL21(DE3). Cultivation was performed in 2-fold LB medium (1 liter: 20 g tryptone, 10 g yeast extract, 10 g NaCl) and the expression (1 l culture, 37°C, 200 rpm, baffled flasks, 3 h) was induced by the addition of 1 mM IPTG to exponentially growing cultures (OD_{600} of 0.6 to 0.8). The cells were pelleted at 4°C for 20 min at 4 000 rpm and washed once with buffer W (100 mM Tris-HCl pH8.0, 150 mM NaCl, 1 mM EDTA). Cells lysis was carried out using French press (18 000 p.s.i., 138 000 kPa, three passes, SLM Aminco, United States), subsequently followed by centrifugation of the crude extracts at 35 000 rpm for 30 min. Purification was done at RT using StrepTrap columns (2x 5 ml, GE Healthcare). Crude extract was loaded onto the column (flow rate 0.5 ml min^{-1}, max. 0.5 MPa). StrepTraps were washed with buffer W until the 280 nm absorbance reached the base line. We used 2.5 mM d-desthiobiotin for elution (5 ml fractions; flow rate 1 - 1.5 ml min^{-1}, max. 0.5 MPa). Purification and purity of proteins (>98%) were checked with SDS-PAGE and Colloidal Coomassie staining (Dyballa and Metzger, 2009). Proteins were dialyzed against buffer W using VivaSpin columns (MCO 5 kDa, Sartorius, Göttingen). The pure proteins were frozen in aliquots in liquid nitrogen and stored at -80°C.

Enzyme-linked immunosorbent assay (ELISA). The binding of immunoglobulins and other human serum proteins by MPN400 was quantified in ELISA experiments. Recombinant MPN641 was used as negative mycoplasmal protein control. MPN641 is lipoprotein with unknown function. Further, we used human serum alsbumin and buffer as additional negative controls. MPN400 and a truncated version lacking the predicted C-terminal domain (A446STOP; compare C-term. of Protein M; Grover *et al.*, 2014) were used to address Ig binding. Frozen aliquots were thawed and diluted (2, 3, 4, 5, 10, 50 µg ml^{-}

[1]) and subsequently coated onto 96-well plates. The plates were incubated overnight at 4°C and mild shaking (50 rpm). Afterwards, wells were washed (buffer + 0.05% Tween20) and blocked (1% skim milk, 1 h, 50 rpm, 4°C) three times, followed by a last washing step. The antibodies (IgA / IgM / IgG; 0.2 ng ml^{-1}) were added to the wells with immobilized recombinant proteins and incubated overnight at 4°C (50 rpm). The wells were washed three times before detection. For detection we used an antibody with affinity to human Igs conjugated to horseradish peroxidase (goat α-Ig HRP detecting IgG, IgM, IgA; Thermofisher 0.5 ng ml^{-1}). For detection we incubated wells with 100 µl of α-Ig HRP for 1 h at 4°C (50 rpm). After washing three times, ABTS solution (1-Step™ ABTS, Thermofisher) was added and incubated (20 mins, dark, RT). Absorbance detection of bound antibodies was indicated by green color formation, measured in a plate reader (395 - 415 nm, λ_{max} = 405 nm).

Pull Down of MPN400 binding proteins from human Serum (HuSe). To isolate MPN400-binding proteins from human serum (ThermoScietific; H4522), we cultivated *E. coli* strains harboring either pGP3215 (Strep-MPN400) or the empty vector pGP172. Protein extracts were prepared as described earlier (Expression and purification of recombinant proteins). StrepTactin columns (CV = 250 µl) were saturated with MPN400 (4 columns) or the empty vector crude extract (1 column). After extensive washing (10 times 2 ml buffer W) human serum was applied to all columns. For the empty vector column and one with bound MPN400 we used 5 µg HuSe. The remaining MPN400 columns were incubated with 3, 2 and 1 µg each. After 10 washing steps we eluted the bound proteins 4 times with buffer W containing D-desthiobiotin (2.5 mM). From elution fractions we used 20 µl for SDS-PAGE analysis, followed by silver staining. Significant bands were further processed by LC-MS/MS analysis.

Protein digestion with trypsin and protein identification with LC-MS/MS. Trypsin digestion of proteins was performed as described earlier (Shevchenko *et al.*, 1995). Briefly, the Stage TipStageTip method was used to purify peptides (Rappsilber *et al.*, 2007), which were subsequently separated by reversed-phase liquid chromatography. For analysis an RSLCnano Ultimate 3000 system (Thermo Scientific) followed by mass analysis with an Orbitrap Velos ProHybrid mass spectrometer (Thermo Scientific) was applied as described in more detail elsewhere (Lin *et al.*, 2015; Schmitt *et al.*, 2017). MS/MS2 data processing for peptide analysis and protein identification was performed with the Proteome Discoverer 1.4 software (Thermo Scientific) and the Mascot and SequestHT search algorithms. Proteins identified in empty vector control (pGP172 with human serum) were regarded as unspecific binding and excluded.

HeLa cell cytotoxicity assay. Infection of HeLa cultures with M. pneumoniae cells was done as described previously (Hames *et al.*, 2009; Schmidl *et al.*, 2010a). DMEM medium complemented with 10% FBS was used to grow cells. After four days post infection, HeLa cultures were stained with crystal violet (10 min fixation in 10% formalin; 150 µl 0.1% crystal violet solution for 30 min at RT; 3 times washing) and photographed. For quantification the survived cells, disruption was carried out with 0.5 % SDS solution. The OD_{595} served as indication for cell survival and therefore the cytotoxicity of *M. pneumoniae*.

RESULTS

Homology comparison of Ig-binding proteins. The amino acid sequence of MPN400 was used to search for homologs of in other *Mycoplasma* species. Therefore, we used BLASTp search with standard settings. Only four different species and with low amino acid identity showed homology to MPN400. Since the IBP homolog in *M. genitalium* (MG281) was already known, both proteins were aligned separately and showed 53% amino acid identity (see Fig S4.1). The alignment of other potential Ig-binding proteins in *Mycoplasma* revealed even less sequence conservation (*Mycoplasma iowae* 19.7%, *Mycoplasma imitans* 19.9%, *Mycoplasma gallisepticum* 21%).

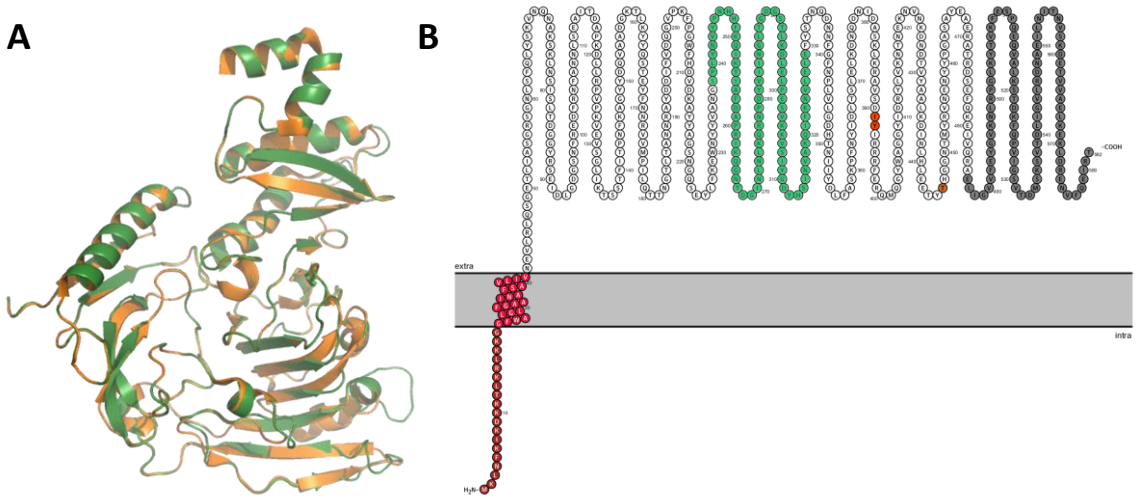

Figure 4.1 | Structural analysis of IbpM (MPN400). (A) Structural alignment of the predicted tertiary structure of IbpM from *M. pneumoniae* (green) to the resolved crystal structure of Protein M TD (PDB: 4NZR) from *M. genitalium* (orange). The figure was created by PyMOL. (B) The ProtterBlot shows the domain architecture of IbpM (using UniProt accession number P75383) anchored in the plasma membrane. Amino acids in dark red indicate signal peptide and light red the predicted transmembrane domain. Colored residues in light green indicate LRR-like domain and dark grey the C-terminal disordered domain. Insertion point for the mini-transposon Tn*4001* is indicated in orange (aa 391-392) and the truncation point for recombinant mutant in brown (aa 446).

For further analysis, structural modeling was used to analyze the structure of MPN400 in comparison to the crystal structure of Protein M of *M. mycoides* (PDB: 4NZR). The calculated structural alignment was visualized using PYMOL (Omasits *et al.*, 2014) (see Fig. 4.1A). The calculated structure seems to be highly similar comparing both IBPs. The sequence and structural comparison revealed a very similar domain architecture as described for Protein M (see Fig. 4.1B).

Surface localization of MPN400. We hypothesized that MPN400 is surface located based on a putative transmembrane domain (identified using "DAS"-TM prediction (Cserzö *et al.*, 1997); amino acids: 21 - 40 Fig. S4.3) and the described activity of homologs on the surface in other *Mycoplasma* species (Arfi *et al.*, 2066; Grover *et al.*, 2014). The surface localization was corroborated with colony blotting (Fig. 4.2A), mild proteolysis (Fig. 4.2B) and immunofluorescence (Fig. S4.4).

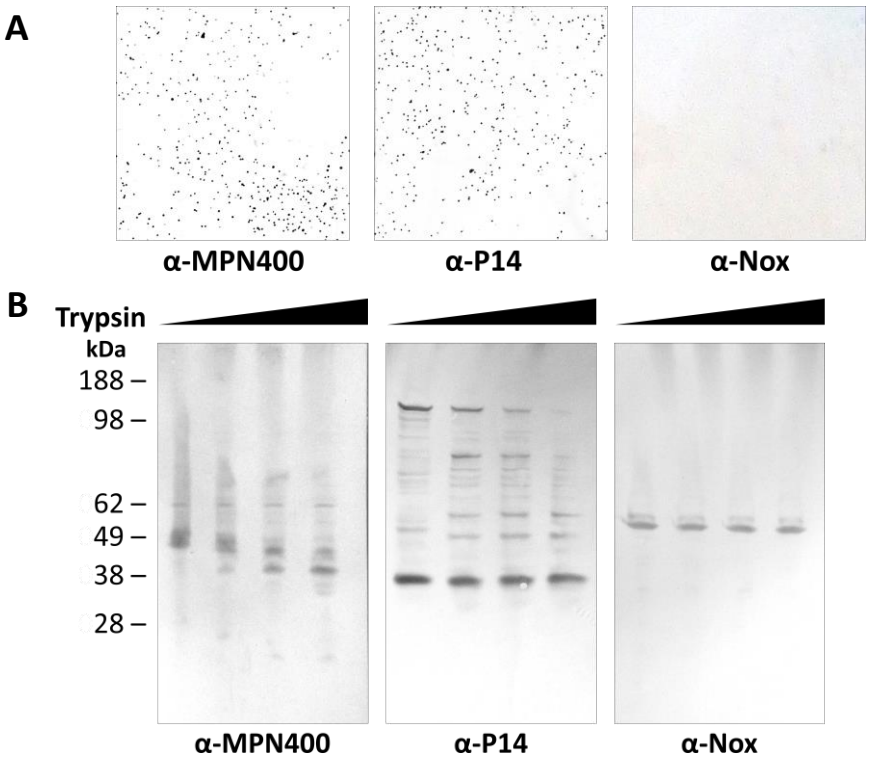

Figure 4.2 | Localization of IbpM (MPN400) on the surface of *M. pneumoniae* cells. (A) Results of colony blot of freshly grown *M. pneumoniae* colonies. Blotted colonies were treated with guinea pig α-MPN400, α-P14 (positive control), and α-NADH oxidase (Nox, negative control), respectively. (B) Reactivity of SDS-PAGE-separated and blotted whole *M. pneumoniae* proteins after mild treatment with increasing concentrations of trypsin. Lane 1: 0 µg ml^{-1}, lane 2: 10 µg ml^{-1}, lane 3: 40 µg ml^{-1} and lane 4: 100 µg mL^{-1} trypsin. Western blots were incubated with guinea pig α-MPN400, α-Nox and α-P14, respectively. Guinea pig antibodies were detected using rabbit α-guinea pig HRP conjugated antibody.

In the colony blotting experiment strong signals could be detected for MPN400 and the surface localized protein P14 (positive control). Moreover, the trypsin proteolysis showed with increasing concentrations stronger degradation for the surface protein P14 as well as for MPN400. Control experiments with the cytosolic protein Nox remained negative in colony blotting and the immunofluorescence assay. Furthermore, Nox was stable after protease treatment in contrast to the surface located protein P14 and MPN400. The experiments show clearly the surface localization of MPN400.

Isolation of a *mpn400* transposon mutant. Since *mpn400* was not annotated as essential (Lluch *et al.*, 2015) it was screened for a transposon mutant. The mutant was isolated from a transposon library as described earlier (Halbedel *et al.*, 2006). The pooled *M. pneumoniae* mutants were screened within a PCR reaction to detect the presence of the mini-transposon disrupting *mpn400* (see Fig. 4.3A). The successful interruption of *mpn400* and the single transposon integration were verified by Southern blot analysis (see Fig. 4.3B).

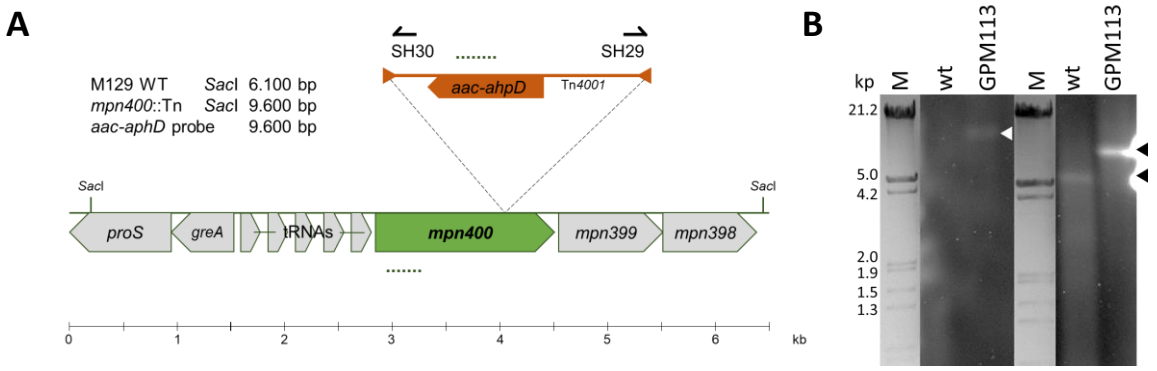

Figure 4.3 | Isolation of a *mpn400* transposon insertion mutant. (A) Schematic representation of the genomic region of *mpn400* in *M. pneumoniae* and the transposon insertion site in the *mpn400*::Tn-*4001* mutant GPM113. (B) Southern blot analysis to confirm single transposon integration using chromosomal DNA of the wild type (wt) and strain GPM113 were digested using SacI. Detection was carried out with a probe specific for the *aac-ahpD* resistance cassette (white arrow, left) and a probe hybridizing to the gene *mpn400* (right) which is upshifted after transposon integration (black arrows). λ-marker (HindIII/EcoRI) served as a size standard.

Only one single band for the *aac-aphD* probe in the mutant could be detected (white arrow). For the *mpn400* specific probe a clear shift is visible compared with the wild type signal (indicated by black arrows, Fig. 4.3B), this shift corresponds to the bigger size due to transposon integration. The exact integration was determined by DNA sequencing, showing that *mpn400* is interrupted at its 1178th nucleotide, resulting in a 191 amino acid (from total 582 amino acids) truncated protein. The isolated mutant was named GPM113 (*mpn400*::Tn*4001*). The isolation of a clean deletion, using the GP35 recombinase

dependent deletion system (Piñero-Lambea *et al.*, unpublished) failed several times under various conditions.

Characterization of the *mpn400* mutant. When the growth of the mutant strain GPM113 was compared with the wild type M129, no changes could be observed, irrespectively of the carbon source (glucose or glycerol). Colony blotting with GPM113 showed no surface localization at all (see Fig. S4.5). In a Western blot using crude extracts from the wild type and GPM113 showed a weak band with reduced size (~55 kDa) compared to the wild type MPN400 band at 65 kDa (data not shown). Using HeLa cytotoxicity assay showed only a slight reduction (see Fig S4.6). After 48 h post infection wild type cells cause ~50% cytotoxicity while GPM113 cause less than 35%. This toxicity effect is no longer detectable after 96 h or 120 h post infection.

Expression of recombinant proteins. For recombinant expression the respective genes (*mpn400*, a truncated version of *mpn400* lacking the C-terminal domain (A446STOP) and the lipoprotein *mpn641* as control) were cloned into *E. coli* overexpression vector pGP172 adding a STREP-tag for purification. The signal peptide and the transmembrane domain were not cloned in the recombinant expression vectors (see Fig. 4.1B; amino acids 1 - 40). After the exchange of opal stop codons in *mpn400* and sequencing of the plasmids pGP3215 (STREP-MPN400), pGP3217 (STREP-MPN400 A446STOP), and pGP3235 (STREP-MPN641) the proteins were expressed in *E. coli* BL21. Overexpressed proteins were purified under native conditions and checked by SDS-PAGE. Coomassie stained gels (see Fig. S4.2) showed clean (>98%) protein bands at the expected sizes. Recombinant MPN400 was used to raise polyclonal antisera in guinea pigs. MPN400 and its truncated derivative as well as MPN641 were used for ELISA assays.

Pull-down of human serum proteins bound by MPN400. The binding capacity of human serum components, which includes antibodies and proteins from the immune system, to MPN400 was addressed in a pull-down experiment. Therefore, recombinant MPN400 was immobilized on StrepTactin columns and incubated with different concentrations of human serum. The bound proteins were analyzed with silver stained SDS-PAGE (see Fig. 4.4) and LC-MS/MS analysis. We analyzed proteins over 50 kDa for empty vector control and same sizes for MPN400 bound proteins. Indeed, we identified 1510 unique peptide-spectrum matches (PSMs) for MPN400, which was expected. Furthermore, we could identify under the 30 most abundant PSMs the apolipoprotein B-100 and more than 15 different immunoglobulin heavy chains or immunoglobulin-like peptides. This directed us to analyze detailed binding ability of MPN400.

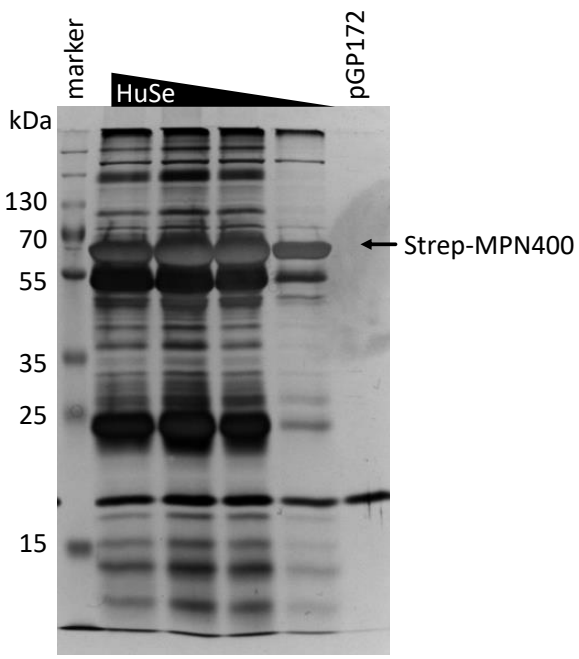

◄ Figure 4.4 | Detection of proteins bound by immobilized MPN400. The binding was performed with recombinant MPN400 (from *E. coli* BL21::pGP3215) immobilized to StrepTactin matrix, which was incubated with different concentrations of human serum (HuSe). Columns were washed extensively, and bound proteins eluted four times with D-desthiobiotin. We used the fractions from elution 3 to analyze the protein content by 12% SDS-PAGE stained with silver. Lane 1, Pre-stained protein ladder plus (ThermoFisher); lane 2 - 5, rMPN400 incubated with 5, 3, 2, and 1 µg protein from HuSe, respectively; lane 6 empty vector crude extract from *E. coli* incubated with 5 µg HuSe.

Binding of immunoglobulins to MPN400. The binding of Igs to MPN400 was characterized via an enzyme linked immunosorbent assay (ELISA). Recombinantly expressed proteins (MPN400, MPN400 without C-terminal domain, negative control lipoprotein MPN641) were coated onto 96-well plates. Coated wells were incubated with different Igs in various concentrations. The negative controls (human serum albumin coated or MPN641-coated as well as blank wells with only buffer) showed no binding to the Igs. For MPN400 coated wells we saw that the tested Igs (IgG, IgA, and IgM) bound even at low concentration (2 µg ml^{-1}) strongly (see Fig. 4.5). However, for the C-terminal truncated MPN400 mutant, its Ig-binding is reduced at lower concentrations (see Fig. 4.5). The binding showed that IbpM has different affinities towards the tested Igs, with the order as follows: IgG > IgA > IgM. In addition, we tested the capabilities of IbpM to bind other human proteins. For fibronectin and plasminogen, we saw also binding to MPN400 (see Fig. 4.6). This was again not seen for the negative controls. We therefore named *mpn400* the **i**mmunoglobulin **b**inding **p**rotein gene of ***M****. pneumoniae* (*ibpM*) and the protein IbpM, respectively.

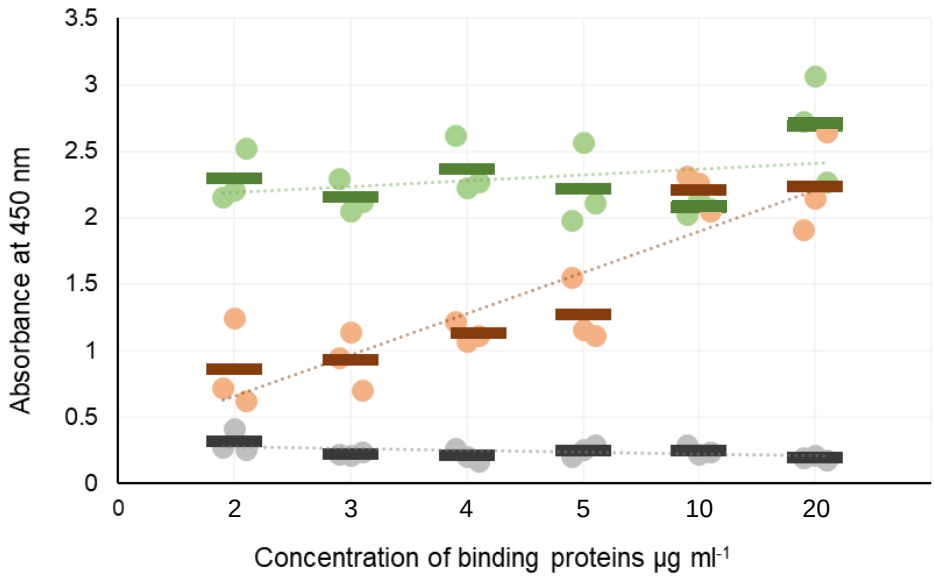

Figure 4.5 | Binding of different Ig's towards IbpM in an ELISA experiment. Purified full-length IbpM, C-terminal truncated IbpM, and HSA were coated in different concentrations onto 96-well plates and incubated with IgG, IgA or IgM. Binding of Igs was quantified by the detection with rabbit α-human Ig -AP antibody responsible for ABTS color formation and detection at 405 nm. Single dots are means for technical triplicates of three independent biological replicates, the bars represent the average of all measurements. Full-length IbpM in green, truncated IbpM in reddish, and HSE in grey. Values from IgG measurement in the graphic are representative as well for IgA and IgM.

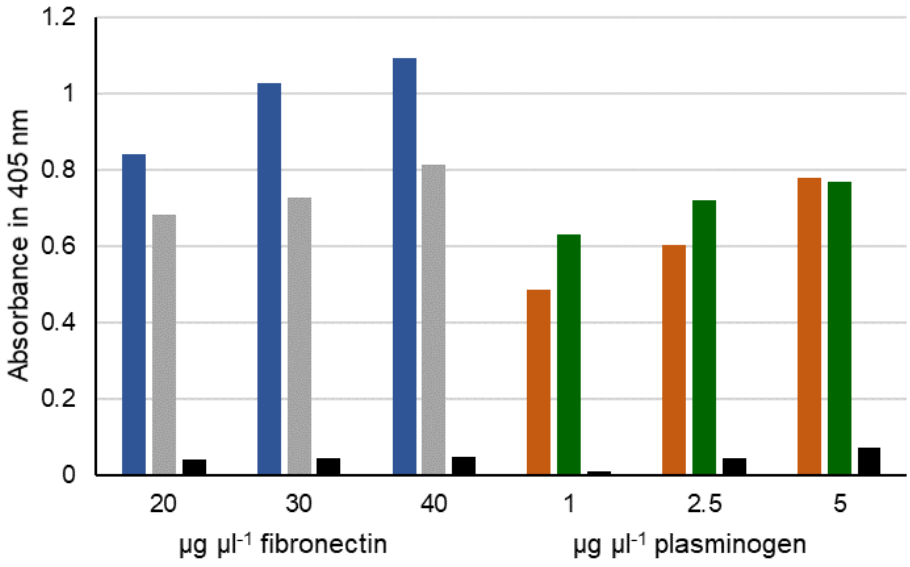

Figure 4.6 | Interaction of fibronectin and plasminogen with IbpM. Purified IbpM (blue and brown) or whole cells of *M. pneumoniae* (grey and green) were coated onto 96-well plates and incubated with different concentrations of fibronectin (left) or plasminogen (right). Interaction of IbpM with the human proteins was quantified with peroxidase-conjugated antibodies detecting the corresponding human proteins. Absorbance was detected at 405 nm. BSA (black bars) served as negative control.

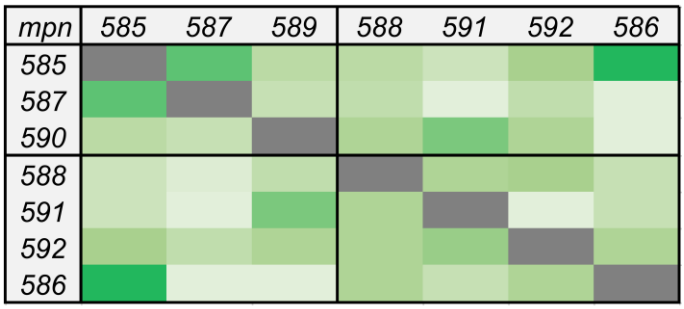

Figure 4.7 | Amino acid identity heat-map of *M. pneumoniae* DUF31 proteins. Protein sequences were aligned and compared using BLASTp. Amino acid sequences that covered at least 24% (up to 99%) of the proteins were used to detect identical residues, grouped by their identity and color coded. Grey 100%, dark green >75%, medium green ~40% and light green <35% amino acid identity; white means no identity at all.

Analysis of putative immunoglobulin proteases in *M. pneumoniae*. The protease from the MIB-MIP system (Arfi *et al.*, 2016) was annotated as putative protease bearing a conserved domain of unknown function DUF31. We used the predicted domain DUF31 to scan the *M. pneumoniae* protein sequences for presence of similar domians. The function of this domain still remains elusive, but the amino acid sequence is similar to that of serine-proteases. We found sixteen proteins containing a DUF31 domain. Multiple genes encoding the DUF31-proteins localize in one hotspot of the *M. pneumoniae* genome (listed in Table 4.1). It is worth mentioning, that a similar comparison was done with many other Mollicutes and it seems, that only animal and human pathogenic *Mycoplasmas* encode such DUF31 containing proteins (Arfi *et al.*, 2016). Furthermore, the presence of multiple copies of DUF31 proteins was only found in species lacking the MIB-MIP system (Arfi *et al.*, 2016). This indicates that MIB-MIP and Protein M are mutually exclusive. However, we identified 17 genes containing the DUF31 domain ordered in one genomic locus encoded by the genes *mpn577, mpn580* to *mpn592* plus the paralogs *mpn083* and *mpn084*. We compared all selected proteases with each other resulting in a heat map representing the amino acid identities (see Fig. 4.7). Further experiments either failed to express these proteins in *E. coli* or no specific activities against Igs could be detected. We also used the MIB-MIP system to test whether IbpM can substitute for the MIB binding protein from *M. mycoides*, but no binding to MIP, nor MIP activity could be reported when MIB was exchanged by IbpM (data not shown).

Table 4.1 | Genes encoding DUF31 domains of *M. pneumoniae.*

Gene	Motif/Domain	Size (bp)	Location*/Information
mpn083	Peptidase S7	1602	membrane-external
mpn084	Peptidase S7	1575	membrane-external
mpn577	Peptidase S7	1041	cytoplasm
mpn580	Peptidase S7	423	cytoplasm
mpn581		798	cytoplasm
mpn582	Peptidase S7	1320	membrane-external
mpn583		678	cytoplasm
mpn584	Peptidase S7	408	cytoplasm
mpn585		909	membrane-external
mpn586	GS**S**GS/Peptidase S7	1044	membrane-external
mpn587		453	membrane-external
mpn588	GS**S**GS/Peptidase S7	1596	membrane-external, [#]
mpn589	Peptidase S7	474	cytoplasm
mpn590		654	membrane-external
mpn591	GS**S**GS/Peptidase S7	1062	membrane-external, [#]
mpn592	GS**S**GS/Peptidase S7	1566	membrane-external, [#], [+]

*predicted; [#]Hallamaa *et al.*, 2008; upregulated after A549 contact; [+]similar to v8 protease (PDB: 1WCZ) from *S. aureus;* GS**S**GS conserved catalytic serine, all putative proteases encode DUF31 domains.

DISCUSSION

After successful adherence to epithelial cells, bacteria are exposed to the defense mechanisms of the human host, mainly cell-mediated and humoral immunity. The latter includes antibody-dependent cellular cytotoxicity (ADCC) and activation of complement proteins. The complement can detect antibody-antigen labelled complexes (opsonization) and consequently trigger a degradation cascade for bacterial clearance. To overcome opsonization, phagocytosis, cell lysis and successfully infect host tissue, bacteria must subvert or manipulate the innate immune system. There are two possibilities, on one hand they could modulate effectors required for detection and degradation of bacterial antigens while on the other hand they could evade mode the recognition by neutrophils and macrophages in a stealth-like (reviewed in Reddick and Alto, 2014; van Avondt *et al.*, 2015).

In this study, we showed the surface localization of IbpM (MPN400) via three different approaches: colony blot, trypsin digestion and immunofluorescence microscopy. Furthermore, we demonstrate binding of IgG, IgA, and IgM to recombinant IbpM with ELISA experiments. Additionally, we also tested and confirmed the binding capabilities to human

plasminogen and fibronectin, which are required for innate immune response against bacterial infection. The C-terminal domain of the IbpM homolog in *M. genitalium* was thought to be not influencing the binding of Igs (Grover *et al.*, 2014) but a truncated version of IbpM showed already a reduced binding affinity. However, the function of the C-terminal domain remains elusive. As discussed earlier (Grover *et al.*, 2014), after binding of IbpM the C-terminal domain could allow to cover the antigen-binding site and therefore hinder antigen-antibody union. Such a masked Ig could not be detected by the complement or in turn an Ig-wrapped *Mycoplasma* cell could be barely detectable for the host defense mechanism. Lastly, strong binding of IgG by IbpM could invert the effect of opsonization and prevent ADCC (Wang *et al.*, 2015) hindering natural killer cells to eliminate *Mycoplasma* cells. These ideas are in agreement with the chronicity of *Mycoplasma* infection and low mortality rates. To test this hypothesis infection assays in animal models with wild type cells, mutants of IbpM (truncation) and a knock-out mutant seem to be indispensable. This further analysis would elucidate the function of IbpM in virulence of *Mycoplasma* and the responsibilities of the different domains in these processes.

We evaluated proteases in *M. pneumoniae*, based on the described MIB-MIP system from *M. mycoides* (Arfi *et al.*, 2016). Our results revealed the presence of several DUF31 containing proteases in the genome of *M. pneumoniae.* However, either expression failed, or specific Ig activity was not detectable for selected proteases. Furthermore, partial cleavage of Ig without fragment release could be barely detectable (Brezski *et al.*, 2009). We cannot exclude the possibility that an Ig-specific protease is encoded in the genome of *M. pneumoniae.* The protease needs maybe an equivalent binding order as described for *M. mycoides* for being active. In *M. mycoides* the protease is only active when Igs are in a complex with the binding protein already (Arfi *et al.*, 2016). Thus, we would need a proper expression of putative proteases before testing the Ig-specificity *in vitro*. However, it would be interesting if any of the proteases contributes to the virulence of *M. pneumoniae* even if not involved in Ig degradation. Proteases are known to impact the pathogenicity of bacteria, *e.g*. the proteases InhA and ClpX of *Bacillus anthracis* contribute to invasion and survival of the pathogen in host tissue (McGillivray et a., 2009; Tonry *et al.*, 2012). Moreover, we show the binding of fibronectin and plasminogen to IbpM. For surface displayed proteins and lipoproteins in *M. pneumoniae* and other *Mycoplasma* species, the binding of plasminogen and fibronectin was already described (Chen *et al.*, 2018b; Gründel *et al.*, 2016a; Gründel *et al.*, 2016b; Guo *et al.*, 2017; Hagemann *et al.*, 2017; reviewed in Henderson *et al.*, 2011; Yavlovich *et al.*, 2004; Qi *et al.*, 2018) The binding of plasminogen could be mediated by interactions between the Kringle domains of human plasminogen and the leucine-rich repeat (LRR)-like structure in IbpM (see Fig. 4.1B), as the affinity of these domains towards lysine-residues is well known (Bhattacharya *et al.*, 2012; Sanderson-

Smith *et al.* 2012). Furthermore, the binding of IbpM to host cell components could be important for cell invasion (Dallo and Baseman, 2000). Cell migration through tissue barriers involving LRR-containing proteins is already known. For example, *Listeria monocytogenes* uses InlB, one LRR containing protein, that induces phagocytosis (Marino *et al.*, 1999; Shen *et al.*, 2000). *M. pneumoniae* is thought to be an extracellular pathogen, but it was show, to survive and replicate intracellular as well (Dallo and Baseman, 2000). Further, we could think of a dual mechanism by which the Ig binding is needed, besides plasminogen interaction, for enhanced epithelial crossing. The translocation of extracellular bacteria across the epithelium into the inner space of a cell and the bloodstream was shown in experiments with *Shigella flexneri.* The pathogenic bacteria were coated with secretory IgA and subsequently translocated from host cells without immune exclusion (Kadaoui and Corthésy, 2007). However, the binding of plasminogen to IbpM is tempting to speculate that *M. pneumoniae* already lost the MIP homolog during evolutionary genome minimization. The protease is might replaced by an Ig-specific protease from the human host, *e.g.* the plasmin (active form of plasminogen). Plasmin shares 48% amino acid similarity to serine proteases and is known to cleave IgG (Chuba, 1994; Harpel *et al.*, 1989). In addition, the activation of plasminogen to plasmin, was already shown with different surface proteins of *M. pneumoniae* (Gründel *et al.*, 2015; Hagemann *et al.*, 2017). Moreover, binding of plasminogen and fibronectin for themselves could be important. After binding of fibronectin or plasminogen their activated forms can modulate the complement system which would allow *Mycoplasmas* to survive in host tissue (Barthel et la., 2012; Foley *et al.*, 2016). The use of host derived enzymes to circumvent detection and elimination has been described and summarized for Gram-positive and Gram-negative bacteria (Bhattacharya *et al.*, 2012).

In conclusion, IbpM was confirmed as a surface located multi-immunoglobulin binding protein with affinity for plasminogen and fibronectin. With this, IbpM exhibits all important abilities to subvert the host immune system. Beside other mycoplasmal lipoproteins that facilitate surveillance in the host (Chambaud *et al.*, 1999; Citti and Rosengarten, 1997; Goret *et al.*, 2016), IbpM is a new target for better understanding virulence of *M. pneumoniae.* The functions of IbpM *in vivo* and its implication in virulence, especially potential immunomodulatory effects need to be elucidated in the future. Testing the *mpn400*-deficent mutant in comparison with the wild type in animal models seem to be important. IbpM is an optimal target for developing a vaccine against *M. pneumoniae* and IbpM could be industrially relevant for high affinity immunoglobulin purification.

SUPPLEMENTAL MATERIAL

Acknowledgements. We are grateful to Kerstin Schmitt and Oliver Valerius for initial MS-analysis of a pull down experiment. We want to reward Johannes Gibhardt and Julia Busse for helpful discussions and technical assistance. For carefully proof-reading the manuscript a great thank to Katrin Gunka and Miriam Dormeyer.

Funding. Results have been achieved within the framework of the ERASynBio 2nd Joint Call for Transnational Research Projects: "Building Synthetic Biology Capacity Through Innovative Transnational Projects" with funding from the corresponding ERASynBio National Funding Agencies.

CHAPTER 5 | Peroxide detoxification in *Mycoplasmas*

How to get rid of Peroxides? The Detoxification System and its Regulation in *Mycoplasma pneumoniae*

Cedric Blötz[1], Larissa Krüger[1], Anika Kahle[1], Neil Singh[1], Tenzin Tapkey[1], Achim Dickmanns[2], Eva Yus[3], Julia Busse[1], Luis Serrano[3], and Jörg Stülke[1]

[1]Department of General Microbiology, University of Göttingen, Germany
[2]Department of Molecular Structural Biology, University of Göttingen,
[3]Centre for Genomic Regulation (CRG), The Barcelona Institute for Science and Technology

AUTHOR CONTRIBUTION

CB, LK, and JS designed the study. CB and LK cloned plasmids and prepared protein overexpression. CB performed FOX assays. NS and LK performed MPN drop dilution assays. JB cultivated cells and isolated RNA and performed RT-PCR. CB evaluated all collected data. AK produced single KO-mutants of *B. subtilis*. CB and JB performed *B. subtilis* complementation and drop dilution assays. TT created MPN complementation strains. CB and LK created MPN deletion mutants. EY collected transcriptomic data for the *fur*-mutant under different conditions. CB and JS wrote the manuscript.

ABSTRACT

Mycoplasma species are near-minimal pathogenic bacteria, known to produce hydrogen peroxide (H_2O_2) as virulence determinant. The cells do not have to cope only with metabolism derived H_2O_2, they are also exposed to host-derived reactive oxygen species, which are produced as defense mechanism. Even though, some rare examples of detoxification enzymes protecting from damage of reactive oxygen species (ROS) were described for *Mycoplasmas*, no common detoxification enzyme, such as a catalase or a superoxide dismutase, is encoded in the genomes of *Mycoplasma pneumoniae*. In this study, we examined the function of two enzymes putatively facilitating ROS-resistance in *M. pneumoniae*. These are encoded by the genes *mpn625* and its homolog *mpn668*. Moreover, we investigated the possible regulation of these genes upon peroxide stress and potential regulating mechanisms. We could show that MPN625 binds and degrades H_2O_2, while MPN668 is mainly responsible for organic peroxide detoxification. Furthermore, our results show that internal H_2O_2 production induces the expression of *mpn668* while external *tert*-butyl hydroperoxide stress did not alter the expression of both genes. In addition, we identified the intertwining of the trigger enzyme GlpQ and the major protein kinase PrkC in the detoxification system. Overall, our study provides new insights into the ability of *M. pneumoniae* to cope with oxidative challenges.

INTRODUCTION

Several Gram-positive bacteria and naturally genome-reduced bacteria of the genus *Mycoplasma* have recently come into focus of scientific interest. For systems and synthetic biology *Mycoplasma pneumoniae* and *Mycoplasma genitalium*, become more and more important. *M. pneumoniae* and *M. genitalium* encode only 694 and 420 genes, respectively, representing the smallest viable organisms living independent from its host (Lluch-Senar *et al.*, 2015; Fraser *et al.*, 1995; Dandekar *et al.*, 2000; Himmelreich *et al.*, 1996). Both species are human pathogens, *M. pneumoniae* infects respiratory epithelial cells and *M. genitalium* the urogenital tract (Waites and Talkington, 2004; McGowin and Totten, 2017). For virulent bacteria it is a key feature to produce virulence factors as toxins, adhesion machineries or toxic metabolites (Balish and Distelhorst, 2016). For *Mycoplasma* a CARDS toxin is described but the influence on *in vivo* pathogenicity is still under investigation (Bose *et al.*, 2014; Kannan and Baseman, 2006). A major factor enabling virulence in most of all *Mycoplasma* species are toxic metabolites, including hydrogen peroxide (H_2O_2) and hydrogen sulfide (H_2S) (Großhennig *et al.*, 2016; Hames *et al.*, 2009). *Mycoplasma* species can use glycerol or glycerol-containing compounds, such as glycerol phosphocholine (host derived lipids) in their carbon metabolism to produce toxic amounts of H_2O_2 (Blötz and

Stülke, 2017). Hydrogen peroxide can be used as defense mechanism against other competing bacteria or as a targeted weapon to destroy human cells. Interestingly, for *Mycoplasma mycoides* a mechanism of H_2O_2 injection into host cells is described (Pilo *et al.*, 2007), emphasizing the role of H_2O_2 in mycoplasmal pathogenicity. H_2O_2 belongs with several other harmful molecules, such as superoxide anions (O_2^-) and hydroxyl radicals (·OH), to the group of reactive oxygen species (ROS). In the presence of transition metals, *e.g.* Fe^{2+}, Cu^{2+}, or Mn^{2+}, H_2O_2 can react in the Fenton reaction to O_2^-, OH and the corresponding oxidized metal ion. *Vice versa*, molecular oxygen can be converted into O_2^- by the addition of one electron, furthermore, O_2^- can react with H_2O_2 to form hydroxyl radicals. Therefore, ROS are highly reactive molecules. This reactivity is caused by unpaired electrons that react with nearly all cellular components, including DNA, proteins and lipids. The destructive influence of ROS towards DNA is well known (Gusarov and Nudler, 2005). Several modifications as single- or double stranded DNA-breaks, deletions or other mutations can be induced by ROS. Furthermore, ROS can cross-link proteins onto DNA, adding a steric blockade to abort transcription and replication (Tretyakova *et al.*, 2015). ROS stress can also lead to oxidation or degradation of proteins. Especially proteins associated with metals and thiol group containing amino acids (cysteine, methionine) are prone to oxidation. Membrane damage induced by ROS can lead to lipid peroxidation (Becerra *et al.*, 2006) and in consequence the inactivation of membrane-bound receptors or increased membrane permeability. With this high degenerative potential, H_2O_2 and related ROS are powerful poisons for living cells. Protective mechanisms against ROS seem to be indispensable for any living organism. This raises the question how *Mycoplasmas* protect themselves from ROS, either produced from their own metabolism or as a defense mechanism sequestered from the attacked host (Blötz and Stülke, 2017; Sun *et al.*, 2008).

There are two ways to protect cellular components. First, the repair or reversion of ROS damaged targets. Second, the direct elimination of ROS. The repair or reversion of damaged cell components is happening continuously in cells but could already influence metabolism or surveillance. Therefore, direct degradation of ROS is the preferred protection route, which is achieved by antioxidants. These compounds can reduce ROS to less harmful molecules. Antioxidants can be either non-enzymatic, exemplified by several vitamins (C, E or carotenoids) and glutathione or enzymatic antioxidants. These enzymes can be very different regarding their catalytic mechanism, their localization, regulation on transcriptional level (Knoops *et al.*, 2011) as well as on protein level (Rhee and Woo, 2011). The most prominent examples are catalases, superoxide dismutases (SOD) and peroxidases (*e.g.* glutathione or thioredoxin dependent peroxidases). After bacteria sense ROS, general and specific stress responses are activated (Imlay, 2008; Mols and Abbee,

2011; Zhao and Drlica, 2014). Bacteria evolved several systems to detect harmful ROS and activate a specific protective function. In most bacteria, the presence of H_2O_2 or O_2^- are predominantly detected by OxyR and SoxR. The oxidation of the transcriptional activators leads to conformational changes enabling the proteins to bind to promoter regions of ROS protective enzymes, enhancing their expression (Christman *et al.*, 1985; Dietrich *et al.*, 2008; Imlay, 2015; Nunoshiba *et al.*, 1992; Zheng, *et al.*, 1998). In a few cases OxyR can function also as a transcriptional repressor (Heo *et al.*, 2010; Loprasert *et al.*, 2000; Teramoto *et al.*, 2017). Interestingly, *B. subtilis* uses a different transcription factor PerR to respond peroxide stress (Bsat *et al.*, 1996). PerR is a H_2O_2 sensitive transcriptional repressor, which belongs to the Fur protein family. Other members of this family are responsible for metal ion homeostasis, *i.e*. Fur for iron or Zur for zinc (Fillat, 2014; Helmann, 2014). PerR is highly sensitive to H_2O_2 in its Fe-bound state, not acting any longer as repressor when oxidized (Lee and Helmann, 2006; Ma *et al.*, 2011). Even if the proteins are very similar, the Fur protein of *B. subtilis* is insensitive to H_2O_2 oxidation (Parent *et al.*, 2013). However, the detoxification of ROS and its regulation in *Mycoplasmas* is an underrepresented research topic so far.

Interestingly, many *Mycoplasma* species produce ROS in high amounts, especially hydrogen peroxide, but no protecting enzymes have been identified until recently, a catalase was characterized in *Mycoplasma iowae* (Pritchard *et al.*, 2014) and SOD activity was described for *Mycoplasma hyopneumoniae* (Chen *et al.*, 2000; Machado *et al.*, 2009). In the genomes of *M. iowae, Mycoplasma haemofelis,* and *Mycoplasma haemocanis* genes very similar to genes encoding for SODs from *Bacilli* were identified (Berent and Messick, 2003; do Nasciemento *et al.*, 2012; Wei *et al.*, 2012). Furthermore, several *Mycoplasma* species were sequenced and showed the presence of putative peroxiredoxins, *i.e. ohr* and *osmC* homologs (Atichartpongkul *et al.*, 2001; Machado *et al.*, 2009). Peroxiredoxins (Prx) represent a group of ubiquitous distributed enzymatic antioxidants, only excluded from *Borrelia* species. Overall these enzymes share a similar folding and the mechanism to reduce various peroxides to the corresponding alcohols. These proteins contain a conserved cysteine, as reducing residue Cys^P (peroxidatic cysteine) which is regenerated by another protein/molecule or a resolving cysteine (Cys^R) from a second Prx. The known bacterial peroxiredoxins can be grouped into three main classes, 1-Cys, typical 2-Cys (intermolecular disulfide bonds), and atypical 2-Cys (intramolecular disulfide bonds) peroxiredoxins. More specifically Prx can be sorted into six subfamilies, Prx1 (typical 2-Cys), Prx5, Prx6, Tpx, PrxQ, and AhpE due to their mechanism, localization or the respective reducing agent (Chae *et al.*, 1994; Hall *et al.*, 2009; Nelson *et al.*, 2011). Prx enzymes were identified in different *Mycoplasma* species besides *M. pneumoniae*, but their classification is still controversial. Only few mycoplasmal Prx enzymes have been

investigated in more detail so far. The Tpx enzyme of *M. hyopneumoniae,* classified as atypical 2-Cys peroxiredoxin containing only the Cys^P (lost the Cys^R), was shown to protect DNA from ROS-damage (Machado *et al.* 2009; Gonchoroski *et al.*, 2017). This class of enzymes seems to be conserved only among animal infecting *Mycoplasmas*, but there is no homolog in *M. pneumoniae* or *M. genitalium*. Moreover, little is known about the detoxification system in *M. pneumoniae* or *M. genitalium*. Both species are human pathogens, infecting lung epithelia or the urogenital tract, respectively. Recently, *in vitro* characterization of MPN668 from *M. pneumoniae* revealed organic hydroperoxidase activity (Chen *et al.*, 2018a), but the detailed mechanisms and regulation of ROS detoxification remain unknown. Transposon mutants of the *ohr* gene of *M. genitalium* (MG_454) were sensitive to organic hydroperoxides (OHP) and ectopic gene expression in the foreign host *Pseudomonas aeruginosa* can complement an *ohr* deletion (Saikolappan *et al.*, 2009). The MG_454 expression was significantly upregulated upon physical stresses but not under peroxide stress. In contrast, *ohr* homologs of *Xanthomonas campestris* (Mongkolsuk *et al.*, 1998), *P. aeruginosa* (Atichartpongkul *et al.*, 2001), and *B. subtilis* (Fuangthong *et al.*, 2001; Helmann *et al.*, 2003) are highly and specifically upregulated upon OHP stress. Furthermore, genes for an osmotically inducible protein C (*osmC*) were identified in *Mycoplasmas* to contribute to the detoxification of peroxide stress. A deletion mutant of the *osmC* homolog (MG_427) in *M. genitalium* was shown to be hypersensitive towards peroxides (Zhang and Baseman, 2014). Overall, the mechanisms involved in detoxification of ROS and their regulation are poorly understood in *Mycoplasma* species. The few reports on the existence of proteins involved in the degradation of peroxides in *Mycoplasma* were the driving force to identify enzymes in *M. pneumoniae* involved in the detoxifying pathway sensing different ROS species and counteracting their toxic nature. To unravel the ROS sensing and defense mechanisms in *M. pneumoniae in vitro* and *in vivo*, the putative OsmC/Ohr homologs MPN625 and MPN668 as well as well as the putative Fur homolog MPN329 of *B. subtilis* were investigated.

MATERIALS AND METHODS

Bacterial strains, transformation, and growth conditions. The *M. pneumoniae* strains used in this study were *M. pneumoniae* M129 (ATCC 29342) and its mutant derivatives listed in Table 5.1. *M. pneumoniae* was transformed by electroporation as described (Halbedel *et al.*, 2004) and grown in modified Hayflick medium (Halbedel *et al.*, 2004) or on Blood Agar Plates at 37°C. *Escherichia coli* strains XL1blue and BL21 were used for transformation of plasmids and overexpression of proteins, respectively.

Table 5.1 | *Mycoplasma* and *Bacillus* strains used in this study.

Name	Description	Construction	Reference
Mycoplasma pneumoniae M129			Laboratory collection
GPM11	*prkC*::Tn (*Gm*^{R})	pMT85 → M129	Schmidl *et al.*, 2010a
GPM14	Δ*ptxA::loxE* Δ*mpn668::loxE*	pBSKCre → GPM16	This work
GPM15	Δ*ptxA::loxE* Δ*mpn625::Cm*^{R}	ssDNA of pGP2963→ GPM116	This work
GPM16	Δ*ptxA::loxE* Δ*mpn668::Cm*^{R}	ssDNA of pGP2964→ GPM116	This work
GPM18	Δ*ptxA::loxE* Δ*mpn329/fur::loxE*	1. ssDNA of pGP3240 → GPM116 2. GPM116* → pBSKCre	This work
GPM45	Δ*ptxA::loxE* Δ*mpn625::Cm*^{R} P$_{MG438}$-*mpn625* (*tetM*)	pGP1899 → GPM15	This work
GPM46	Δ*ptxA::loxE* Δ*mpn668::Cm*^{R} P$_{MG438}$-*mpn668* (*tetM*)	pGP1900 → GPM16	This work
GPM81	*glpQ*::Tn (*Gm*^{R})	pMT85 → M129	Schmidl *et al.*, 2011
GPM116	*arcA*::GP35 recombinase Δ*cards/ptxA::loxE*		Piñero-Lambea *et al.*, unpublished
Bacillus subtilis 168 *trpC2*			Laboratory collection
GP1726	Δ*katA::zeo*	LFH → 168	This work
GP1727	Δ*ohrA::tet*	LFH → 168	This work
GP1728	Δ*ohrB::spec*	LFH → 168	This work
GP3153	Δ*ohrA::tet* Δ*ohrB::spec*	GP1728 → GP1727	This work
GP3154	Δ*katA::zeo* Δ*ohrA::tet* Δ*ohrB::spec*	GP1726 → GP3153	This work
GP3167	Δ*katA::zeo* Δ*ohrA::tet* Δ*ohrB::spec* P$_{xyl}$-EV (*kan*)	pGP888 → GP3154	This work
GP3168	Δ*katA::zeo* Δ*ohrA::tet* Δ*ohrB::spec* P$_{xyl}$-*mpn625* (*kan*)	pGP3274 → GP3154	This work
GP3170	Δ*katA::zeo* Δ*ohrA::tet* Δ*ohrB::spec* P$_{xyl}$-*mpn668* (*kan*)	pGP2202 → GP3154	This work

***loxE* indicates the reversion of the chloramphenicol resistance cassette (Cm^R) with the suicide plasmid pBSKCre; Gm^R, gentamicin resistance; *tetM/tet*, tetracyline resistance; zeo, zeocin resistance; spec, spectinomycin resistance; kan, kanamycin resistance.

DNA isolation and plasmid construction. *M. pneumoniae* chromosomal DNA was isolated using the peqlab Blood & Tissue Kit following the manufacturer's protocol. The sequences of the oligonucleotides used in this study are listed in Table S5.1 and plasmids are listed in Table S5.2. Briefly, amplified and purified PCR fragments were digested with

the appropriate restriction enzymes and ligated into the digested plasmid backbone (as indicated in Table S5.1 and S5.2). Plasmids were introduced into *E. coli* DH5α by transformation (Sambrook *et al.*, 1989). For modified genes the multiple mutation reaction was used to exchange codons (Hames *et al.*, 2005). For this purpose, mutational primers (5´-phosphorylated oligonucleotides) were used to exchange the respective codons in a PCR reaction. Resulting plasmids were checked by control digestion, PCR and sequencing.

Clean-deletion of *M. pneumoniae* genes. To delete the genes of interest (*mpn625*, *mpn668*, *mpn329*) we amplified 500 bp on both sites, upstream and downstream of each gene and fused them to the chloramphenicol resistance cassette, encoded on the plasmid pGP2727, flanked by *lox* sites. In a second attempt, we exchanged the resistance marker into the *tetM*-resistance cassette. The resulting plasmids were used to amplify double stranded DNA, where the two strands were tagged differently. One strand must be protected (for further transformation of *Mycoplasma*) and the second one is tagged with biotin. The biotin tag allows the separation of the two strands with magnetic beads under basic conditions. The protected ssDNA is purified, dried and re-suspended in electroporation buffer. The ssDNA was transformation substrate for the deletion of genes in the strain GPM116 (harboring GP35 recombinase (*mpn560*)-*arcA*::GP35-Puro^{R}). After successful deletion of the genes, we also excised the chloramphenicol cassette by transformation with the suicide plasmid pBSK-Cre, which is lost after one generation. The expressed Cre recombinase is sensitive towards *lox*-sites flanking the resistance cassette and excises these leaving a scar called *loxE*. Gene deletions and excision of the chloramphenicol/ tetracycline cassettes were confirmed by PCR and sequencing.

Growth curves. The defined amount 0.25 mg freshly grown cells (wet weight) of *M. pneumoniae* strains were used to inoculate several flasks (2 technical replicates/3 biological replicates) to monitor the growth with different carbon sources. After different time points (days: 2, 3, 4, and 7) the cell layer was recovered, and the wet weight measured.

Drop dilution assays. *M*. *pneumoniae* strains were cultivated and collected in 1x PBS buffer (137 mM NaCl, 2.7 mM KCl, 10 mM Na_2HPO_4, 1.76 mM KH_2PO_4, pH7.4) and adjusted to an OD_{600} of 0.5. The cells were stressed with different concentrations of H_2O_2 and *tert*-butyl hydroperoxide (0, 5, 25, 50, 100 mM). Cells were incubated for 60 min at 37°C. From the incubated cells 1:10 dilutions (up to 10^{-3}) were prepared. 6 µl of the cell suspension were spotted onto MP-agar plates and incubated for several days.

Protein purification. The transformed *E. coli* (BL21) strains harboring the expression plasmids were pre-cultured in LB over night at 28°C, next day cells were grown in 2x LB

(per liter: 20 g tryptone, 10 g yeast extract, 10 g NaCl) at 37°C and 220 rpm in baffled flasks, to an OD_{600} of 0.8 and induced for 3 h with 1 mM IPTG. Cells were pelleted at 5 000 rpm at 4°C for 15 minutes. The pellet was washed once with 1x ZAP buffer (200 mM NaCl and 10 mM Tris-HCl, pH7.5) containing 50 mM imidazole and frozen at -20°C till cell disruption. Cell disruption was carried out using a French Press (3x, 18 000 psi). Pellets were resuspended in 1x ZAP + 50 mM imidazole and 1 mM DTT. Crude cell extracts were centrifuged for 30 minutes at 35 000 rpm at 4°C and subsequently used for Ni-affinity purification of the 6x His-SUMO-tagged proteins. Ni-affinity purification was done as described earlier (Mehne *et al.*, 2014). Briefly, 8 ml 50% Ni-sepharose (IBA, Göttingen) was equilibrated with 10 column volumes of 1x ZAP + 50 mM imidazole, crude extracts were run through the columns, and the columns were washed with 2.5 column volumes of 1x ZAP + 50 mM imidazole. Elution of the purified proteins were archived by applying 2 column volumes of ZAP buffer with 500 mM imidazole. From each fraction, samples were checked by SDS-PAGE. Purified proteins were dialyzed with 1x ZAP to get rid of the excess of imidazole. Afterwards, His-SUMO-proteins were incubated with SUMO protease (Mossessova and Lima, 2000) in the ratio 1:100 at 28°C for 12 hours to cleave the His-SUMO-tag from the native protein. The SUMO protease as well as the His-SUMO-tag were pulled out of the mixture by applying the samples again on Ni-sepharose columns. Native proteins were collected as flow through, dialyzed in the identical buffer 1x ZAP and frozen in liquid nitrogen, stored at -80°C till use.

Triton-X-100 separation. Fresh pellets of *M. pneumoniae* GPM45 and GPM46 (complementation strains of *mpn625* and *mpn668* deletion mutants) were resuspended in 1 ml of 1% Triton buffer (1% Triton X-100 in 1x PBS) and incubated at 10°C for 2 h, at 1000 rpm. The cell debris are pelleted by centrifugation at 14,000 rpm for 10 min at 4°C. The supernatant was transferred to a fresh tube. The treatment separated the fraction containing most of the membrane-associated proteins from the cytosolic proteins. Samples were subsequently used for Western blot analysis.

Enzymatic assays. First, we used Quantofix® peroxide test stripes (Merck, Darmstadt, Germany). For this purpose, the respective enzymes were adjusted to 10 µM (unless otherwise indicated) in 1x ZAP buffer (200 mM NaCl and 10 mM Tris-HCl, pH7.5) including 10 µM DTT. Reactions were started with the addition of peroxides (200 µM). Controls were prepared equally, leaving out the enzyme or peroxide of the reactions, respectively. At different time points, 10 µl samples were taken and applied onto the test stripe. Color development of the test stripe indicates the amount of remaining peroxide in solution by

intensity of the visible color. The color formation was subsequently evaluated by visulal comparison with the color scale from the munufacturer.

In a second approach, the ferrous oxidation xylenol orange (FOX) assay was used to quantify degradation of peroxides (Nelson and Parsonage, 2011). Briefly, FOX indirectly monitors the decreasing peroxide concentrations, using Fe^{2+} and xylenol orange. Under acidic conditions, Fe^{2+} is oxidized by peroxides to Fe^{3+} reacting with xylenol orange to a blue-purple complex, which is detected at 560 nm. Standard curves were created determining peroxide concentrations, by measuring different peroxide concentrations (0 µM, 50 µM, 100 µM, 200 µM, 300 µM; 400 µM, and 500 µM). The activity assay was set up in a reaction tube containing enzyme, DTT (100 µM), H_2O_2 or tBP (500 µM) in 1x ZAP buffer. Reactions were initiated by adding of 20 µM enzyme and incubated at 25°C. At time intervals, 20 µl aliquots were removed, added to 180 µl of FOX working reagent (mixture of 1:10 FOX-A and FOX-B; FOX-A: 25 mM ammonium ferrous sulfate in 2.5 M H_2SO_4 and FOX-B: 100 mM sorbitol and 125 µM xylenol orange), incubated at room temperature for 30 min, subsequently the absorbance was measured at 560 nm. (adapted from Nelson and Parsonage, 2011).

Isothermal titration calorimetry (ITC). For determination of binding isotherms of MPN625, MPN668, and their respective peroxidatic cysteine (C^P, MPN625:C52S and MPN668:C55S) or their resolving cysteine (C^R, MPN625:C115S and MPN668:C119S) mutants, as well as BSA and bovine catalase were dialyzed in the same buffer (1x ZAP) containing 200 mM NaCl and 10 mM Tris-HCl, pH7.5. The isotherms were recorded at 20°C. ITC experiments were carried out with a VP-ITC microcalorimeter (Microcal). The protein concentrations were 10 µM in the sample cell and 100 µM in the injection syringe. Data were analyzed with Origin 7.0, and linear fitting curves were applied.

Real-time PCR. For RNA isolation, cells were grown to confluency in MP-medium with either glucose or glycerol. Afterwards, cells were resuspended for 30 min in fresh MP-medium with glucose or glycerol for glycerol-grown cells. Glucose-gown cells were stressed with hydrogen peroxide (5 mM), *tert*-butyl hydrogen peroxide (5 mM). Stressed cells were collected subsequently in RNA lysis buffer, delivered by the RNeasy Midi Kit (Qiagen). RNA isolation was carried out using the manufacturers protocol followed by DNase I digestion for 30 h at 37°C (25 µl set-up: 2.5 µg RNA; 2.5 µl 10x DNase I buffer; 5 µl DNase I), inactivation for 10 min at 75°C and control PCRs for the cleaning of any remaining DNA. RNA concentrations were measured via NanoDrop and samples stored at -80°C. qRT-PCR was carried out on an iCycler instrument (Bio-Rad) following the manufacturer's recommended protocol by using the oligonucleotides indicated in Table S5.1. The *rpoB* and

rpsL genes encoding constitutively expressed RNA polymerase β-subunit and the 30S ribosomal protein S12, respectively, were used as internal controls. Data analysis and the calculation of expression ratios as fold changes were performed as described by Diethmaier *et al.* 2011. qRT-PCR experiments were performed in biological duplicates.

Bacterial two-hybrid assay (BACTH). Primary protein-protein interactions were identified by bacterial two-hybrid (B2H) analysis (Karimova *et al.*, 1998). The BACTH system is based on the interaction-mediated reconstruction of *Bordetella pertussis* adenylate cyclase (CyaA) activity in *E. coli*. Functional complementation between two fragments (T18 and T25) of CyaA as a consequence of the interaction between bait and prey molecules results in the synthesis of cAMP. The reporter gene encoding for the β-galactosidase is fused to the cAMP dependent CAP (cAMP-catabolite gene activator protein) promotor which allows indirect detection of the protein-protein interaction by measuring the β-galactosidase activity. Plasmids pUT18/pUT18C and p25N/p25 allow the expression of proteins fused to the C- or N-terminal T18 and T25 fragments of CyaA, respectively. For these experiments, we constructed the plasmids pGP2949 – pGP2960. DNA fragments corresponding to the genes *mpn625*, *mpn668, glpQ* and *mpn566* were obtained by PCR, digested and ligated into the vectors pUT18/pUT18C and p25N/p25 (for primers and restriction enzymes, see Table S5.1). These plasmids were used for co-transformation of *E. coli* BTH101, and the protein-protein interactions were then analyzed by plating the cells on LB plates containing 100 µg ml^{-1} ampicillin, 50 mg ml^{-1} kanamycin, 80 mg ml^{-1} X-Gal (5-bromo-4-chloro-3-indolyl-β-D-galactopyranoside), and 1 mM IPTG. The plates were incubated for a maximum of 36 h at 28°C.

Human bronchial epithelial cell (HBEC) cytotoxicity assay. Infection of HBEC cultures with *M. pneumoniae* cells was done as described previously for HeLa cells (Hames *et al.*, 2009; Schmidl *et al.*, 2010a). DMEM medium complemented with 10% FBS was used to grow cells. After four days post infection, HBEC cultures were stained with crystal violet (10 min fixation in 10% formalin; 150 µl 0.1% crystal violet solution for 30 min at RT; 3 times washing) and photographed. For quantification the surviving cells, disruption was carried out with 0.5% SDS solution. The OD_{595} served as indication for cell survival and therefore the cytotoxicity of *M. pneumoniae*.

METHODS FOR *BACILLUS* COMPLEMENTATION

Bacterial strains and growth conditions. *B. subtilis* strains were derived from the laboratory strain 168 (*trpC2*) and are listed in Table 5.1. *B. subtilis* was grown in SP medium (Kunst and Rapoport, 1995) or CE minimal medium supplemented with 40 mM MOPS and 0.5% glucose (CEM, Commichau *et al.*, 2008; Bsat *et al.*, 1996). CE minimal medium

contains 70 mM K_2HPO_4, 30 mM KH_2PO_4, 25 mM $(NH_4)_2SO_4$, 0.5 mM $MgSO_4$, 10 µM $MnSO_4$, 22 mg ferric ammonium citrate liter^{-1}, potassium glutamate (8 g liter^{-1}), tryptophan (50 mg liter^{-1}) and glucose (5 g liter^{-1}).

Construction of *B. subtilis* mutants. Deletion of the genes *ohrA*, *ohrB*, *katA* was achieved by transformation with PCR products constructed using oligonucleotides (see Table S5.1) to amplify DNA fragments flanking the target genes and intervening antibiotic resistance cassettes as described previously (Guérout-Fleury *et al.*, 1995; Wach, 1996). Mutants constructed in this work are listed in Table 5.1.

Transformation and phenotypic analysis. *B. subtilis* was transformed with plasmid or genomic DNAs according to the two-step protocol (Kunst and Rapoport, 1995). Transformants were selected on SP plates containing chloramphenicol (5 µg ml^{-1}), kanamycin (10 µg ml^{-1}), tetracycline (12.5 µg ml^{-1}), zeocin (35 µg ml^{-1}) or spectinomycin (150 µg ml^{-1}).

Construction of strains allowing controlled expression of *Mycoplasma pneumoniae* proteins. First, we constructed the plasmid pGP3273, an *amyE*-integrative plasmid, which allows the expression of proteins in *B. subtilis* under IPTG-inducible promoter. Briefly, the vector pHT01 (MoBiTec, Göttingen, Germany) was used as source for the *lacI*-operator-RBS unit and ligated into pAC5 (Martin-Verstraete *et al.*, 1992) with the enzymes SacI and BamHI. Finally, we constructed the plasmids pGP3274 and pGP3275 integrating in the *ganA* or *amyE* loci in *B. subtilis*, respectively. There, MPN625 or MPN668 can be expressing ectopically when xylose is added to the medium. We amplified the genes *mpn625* and *mpn668* from *M. pneumoniae* M129 chromosomal DNA with the oligos listed in Table S5.1. The genes *mpn625* and *mpn668* were digested with the restriction enzymes given in Table S5.1 and S5.2 and subsequently ligated into pGP884 (Gunka, 2011) and pGP3273, respectively, linearized with the same enzymes. The controlled expression of MPN625 and MPN668 in *B. subtilis* was verified by Western blotting (data not shown), using isogenic strains harboring 6xHis-tagged versions of *mpn625* or *mpn668* that were introduced into the respective loci with the plasmids pGP3276 and pGP3277 (used oligonucleotides in Table S5.1).

Western blotting. For Western blotting, *B. subtilis* strains were grown in CEM medium at 37°C. Induction was carried out when cells reached OD_{600} of 1. At different time points 2 ml samples were taken. The cells were disrupted using 100 µl lysozyme-DNase I mix (10 mg lysozyme, 1 mg DNase I ml^{-1}) in 900 µl 1xPBS. Disruption was done for 1 hour at 37°C and 400 rpm. The cell debris were pelleted by centrifugation (10 min, 4000 rpm, 4°C), and the

protein content of the supernatant was measured using Nanodrop. From each sample 10 µg total protein was mixed with SDS-loading buffer, boiled for 10 min at 95°C and separated in 12.5% SDS-polyacrylamide gels. After electrophoresis, the proteins were transferred to a polyvinylidene difluoride (PVDF) membrane (Bio-Rad) by electroblotting (80 mA/membrane, 1 hour). Proteins were detected using antibodies recognizing the 6xHIS tag (Sigma). The primary antibody was visualized by using α-rabbit IgG-alkaline phosphatase (AP) secondary antibodies (Promega) and the CDP* detection system (Roche Diagnostics) (Schmalisch *et al.*, 2002).

RESULTS

Structural modelling. For the structural prediction of MPN668 we used the crystal structure of the homolog MPN625 (PDB: 1LQL; Choi *et al.*, 2003) as template. In a second approach we used the available structure from *Vibrio cholerae* (3EER.1.A 36.23% identity), which was not significally different. We compared the overall folding of the modelled proteins. As shown in Figure 5.1A the modelled structure of MPN668 strongly resembles the crystal structure of the MPN625 dimer (Fig. 5.1B).

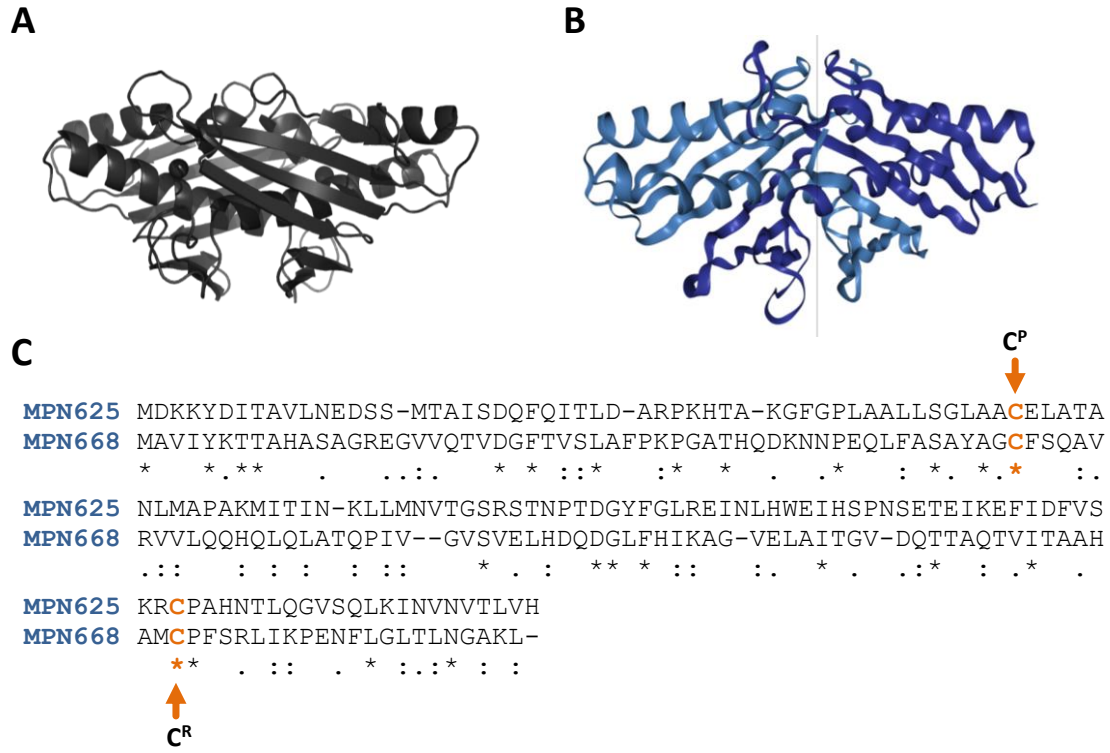

Figure 5.1 | Comparison of MPN625 and MPN668. (A) Structural modelling of MPN668 on the basis of the peroxiredoxin structure from *Vibrio cholerae* (3EER.1.A) and the structure from MPN625 (1LQL). (B) Crystal structure of MPN625 from *M. pneumoniae* (PDB: 1LQL; Choi *et al.*, 2003). (C) Amino acid comparison of MPN625 and MPN668 from *M. pneumoniae*. The highly conserved cysteine residues for peroxidatic activity (C^P) and regeneration (C^R) are highlighted in orange. * identical amino acids, **:** highly similar amino acids, **.** less similar amino acids.

The depicted structures show that there is near no difference in protein folding, even if the sequence of both proteins is different (16.5% identity, 46.9% similarity). The alignment of MPN625 and MPN668 shows the limited sequence conservation between both proteins (see Fig. 5.1C). However, MPN625 shares ~30% identity with related OsmC proteins, *e.g*. from *Enterococci* or *Bacilli.* MPN668 is up to 40% similar to Ohr homologs in *e.g*. *Mycobacteria*. Overall, MPN625 and MPN668, as well as their homologs in *M. genitalium*, contain two characteristically conserved cysteine residues. These residues are responsible for catalytic activity and regeneration in the Ohr/OsmC-protein family.

Interaction analysis. For the characterization of the OsmC/Ohr homologs MPN625/MN668 we were interested in the dimerization potential and interaction between both proteins. In the BACTH system, the T25 and the T18 fragments of the catalytic domain of the *B. pertussis* adenylate cyclase were fused to full-length copies of MPN625 and MPN668. The leucine zipper of the yeast GCN4 transcription factor served as a positive control for strong self-interaction (Karimova *et al.*, 1998). The results are shown in Figure 5.2, which shows that MPN625 and MPN668 form dimers. This is in agreement in comparison to other hydroperoxide resistance proteins. No interaction between MPN625 and MPN668 was observed in this experiment, even if a very similar folding is expected. Furthermore, no interaction between MPN625/668 with the moonlighting protein GlpQ nor its paralogue MPN566 could be observed (data not shown).

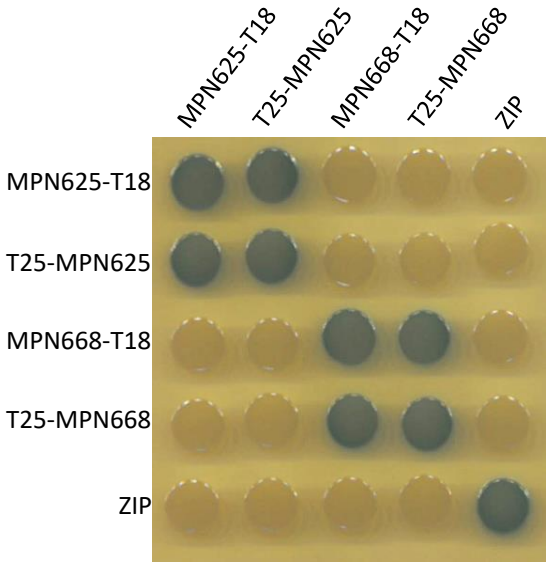

Figure 5.2 | Interactions between MPN625 and MPN668. Bacterial two-hybrid analysis of N- or C-terminal fusions of MPN625 and MPN668 to domains of CyaA (T18 and T25) (Karimova *et al.*, 1998).

Peroxidase activity. The activity of MPN625 and MPN668 to degrade peroxides was determined using test stripes, FOX-assay and for quantitative analysis, ITC measurements. In the first experiments with test stripes we detected that both proteins can degrade a certain

extent of hydrogen peroxide (data not shown). To confirm the results and use adequate controls, we created for each protein, mutants' defect in either the catalytic cysteine (C^P) or the resolving cysteine residue (C^R), respectively. We exchanged the cysteines with serine residues (C^P, MPN625:C52S and MPN668:C55S or C^R, MPN625:C115S and MPN668:C119S). All proteins were analyzed using FOX-assay (see Fig 5.3). We detected activity of MPN625 towards hydrogen peroxide degradation and activity of MPN668 to degrade organic peroxides, *i.e*. *tert*-butyl hydroperoxide (tBP). However, for none of the tested mutants we could detect activity at all. Indeed, MPN625 and MPN668 degrade hydrogen peroxide and tBP, respectively, but not *vice versa* and none of the mutants showed activity. These results are corroborated by ITC measurements. To show the usability of this technique for the affinity detection of peroxides we initially tested H_2O_2 with catalase from bovine liver or BSA. The latter one, did not show any interaction with H_2O_2 while strong interaction occurred with the positive control in form of the catalase (Fig. S5.1).

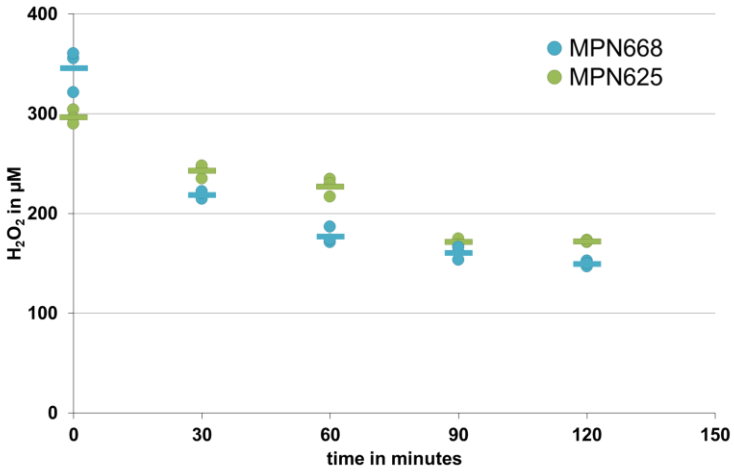

Figure 5.3 | FOX assay determining hydrogen peroxide concentrations *in vitro*. Peroxidase activities of MPN625 (green) and MPN668 (blue) (each 20 µM) in the presence of 500 µM hydrogen peroxide and 100 µM DTT. Negative controls (BSA, mutants and buffer) showed no values below 350 µM (not shown).

These results proved the functionality of ITC to detect protein-peroxide interactions. Our ITC experiments clearly showed affinity of MPN625 towards hydrogen peroxide (Fig. 5.4A) but not towards tBP (Fig. 5.4C) and in contrast a strong affinity of MPN668 towards tBP (Fig. 5.4D) but not towards H_2O_2 (Fig. 5.4B). Furthermore, integrated heat curves for MPN668 with tBP indicate two phases of enzymatic binding, due to two peaks. This indicates substrate specificity for each of the enzymes and their putative role in peroxide degradation and even super oxidation of MPN668 by tBP.

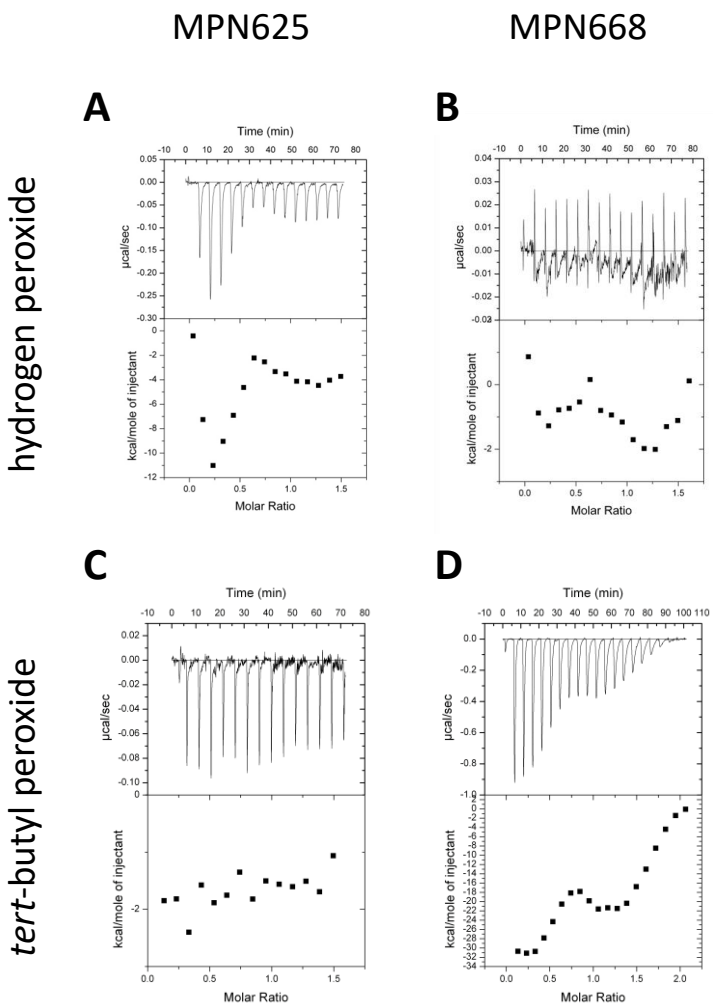

Figure 5.4 | Peroxide binding of MPN625 or MPN668 are measured by ITC. (A) MPN625 with hydrogen peroxide, (B) MPN668 with hydrogen peroxide, (C) MPN625 with *tert*-butyl hydroperoxide, (D) MPN668 with tert-butyl hydroperoxide. Upper panels show original titration data and the lower panels the integrated heat measurements.

Mutant characterization. To compare the growth of mutants lacking either *mpn625* or *mpn625* we grew the strains in MP liquid medium over a period of 4 days. Irrespective of the carbon source (glucose or glycerol), no growth defect was observed compared with the wild type (see Fig. S5.2). To test whether the external ROS stress is influencing the survival of *M. pneumoniae,* we stressed the cells with different concentrations (0, 5, 25, 50, 100 mM) of *tert*-butyl hydroperoxide or H_2O_2. Cell were serial diluted and dropped as spots to MP agar. With increasing H_2O_2 concentrations (>5mM) the *mpn625* and *mpn668* mutants showed a slight increase in growth. At 100 mM H_2O_2 only the *mpn668* mutant showed enhanced growth (see Fig. 5.5). However, on agar with tBP stressed cells we could not see significant differences in growth.

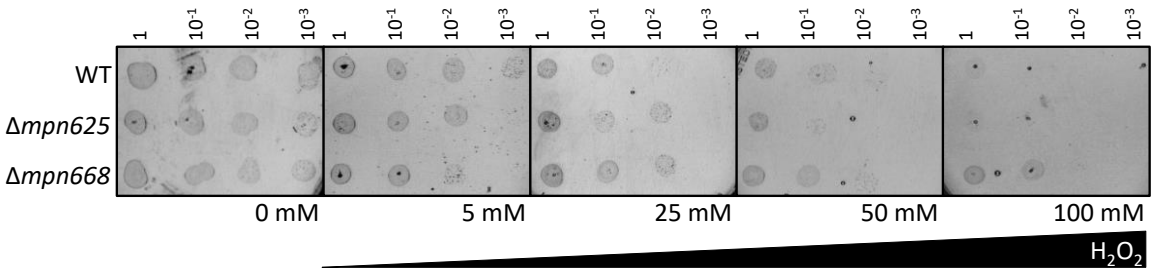

Figure 5.5 | Sensitivity of *M. pneumoniae* to H_2O_2. The sensitivity was determined with a drop dilution assay. Dilution series of wild type cells (GPM116) and the mutants Δ*mpn625* and Δ*mpn668* (OD_{600} 0.1) were treated with different concentrations of H_2O_2 (5 mM, 25 mM, 50 mM and 100 mM). Samples that were not stressed served as growth control. Spots of 10 µl of the dilution series were pipetted on MP agar plates and incubated (37°C, 7 days).

Corroborating the observed phenotype, the deletion of *mpn625* or *mpn668* were complemented with plasmids constitutively expressing the respective gene from plasmids pGP1899 and pGP1900, based on pGP2756 (Blötz *et al.*, 2018). Complemented strains showed growth when stressed with ROS comparable to the wild type (data not shown). In addition, we determined the localization of MPN625 and MPN668. Therefore, we fractionated the complemented strains into cytosolic and membrane fractions and performed Western blot analysis. Our results show that MPN625 and MPN668 are expressed as 6xHis-tagged proteins. We detected both proteins only in the cytosolic fractions, when *M. pneumoniae* was grown in glucose supplemented medium (data not shown).

Transcriptional regulation of *mpn625* and *mpn668*. The detoxifying activity against ROS directs us to investigate a regulatory mechanism of the involved enzymes in *M. pneumoniae*. Therefore, we cultivated different strains (WT, deletion mutants of *mpn625*, *mpn668* and *fur*, transposon mutants of *glpQ* and *prkC*) and stressed them with *tert*-butyl hydroperoxide and H_2O_2 or grew them in glucose or glycerol to elucidate the regulatory network of the proteins. Subsequently, we isolated RNA from stressed cells and performed quantitative real-time PCR (qRT PCR). We compared expression of seven genes potentially involved in regulation of the detoxification enzymes, *i.e. mpn625, mpn668, fur, spx, prkC, glpQ, trxA,* and *mraZ* as well as the house-keeping genes *rpoB* and *rpsL*. The gene *mraZ* was chosen, since it was suggested to be involved in regulatory processes and is similar to *ohrR* genes (Eiler, 2010; Chen *et al.*, 2018).

As expected, for the mutant strains no expression could be detected for the disrupted or deleted genes. The obtained results are comparisons of stressed cells with wild type cells grown in glucose without stress. For the *mraZ* gene under all tested conditions and in all mutants no regulation was observed. The *trxA*-mRNA was only reduced (-11-fold)

in a *glpQ*-mutant grown in glucose. For the mRNA levels of *spx* and *fur* high perturbations in were detected, making the evaluation from our experimental set-up impossible. Wild type cells grown with glycerol have 13.8-fold upregulated mRNA levels of *mpn668,* while *mpn625* is not regulated (see Fig. 5.6). Interestingly, in mutants lacking *glpQ* a reduced expression of *mpn668* (-13-fold) and *mpn625* (-6-fold) was observed. This effect is nearly gone for *mpn625* and completely for *mpn668* if the *glpQ*-mutant is grown in glycerol. In addition, if *prkC* is deleted, *mpn668* is slightly (4-fold) increased but not when grown in glycerol containing medium (see Fig. 5.6).

Figure 5.6 | Control of the genes *mpn625* and *mpn668* by different carbon sources. Fold changes in expression of *mpn625* and *mpn668* were investigated in the labeled mutant strains. The strains were grown in MP medium with glucose or glycerol till confluent. RNA was purified from each strain. Quantitative PCR was performed using oligonucleotides specific for the genes. Gene expression in the wild type strain M129 was set "1". *rpoB and rpsL* were used as controls. Glc, glucose; glyc, glycerol.

In mutants lacking *mpn625* or *mpn668* no significant difference in gene expression dependent on the carbon source was observed. Comparing *mpn625* and *mpn668* expression in the strains stressed with H_2O_2 (see Fig. 5.7), only a slight increase of *mpn668* was seen for the *mpn625*-mutant (8.3-fold), while *mpn625* was not regulated in any strain.

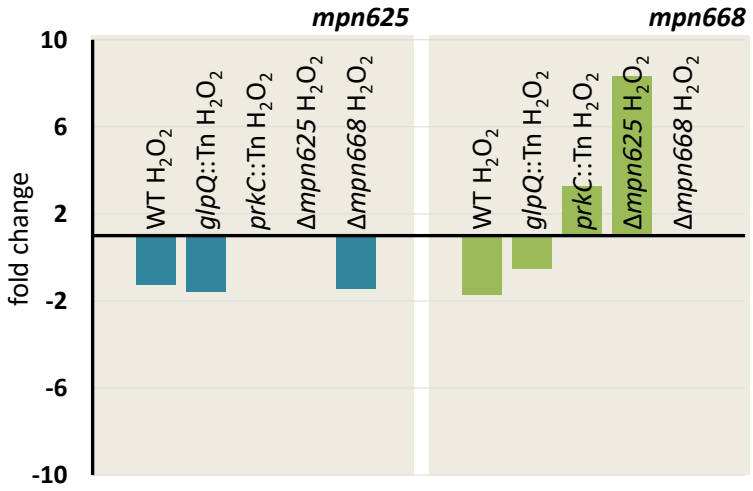

Figure 5.7 | Control of the genes *mpn625* and *mpn668* under hydrogen peroxide stress. Fold changes in expression of *mpn625* and *mpn668* were investigated in the labeled mutant strains. The strains were grown in MP medium with glucose or glycerol till confluent. Cells were stressed with 5 mM hydrogen peroxide for 20 min. Subsequently RNA was purified from each strain. Quantitative PCR was performed using oligonucleotides specific for the genes. Gene expression in the wild type strain M129 was set "1". *rpoB and rpsL* were used as controls. H_2O_2, hydrogen peroxide.

Since we observed an impact on regulation of *mpn625* and *mpn668* in deletion mutants of *prkC* and *glpQ* we analyzed the expression of the protein kinase C (*prkC*) and the trigger enzyme *glpQ* in different strain backgrounds (see Fig. 5.8A - C). Our results show that expression of *glpQ* is increased when the wild type is grown in glycerol instead of glucose (53-fold, see Fig. 5.8A). The increase in *glpQ* expression is even higher in a *prkC* deletion strain grown in medium with glucose (73-fold) but decreased in medium with glycerol (-11-fold). Interesingly, *prkC* seems to be regulated with different carbon sources as well. If the wild type is grown in glycerol the expression of *prkC* is increased (31-fold), but *prkC* expression is decreased when *glpQ* is deleted (-29-fold). However, in a *glpQ* mutant the *prkC* levels reach again wild type levels when grown with glycerol, which could be a hint for the induction of *prkC* with glycerol as carbon source. When we compared deletion mutants of *mpn625* and *mpn668* stressed with H_2O_2 with non-stressed wild type cells (see Fig. 5.8B), we saw a strong effect of the *mpn625* deletion for *glpQ* expression, which is highly induced (>60-fold). In contrast, if *mpn668* is absent, the expression of *glpQ* is reduced in glucose (-14-fold) and slightly increased when the mutant cells were stressed with H_2O_2 (5-fold). A similar expression pattern was observed for the expression of *prkC* in *mpn625* mutant cells (see Fig. 5.8B). In these cells the levels of *prkC* increase in the presence of glucose (10-fold) and under H_2O_2 stress (50-fold). However, when *mpn668* is deleted no change was detected. Moreover, we analyzed the expression of *glpQ* and *prkC* in the respective mutants and wild type under H_2O_2-stress (see Fig. 5.8C). The *glpQ* mRNA is increased (14-fold) in the wild type and strongly (>200-fold) in a *prkC* -mutant (see Fig. 5.8C). The *prkC* mRNA is

also increased (6-fold) and (29-fold) in the wild type and the *glpQ* mutant respectively, when stressed with H_2O_2. When the same strains were stressed with *tert*-butyl hydroperoxide, no gene regulation in the wild type nor the *glpQ*-mutant was observed (see Fig. 5.9).

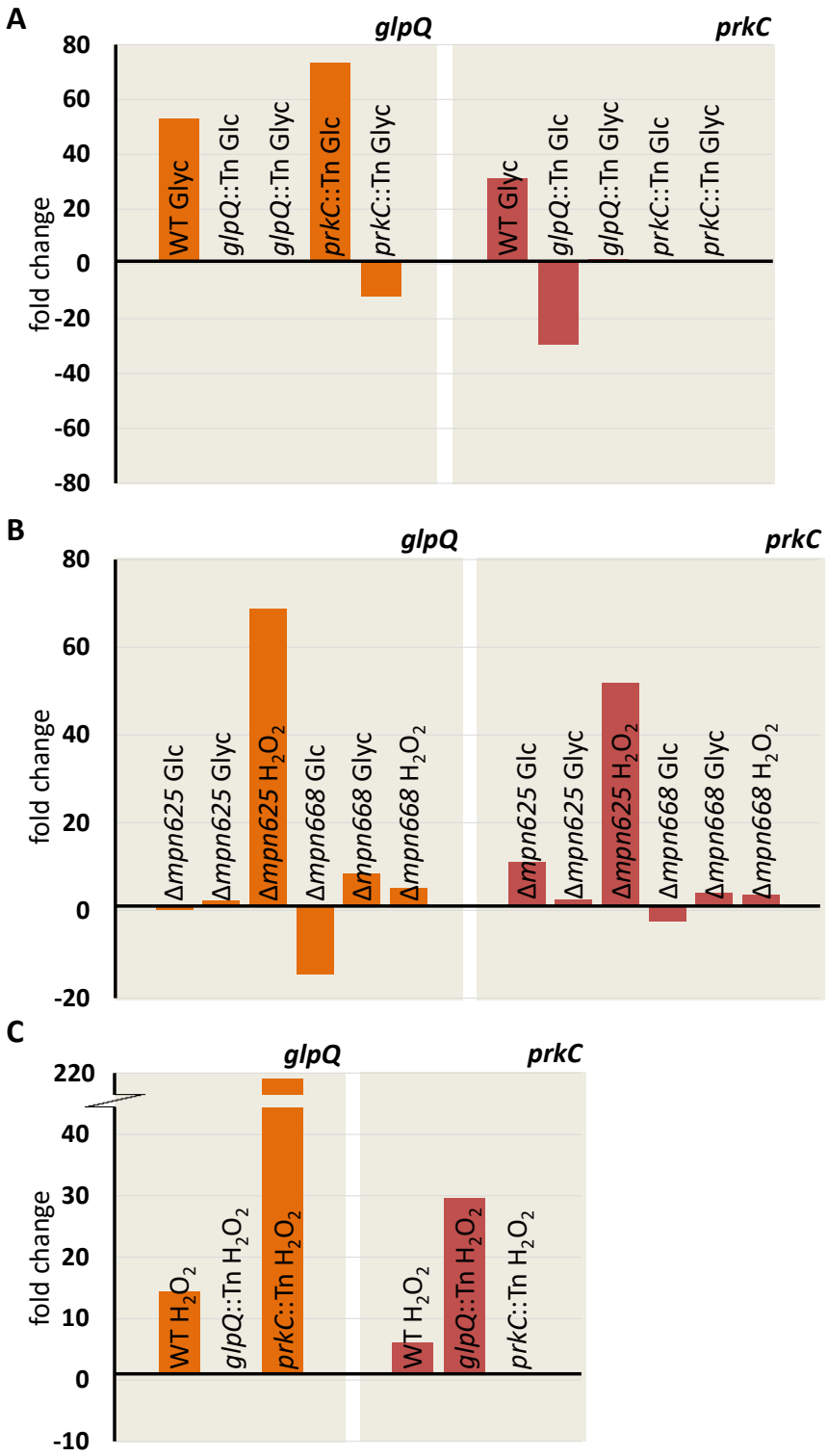

Figure 5.8 | Control of the genes *glpQ* and *prkC* by under various conditions. Fold changes in expression of *prkC* and *glpQ* were investigated in the labeled mutant strains under (A) different carbon sources, (B) in the *mpn625* and *mpn668* mutants, (C) under hydrogen peroxide stress. The strains were grown in MP medium with glucose or glycerol till confluent. Cells were stressed with 5 mM hydrogen peroxide or 5 mM tBP for 20 min or

incubated with fresh medium. Subsequently, RNA was purified from each strain. Quantitative PCR was performed using oligonucleotides specific for the genes. Gene expression in the wild type strain M129 was set "1". *rpoB and rpsL* were used as controls. Glc, glucose; glyc, glycerol; H_2O_2, hydrogenperoxide.

Interestingly, strong induction of *glpQ* was detectable in a *prkC* transposon mutant (>290-fold). This is also the case for the strains lacking *mpn625* or *mpn668*, there glpQ is 55-fold and 22-fold induced, respectively. Only a minor change for *prkC* expression was observed in the *mpn668* mutant (5.6-fold induction) but no change of expression in the other strains.

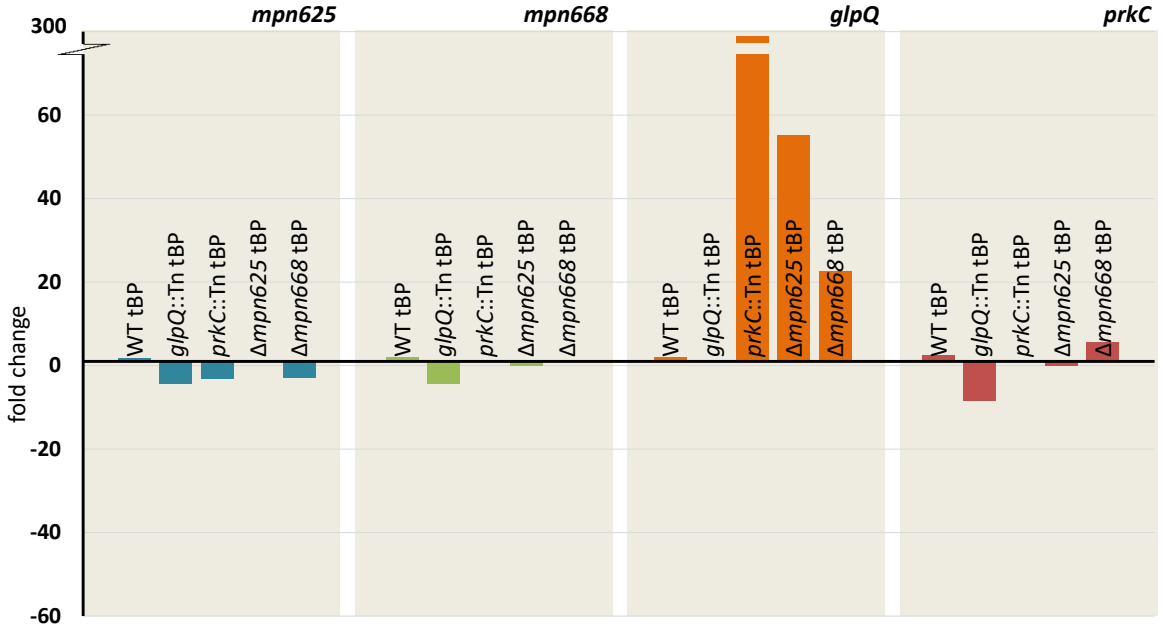

Figure 5.9 | Control of the genes *mpn625, mpn668, glpQ and prkC* under *tert*-butyl hydroperoxide stress. Fold changes in expression of various genes were investigated in the labeled mutant strains under (A) different carbon sources, (B) in the *mpn625* and *mpn668* mutants, (C) under hydrogen peroxide stress. The strains were grown in MP medium with glucose or glycerol till confluent. Cells were stressed with 5 mM hydrogen peroxide for 20 min. Subsequently, RNA was purified from each strain. Quantitative PCR was performed using oligonucleotides specific for the genes. Gene expression in the wild type strain M129 was set "1". *rpoB and rpsL* were used as controls. tBP, *tert*-butyl hydroperoxide.

Analysis of a *fur* mutant. We speculated that the iron homeostasis could influence the detoxification systems due to the Fenton reaction. We analyzed the expression of the putative ferric ion uptake regulator (Fur; *mpn329*) in more detail. The gene *mpn329* was annotated as non-essential (Lluch-Senar *et al.*, 2015; Glass *et al.*, 2006) and no mutant could be isolated and characterized so far (Eilers, 2010). However, we have created a knock-out strain (GPM18) which showed that *mpn329* is not essential in *M. pneumoniae*. The *mpn329* mutant showed no significant difference in growth in MP medium, compared with the wild type. Transcriptomic analysis of the mutant revealed that Fur seems to share its target genes with GlpQ, *i.e. glpF*, *cbiO1* and *cbiO2*, *mpn162*. These data are supported further when MPN329 was overexpressed (Güell *et al.*, 2009), resulting in expression

alterations of the same targets. Furthermore, our transcriptomic analysis showed Fur targets were upregulated when we incubated the mutant with thiolutin, which acts as a zinc chelator. This was not the case when *fur* was deleted. Under zinc chelating conditions *glpQ* expression is decreased independent of Fur. This indicates that MPN329 is a Zur protein, rather a Fur or a PerR-like protein (Yus *et al.*, submitted).

Heterologous expression of *mpn625* or *mpn668* in *B. subtilis*. We constructed a *B. subtilis* strain deficient of the genes *ohrA*, *ohrB* and *katA* (GP3154). This strain allows the observation of phenotypes, when stressed with *tert*-butyl hydroperoxide or H_2O_2, due to the lack of the native detoxification enzymes. The genes *mpn625* or *mpn668* were integrated with xylose-inducible promoters in the *ganA*-locus of GP3154. We used the plasmids pGP888 (P_{xyl}-empty vector; Diethmaier *et al.*, 2011), pGP3274 (P_{xyl}-*mpn625*), and pGP2202 (P_{xyl}-*mpn668*) to transform GP3154. We stressed the different strains with H_2O_2 and *tert*-butyl hydroperoxide and performed drop dilution assays (see Fig 5.10). Our results show sensitivity of GP3154 to the applied ROS, as well as the isogenic strain harboring the empty vector. Interestingly, both heterologously expressed genes can compensate partially for *tert*-butyl hydroperoxide stress. For the *Bacillus* strain expressing *mpn668*, a slight better growth could be observed compared with the strain expressing *mpn625*. The effects were already seen even if no xylose was added to the medium, which could be due to the fact that the xylose-promoter is “leaky” or mutated already.

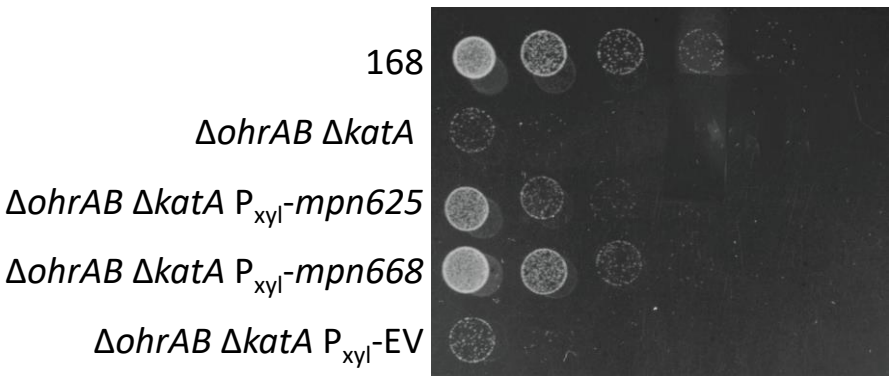

Figure 5.10 | Drop dilution of *B. subtilis* mutant sensitive to ROS complemented with MPN625 or MPN668. GP3154 (Δ*ohrAB* Δ*katA*) is sensitive to hydrogen peroxide while the *B. subtilis* wild type can cope with ROS stress**.** Complemented strains with plasmids incorporating in the *ganA* locus express after xylose addition the genes mpn625 or mpn668, respectively. As negative control we used GP3154 complemented with the empty vector. *B. subtilis* cells (OD_{600} = 1) were stressed for 20 min with 5 mM *tert*-butyl hydroperoxide and subsequently plated on CEM defined medium. Plates were incubated for 20 h at 37°C.

HBEC cytotoxicity assay. To address whether *mpn625* or *mpn668* influence the virulence of *M. pneumoniae* we infected layers of human bronchial epithelial cells with the mutant strains GPM15 and GPM16, lacking *mpn625* or *mpn668,* respectively. The toxicity of the mutants was compared with wild type infected cells and no significant difference could be

detected (data not shown; ~98%). In contrast, HBECs infected with GPM18 (*fur* mutant) showed decreased levels of cytotoxicity (20%). We used, the *prkC*-mutant as a negative control, as expected, the *prkC*::Tn mutant showed reduced cytotoxicity (15%) as described earlier (Schmidl *et al.*, 2010b), while wild type cells killed nearly all HBECs (98%).

Hemolytic activity of *M. penumoniae*. Analyzing the hemolytic activity, we tested the growth of all *M. pneumoniae* strains of this study on blood agar plates (for strains see Table 5.1). Growth was visible for non-diluted cells after 2 days and for dilutions after 5 days. Drop dilutions of all strains of *M. pneumoniae* showed no significant phenotype on blood agar plates (data not shown). Slight brownish coloration could be due to initial α-hemolytic activity, dueto the hydrogen peroxide production of the cells.

DISCUSSION

High amounts of oxygen and its harmful radicals can be poisonous for any living cell. Microorganisms have evolved detoxifying enzymes allowing the degradation of reactive oxygen species. Surprisingly, the aerobic *Mycoplasmas* lack common detoxification enzymes with few exceptions. Even though *M. pneumoniae* an *M. genitalium* can produce high amounts of hydrogen peroxide, no efficient degrading enzyme was discovered so far.

In the present work, we provide evidence for detoxifying activity for two proteins from *Mycoplasma pneumoniae*, MPN625 and MPN668. MPN625 is very similar to known osmotically inducible protein C (OsmC) homologs, MPN668 seems to be related with organic hydroperoxide resistance (Ohr) proteins (Jenkins *et al.*, 2008). The OsmC and Ohr proteins appear mainly as peroxidatic active dimers. We show that MPN625 and MPN668 form homodimers, but they cannot form heterodimers. Structural modelling and a sequence alignment revealed that MPN625 (structure at PDB: 1LQL; Choi *et al.*, 2003) and MPN668 have highly different sequences, but they are structurally very similar. Both proteins contain the important and conserved cysteine residues C^P and C^R for catalytic activity and regeneration, respectively. Interestingly, the protein MGA1142 from *M. gallisepticum* is structurally very similar to MPN625. For MGA1142 an affiliation to the more outsourced subgroup III (within OsmC/Ohr family) with an unknown function was suggested (Jenkins *et al.*, 2008). Moreover, the size of the active site in MPN625 and MGA1142 implies larger substrates than for other Ohr proteins (Jenkins *et al.*, 2008). In addition, in *M. genitalium* Ohr and OsmC homologs are present as well (MG_454 for Ohr and MG_427 for OsmC). In *M. genitalium* the OsmC-like protein MG_427 shows activity to organic peroxides and in a lesser extent to hydrogen peroxide (Zhang and Baseman, 2014). In addition, the Ohr related protein MG_454 was shown to facilitates organic peroxide stress resistance as well (Saikolappan *et al.*, 2009). As a consequence, it was hard to predict if and which protein of

M. pneumoniae could degrade peroxides. While working on the experiments investigating the protein activity for MPN625 and MPN668, Chen and his colleagues showed that MPN668 (Ohr homolog) has activity degrading hydrogen peroxide and even stronger to degrade *tert*-butyl hydroperoxide (Chen *et al.*, 2018a). The observed activity fits well to former characterized Ohr proteins in other bacteria, *e.g. X. campestris* Ohr (Mongkolsuk *et al.,* 1998). In the present work, we showed activity as well for MPN668 using FOX assay. MPN668 is able to degrade tBP and in a lesser extent H_2O_2, but not a C^P or a C^R mutant showed activity. However, the role of MPN625 in *M. pneumoniae* was not investigated so far. Activity of the *M. genitalium* MG_427 homolog indicates a similar protective function as for MPN668 in *M. pneumoniae.* Our FOX assay showed degradation of H_2O_2 by MPN625 comparable to MPN668. In our ITC experiments we were able to show that recombinant MPN625 can bind and slightly degrade H_2O_2 but not organic peroxides *in vitro*. In contrast, recombinant MPN668 was only able to bind to tBP but not H_2O_2 in ITC measurements. The degradation of H_2O_2 by MPN625 could be reasoned by the interaction of peroxide with the reactive cysteines. This would result in the formation of sulfur bridges decreasing the overall peroxide content, rather being a degradation activity. On the other hand, MPN625 is known to be phosphorylated *in viv*o (Schmidl *et al.*, 2010b), which could influence the activity drastically (Wood *et al.*, 2003; Rhee *et al.*, 2012). Investigation of the biological relevant reducing agent would give more insights for the *in vivo* function of both, MPN625 and MPN668. The identification of the regeneration system would allow a more precise annotation and grouping to functional categories, 1-Cys, 2-Cys or atypical 2-Cys peroxiredoxins (Hall, 2009). The reducing agent could be the thioredoxin system, which is encoded by the *trxA* and *trxB* in *M. pneumoniae*. Further, reduction could happen by non-thiolic electron donors, such as ascorbate (Monteiro *et al.*, 2007) or by lipoylated proteins, as described for a peroxidase from *Xylella fastidiosa* (Cussiol *et al.*, 2010). However, the current results lead to the conclusion that maybe DTT as an artificial reducing agent is not sufficient to show enzymatic activity. To address the *in vivo* functionality of the proteins MPN625 and MPN668 in a surrogate host, we created a *B. subtilis* strain lacking major ROS detoxification enzymes increasing its ROS sensitivity. Indeed, the *Bacillus* mutant showed a severe growth defect after tBP exposure. The mutant expressing MPN625 or MPN668 showed again increased growth. This indicates that the proteins in *B. subtilis* could have overlapping functions *in vivo*. Surprisingly, *M. pneumoniae* deletion mutants lacking *mpn625* or *mpn668* showed higher resistance towards H_2O_2 than the wild type. This might indicate the regulation of the remaining ROS detoxification enzyme. Since the expression of detoxification enzymes is in general strongly controlled by transcription factors, such as OhrR or OxyR, we were interested in any regulatory mechanism controlling the expression of *mpn625* and/or *mpn668.* In contrast to other *ohr* genes, *e.g*. *ohrA* in *B. subtilis*

(Fuangthong *et al.*, 2001), the homologs in *M. genitalium* and *M. gallisepticum* do not seem to be regulated upon peroxide stress, but under physical stress conditions, *i.e*. osmotic or ethanol shock (Saikolappan *et al.*, 2009; Jenkins *et al.*, 2008). Counterintuitive, the OsmC homologe in *M. genitalium* (*mg_427*) is decreased among several stress conditions (Zhang and Baseman, 2014). In our study, we analyzed with quantitative PCR the expression pattern of *mpn625* and *mpn668*. Using glycerol as carbon source, which mimics the *in vivo* growth, expression of *mpn668* is induced but not the expression of *mpn625*. No altered expression due to applied stresses, neither tBP nor H_2O_2, could be observed. This contrasts with our observations in drop dilution experiments, which suggests overexpression of a detoxifying enzyme under H_2O_2 stress. Additionally, previous experiments showed induction of *mpn668* upon tBP exposure (Chen *et al.*, 2018a). Repeating the experiments as described failed several times. Maybe, in our approach the peroxide concentration was to low to induce significant expression changes. Interestingly, using different mutants under the same stress conditions suggests a complex regulatory network, formed by GlpQ, PrkC, MPN625 and MPN668. Chen and his colleagues suggested that MraZ (MPN314) shows 32% homology to OhrR transcription factors (Chen *et al.*, 2018a). Therefore, we also analyzed the *mraZ* expression. For all tested strains and under all conditions no regulation of the *mraZ*-levels could be detected. It would be interesting to test if MraZ or GlpQ can bind DNA or more specific, binding upstream of *mpn625* or *mpn668*. In addition, the analysis of gene expression in a *mraZ*-deletion mutant could lead to new insights of the MraZ targets. Furthermore, the Fur protein influences the iron homeostasis and the expression of *glpQ* which in turn could influence the peroxide stress of the cells. It would be interesting to analyze the expression of *mpn625* and *mpn668* in different double and triple mutants. However, the data tempt us to speculate that MPN625 has more a regulating function rather than an enzymatic. Since MPN625 is phosphorylated and strongly altered in a PrkC mutant, the phosphorylation status might be important for its activity and regulation. It seems that the phosphorylation of proteins (MPN625, GlpQ), peroxide and ion concentrations in cells and the available carbon source influence the response of *M. pneumoniae* to maintain cell viability under peroxide stress.

We identified MPN625 and MPN668 as cytosolic proteins, even if they are speculated to be exported or integral membrane proteins (Jenkins *et al.*, 2008). In *M. gallisepticum* the MPN625 homolog, MGA1142, was found to localize cytosolic and also in the membrane. Furtheromre, a transmembrane domain in MGA1142 was predicted (Jenkins *et al.*, 2008). This putative transmembrane domain is also present in MPN625, but not in MPN668. The localization could change upon infection or the available carbon source. More experiments should be performed to test the possible membrane localization of the

peroxiredoxin-like proteins in *M. pneumoniae*. The *in vivo* functionality and the regulation of the proteins will be addressed in more detail in future experiments.

SUPPLEMENTAL MATERIAL

Table S5.1 | Oligonucleotides used in the study of chapter 5.

Table S5.2 | Plasmids used in the study of chapter 5.

Figure S5.1 | Peroxide binding of catalase or BSA are measured by ITC.

Figure S5.2 | Growth curves with *M. pneumoniae* strains.

Acknowledgements. We are grateful to Christina Herzberg supporting the creation of *Bacillus subtilis* mutants. We want to thank Alexander Mehr and Julian Schwanbeck for testing protein expressions and offering blood agar plates, respectively. For fruitful discussions, we want to thank especially Katrin Gunka, Anika Klewig and Johannes Gibhardt.

Funding. Results have been achieved within the framework of the ERASynBio 2nd Joint Call for Transnational Research Projects: "Building Synthetic Biology Capacity Through Innovative Transnational Projects" with funding from the corresponding ERASynBio National Funding Agencies.

CHAPTER 6 | Discussion

C-di-AMP metabolism in a genome reduced bacterium

The detection of environmental perturbations and its resulting response in *M. pneumoniae* is still a striking question, since common two-component regulatory systems are absent. In general, such systems transfer external signals into processes for adaptation, *i.e*. gene expression or repression. Furthermore, only few transcription factors are known or identified so far. This is in good agreement with the habitat, the human lung epithelium, where near constant conditions predominate. Nevertheless, *Mycoplasmas* can survive as free-living organisms and must adapt to changing temperatures, nutrient and salt conditions as well as in response to human defense mechanisms or other competing bacteria. This indicates that *M. pneumoniae* somehow alters its gene expression. It is noteworthy that the alarmone ppGpp was detected in *M. pneumoniae* (Eilers, 2010). The second messenger ppGpp is one of the best characterized second messengers. It is induced by nutrient starvation and responsible for the stringent response for stress adaptation. Cultivating *M. pneumoniae* in the presence of the synthetic tRNA synthetase inhibitor serine hydroxamate mimics nutrient starvation and leads to the formation of ppGpp. In a *spoT*-transposon mutant under the same conditions no ppGpp was detectable, allowing the assignment of SpoT as the only ppGpp synthase in *M. pneumoniae*. To analyze the signal transduction in *M. pneumoniae* further, we analyzed the pool of nucleotides from whole cell extracts. Indeed, we identified besites the second messenger ppGpp, also significant amounts of cyclic di-AMP (c-di-AMP). Interestingly, this cyclic dinucleotide is the only essential second messenger, *i.e.* most of c-di-AMP producing bacteria need this molecule to be viable. On the other hand, if cells accumulate c-di-AMP it is toxic for many bacteria indicating the precisely controlled homeostasis of this messenger (Gundlach *et al.*, 2017; Huynh *et al.*, 2015). The presence of c-di-AMP in a representative of the *Mollicutes* supports the essentiality of this second messenger in all *Firmicutes* investigated so far (Commichau *et al.*, 2015). The occurrence of this second messenger, even in a near-minimal organism, points out that c-di-AMP plays an important role in mycoplasmal cell homeostasis. C-di-AMP is produced by proteins containing a diadenylate cyclase (DAC) domain and degraded by proteins with DHH-DHHA1/HD domains (see Fig 6.1). We identified *mpn244/cdaM* in *M. pneumoniae* as a *cdaS* ortholog. CdaS is one of the diadenylate cyclases of *B. subtilis* and responsible for c-di-AMP production, besides CdaA and DisA (Commichau *et al.*, 2018). Surprisingly, the N-terminus of CdaM is very different compared to other investigated DACs, it contains only a single transmembrane domain similar to the membrane-bound CdaA from *L. monocytogenes*, that contains three transmembrane domains (Rosenberg *et al.*, 2015). Thus, CdaM represents a novel class of DACs. Other bacterial species encode DACs with

additional domains besides the cyclase domain, required for regulation of enzymatic activity (Huynh *et al.*, 2016; Mehne *et al.*, 2014; Witte *et al.*, 2008). The absence of regulatory domains in CdaM is in good agreement with the host adapted minimizing evolution of *Mycoplasmas*, that led also to the lack of common two-component systems and few transcription factors.

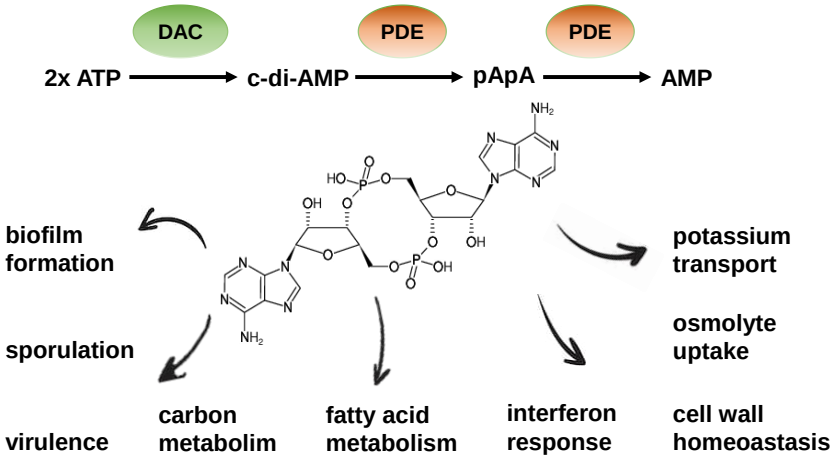

Figure 6.1 | Production and degradation of c-di-AMP and its biological importance. C-di-AMP is produced from two molecules of ATP by diadenylate cyclases (DAC), its degradation into 5'-phosphadenylyl-adenosine (pApA) is catalyzed by specific phosphodiesterases (PDE) and further degradation occurs as well via PDEs producing AMP.

Furthermore, we compared the activities and cofactors of CdaM with CdaA from *L. monocytogenes.* CdaA from *L. monocytogenes* has an unusual affinity for cobalt and manganese ions (Rosenberg *et al.*, 2015). Thereby the question raised, if a similar cofactor requirement for CdaM could exist. The use of unusual ions could be of great evolutionary importance for pathogens and their survival, since a competition regarding metal ions of these bacteria and their hosts could exist (Agranoff and Krishna, 1998). The heterologous expression of CdaM in c-di-AMP deficient *E. coli* provided unequivocal evidence for DAC activity of CdaM. However, overproduction was not possible due to the toxicity of c-di-AMP in *E. coli*. *In vitro* analyses with purified CdaM will be important to unravel the cofactor requirements. Moreover, we identified two putative c-di-AMP phosphodiesterases (PDE) degrading the second messenger (MPN140 and MP549), only MPN549/PdeM showed c-di-AMP specificity. However, MPN140 seems to be involved in the nucleotide metabolism since we detected phosphodiesterase activity, which could be responsible for pApA recycling, the product of c-di-AMP degradation, into AMP (see Fig. 6.1). These observations fit perfectly to the well characterized degradation of c-di-AMP in *B. subtilis* and *Streptococcus* spp. (Rao *et al.*, 2010; Bai *et al.*,2013). Furthermore, the degradation of 5- to 24-mers of RNA and more interestingly pAp, was shown *in vitro* for MPN140, as well for

the homolog in *Mycobacterium tuberculosis* (Postic *et al.*, 2012). For MPN140 again cobalt seems to be the cofactor rather than manganese or magnesium. This would support the hypothesis of unusual cofactor requirements in minimal pathogenic bacteria. Trace elements are not limiting in bacteria. As an example, the intracellular concentrations of trace elements such as copper, zinc or iron are more than 100-fold higher in the cytoplasm of *E. coli* than extracellular (reviwed in Porcheron *et al.*, 2015). Too high concentrations of trace elements, especially cobalt, are toxic for bacteria and human cells, which indicate tight regulation. Copper is thought to enter human cells predominantly over the lung tissue with air pollution (Simonsen *et al.*, 2012). This fact could explain the putative evolution of proteins in *M. penumoniae* using copper instead of more abundant ions. Even if no regulatory domains are annotated in CdaM, regulation upon ion-specificity or metabolite binding could be possible. Interestingly, in *Staphylococcus aureus* the PDE GdpP is feedback inhibited by pApA (Bowman *et al.*, 2016). Host derived heme or nitric oxide (NO) are important compounds for iron acquisition or produced as defense from host cells, respectively. The impact of both, heme and NO, on the activity of PDEs was observed in *Lactococcus lactis*. A PDE mutant of *L. lactis* is strongly heme sensitive (Tan *et al.*, 2013). The importance of iron or heme for *Mycoplasmas* is not clear. *Mycoplasmas* lack iron-sulfur cluster proteins, which are important in most other bacteria (Johnson *et al.*, 2005). In *Streptococcus suis* a PDE mutant showed reduced hemolytic activity (Du *et al.*, 2014). For *L. monocytogenes* it is known, that PdeA is more abundant in eukaryotic cells compared to protein levels *ex situ,* suggesting a regulation upon infection (Huynh *et al.*, 2015; Rao *et al.*, 2011). Thus, a regulation of c-di-AMP metabolism by iron (heme), NO or host cells cannot be excluded. *Vice versa* c-di-AMP putatively impacts the acquisition of iron that is withhold by the host and may supports virulence of bacteria.

Functionality and essentiality of c-di-AMP in *M. pneumoniae*

To gain more insights into essential genes of *M. pneumoniae* we challenged the essentiality of *cdaM* and *pdeM.* For *B. subtilis* and other bacteria, *i.e. L. monocytogenes* or *S. aureus,* the creation of conditional mutants of either producing or degrading enzymes of the c-di-AMP metabolism are described (Whiteley *et al.*, 2015; Gundlach *et al.*, 2017; Devaux *et al.*, 2018; Zeden *et al.*, 2018). Despite the annotation for c-di-AMP-related genes in *M. pneumoniae* as essential (Lluch-Senar *et al.*, 2015), we screened in different attempts our mutant collection for *cdaM* and *pdeM* transposon mutants. A successful deletion of the PDE was unlikely, since the toxic effect of c-di-AMP accumulation is well known for *B. subtilis, L. monocytogenes, Borrelia burgdorferi* or *E. coli*, where the latter one is naturally deficient of c-di-AMP (Gundlach *et al.*, 2015b; Ye *et al.*, 2014; Whiteley *et al.*, 2017a). In a PDE mutant, the levels of c-di-AMP would rise to toxic levels. Unfortunately, no PDE nor

DAC mutant could be isolated, which is may explained by the standard growth conditions used for the creation of the transposon library in complex PPLO broth. In complex medium c-di-AMP metabolism seem to be indispensable (Whiteley *et al.*, 2015; Gundlach *et al.*, 2017). This reflects the restriction of our mutant collection and highlights two missing methodologies when working with *M. pneumoniae*; first a (complex) defined medium with the possibility to test single compounds, or even better a minimal medium, and secondly an approach for targeted gene deletion. Interestingly, the synthetic minimal organism JCVI-syn3.0 does not encode homologs of *cdaM* or *pdeM*, or other homologs related to second messenger metabolism (*e.g. spot/relA* is not essential for survival) suggesting that these genes are synthetic lethal rather essential. Another explanation could be changed deletion conditions or other gene deletions (of target proteins) allowed the DAC and PDE removal (Hutchison III, 2016). Interestingly, there is clear evidence for cross-regulation of second messengers in bacteria (Corrigan *et al.*, 2015). Experiments revealed, that c-di-AMP degradation is inhibited by ppGpp, but none of the c-di-AMP specific PDEs analyzed so far is able to hydrolyze ppGpp (Huynh *et al.*, 2015). *Vice versa* c-di-AMP levels have an influence on the ppGpp levels, and consequently on the stringent response in bacteria (Corrigan *et al.*, 2015; Liu *et al.*, 2006). The connection between ppGpp and c-di-AMP is proposed to be the result of the metabolic imbalance when c-di-AMP homoeostasis is altered, leading to the production of the alarmone signal molecule for stringent response (Huynh *et al.*, 2016; Sureka *et al.*, 2014). Furthermore, in *B. subtilis* and *L. monocytogenes*, c-di-AMP is an important regulator in the central carbon metabolism (Krüger *et al.*, unpublished; Whiteley *et al.*, 2017a). In *L. monocytogenes*, *S. aureus* and *L. lactis* c-di-AMP binds and inhibits the activity of the pyruvate carboxylase PycA (Choi *et al.*, 2017; Sureka *et al.*, 2014; Whiteley *et al.*, 2017a). PycA converts pyruvate into oxaloacetate in the anaplerotic reaction of the citric acid cycle. In *L. monocytogenes* and *L. lactis* this reaction is of great importance for energy production due to the incomplete citric acid cycles in both bacteria (Schär *et al.*, 2010; Wang *et al.*, 2000). *Mycoplasmas* lack the complete citric acid cycle and homologs of PycA, but it would be interesting to investigate if c-di-AMP is influencing the carbon metabolism in *M. pneumoniae*. Accordingly, we attempt the isolation of c-di-AMP interaction partners. Indeed, in a first attempt we identified MPN461, a KtrC homolog of *B. subtilis*, binding to c-di-AMP *in vitro*. This makes perfectly sense because KtrC of *B. subtilis* is as well c-di-AMP regulated (Gundlach *et al.*, 2017). In *B. subtilis* KtrCD forms the low-affinity potassium transporter system (Holtmann *et al.*, 2003), which is negatively controlled by c-di-AMP (Corrigan *et al.*, 2013). The homeostasis of potassium is likely the main cause of the essential nature of this second messenger. Elevated levels of potassium are toxic for bacteria while potassium is itself essential for cell survival (Nissen *et al.*, 2000; Gundlach *et al.*, 2017). However, it needs further investigation to determine in

which extent the regulation of potassium is responsible for the c-di-AMP essentiality in *Mycoplasma*s. Moreover, under different conditions in a more extended pull-down experiment other c-di-AMP binding partners could be addressed. A modified pull-down approach could also reveal ppGpp binding proteins. In addition, new techniques could allow the analysis of mutants lacking c-di-AMP at all in *M. pneumoniae* (deletion of *cdaM* and *pdeM*). The impact of ppGpp on c-di-AMP levels and *vice versa* could be tested with new measurements in a *spoT* mutant as well as in strains overexpressing PDEs or DACs *in vivo*. Lastly, the identification of putative other c-di-AMP regulated proteins is interesting, not only for metabolism and regulation in *M. pneumoniae,* but also for evolution-related questions and basic research of c-di-AMP in other bacteria. Further we hypothesize an influence of c-di-AMP on the pathometabolism of *Mycoplasmas.*

C-di-AMP influenced pathogenicity

Noteworthy is the fact, that c-di-AMP is widely distributed among Firmicutes but excluded from eukaryotic cells. Therefore, c-di-AMP is a perfect candidate for developing new antibiotics or the production of vaccines against many pathogenic bacteria. Recently, first experimental evidence for therapeutically importance of c-di-AMP is given by Quintana as well as Zheng and their colleagues, respectively (Chen *et al.*, 2018c; Quintana *et al.*, 2018; Zheng *et al.*, 2014). Interestingly, c-di-AMP is inducing inflammation reactions in mouse and human tissues (Gries *et al.*, 2010; Ebensen *et al.*, 2011), which indicate a connection to virulence. However, the relationship of c-di-AMP metabolism and virulence was already proven for some bacteria, *i.e*. *L. monocytogenes*, *Mycobacterium tuberculosis* or *Chlamydia* spp. (Barker *et al.*, 2013; Dey *et al.*, 2017; Witte *et al.*, 2013; Ye *et al.*, 2014). The recognition of foreign nucleotides (bacterial derived) by the host defense system is an established way to detect infecting bacteria (Desmet and Ishii, 2012). The recognition of c-di-AMP and c-di-GMP by human cells is a very recent finding. The transmembrane receptor STING (stimulator of interferon genes, controlling innate immunity) binds beside human cyclic nucleotides, bacterial produced c-di-GMP and c-di-AMP. In contrast, RECON (reductase controlling NF-kB) binds with high affinity only bacterial c-di-AMP (Burdette *et al.*, 2011; McFarland *et al.*, 2017; Zhang *et al.*, 2013). When bacteria produce or release c-di-AMP in host cells, RECON soaks up the cyclic nucleotides and thus is inhibited. Consequently, NF-kB repression is abolished. Higher levels of NF- kB leads to antibacterial inflammation and in principle the clearing of bacterial infections (McFarland *et al.*, 2017). Interestingly, *L. monocytogenes* and may also *B. subtilis* can export c-di-AMP (Townsley *et al.*, 2018; Woodward *et al.*, 2010). Surprisingly, there is evidence that the secretion of c-di-AMP rather promotes *L. monocytogenes* infection and not its clearance (McFarland *et al.*, 2018). Balanced doses of c-di-AMP secretion by *L. monocytogenes* can elevate beta-interferon

(IFN-β) levels, leading to anti-inflammatory immune modulation (Schwartz *et al.*, 2012). Since 17% of all *M. pneumoniae* ORFs encode for transporters (Großhennig *et al.*, 2013), it is worth to analyze a possible secretion of c-di-AMP and the resulting host cell response. The activation of the NF-kB pathway was shown to clear *M. pneumoniae* infection in mice (Jiang *et al.*, 2012), however, the study focused solely on the NF-kB pathway and not on the overall changes in immune response, *e.g.* regulators or INF production. In addition to c-di-AMP, the lipoproteins MPN611 and MPN162 (putative lipoproteins involved in phosphate uptake) stimulate NF-kB production via toll-like receptors (receptors for innate immunity and inflammation) (Akira and Takeda, 2004). The same group elucidated also that the ABC-transporter MPN333 and the ε subunit of the F_0F_1 ATP-synthase stimulate inflammation via autophagy (Shimizu *et al.*, 2007; Shimizu *et al.*, 2014; reviewed by Shimizu *et al.*, 2016). The mechanisms controlling inflammation and bacterial clearance seem to be even more complex after c-di-AMP entered the stage. It was already suggested that bacteria use c-di-AMP to exacerbate the infection, either by intervening into the balance of the immune system or simply by overloading the STING pathway (Devaux *et al.*, 2018). Unfortunately, the stimuli regulating c-di-AMP metabolism and more interesting, the influence of making and breaking of c-di-AMP in *M. pneumoniaes'* pathometabolism and virulence remains still elusive.

Impact of immunoglobulin binding proteins on mycoplasmal virulence

Bacteria can adhere to surfaces, often forming biofilms to be protected from environmental changes, competing bacteria or to defend antimicrobial substances (Feng *et al.*, 2018; Raymond *et al.*, 2018; Ryan-Payseur and Freitag, 2018; Vlamakis *et al.*, 2013). For many pathogenic bacteria the adherence to host cells is the prerequisite for host colonization. The adherence can happen through bacterial attachment proteins such as pili or through protein-protein interactions from the bacterial surface to hostcell proteins. For several pathogenic *Streptococci* and *Staphylococci* Ig(A)-binding proteins, which supports adhesion, were identified (Christensen and Oxelius, 1975; Lindahl and Åkerström, 1989; Russell-Jones *et al.*, 1984). Contemporary, other classes of Ig binding proteins were discovered and stepwise characterized in different bacterial species (summarized in Collin and Kilian, 2014; Tab. 18.2). They differ in Ig-binding site, size, structure or are species specific. Overall, IBPs are postulated to confer bacteria with the ability to withstand clearance from their hosts, initiated by antibodies (Pleass *et al.*, 2001). Recently, IBPs were identified in several *Mycoplasma* species. Two IBPs were characterized in more detail, first the IBP from *M. genitalium*, Protein M, and later the IBP system called MIB-MIP in *M. mycoides* (Arfi *et al.*, 2016; Grover *et al.*, 2014). Unfortunately, their potential role in virulence was not experimentally addressed and remains an open question. Notwithstanding, we identified by structural

homology MPN400 in *M. pneumoniae* as potential IBP candidate. We demonstrated that MPN400 binds different human immunoglobulins and is *de facto* the IBP of *M. pneumoniae*. Therefore, we renamed MPN400 accordingly IbpM (Immunoglobulin bindin protein of *M. pneumoniae*). The data for IBPs in different *Mycoplasma* species suggests a significant influence on the virulence and the evasion from host immune system. Similarly, *S. aureus* contains two IBPs, Protein A (SpA) and Sbi, where the latter contains in addition to Ig-binding domain two auxiliary domains, which can bind complement factors, damping the degradation of the pathogen (Smith *et al.*, 2011). It would be interesting to test more human proteins, that are involved in bacterial defense and immunity, putatively bound by IbpM. It is likely to identify plenty, when compared to the huge repertoire of proteins bound by SpA and Sbi, such as von Willebrand factor, tumor necrosis factor receptor-1, complement receptors or complement proteins. Co-immunoprecipitation experiments of IbpM with extracts from *Mycoplasma* and/or extracts from human tissues could reveal other unidentified interactions partners and target proteins. Deletion of IBP in *S. aureus* leads to a less pathogenic strain (Patel *et al.*, 1987; Kim *et al.*, 2012), which should be addressed within animal models for *M. pneumoniae* lacking IbpM. Interestingly, the *in vivo* functionality for the MIP-MIP system was shown very recently. Specific Ig cleavage products could be measured in serum of animals infected with *M. mycoides*, but not animals infected with a mutant lacking the MIB-MIP system (Jores *et al.*, 2019). Besides Ig-cleavage *in vivo,* the influence on the host and overall pathogenicity remains doubtful. According to the described mechanism in *M. mycoides* where MIB binds Igs and MIP cleaves off the heavy chain from the Ig, we tested several proteases from MPN for activity against Igs. Unfortunately, none of the candidates showed Ig specific cleavage. For the protease MPN588 slight Ig degradation was observed, however, specificity and activity towards Igs need further experiments and controls. The ClpX protease of *Bacillus anthracis* impacts defense and virulence, underlying the importance of protease activity for pathogens (McGillivray *et al.*, 2009). The existence of many proteases in the *M. pneumoniae* genome suggests a vital role in either nutrient acquisition, protection or virulence. However, no protease binding to IbpM and/or specific cleavage of Igs could be identified in our experiments. Interestingly, there is clear evidence that the IBPs of *Streptococci* are modified due to the extracellular protease SpeB, increasing surface variation and modifying binding affinities (Raeder *et al.*, 1998). This could be true for *M. pneumoniae* as well, as antigenic variation is well known for *Mycoplasma* spp. (Bhugra *et al.*, 1995; Chopra-Dewasthaly *et al.*, 2008; reviewed by Citti *et al.*, 2010; Lysnyansky *et al.*, 1999; Lysnyansky *et al.*, 2001; Ma *et al.*, 2007). We therefore propose different mechanisms for the *in vivo* function of IbpM in comparison to the MIB-MIP system (see Fig. 6.2). The function of the putative disordered C-terminal domain of IbpM and Protein M (MGE), could be subject to protease post-translational

modification which was observed for mycoplasmal surface proteins (see Fig. 6.2a; Tacchi *et al.*, 2016). The modification could change binding properties or the recruitment of other surface proteins. Furthermore, a conformational change of the C-terminus could result in Fc-masking of the bound Igs lowering detection of the bacteria by the host immune system (Fig. 6.2b). It is possible that the complex of IbpM-bound Igs could not longer trigger bacterial degradation through B cell cells (Fig. 6.2c) and rather lead to B cell apoptosis. Interestingly, this is supported by experiments done with *S. aureus* where B cell apoptosis was induced by SpA (Goodyear and Silverman, 2004). In addition to the Ig binding properties, we observed affinities for fibronectin and plasminogen. It would be interesting to test if the binding protein (MIB) from *M. mycoides* is able to bind fibronectin or plasminogen like IbpM. This could raise another direction for the functionality of IbpM and could explain the varying modes of action in different *Mycoplasmas*.

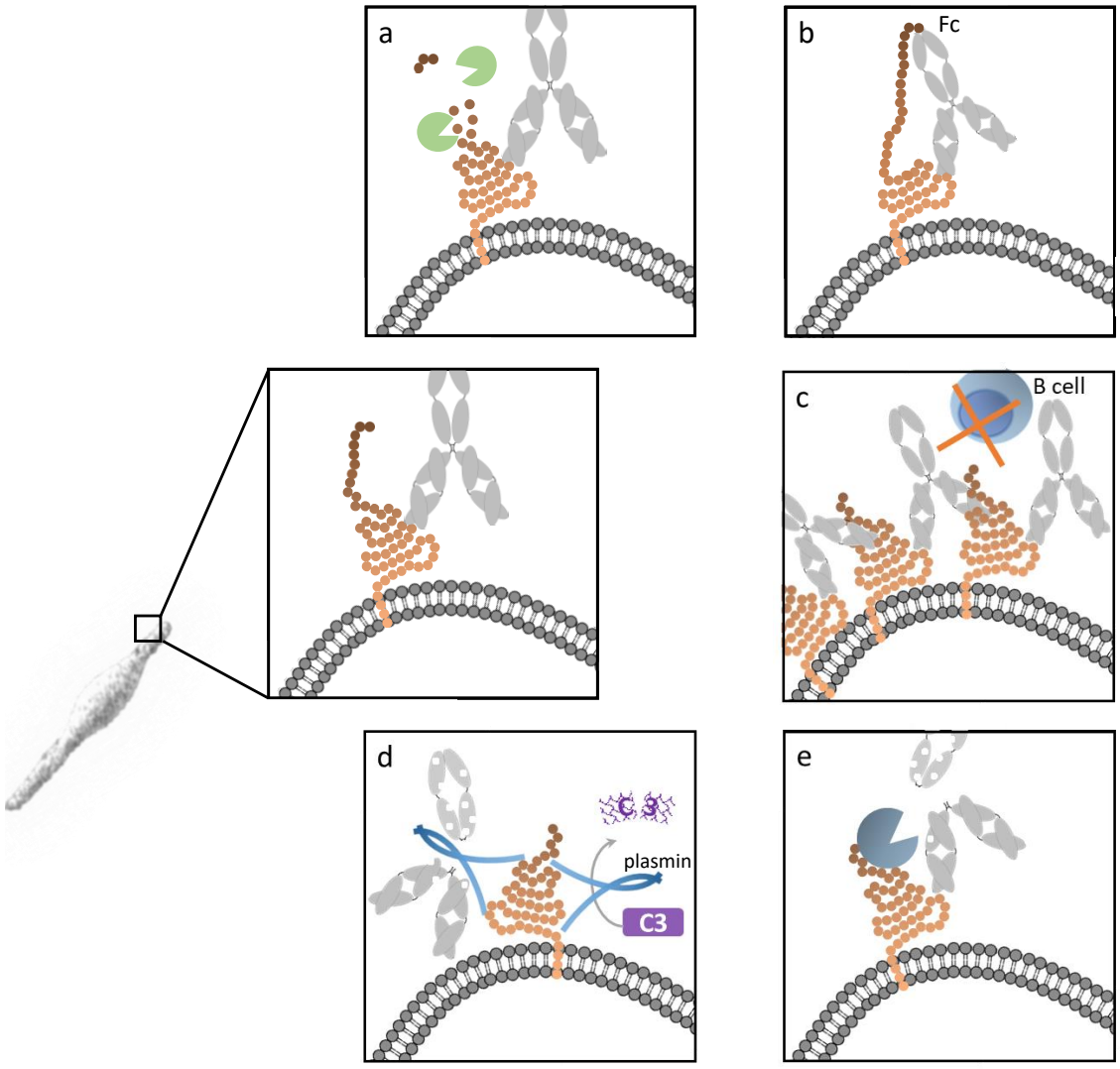

Figure 6.2 | Potential mechanisms for the use of IbpM in *M. pneumoniae*. IbpM is a surface protein of *M. pneumoniae* (orange) which binds human immunoglobulins (Igs, grey). After binding of human Igs to IbpM secreted or surface localized proteases (indicated in green) could degrade bound proteins (a), binding of Igs

could lead to a conformational change which blocks the antigen binding site of the Ig (b), clotting of the IbpM-Ig complexes could lead to shielding from B cell recognition or B cell apoptosis (c), bound plasminogen can be activated to plasmin and degrade bound Igs and complement factors, *e.g*. C3 convertase (d), and recruitment of host proteases (indicated in dark blue) can result in Ig degradation.

The binding of bacterial and more specific of mycoplasmal surface proteins to human proteins such as fibronectin, vitronectin, fibrinogen and plasminogen is proven for many different surface proteins. This variety of multifunctunal surface proteins enables the bacteria to combine multiple protein properties, to evade the host defense. Bound Igs or complement proteins, could be degraded or inactivated by plasmin (see Fig. 6.2d). Interestingly, *S. aureus* uses the staphylokinase to activate plasminogen (Rooijakkers *et al.*, 2005). Aside from the activation, active plasmin was shown to degrade Igs and complement factors (Chuba *et al.*, 1994; Harpel *et al.*, 1989; Rooijakkers *et al.*, 2005). In addition, mycoplasmal or even human proteases could be responsible for the plasminogen activation or directly degrade IbpM-bound proteins. This could confer *M. pneumoniae* with the ability to use host proteins for immune evasion (see Fig. 6.2e). Besides the Ig-binding function, IbpM may exhibits the ability to evade host immune response in a more defined way, which is undiscovered so far.

Multiple surface proteins mediate host immune evasion

For Firmicutes such as *L. monocytogenes, L. lactis* or *Enterococcus faecalis* it was shown that surface proteins could be target of complex processing (Guillot *et al.*, 2016). Secreted or membrane-anchored proteases can lead to the modification of surface proteins. Processed and modified proteins can increase the surface (antigenic) variation of the mycoplasmal cell and in consequence an easier evasion from the human immune system. *M. pneumoniae* encodes for many lipoproteins (6.68% of all genes; Hallamaa *et al*., 2008) and even translocates cytoplasmic proteins to the surface, that act as moonlighting proteins. Moonlighting proteins are proteins exhibiting an unrelated secondary function in addition to their primary activity (Huberts and van der Klei, 2010; Jeffery, 1999). In addition to processed lipoproteins, the processing of moonlighting proteins by proteases creates the possibility for near unlimited variation of *M. pneumoniae.* Such processing of moonlighting proteins on the mycoplasmal cell surface was already described (Tacchi *et al.*, 2016; Widjaja *et al.*, 2017). Modified and processed proteins from the cytosol, acting on the cell surface, add a further layer of complexity to the host-pathogen interaction. Translation elongation factor Tu (Ef-Tu) is one of the most prominent moonlighting proteins localizing on the cell surface. Moonlighting function of Ef-Tu is to bind human proteins, including fibronectin. The interaction between Ef-Tu and host proteins is established for several *Mycoplasmas, S. aureus,* and *Helicobacter pylori* (Balasubramanian *et al.*, 2008; Chiu *et*

al., 2017; Widjaja *et al.*, 2017; Yu *et al.*, 2018). Ef-Tu is a highly abundant protein and was seen to be very “sticky”, which means unspecific binding to many proteins. This was not only observed in *M. pneumoniae*, but also in *B. subtilis* (laboratory experience). Therefore, its specific role in host adhesion and the moonlighting function is still an open question. However, very good characterized moonlighting proteins have a common primary activity - they are involved in bacterial carbon metabolism. For *Mycoplasmas* several examples are described: lactate dehydrogenase (Ldh), glyceraldehyde-3-phosphate dehydrogenase (GAPDH, GapA), pyruvate dehydrogenase (PdhABC), phosphoglycerate mutase (Pgm), transketolase (Tkt), pyruvate kinase (Pyk), or enolase (Eno) are surface expose and interacts with several host proteins (Bao *et al.*, 2014; Chen *et al.*, 2011; Grimmer *et al.*, 2019; Gründel *et al.*, 2015; Gründel *et al.*, 2016a; Gründel *et al.*, 2016b; Schreiner *et al.*, 2012; Tacchi *et al.*, 2016; Thomas *et al.*, 2013; Yavlovich *et al.*, 2007). Recently, also the chaperone complex GroEL and DnaK of *M. pneumoniae* were detected on the surface and seem to interact with human extracellular components (Hagermann *et al.*, 2017). It is interesting to note, that all this moonlighting proteins lack signal motifs for their export, raising the question how they can localize on the cell surface. However, there is experimental evidence in several pathogenic bacteria that most of all investigated glycolytic enzymes, contribute to pathogenicity and can cause cytopathic effects in host cells (Henderson and Martin, 2011). Another example of virulence associated moonlighting protein is the glycerophosphodiester phosphodiesterase GlpQ of *M. pneumoniae*. GlpQ was shown to be a trigger enzyme (Schmidl *et al.*, 2011). Trigger enzymes are more specific moonlightners, as they are active in metabolism and, as second function, control gene expression (Commichau and Stülke, 2008). In the metabolism GlpQ is necessary for degradation of glycerophosphocholine subsequently leading to the formation of H_2O_2 (Schmidl *et al.*, 2011). Interestingly, in a GlpQ deficient mutant, the H_2O_2 production is not abolished when grown with glycerol. More important is the fact, that the mutant is not cytotoxic anymore even if *M. pneumoniae* is still able to produce H_2O_2 (Schmidl *et al.*, 2011). How other metabolic enzymes and moonlighting proteins of *M. pneumoniae* influence the cytotoxicity would be an interesting question to be adressed. Nevertheless, the detailed mechanism of interactions between moonlighting proteins of *M. pneumoniae* and host proteins is still elusive. Unfortunately, *in vivo* experiments are missing that would give clear evidence for this survival mechanism. The interaction of IBPs with Igs and components from the immune system, moonlighting proteins on the surface interacting and modifying host proteins make the pathogenicity of *Mycoplasmas* more complex.

Peroxide detoxification in *M. pneumoniae*

Pathogenic bacteria evolved various strategies to invade and persist in host tissues. In contrast to other bacteria, *Mycoplasmas* lack common virulence factors, such as toxins, invasins and cytolysins (Pilo *et al.*, 2005). Nevertheless, *M. pneumoniae* and relatives are very effective pathogens invading their host and overcome detection by the immune system (discussed above), forming chronic infections (Parrott *et al.*, 2016). As a virulence factor many *Mycoplasma* species use hydrogen peroxide as byproduct from their metabolism (Blötz and Stülke, 2017). On the other hand, human cells can produce hydrogen peroxide, nitric oxide or other reactive oxygen species (ROS) to defend themselves. Overall, *M. pneumoniae* is exposed to various ROS when infecting their host. Interestingly, the mechanisms how *M. pneumoniae* can tolerate high concentrations of internal and external ROS remains elusive. Recently, in some *Mycoplasmas* proteins were identified enabling these species to cope with ROS stress, *e.g*. superoxide dismutase or catalase, which are acquired likely by horizontal gene transfer (Perkins *et al.*, 2014; Chen *et al.*, 2000). In addition, the class of peroxiredoxins come more into the focus of research, since they act as antioxidants and degrade ROS. In many *Mycoplasmas* genes were identified which belongs to the large peroxiredoxin OsmC/Ohr superfamily. Some genomes, including *Mycoplasma*, *Bacilli*, or *Pseudomonas* spp., encode *ohr* and *osmC* homologs simultaneously and not only a single one. Despite their structural and functional similarities, it is possible that the proteins encounter different substrate specificities as discussed earlier (Lesniak *et al.*, 2002). One enzyme might be responsible for organic peroxide degradation from external sources, while the other could convert internal peroxide from their own metabolism. We identified these proteins building a putative system for ROS detoxification in *M. pneumoniae*, where MPN668 detoxifies organic peroxides, *i.e*. *tert*-butyl hydroperoxide, and MPN625 is might specific for hydrogen peroxide degradation. Our *in vitro* experiments clearly showed activity for MPN668, which is supported in a second study analyzing MPN668 function (Chen *et al.*, 2018a). Even though, we saw binding of H_2O_2 to MPN625 (ITC measurements) and decrease in H_2O_2 concentration in our *in vitro* assays, its function in detoxification is still questionable. The *in vitro* activity of the analyzed proteins could be impaired, due to the fact that DTT was used as an artificial reducing agent, instead of the intrinsic reducing factor. The identification of the native reducing agent would be of great importance. The reduction of peroxiredoxins is in general mediated by thioredoxins, thioredoxin-like proteins, or the glutathione reducing system. In *Mycoplasmas* no glutathione nor glutathione reductase is present. In contrast, the tested *Mycoplasmas* so far, showed high levels of thioredoxin reductase activity (Ben-Menachem *et al.*, 1997). For Ohr from *Xylella fastidiosaist* it was proven that the protein can be reduced only with DTT or its own thioredoxin, but not from Trx from yeast or *Spirulina* (Cussiol *et al.*, 2003). If the

thioredoxin system is really the reducing factor of MPN625 or MPN668 needs further investigations. Interestingly, the antioxidant ascorbic acid, better known as vitamin C, can also reduce peroxiredoxins (Monteiro *et al.*, 2007). The lack of vitamin synthesis genes would implicate that the reduction of detoxification enzymes relies only on the uptake of vitamin, which is rather unlikely. Recently, the reducing power of lipoylated proteins was proven for a peroxidase (Cussiol *et al.*, 2010). Noteworthy is the putative interaction of MPN668 with subunits of the pyruvate dehydrogenase complex (PDHC), containing lipoyl moieties (O'Reilley *et al.*, unpublished). Moreover, in previous studies MPN625 was identified to be phosphorylated (Schmidl *et al.*, 2010b). This could be a hint for post-translational modification of the enzyme to control its activity. Peroxiredoxins are known to be regulated in their activity by several modification, including phosphorylation (Antelmann and Helmann, 2011; Wood *et al.*, 2003; Rhee *et al.*, 2012). Modified *in vitro* enzyme assays, including purified TrxAB, PDHC or vitamin C should uncover the native reducing factor. Nevertheless, our interactome analysis (whole cell protein-protein interactions; O'Reilley *et al.*, unpublished) could directs the characterization of the detoxification system in more precise way. Not to neglect should be the possible impact of modifications on enzymes in the detoxification system, which should be addressed in future experiments as well.

Unexpected regulatory stress response

Different studies investigating OsmC and Ohr proteins had proven that the expression pattern of the respective genes change after exposure to different stress conditions. A putative upregulation upon tBP exposure of *mpn668* was discussed recently (Chen *et al.*, 2018a), but could not be reproduced under our conditions so far. In our experiments, no significant regulation of neither *mpn625* nor *mpn668* upon ROS was seen. This could be explained by differences in the experimental set-ups or simply too low amounts (5 mM) of peroxide stress. Additionally, the homologs in *M. genitalium* did not show regulation by ROS stress. Interestingly, the *osmC* homolog is induced under physical stress conditions, while the *ohr* homolog is reduced (Saikolappan *et al.*, 2009; Zhang and Baseman, 2014). This contrasts with the regulation of the respective genes investigated so far in various species, where ROS stress induces *ohr* genes and physical stress is responsible for expression of *osmC* genes, *i.e*. in *E. coli*, *X. campestris*, *B. subtilis*, and *Mycoplasma* spp. (Atichartpongkul *et al.*, 2001; Fuangthong *et al.*, 2001; Gutierrez and Devedjian, 1991; Jenkins *et al.*, 2008; Mongkolsuk *et al.*, 1998; Völker *et al.*, 1998). Interestingly, the putative *prx* gene from *M. hyopneumoniae* is constitutively expressed under all tested conditions (Schafer *et al.* 2007). Easily, the problem of too low concentrations of ROS stress could be addressed when using raising peroxide concentrations or extending incubation times (increasing from 20 to 60 minutes). Nevertheless, the hypothesis of *mpn625* and *mpn668* regulation is

supported by putative OhrR-like boxes upstream of the respective genes. These boxes were already described for *X. campestris*, *B. subtilis, Streptomyces coelicolor* or *Agrobacterium tumefaciens* (Chuchue *et al.*, 2005; Fuangthong *et al.*, 2001; Oh *et al.*, 2007; Sukchawalit *et al.*, 2001). The described boxes act as upstream DNA-binding *cis*-elements enhancing or silencing gene expression or act directly as repressor binding sites in the promoter region. In addition, our *M. pneumoniae* growth assay with *mpn625*/*mpn668*-mutant strains showed increased tolerance for H_2O_2 when one gene is missing. This could indicate an overexpression of the remaining gene to better cope with the stress conditions. Such compensatory effects are not unusual. As an example, when exposed to H_2O_2 *B. subtilis* strongly expresses the *katA* gene and auxiliary genes supporting ROS resistance, *i.e*. *ahpCF* and *mrgA* (Bsat *et al.*, 1996; Dowds, 1994; Herbig and Helmann, 2001; Tu *et al.*, 2012). In a mutant lacking *ahpCF* compensatory effects were observed. In these mutants near all remaining peroxide stress regulated genes are induced (Bsat *et al.*, 1996). However, also in *M. genitalium* putative DNA-regulatory elements were identified. The promoter region of the *osmC* homolog encounters a sequence for alternative sigma (σ^{70}) binding (Chen *et al.*, 2018a). Additionally, similar regulatory DNA-sequences were also identified in *A. tumefaciens* (Chuchue *et al.*, 2005). This could be true for the *M. pneumoniae mpn625* and/or *mpn668* promoters as well. Analyzing wild type and rendered OhrR-like boxes or promoter regions (σ^{70}) with *lacZ*-fusions could address possible regulation and their relevance.

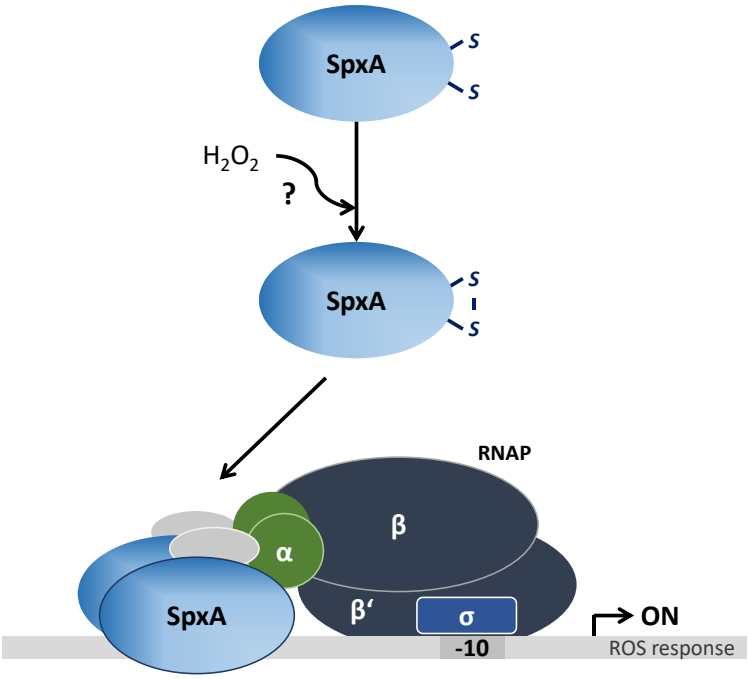

Figure 6.3 | Putative mechanism regulating ROS response in *Mycopalsma pneumoniae*. Under native conditions, SpxA has a redox-active CxxC motif that could be oxidized by peroxides and thereby activates SpxA as RNAP regulating transcription factor. Oxidized SpxA contacts the RNAP activating the transcription of detoxifing enzymes to cope with peroxide stress. Adapted from Antelmann and Helmann, 2011.

Moreover, potential regulatory proteins (transcription factors) could be investigated within DNA binding experiments (electromobility shift assays) with special focus on OhrR-like boxes. Interestingly, when *spxA* was overexpressed in *M. gallispeticum*, the levels of protective enzymes against ROS were increased (including the *osmC* homolog) (Matyushkina *et al.*, 2016). The *spxA* gene and therefore *osmC* upregulation occurred *in vivo* after infecting host cells (Matyushkina *et al.*, 2016). However, *spxA* is known to be induced upon infection (Galvão *et al.*, 2015). This observations could link virulence and ROS detoxification in *Mycoplasmas*. In *M. pneumoniae* the interaction of SpxA and the RNA-polymerase was recently shown (Eilers, 2010; Yus *et al.*, unpublished). SpxA is able to modulate the RNA polymerase affinity promoting or disturbing the expression of a certain gene. In *B. subtilis* Spx controls disulfide and cell wall stress related genes (Rojas-Tapias and Helmann, 2018). Since *Mycoplasmas* lack cell wall components, this protein might evolved to a different stress response mechanism. The oxidation of cysteines in SpxA by peroxides might lead to binding activity in *M. pneumoniae* (see Fig. 6.3). When analyzing diamide stress in *M. pneumoniae*, we saw upregulation of *spxA* and in addition the increase of oxidative stress related genes, *i.e*. *mpn625*, *mpn607* (*msrA*), and *mpn622* (*msrB*) (Yus *et al.*, unpublished). This indicates a regulatory function of SpxA after activation by reducing the cysteines due to diamide addition. It would be interesting to address the possible regulation of oxidative stress genes in *M. pneumoniae* with special regards on SpxA and its activation by peroxides and further a putative inducing effect after human cell contact.

Furthermore, we investigated the influence of the trigger enzyme GlpQ (Schmidl *et al.*, 2011), the protein kinase PrkC (Schmidl *et al.*, 2010b) and putative ferric uptake regulator Fur (Yus *et al.*, unpublished) on the expression of *mpn625* and *mpn668* and the ROS response in *M. pneumoniae*. We hypothesized that GlpQ could regulate the expression of ROS related genes, by sensing its substrate glycerophosphocholine or simply peroxides. The activating and repressing effects of GlpQ on *cis*-elements are known (Schmidl *et al.*, 2011). Such a dual role of regulation was also shown in *Streptomyces coelicolor* facilitated by the OhrR regulator in response to organic hydroperoxides (Oh *et al.*, 2007). However, we could not exclude that GlpQ or its enzymatic inactive homolog MPN566 directly bind MPN625 or MPN668 for regulatory purposes. We therefore analyzed their interaction in a BACTH, which revealed no direct protein interactions at all. Thereafter we focused on gene regulation by GlpQ. Our data suggests that *glpQ* is induced when H_2O_2 stress is detected in the cells, irrespective of an internal H_2O_2 production via glycerol or by an external H_2O_2 stimuli. This was also observed for the *glpQ* gene from *B. subtilis*, when 104 growth conditions were analyzed. The *glpTQ* operon is induced in the presence of glycerol, G3P, and H_2O_2 (Nicolas *et al.*, 2012; Nilsson *et al.*, 1994). The expression is tightly controlled by several transcription factors. In *B. subtilis* inverted repeats in front of *glpTQ*

can form stem-loops might influencing the expression as well (Nilsson *et al.*, 1994). How secondary mRNA structures influence the gene regulation in *Mycoplasmas* is an underrepresented topic so far. It would be interesting to analyze putative riboswitches that might sense substrates and alter gene expression. Surprisingly, the expression of *glpQ* is increased when *mpn625* is absent and H_2O_2 stress applied to the cells. This observation might imply an *in vivo* functionality of *mpn625* degrading H_2O_2 in the cells but not *in vitro*. When *mpn625* is absent, intracellular peroxide concentrations raise and lead to the induction of *glpQ*. The moonlighting properties of GlpQ seem to have an even greater impact on regulation with respect on the detoxification system. We uptated the existing mechanism and added our proposed influence on the detoxification system as shown in Figure 6.4.

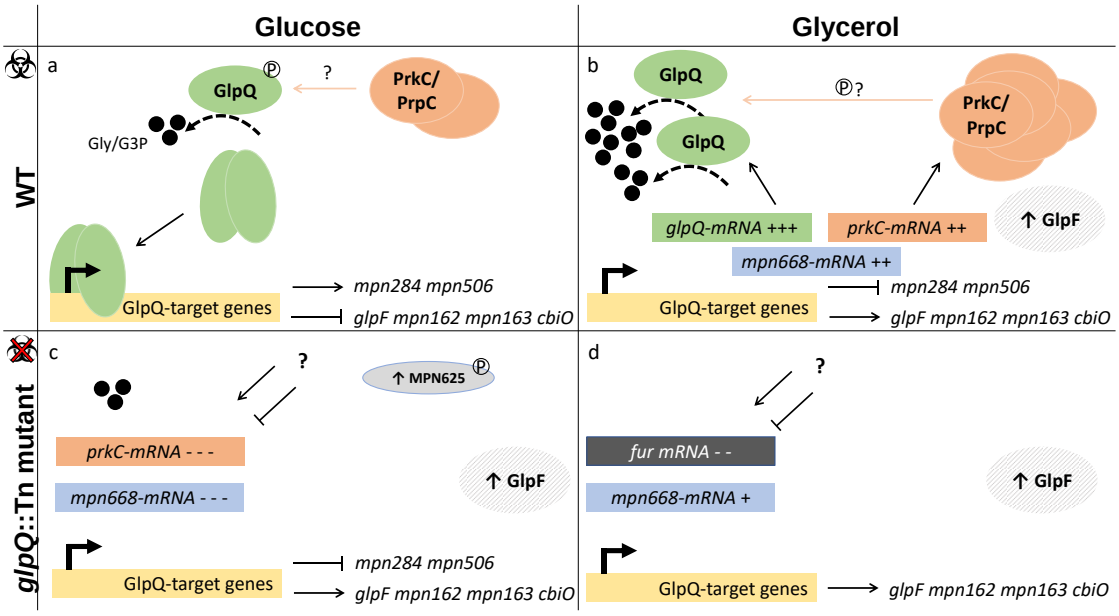

Figure 6.4 | Influences of GlpQ as trigger enzyme under glucose and glycerol conditions. (a) Wild type *M. pneumoniae* cells grown in glucose have low intracellular glycerol/G3P concentrations, resulting in a low *glpQ* activity. Enzymatic inactive GlpQ proteins are "free" and can trigger gene expression and repression. Wild type cells are cytotoxic to human cells. (b) Under glycerol and G3P growth conditions *glpQ*-activity is high and enzymatic active GlpQ cannot regulate gene expression. Regulation on *cis*-elements is reversed and mRNA of the glycerol facilitator *glpF* and other GlpQ repressed targets, *e.g.* the gene for the ion transport protein *cbiO* are induced. Further, mRNA levels of *prkC* and *prpC* as well as their protein levels raise. (c) Deletion of *glpQ* leads to mimicry of glycerol conditions for GlpQ targets even in glucose grown cells. Striking is the strong decrease of *prkC* and *mpn668* levels, protein levels of MPN625 increase. A *glpQ* mutant is not cytotoxic anymore. (d) GlpQ repressed targets are induced in a glpQ mutant under glycerol growth conditions, while no repression could be observed. Comapring the abundance of of *prkC* and *mpn668* mRNA in a *glpQ* mutant under glucose and glycerol growth conditions suggests an unidentified regulator (?) sensing the change of carbon sources or the peroxide production from the glycerol catabolism. mRNA in colored boxes, proteins in circles, mRNA levels are relative comparisons to mRNA levels of glucose grown wild type cells. Phosphorylation and abundance of proteins from Schmidl *et al*., 2010b, *glpQ*-targets were identified in Schmidl *et al*., 2011, G3P, glycerol 3-phosphate; P, phosphorylation.

Post-transcriptional regulation of the detoxification system

Phosphorylation is a fundamental control mechanisms of bacteria to post-transcriptional regulate their proteins (Mijakovic *et al.*, 2016). Since MPN625 and GlpQ are phosphorylated proteins (Schmidl *et al.*, 2010b), we hypothesized a connection of the major kinase PrkC in *M. pneumoniae* with the detoxification system (see Fig. 6.4). Therefore, we tested the *prkC*-mutant for regulatory effects on expression of *glpQ*, *mpn625* and *mpn668*. Our results showed no significant impact on *mpn625* or *mpn668* expression, when *prkC* was disrupted. Interestingly, the *glpQ* expression was strongly influenced by the absence of *prkC*. This might indicate, contradictory to former results (Schmidl *et al.*, 2010b), that PrkC phosphorylates GlpQ and influences its activity or stability. In consequence, PrkC could indirectly influence the detoxification of ROS by acting on GlpQ. Interestingly, in the *mpn625* mutant we saw upregulation of *prkC* when exposed to H_2O_2, which could indicate a lack of phosphorylation on GlpQ for its stability. This is in good agreement with the H_2O_2 stress induced expression of *glpQ*. A connection of phosphorylation and oxidative stress is given even in *B. subtilis*, where ROS protective enzymes are phosphorylated, *e.g.* SodA or KatA (Schmidt *et al.*, 2014). Another link of phosphorylation and protein regulation under peroxide stress is exemplified in *Streptomyces* species. The protein SenS was shown to play a major role in sensing peroxide stress. Phosphotransfer from SenS to SenR results in the derepression and the subsequent induction of the major catalase-peroxidase and iron homeostasis genes (de Orué Lucana *et al.*, 2005). New analysis of GlpQ and its phosphorylation status in the cell should be addressed. Artificially phosphorylated or dephosphorylated GlpQ proteins, and also MPN625, should be investigated with focus on activity and stability.

Sensing peroxide and ion concentrations in *M. pneumoniae*

In many bacteria the regulation of oxidative stress is strongly interconnected with metal ion homeostasis. If intracellular concentrations of free iron raise, the amount of deleterious reactive oxygen species increase as well, due to the Fenton reaction. To prevent ROS stress from iron imbalances, bacteria control their iron acquisition carefully (Cornelis, 2011; Touati, 2000). The ferric uptake regulator (Fur) is conserved in many bacteria, where it can act as repressor or activator. The Fur protein family contains metal and peroxide sensing transcription factors, *i.e*. Mur, Zur, PerR and Fur itself (Troxell and Hassan, 2013; Waldron and Robinson, 2009). Interestingly, the gene *mpn329* encodes a Fur-protein and is one of the rare transcription factors in *M. pneumoniae*. In *B. subtilis* three regulatory proteins of this class exist at the same time, namely Zur, Fur and PerR. The relationship of MPN329 with PerR proteins lead us to the comparison of the amino acid

sequence of MPN329 with the proteome of *B. subtilis*. Indeed, there is high homology of MPN329 and PerR (58% similarity, 25% identity) and to Zur (61% similarity, 17% identity) from *B. subtilis.* PerR and Fur of *B. subtilis* carry one structural zinc ion in each monomer. When PerR has bound additionally an iron ion as regulatory metal, it is able to sense peroxides (Lee and Helmann, 2006; Traoré *et al.*, 2009). The lack of a regulatory PerR protein in *M. pneumoniae* might be the result of genome minimization and end up in the evolution of another protein able to sense peroxides, such as SpxA, Fur or GlpQ. This observation promotes our hypothesis that a peroxidative stimulus is detected by *M. pneumoniae* and translated into gene regulation.

In *B. subtilis* the proteins Fur and PerR bind very similar DNA-sequences but control distinct sets of genes in responds to different stimuli (Baichoo and Helmann, 2002). In *Campylobacter jejuni*, Fur and PerR have overlapping regulatory functions, *e.g*. the catalase gene is controlled by both regulatory proteins (van Vliet *et al.*, 1999). Overall, Fur and PerR seem to evolved from a common ancestor, where Fur retained its original function and PerR get specialized to sense peroxide stress. Noteworthy is that Fur appears to be essential in some bacteria, *e.g*. in *P. aeruginosa* or *Mycobacterium tuberculosis* (Barton *et al.*, 1996; Rodriguez *et al.*, 2002). However, we were able to delete the *mpn329* gene in *M. pneumoniae* without any obvious growth defects in complex medium. Transcriptomic comparison of the *mpn329* mutant with the wild type and in a second experiment, incubation of both strains with thiolutin, a zinc chelator, provoked the major upregulation of MPN329 targets and down-regulation of *glpQ*. In addition, thiolutin incubated wild type cells upregulate *mpn625* significantly (Yus *et al.*, unpublished). Interestingly, when crystallizing the Ohr protein from *Vibrio cholerae* it was found that zinc ions were bound to the dimer (Nocek *et al.*, unpublished; PDB: 3EER), which could influence activity and explain the low activity in *in vitro* assays and its upregulation under zinc limitation. Higher amounts of MPN625 could compensate for their low activity. Similarly, in a *B. subtilis perR* mutant ROS related genes as well as *fur* are induced (Chen *et al.*, 1995; Faulkner *et al.*, 2012). The interconnection of MPN329 and GlpQ targets tempted us to the assumption, that both genes are involved in balancing metal ion homeostasis and oxidative stress in *M. pneumoniae*. This is supported by experimental data where the overexpression of MPN329 protein leads to significant altered regulation of *glpQ* targets and the other way around, a deletion of *glpQ* influences the regulation of MPN329 targets (Güell *et al.*, 2009; Schmidl *et al.*, 2011; Yus *et al.*, unpublished). The impact of zinc limitation by thiolutin suggests that MPN329 is regulated by zinc and hence be considered as Zur protein, rather as iron regulated protein. Further investigation of Zur and GlpQ regulating the metal ion homeostasis and oxidative stress response in *M. pneumoniae* are indispensable when

deciphering the detoxification system. Using foot printing analysis of the known transcription factors under different conditions (Fe^{2+}/Zn^{2+}-limitation or peroxide stress) to the genome of *M. pneumoniae* could reveal target for each regulatory protein. In consequence, we might be able to reveal how different control elements in *M. pneumoniae* are interconnected. Lastly, it should be noted, that the production of H_2O_2 is strongly influencing mycoplasmal virulence and the detoxification enzymes might only reduce intracellular ROS stress to a non-toxic level instead of detoxifying extracellular peroxides, that are secreted to kill cells in their surroundings.

CHAPTER 7 | Supplementary Material

SUPPLEMENTARY TABLES

Table S2.1 | Oligonucleotides used in the study of chapter 2.

Primer	Sequence	Restriction sites
Construction of *mpn244, mpn140, mpn549* and *gdpP* overexpression plasmids		
***mpn244*-plasmid (pGP2036)**		
AS95	5‘-AAACATATGATGATGACAGTGGAAGTCTTTTCG	NdeI
AS96	5‘-TTTGGATCCTTAACCCGGCTTTACCGTCAG	BamHI
***mpn140*-plasmid (pGP2717)**		
KT21	5‘-AAACATATGAATAGCCAAGTACACCGCAAG	NdeI
KT22	5‘-TTTGGATCCTACAGCAATTTGCTTTTGGCAATCTTG	BamHI
KT23	5‘-p-AACTTTCCC**TGG**TTGGAGATGGTTTTCAC	
KT24	5‘-p-TAATACATCA**TGG**AGAACACTATATCTAGGATCTATG	
***mpn549*-plasmid (pGP2718)**		
KT25	5‘-AAACATATGATTAACATCGATCCCCATTTTATTC	NdeI
KT26	5‘-TTTGGATCCGCTGTTGACATGCTTTTGTTTGG	BamHI
KT27	5‘-p-AAGACATTAAGAAG**TGG**ATTGGTTCCATTCGTTC	
***gdpP*-plasmid (pGP2720)**		
KT30	5‘-AAACATATGCCGATTGGAATCATGCTTTTTAATGACC	NdeI
KT31	5‘-TTTGGATCCTCTCTGTACGCCTCCCTCAAAATAC	BamHI
Screening oligos		
mpn244		
KT17	5‘-CTCCAGAGCGTTTTACTGACACT	
KT18	5‘-GTATGGCATTATTCCCGGCATTG	
mpn140		
KT63	5‘-AGTCTACAGTTATTTAGGCGGATCG	
KT64	5‘-CCTAAAGACACCTATACTCAAAGGC	
mpn549		
KT19	5‘-GAGTTGAGTCATATTAGTCTGGAAGG	
KT20	5‘-GCAAACCGTGGTATGAAGCTAAG	
KT65	5‘-CAGGTATTACGATCAATTCGGTGC	
KT66	5‘-GTGGCATAGACAGTCCAGTAGC	
Tn*4001*		
SH29	5‘-ATGAGTGAGCTAACTCACAG	
SH30	5‘-CAATACGCAAACCGCCTC	

Restriction sites are underlined, mutation sites in bold letters, p denotes phosphorylation

Table S3.1 | Oligonucleotides used in the study of chapter 3.

Primer	Sequence	Restriction sites
Construction of *oriC plasmids*		
***tetM* cassette**		
CB61	5‘-ATGAATTCATGAAAATTATTAATATTGGAGTTTTAGCTCATG	EcoRI
CB62	5‘-ATGGATCCAGTTATTTTATTGAACATATATCGTACTTTATCTAT	BamHI
***full-length oriC* region (pGP2756)**		
CB55	5‘-ATGAATTCGCCATGGTTGTTTTTAAAACGCCAC	EcoRI
CB56	5‘-ATTCTAGAAGAGTGGTATGGTTTCATCTTATTGTTAG	XbaI
***5’- oriC* region (pGP2732)**		
CB103	5‘-TTTTCTAGATAATATTAGCCTAATACTATAGATAATATTAAGATAATA	XbaI
***3’- oriC* region (pGP2733)**		
CB104	5‘-TTTGAATTCTATTATCTTAATATTATCTATAGTATTAGGCTAATATTA	EcoRI
***glpQ* complementation plasmid (pGP2496)**		
CB105	5‘-TTTGACGTCCAAATCTAAATACGGTTTTCCTCTCAC	AatII
CB106	5‘-TTTGATATCTTACACTTCAAACTTCTTGTTGGCAATTTG	EcoRV
Check PCR for integration		
AS30	5‘-CGCGGTTGGGCACATTTTAATA	
AS31	5‘-GGGGCATGTCCTTAGAAAAGAA	
CB158	5‘-GCGTGGACAAAGGTACAACGA	
CB159	5‘-CTTCTGCTAAGAAATCCATATGTCCTGG	
Probing oligos		
oriC		
CB75	5‘-TTAGTATTATTCCGGTATTATTTACCGAC	
CB76	5‘-*CTAATACGACTCACTATAGGGAGA* TGCCTATTATATATAATGTCATGGTAGC	
***aac-ahpD* (Gm^R)**		
SH62	5‘-TAGAATTTTATGGTGGTAGAG	
SH63	5‘-*CTAATACGACTCACTATAGGGAGA* ACACTATCATAACCACTACC	
RT oligos		
rpoB		
CB160	5’-CCAGTAGTGTCGATGGCGTT	
CB161	5’-ACAATTTTAACTGGGACTTAGTGAGCA	
tetM		
CB158	5’-GCGTGGACAAAGGTACAACGA	
CB159	5’-CTTCTGCTAAGAAATCCATATGTCCTGG	

Restriction sites are underlined, T7 RNA polymerase extension in *italic*

Table S3.2 | Plasmids used in the study of chapter 3.

Plasmid name	Backbone	Restriction sites	Purpose	Reference
pET3c		XbaI BamHI	T7 driven expression plasmid	Novagene
pGP2496	pGP2756	AatII EcoRV	Expression of *glpQ* with native promoter	This work
pGP2732	pET3c	XbaI BamHI	5'-*oriC* (PCR CB55-CB103)	This work
pGP2733	pET3c	XbaI BamHI	3'-*oriC* (PCR CB104-CB56)	This work
pGP2756	pET3c	XbaI BamHI	*oriC* (PCR CB55-CB56)	This work
pGP2777	pET3c	EcoRI BamHI	*tetM* (PCR CB61-CB62 from pMTn*tetM438*)	This work
pMCO3			Replicative vector for *M. capricolum*	Lartigue *et al.*, 2003
pMgalloriC			Replicative vector for *M. gallisepticum*	Lartigue *et al.*, unpublished
pMTn*tetM*438			Transposon mutagenesis in *M. genitalium*	Pich *et al.*, 2006
pSRT2			Cloning vector	Lartigue *et al.*, 2002

Table S4.1 | Oligonucleotides used in the study of chapter 4.

Primer	Sequence	Restriction sites
Screening oligonucleotides *mpn400*::Tn4001		
CB37	5'-GAGAAGAACACTATATCTTTAATAGGTG	
CB38	5'-GCCAAGACCTAACAAAACCAAAAAG	
SH29	5'-ATGAGTGAGCTAACTCACAG	
SH30	5'-CAATACGCAAACCGCCTC	
Southern blot probes		
mpn400-probe		
CB53	5'-TTTCCGCAGTTCTAATCGTTAATGAG	
CB54	5'-**CTAATACGACTCACTATAGGGAGA-**GGGACACCTTGATCGACAAAG	T7-extension
aac-ahpD-probe		
SH62	5'-TAGAATTTTATGGTGGTAGAG	
SH63	5'-**CTAATACGACTCACTATAGGGAGA-**ACACTATCATAACCACTACC	T7-extension
Construction of overexpression plasmids		
mpn400		
CB57	5'-**AT***GGTACC***A**ATGAAATTAAATTTCAAAATCAAGGACAAAAAGAC	KpnI

CB58	5‘-**AT***GGATCC***TTA**AGTTCGAATCTCTTGGAAAACATTTTC	BamHI
CB59	5‘-[phos]-GGTGGTTTCTGGGCGCTTGGTCT	MMR
CB60	5‘-[phos]-AAATGCAAGGTTACTGGGCTGGTGGTTAC	MMR
CB177	5‘-**AAA***GGTACC***A**GTTAATGAGGTATTAAGGCTACAAAGT	KpnI
CB179	5‘-**AAA***GGATCC***TTA**AGCGCGTTGTACAATTTCCTTTTG	BamHI
mpn641		
CB228	5‘-**AAA***GAGCTC***T** TGTTCTAATTCTGATTTTCAAACTAATTTA-ACAA	SacI
CB229	5‘-**AAA***GGATCC***TTA** TTAGAGAATGGAATAAAGCAAGTAAGG	BamHI
Gene deletion plasmid		
CB87	5‘-TTT *AAGCTT* GCCGGTTCAAGTCCGGC	HindIII
CB88	5‘-TTT *CTGCAG* GTCTTTTTGTCCTTGATTTTGAAATTTAATT-TCAT	PstI
CB89	5‘-TTT *GGATCC* GAAAATGTTTTCCAAGAGATTCGAACTTAA	BamHI
CB90	5‘-TTT *TCTAGA* TTTATTTGCTTTTCGTACTCCTCTAACT	XbaI

restriction sites are *italic*, mutation bases are underlined, additional bases in **bold**

Table S4.2 | Plasmids used in the study of chapter 4.

Plasmid name	Backbone	Oligos/ Restriction sites	Purpose	Reference
pBSKII(-)			Cloning vector / blue-white selection	Stratagene
pGP172			Expression of N-terminal STREP-tagged proteins	Merzbacher *et al.*, 2004
pGP2727 pBSKII (-)	lox71-P_{438}-cat-lox66 (PCR product	CB87 - CB88 HindIII / PstI + CB89 - CB90 BamHI / XbaI	GP35-dependent deletion of genes	This work
pGP2729	pGP2727	deletion *mpn400* 5'-HR + 3'-HR	Deletion of *mpn400*	This work
pGP2743	pBSKII(-)	CB57 / CB58 CB59* CB60* KpnI / BamHI	MMR* reaction to reverse TGA into TGG codons	This work
pGP3215	pGP172	CB177 / CB58 KpnI / BamHI	Overexpression of Strep-MPN400 w/o transmembrane domain	This work
pGP3217	pGP172	CB177 / CB179 KpnI / BamHI	Overexpression of Strep-MPN400 A446STOP w/o transmembrane domain	This work

pGP3235	pGP172	CB228 / CB229 SacI / BamHI	Overexpression of Strep-MPN641 w/o transmembrane domain	This work

*Hames *et al.*, 2005

Table S5.1 | Oligonucleotides used in the study of chapter 5.

Primer	Sequence	Restriction sites
Construction of BACTH plasmids		
mpn625		
LK41	5‘-AAA GGTACC GCATGCACTAAAGTTACATTAACGTTAATCTTG-AGTTGAC	KpnI
LK44	5’-AAA TCTAGA AATGGACAAAAAGTACGACATCACTGCTGTTTT-AAA	XbaI
mpn668		
LK42	5‘-TTT GGTACC GCAAGCTTGGCACCGTTCAAGGTTAAACC	KpnI
LK14	5‘-AAA TCTAGA AATGGCAGTAATTTACAAAACAACAGCACACGC	XbaI
mpn566		
LK16	5‘-AAA TCTAGAA ATGCGCAAACAGTTTTTAATTGCACACCGTG	XbaI
LK43	5‘-AAA GGTACC GCGTAAAGTTGTGCTGCTATTTGAAATTTAAC-AAAGCG	KpnI
Protein overexpression		
CB162	5‘-AAA GGATCC GAATGGACAAAAAGTACGACATCACTG	BamHI
CB163	5‘-AAA GCGGCCGC TTAATGCACTAAAGTTACATTAACGTTAAT-CT	NotI
CB164	5‘-AAA GGATCC GAATGGCAGTAATTTACAAAACAACAGCAC	BamHI
CB165	5‘-AAA GCGGCCGC TTAAAGCTTGGCACCGTTCAAGG	NotI
CB172	5‘-AAA GGATCC GAATGGTAACTGAAATTAAAAGTCTCAAACAAC	BamHI
CB173	5‘-AAA GCGGCCGC TTATTGGCTGACAAGTTGCACGAT	NotI
CB174	5‘-[Phos]GTAATTATTGATTTTTGGGCAGAATGGTGTGGG	
CB175	5‘-AAA GGATCC GAATGCTTAAAGTAAAGTCAGATTTTTTAACTA-AAG	BamHI
CB176	5‘-AAA GCGGCCGC CTAAAGGACATCACGGATCGTTAA	NotI
CB194	5‘-[Phos]TCTGGTTTAGCTGCTAGTGAATTGGCAAC	
CB195	5‘-[Phos]TCCAAACGCTCCCCAGCGCAC	
CB196	5‘-[Phos]TCAGCTTATGCTGGTTGATTTTCGCAAGCT	
CB197	5‘-[Phos]TCAGCTTATGCTGGTTGATTTTCGCAAGCT	
RT oligos		
rpoB		
CB160	5’- CCAGTAGTGTCGATGGCGTT	
CB161	5’- ACAATTTTAACTGGGACTTAGTGAGCA	
spx		
LK51	5’- GATTTGACCATTCCTGAATTGATTAAGTTAATTCGC	
LK52	5’- TACTTCTTTACTGTACGCACTTTAGGTTCCATTAA	
fur		
LK53	5’- TTAAGACACGAAAACCACAAGCACATTTACTTCTTT	

LK54	5’- CTTATTGATCATCTTCAAGTGTACCGCTAGC	
mpn625		
LK01	5’-ATGGACAAAAAGTACGACATCACTGCTGTTTTAAA	
LK02	5’-ATCAAGTTAGCGGTTGCCAATTCACAAGC	
mpn668		
LK03	5’-ATGGCAGTAATTTACAAAACAACAGCACACGC	
LK04	5’-CAGCTTGCGAAAAACAACCAGCATAAGC	
rpsL		
CB404	5’- ATGACTCCAAAAAAACCGAACTCTGCTTTG	
CB405	5’- ACGAACAATGTGGTAACGCACACCAG	
mraZ		
CB400	5’- TGCAAAAAACAGGATCAGTCTGCCAGC	
CB401	5’- TTAAGCGCTTGAGTGTTCTAGTGTCTTTTTG	
prkC		
CB402	5’- TCACACAAAAATCTGGTGCAAACCTTTGATG	
CB403	5’- GTACACCACCTCCTGCACACTAAAGT	
glpQ		
SG23	5’- CTTTGCTTCCTTACAGCGC	
SG24	5’- TTTTCGTAAATGTTTGTTCAGGGATG	
Gene deletion in *M. pneumoniae*		
CB125	5’- AAA CTCGAG AGCGGTTGAGCAAACTCAAACC	XhoI
CB126	5’- AAA CTGCAG TTTAGTGTTTGGTTATCGTGCTCCA	PstI
CB127	5’- AAA TCTAGA ACATAGTCGCTAGCGGTACAC	XbaI
CB128	5’- AAA GCGGCC GCTGAGTGCTTGAAAGAAGGAAAAGC	NotI
CB128	5’- AAA GCGGCC GCTGAGTGCTTGAAAGAAGGAAAAGC	NotI
CB426	5’- AAA CTGCAG TAGTATTTAGAATTAATAAAGTATGAAAATTAT-TAATATTGG-AGTTTTAGCTCATG	PstI
CB62	5’- AT GGATCC AGTTATTTTATTGAACATATATCGTACTTTATCT-AT	BamHI
CB85	5’- TTT CTGCAG TACCGTTCGTATAGCATACATTATACGAAGT-TAT*TAGTATTTAGAATTAATAAAGT* ATGAACTTTAATAAAATTGATTTAGACAATTGGAA	PstI *MG438 promoter*
CB86	5’- TTT *GGATCC* TACCGTTCGTATAATGTATGCTATACGAAGT-TATCCAGCGTGGACCGGCG	BamHI
LK20	5’-AAA GAATTC CGACAAGCGCATTAGCCCTCTCC	EcoRI
LK21	5’-TTT CTGCAG ATTTACTATATGGATTTAAGTTTAATTTAACTCT-AGCGCGC	PstI
LK22	5’-AAA GGATCC TGGGTAAAAAACGAGCGAAAAATGCTGAAAAA-ATAC	BamHI
LK23	5’-TTT TCTAGA TTCTTGGCTTTCTTAAACGCTAAGTGCACC	XbaI
LK26	5’-AAA GAATTC AAACCGCGTTCCCAACGAGCACTAAA	EcoRI
LK27	5’-TTT CTGCAG GTTACTGATATTATATTTAGAAAGATGACAAAA-GATCTCCTA	PstI
LK28	5’-AAA GGATCCC AAATTCCTTGAGGATGGCCAAGACTTCA	BamHI
LK29	5’-TTT TCTAGA CTTTGCCGTCCTTTTAGGTGATGATGTC	XbaI
LK45	5’-C*G*A*C*AAGCGCATTAGCCCTCTCC	*protecctedd
LK46	5’- biotin-TEG-TTCTTGGCTTTCTTAAACGCTAAGTGCACC	biotinylated

LK47	5'-C*T*T*T*GCCGTCCTTTTAGGTGATGATGTC	*proteccted
LK48	5'-biotin-TEG-AAACCGCGTTCCCAACGAGCACTAAA	biotinylated
***Bacillus subtilis* work**		
CB296	5'-AAA GCGGCC GCATGGCAGTAATTTACAAAACAACAGCAC	NotI
CB320	5'-AAA GGATCCA GACAAAAAGTACGACATCACTGC	BamHI
CB320	5'-AAA GGATCC AGACAAAAAGTACGACATCACTGC	BamHI
CB321	5'-AAA GTCGAC TTATTAATGCACTAAAGTTACATTAACGTTAAT-CT	SalI
CB322	5'-AAA GTCGAC TTATTAATGATGATGATGATGATGCACTAAAG-TTACATTAACGTTAATCT	SalI
CB323	5'-AAA GGATCC AATGGCAGTAATTTACAAAACAACAGCAC	BamHI
CB324	5'-AAA GAATTC TTATTAAAGCTTGGCACCGTTCAAGG	EcoRI
CB325	5'-AAA GAATTC TTATTAATGATGATGATGATGATGAAGCTTGGC-ACCGTTCAAGG	EcoRI
CB394	5'- AAA ACTAGT TTATTAATGATGATGATGATGATGCACTAAAGT-TA	BcuI
CB395	5'-AAA ACTAGT TTATTAATGATGATGATGATGATGAAGCTTGG	BcuI
CB396	5'-AAA GCGGCC GCATGGATCCAGACAAAAAGTACGACATC	NotI
tet-fwd	5'-*CAGCGAACCATTTGAGGTGATAGG* GCTTATCAACGTAGTA-AGCGTGG	
tet-rev	5'-*CGATACAAATTCCTCGTAGGCGCTCGG* GAACTCTCTCCCAA-AGTTGATCCC	
spec-fd	5'-*CAGCGAACCATTTGAGGTGATAGG* GACTGGCTCGCTAATAA-CGTAACGTGACTGGCAAGAG	
spec-rev	5'-*CGATACAAATTCCTCGTAGGCGCTCG* GTTTCCACCATTTT-TTCAATTTTTTTATAATTTTTTTAATCTG	w/o terminator
zeo-fwd	5'-*CAGCGAACCATTTGAGGTGATAGG* GAACGATGACCTCTA ATAATTG	
zeo-rev	5'-*CGATACAAATTCCTCGTAGGCGCTCGG* GTAGTATTTTTTG AGAAGATCAC	

restriction sites are underlined, overhangs highlighted in *italic*, protected, biotinylated and phosphorylated oligonucleotides are indicated

Table S5.2 | Plasmids used in the study of chapter 5.

Plasmid name	Backbone	Purpose / Used Oligonucleotides	Restriction sites	Reference
BACTH plasmids				
p25-N		N-terminal fusion of the target protein to the T25 fragment of adenylate cyclase		Karimova *et al.*, 1998
pET-SUMO		Fusion of protein with N-terminal His-tag, overexpression in *E. coli*		Mossessova and Lima, 2000
pGP2001	pUT18	N-terminal fusion of *glpQ* to the T18 fragment of adenylate cyclase		Schmeisky, 2013

pGP2002	pUT18C	C-terminal fusion of *glpQ* to the T18 fragment of adenylate cyclase		Schmeisky, 2013
pGP2003	p25-N	N-terminal fusion of *glpQ* to the T25 fragment of adenylate cyclase		Schmeisky, 2013
pGP2004	pKT25	C-terminal fusion of *glpQ* to the T25 fragment of adenylate cyclase		Schmeisky, 2013
pGP2949	pUT18	N-terminal fusion of *mpn625* to the T18 fragment of adenylate cyclase	XbaI KpnI	This work
pGP2950	pUT18C	C-terminal fusion of *mpn625* to the T18 fragment of adenylate cyclase	XbaI KpnI	This work
pGP2951	p25N	N-terminal fusion of *mpn625* to the T25 fragment of adenylate cyclase	XbaI KpnI	This work
pGP2952	pKT25	C-terminal fusion of *mpn625* to the T25 fragment of adenylate cyclase	XbaI KpnI	This work
pGP2953	pUT18	N-terminal fusion of *mpn668* to the T18 fragment of adenylate cyclase	XbaI KpnI	This work
pGP2954	pUT18C	C-terminal fusion of *mpn668* to the T18 fragment of adenylate cyclase	XbaI KpnI	This work
pGP2955	p25N	N-terminal fusion of *mpn668* to the T25 fragment of adenylate cyclase	XbaI KpnI	This work
pGP2956	pKT25	C-terminal fusion of *mpn668* to the T25 fragment of adenylate cyclase	XbaI KpnI	This work
pGP2957	pUT18	N-terminal fusion of *mpn566* to the T18 fragment of adenylate cyclase	XbaI KpnI	This work
pGP2958	pUT18C	C-terminal fusion of *mpn566* to the T18 fragment of adenylate cyclase	XbaI KpnI	This work
pGP2959	p25N	N-terminal fusion of *mpn566* to the T25 fragment of adenylate cyclase	XbaI KpnI	This work
pGP2960	pKT25	C-terminal fusion of *mpn566* to the T25 fragment of adenylate cyclase	XbaI KpnI	This work

pKT25		C-terminal fusion of the target protein to the T25 fragment of adenylate cyclase		Karimova *et al.*, 1998
pKT25-ZIP		Control plasmid carrying leucine zipper fused to T25 fragment of adenylate cyclase		Karimova *et al.*, 1998
pUT18		N-terminal fusion of the target protein to the T18 fragment of adenylate cyclase		Karimova *et al.*, 1998
pUT18C		C-terminal fusion of the target protein to the T18 fragment of adenylate cyclase		Karimova *et al.*, 1998
pUT18-ZIP		Control plasmid carrying leucine zipper fused to T25 fragment of adenylate cyclase		Karimova *et al.*, 1998
Protein expression plasmids				
pBSK(II)-		Cloning vector / blue-white selection		Stratagene
pGP1899	pGP3260	*mpn625*-6xHis CB396-CB394 (from pGP3276)	NotI BcuI	This work
pGP1900	pGP3261	*mpn668*-6xHis CB296-CB395 (from pGP3277)	NotI BcuI	This work
pGP3210	pET-SUMO	*mpn625* CB162-CB163	NotI BamHI	This work
pGP3211	pET-SUMO	*mpn668* CB164-CB165	NotI BamHI	This work
pGP3212	pET-SUMO	*trxA** CCR CB172-CB173-CB174 (from pGP3214)	NotI BamHI	This work
pGP3213	pET-SUMO	*trxB* CB175-CB176	NotI BamHI	This work
pGP3214	pBSKII (-)	*trxA* CB172-CB173	NotI BamHI	This work
pGP3241	pET-SUMO	*mpn625*-mutated Cys: S^{P}-C^{R} CB162-CB163-CB194	NotI BamHI	This work
pGP3242	pET-SUMO	*mpn625*-mutated Cys: C^{P}-S^{R} CB162-CB163-CB195	NotI BamHI	This work
pGP3243	pET-SUMO	*mpn668*-mutated Cys: S^{P}-^{CR} CB164-CB165-CB196	NotI BamHI	This work
pGP3244	pGP2962	*mpn668*-mutated Cys: C^{P}-S^{R} CB164-CB165-CB197	NotI BamHI	This work
pULP				Mossessova and Lima, 2000
Gene deletion plasmids				
pBSKP438-Cre	pBSKII	Excision of CmR cassette with Cre recombinase		Mariscal *et al.*, 2016
pGP1704	pGP2964	*tetM* from pGP2756 CB62-CB426	BamHI PstI	This work
pGP1705	pGP2963	*tetM* from pGP2756 CB62-CB426	BamHI PstI	This work

pGP2727	pBSKII (-)	lox71-P_{438}-cat-lox66 (PCR product CB85-CB86)		This work
pGP2756		Replicative plasmid in *M. pneumoniae*		Blötz *et al.*, 2018
pGP2961	pGP2727	Insertion of the 5'HR of *mpn625*	EcoRI BamHI	This work
pGP2962	pGP2727	Insertion of the 5'HR of *mpn668*	EcoRI BamHI	This work
pGP2963	pGP2961	Insertion of the 3'HR of *mpn625*	EcoRI BamHI	This work
pGP2964	pGP2962	Insertion of the 3'HR of *mpn668*	EcoRI BamHI	This work
pGP3239	pGP2727	Deletion of *mpn329* (*fur*) 3'-HR CB127-CB128	XbaI NotI	This work
pGP3240	pGP3239	Deletion of *mpn329* (*fur*) 5'-HR + 3'-HR CB125-CB126	XhoI PstI	This work
***Bacillus* subtilis plasmids**				
pAC5		Integrative vector for the *amyE* locus in *B. subtilis*		Martin-Verstraete *et al.*, 2011
pDG148		phelo(zeo)-resistance cassette		Joseph *et al.*, 2001
pDG1514		tet-resistance cassette		Guérout-Fleury *et al.*, 1995
pDG1726		spec-resistance cassette		Guérout-Fleury *et al.,* 1995
pGP2202	pGP888	*mpn668* PCR CB323-CB324	EcoRI BamHI	This work
pGP3273	pAC5	P_{grac} and *lacI* go into the backbone with *cat* and both *amyE* sites; pHT01 (digested: SacI BamHI and EcoRI ClaI)		This work
pGP3274	pGP884	*mpn625* CB320-CB321 (from pGP3210)	BamHI SalI	This work
pGP3275	pGP3273	*mpn668* CB323CB-324 (from pGP3211)	BamHI EcoRI	This work
pGP3276	pGP884	*mpn625*-6xHis CB320-CB322 (from pGP3210)	BamHI SalI	This work
pGP3277	pGP3273	*mpn668*-6xHis CB323-CB325 (from pGP3211)	BamHI EcoRI	This work
pGP884		xylose-inducible protein expression in *B. subtilis;* integrative in the *ganA* locus		Gunka, 2011
pGP888		xylose-inducible protein expression in *B. subtilis;* integrative in the *ganA* locus		Diethmeier *et al.*, 2011
pHT01		Expression vector for high level protein production in *B. subtilis*		MoBiTec

SUPPLEMENTARY FIGURES

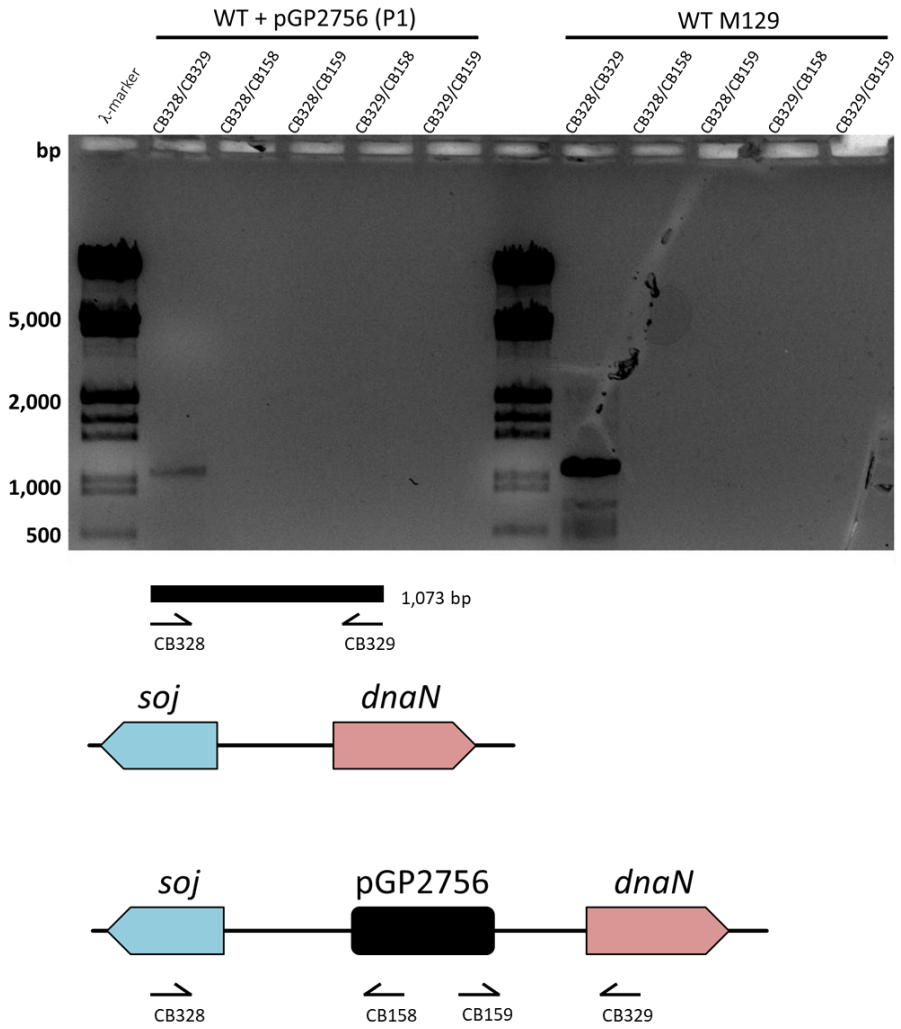

Figure S3.1 | Verification of the possible integration of pGP2756 in the *M. pneumoniae* chromosome. Isolated DNA was used in PCR reactions checking the native *oriC* locus (left: WT + pGP2756 | right: WT). For the possible integration different combinations of oligos amplifying from the plasmid into the chromosome as depicted in the left part of the figure were used. Only native *oriC* loci could be detected in cells transformed with pGP2756 as in the wild type control. Primer pairs and product size: CB328-CB329 (WT 1,073 bp), CB328-CB158 (WT no product), CB328-T7p (WT no product, Integrant 1,017 bp), CB329-CB159 (WT no product, Integrant 1,250 bp).

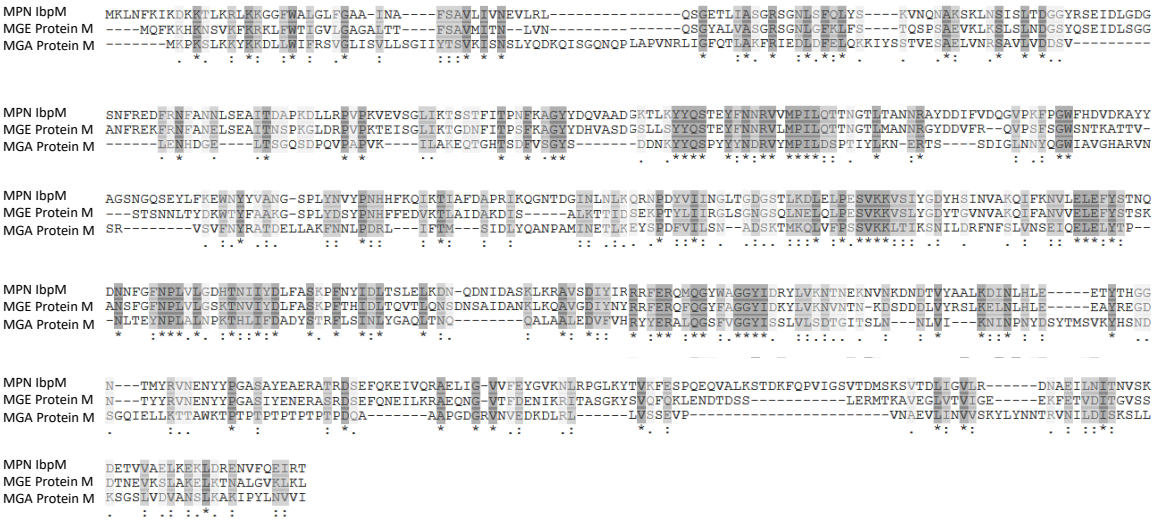

Figure S4.1 | Alignment of immunoglobulin binding proteins from *Mycoplasmas*. For the alignment BLASTp was used to align the putative immunoglobulin binding protein of *M. pneumoniae* (MPN IbpM former MPN400) with the Protein M (MG281) from *M. genitalium* (MGE) and the homology of *M. gallisepticum*. Identical residues are indicated by asterix (dark grey), similar amino acids indicated by **:** (medium grey) and less similar amino acids only with a point (light grey).

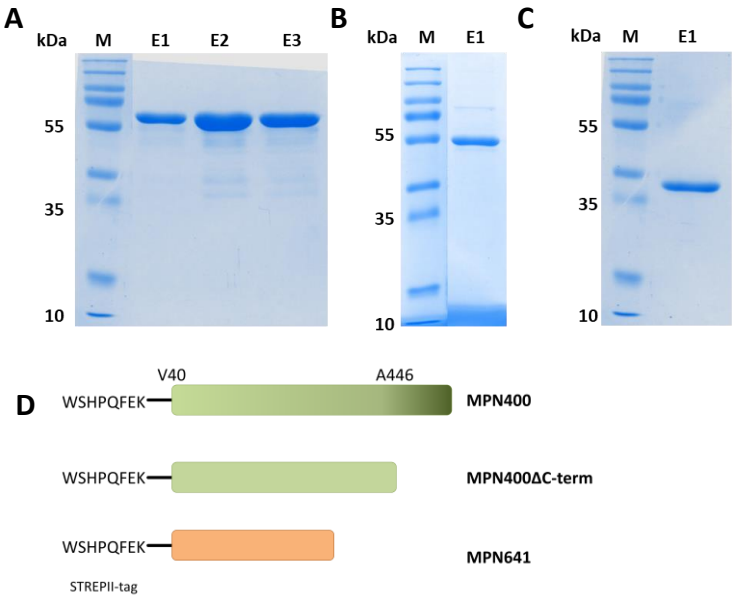

Figure S4.2 | Overexpression of recombinant proteins for *in vitro* characterization. Proteins were expressed in E. coli BL21 in 2fold LB medium for 3 hours with IPTG. STREP-tagged proteins were purified from cell lysates after cell disruption (French pressure) with Streptactin columns. After extensive washing proteins were eluted with d-desthiobiotin. Fractions of the purification were checked via SDS-PAGE and stained with Colloidal Coomassie. (A) Elution fractions of recombinant IbpM (64 kDa). (B) Elution fraction of C-terminal truncated IbpM (51 kDa). (C) Elution fraction of MPN641 (31 kDa). (D) STREP-tagged proteins that were generated for *in vitro* enzyme assays.

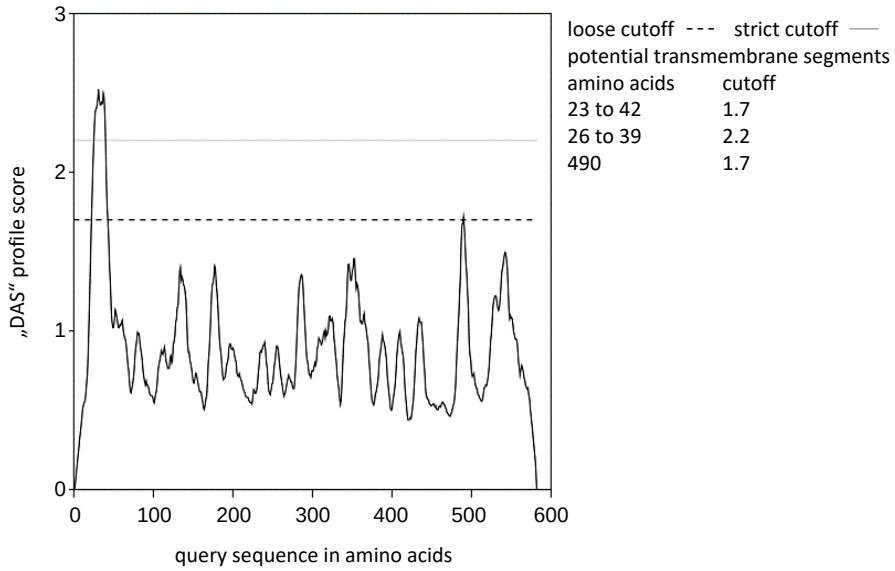

Figure S4.3 | Transmembrane prediction of MPN400 using „DAS". Transmembrane alpha-helices are predicted by reaching the strict threshold. Peaks above loose cut off (dashed line aa 23-42 and aa 490) indicate a potential for being transmembrane domain. Peaks reaching strict cut off (gray line aa 26-39) are likely transmembrane alpha-helices (according to Cserzo *et al.*, 1997).

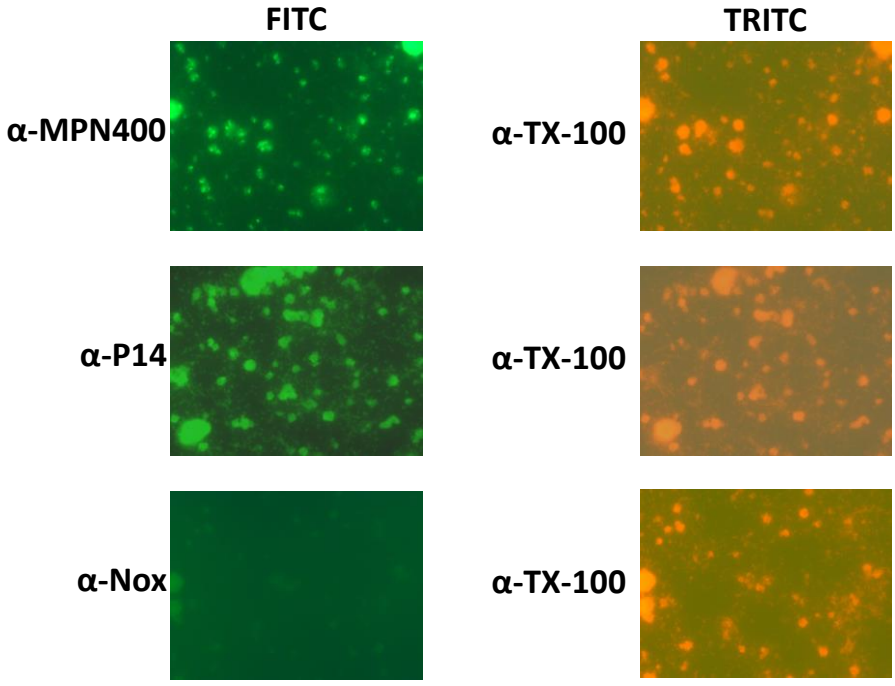

Figure S4.4 | Immunofluorescence microscopy of *M. pneumoniae* cells. Cells were incubated with guinea pig antibodies against MPN400, NADH oxidase (Nox, negative control) and to P14 (positive surface proteins control), respectively. The rabbit antiserum to the Triton X 100-insoluble fraction (TX 100) of *M. pneumoniae* proteins was used as cell staining control. Signals were detected after incubation with a mixture of FITC- labeled anti-guinea pig IgG and TRITC-labeled anti-rabbit IgG.

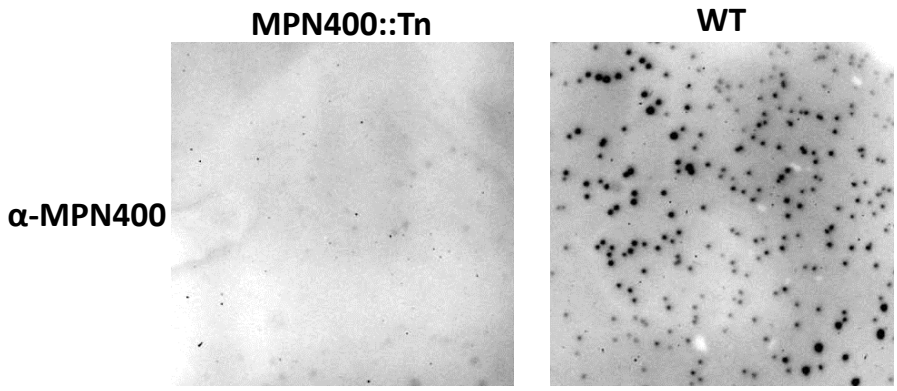

Figure S4.5 | Localization of lbpM on the surface of *M. pneumoniae* wild type colonies and *mpn400*::Tn mutant (GPM113). Results of colony blot of freshly grown *M. pneumoniae* colonies. Blotted colonies were treated with guinea pig α-MPN400. Guinea pig antibodies were detected using rabbit α-guinea pig -HRP conjugated antibody.

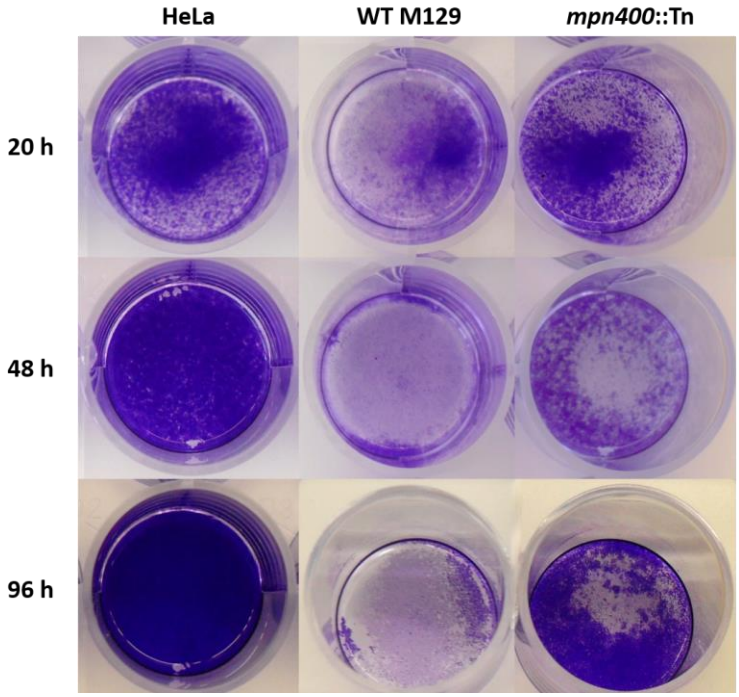

Figure S4.6 | Crystal violet stain of HeLa cells after mycoplasmal infection. Cytotoxicity of *M. pneumoniae* toward HeLa cell cultures. Confluent HeLa cell culture without infection or with M129 wild type cells and with GPM113 (*mpn400*::Tn) mutant cells. After 20h, 48 h, and 96 h post infection HeLa cells were stained with crystal violet and photographed.

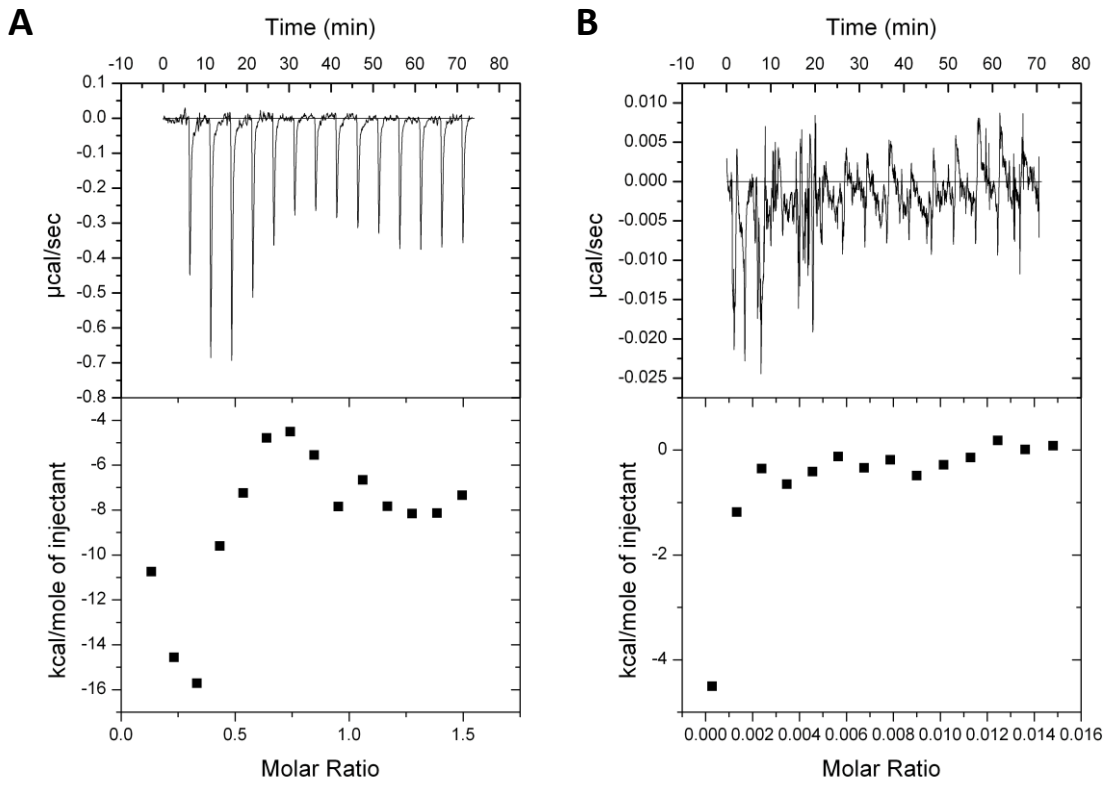

Figure S5.1 | Peroxide binding of catalase or BSA are measured by ITC. (A) Bovine catalase with hydrogen peroxide (left), (B) Bovine serum albumin (BSA) with hydrogen peroxide (right). Upper panels show original titration data and the lower panels the integrated heat measurements

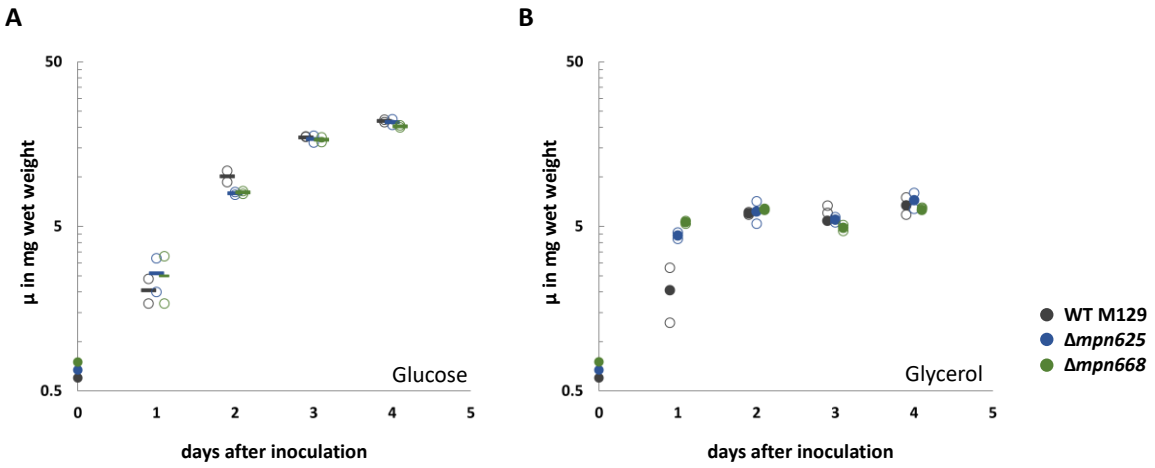

Figure S5.2 | Growth curves with *M. pneumoniae* strains. Wild type, GPM15 (Δ*mpn625*), and GPM16 ((Δ*mpn668*) were inoculated to 0.5 mg per T25 flash in MP medium either with glucose (A) or glycerol (B). Growth was measured in triplicates after 1, 2, 3, and 4 days after inoculation. µ, growth rate.

CHAPTER 8 | Closing remark

The **Answer to the Ultimate Question of Life, The Universe, and Everything** was answered by Douglas Adams by 42. The real answer might be closer to 473 – the minimum number of genes required for life.

The Hitchhiker's Guide to the Galaxy
Douglas Adams (Sleator, 2016)

CHAPTER 9 | References

Aanen, D.K., and Eggleton, P. (2017) Symbiogenesis: Beyond the endosymbiosis theory? *J Theor Biol* **434**: 99–103.

Agranoff, D.D., and Krishna, S. (1998) Metal ion homeostasis and intracellular parasitism. *Mol Microbiol* **28**: 403–412.

Akerström, B., and Björck, L. (1989) Protein L: an immunoglobulin light chain-binding bacterial protein. Characterization of binding and physicochemical properties. *J Biol Chem* **264**: 19740–6.

Akira, S., and Takeda, K. (2004) Toll-like receptor signalling. *Nat Rev Immunol* **4**: 499–511.

Alteri, C.J., Xicohténcatl-Cortes, J., Hess, S., Caballero-Olín, G., Girón, J.A., and Friedman, R.L. (2007) *Mycobacterium tuberculosis* produces pili during human infection. *Proc Natl Acad Sci USA* **104**: 5145–50.

Antelmann, H., and Helmann, J.D. (2011) Thiol-based redox switches and gene regulation. *Antioxid Redox Signal* **14**: 1049–1063.

Antelmann, H., Engelmann, S., Schmid, R., and Hecker, M. (1996) General and oxidative stress responses in *Bacillus subtilis*: cloning, expression, and mutation of the alkyl hydroperoxide reductase operon. *J Bacteriol* **178**: 6571–8.

Arfi, Y., Minder, L., Primo, C. Di, Roy, A. Le, Ebel, C., Coquet, L., *et al.* (2016) MIB-MIP is a mycoplasma system that captures and cleaves immunoglobulin G. *Proc Natl Acad Sci U S A* **113**: 5406–11.

Atichartpongkul, S., Loprasert, S., Vattanaviboon, P., Whangsuk, W., Helmann, J.D., and Mongkolsuk, S. (2001) Bacterial Ohr and OsmC paralogues define two protein families with distinct functions and patterns of expression. *Microbiology* **147**: 1775–1782.

Atkinson, T.P., Balish, M.F., and Waites, K.B. (2008) Epidemiology, clinical manifestations, pathogenesis and laboratory detection of *Mycoplasma pneumoniae* infections. *FEMS Microbiol Rev* **32**: 956–73.

Avondt, K. Van, Sorge, N.M. van, and Meyaard, L. (2015) Bacterial Immune Evasion through Manipulation of Host Inhibitory Immune Signaling. *PLoS Pathog* **11**: 1–8.

Baba, T., Ara, T., Hasegawa, M., Takai, Y., Okumura, Y., Baba, M., *et al.* (2006) Construction of *Escherichia coli* K-12 in-frame, single-gene knockout mutants: the Keio collection. *Mol Syst Biol* **2**: 2006-08.

Bai, Y., Yang, J., Eisele, L. E., Underwood, A. J., Koestler, B. J., Waters, C. M., *et al.* (2013). Two DHH subfamily 1 proteins in *Streptococcus pneumoniae* possess cyclic di-AMP phosphodiesterase activity and affect bacterial growth and virulence. *J. Bacteriol.* **195**: 5123–32.

Baichoo, N., and Helmann, J.D. (2002) Recognition of DNA by Fur: A reinterpretation of the Fur box consensus sequence. *J Bacteriol* **184**: 5826–32.

Bajantri, B., Venkatram, S., and Diaz-Fuentes, G. (2018) *Mycoplasma pneumoniae*: A Potentially Severe Infection. *J Clin Med Res* **10**: 535–44.

Balasubramanian, S., Kannan, T.R., and Baseman, J.B. (2008) The surface-exposed carboxyl region of *Mycoplasma pneumoniae* elongation factor Tu interacts with fibronectin. *Infect Immun* **76**: 3116–23.

Balish, M.F., and Distelhorst, S.L. (2016) Potential molecular targets for narrow-spectrum agents to combat *Mycoplasma pneumoniae* infection and disease. *Front Microbiol* **7**: 1–12.

Balish, M.F., and Krause, D.C. (2006) *Mycoplasmas*: a distinct cytoskeleton for wall-less bacteria. *J Mol Microbiol Biotechnol* **11**: 244–55.

Bao, S., Guo, X., Yu, S., Ding, J., Tan, L., Zhang, F., *et al.* (2014) *Mycoplasma synoviae* enolase is a plasminogen/fibronectin binding protein. *BMC Vet Res* **10**: 223.

Barbe, V., Cruveiller, S., Kunst, F., Lenoble, P., Meurice, G., Sekowska, A., *et al.* (2009) From a consortium sequence to a unified sequence: the *Bacillus subtilis* 168 reference genome a decade later. *Microbiology* **155**: 1758-75.

Barker, J.R., Koestler, B.J., Carpenter, V.K., Burdette, D.L., Waters, C.M., Vance, R.E., and Valdivia, R.H. (2013) STING-dependent recognition of cyclic di-AMP mediates type I interferon responses during *Chlamydia trachomatis* infection. *MBio* **4**: 1–11.

Barrick, J.E., and Breaker, R.R. (2007) The distributions, mechanisms, and structures of metabolite-binding riboswitches. *Genome Biol* **8**: R239.

Barthel, D., Schindler, S., and Zipfel, P.F. (2012) Plasminogen is a complement inhibitor. *J Biol Chem* **287**: 18831–42.

Barton, H.A., Johnson, Z., Cox, C.D., Vasil, A.I., and Vasil, M.L. (1996) Ferric uptake regulator mutants of *Pseudomonas aeruginosa* with distinct alterations in the iron-dependent repression of exotoxin A and siderophores in aerobic and microaerobic environments. *Mol Microbiol* **21**: 1001-17.

Baumann, L. (1989) The capacity of *Ureaplasma urealyticum*, *Mycoplasma hominis* and seven other *Mycoplasma* species for hemadsorption, sperm adsorption, hemolysis and peroxide formation. *Arch Exp Veterinarmed* **43**: 789–800.

Becerra, M.C., Páez, P.L., Laróvere, L.E., and Albesa, I. (2006) Lipids and DNA oxidation in *Staphylococcus aureus* as a consequence of oxidative stress generated by ciprofloxacin. *Mol Cell Biochem* **285**: 29–34.

Becker, A., Kannan, T.R., Taylor, A.B., Pakhomova, O.N., Zhang, Y., Somarajan, S.R., *et al.* (2015) Structure of CARDS toxin, a unique ADP-ribosylating and vacuolating cytotoxin from *Mycoplasma pneumoniae*. *Proc Natl Acad Sci U S A* **112**: 5165–70.

Ben-Menachem, G., Himmelreich, R., Herrmann, R., Aharonowitz, Y., and Rottem, S. (1997) The thioredoxin reductase system of *Mycoplasmas*. *Microbiology* **143**: 1933–40.

Ben-Menachem, G., Rottem, S., Tarshis, M., Barash, V., and Brenner, T. (1998) *Mycoplasma fermentans* glycolipid triggers inflammatory response in rat astrocytes. *Brain Res* **803**: 34–38.

Bennett, G.M., and Moran, N.A. (2013) Small, smaller, smallest: the origins and evolution of ancient dual symbioses in a Phloem-feeding insect. *Genome Biol Evol* **5**: 1675–88.

Berent, L.M., and Messick, J.B. (2003) Physical map and genome sequencing survey of *Mycoplasma haemofelis* (*Haemobartonella felis*). *Infect Immun* **71**: 3657–62.

Bergemann, A.D., and Finch, L.R. (1988) Isolation and restriction endonuclease analysis of a *Mycoplasma* plasmid. *Plasmid* **19**: 68–70.

Bhattacharya, S., Ploplis, V.A., and Castellino, F.J. (2012) Bacterial Plasminogen Receptors Utilize Host Plasminogen System for Effective Invasion and Dissemination. *J Biomed Biotechnol* **2012**: 1–19.

Bhavsar, A.P., Guttman, J.A., and Finlay, B.B. (2007) Manipulation of host-cell pathways by bacterial pathogens. *Nature* **449**: 827–34.

Bhugra, B., Voelker, L.L., Zou, N., Yu, H., and Dybvig, K. (1995) Mechanism of antigenic variation in *Mycoplasma pulmonis*: interwoven, site-specific DNA inversions. *Mol Microbiol* **18**: 703–14.

Blötz, C., and Stülke, J. (2017) Glycerol metabolism and its implication in virulence in *Mycoplasma*. *FEMS Microbiol Rev* **41**: 640–52.

B**lötz, C., Lartigue, C., Valverde Timana, Y., Ruiz, E., Paetzold, B., Busse, J., and Stülke, J.** (2018) Development of a replicating plasmid based on the native *oriC* in *Mycoplasma pneumoniae*. *Microbiology* **164**: 1372–82.

Bolland, J.R., Simmons, W.L., Daubenspeck, J.M., and Dybvig, K. (2012) *Mycoplasma* polysaccharide protects against complement. *Microbiology* **158**: 1867–73.

Bose, S., Segovia, J.A., Somarajan, S.R., Chang, T., Kannan, T.R., and Baseman, B. (2014) ADP-Ribosylation of NLRP3 by *Mycoplasma pneumoniae* CARDS. *MBio* **5**: 1–11.

Bowman, L., Zeden, M.S., Schuster, C.F., Kaever, V., and Gründling, A. (2016) New insights into the cyclic di-adenosine monophosphate (c-di-AMP) degradation pathway and the requirement of the cyclic dinucleotide for acid stress resistance in *Staphylococcus aureu*. *J Biol Chem* **291**: 26970–86.

Boyle, M.D.P. (1990) Bacterial immunoglobulin-binding proteins and complement. In Bacterial Immunoglobulin-Binding Proteins. *Elsevier*, **pp**: 369–391.

Brezski, R.J., Vafa, O., Petrone, D., Tam, S.H., Powers, G., Ryan, M.H., *et al.* (2009) Tumor-associated and microbial proteases compromise host IgG effector functions by a single cleavage proximal to the hinge. *Proc Natl Acad Sci U S A* **106**: 17864–9.

Briggs G.S., Smits W.K., Soultanas P. (2012) Chromosomal replication initiation machinery of low-G+C-content *Firmicutes*. *J Bacteriol*; **194**: 5162.

Brown, D.R., Zacher, L.A., and Farmerie, W.G. (2004) Spreading Factors of *Mycoplasma alligatoris*, a Flesh-Eating *Mycoplasma*. *J Bacteriol* **186**: 3922–27.

Bsat, N., Chen, L., and Helmann, J.D. (1996) Mutation of the *Bacillus subtilis* alkyl hydroperoxide reductase (*ahpCF*) operon reveals compensatory interactions among hydrogen peroxide stress genes. *J Bacteriol* **178**: 6579–86.

Burdette, D.L., Monroe, K.M., Sotelo-Troha, K., Iwig, J.S., Eckert, B., Hyodo, M., *et al.* (2011) STING is a direct innate immune sensor of cyclic di-GMP. *Nature* **478**: 515–18.

Burgos, R., Wood, G.E., Iverson-Cabral, S.L., and Tottena, P.A. (2018) *Mycoplasma genitalium* nonadherent phase variants arise by multiple mechanisms and escape antibody-dependent growth inhibition. *Infect Immun* **86**: 1–19.

Buttery, S.H., Lloyd, L.C., and Titchen, D.A. (1976) Acute respiratory, circulatory and pathological changes in the calf after intravenous injections of the galactan from *Mycoplasma mycoides* subsp. *mycoides*. *J Med Microbiol* **9**: 379–91.

Campos, G.B., Marques, L.M., Rezende, I.S., Barbosa, M.S., Abrão, M.S., and Timenetsky, J. (2018) *Mycoplasma genitalium* can modulate the local immune response in patients with endometriosis. *Fertil Steril* **109**: 549–60.

Campos, S. S., Ibarra-Rodriguez, J. R., Barajas-Ornelas, R. C., Ramírez-Guadiana, F. H., Obregón-Herrera, A., Setlow, P., *et al.* (2014). Interaction of apurinic/ apyrimidinic endonucleases Nfo and ExoA with the DNA integrity scanning protein DisA in the processing of oxidative DNA damage during *Bacillus subtilis* spore outgrowth. *J. Bacteriol.* **196:** 568–78.

Cao, J., Kapke, P.A., and Minton, F.C. (1994) Transformation of *Mycoplasma gallisepticum* with Tn*916*, Tn*4001*, and integrative plasmid vectors. *J Bacteriol* **176**: 4459–62.

Chae, H.Z., Robison, K., Poole, L.B., Church, G., Storz, G., and Rhee, S.G. (1994) Cloning and sequencing of thiol-specific antioxidant from mammalian brain: alkyl hydroperoxide reductase and thiol-specific antioxidant define a large family of antioxidant enzymes. *Proc Natl Acad Sci U S A* **91**: 7017–21.

Chambaud, I., Wróblewski, H., and Blanchard, A. (1999) Interactions between *Mycoplasma* lipoproteins and the host immune system. *Trends Microbiol* **7**: 493–9.

Chaudhry, R., Ghosh, A., and Chandolia, A. (2016) Pathogenesis of *Mycoplasma pneumoniae*: An update. *Indian J Med Microbiol* **34**: 7.

Chaudhry, R., Varshney, A.K., and Malhotra, P. (2007) Adhesion proteins of *Mycoplasma pneumoniae*. *Front Biosci* **12**: 690–9.

Chen, H., Yu, S., Shen, X., Chen, D., Qiu, X., Song, C., and Ding, C. (2011) The *Mycoplasma gallisepticum* α-enolase is cell surface-exposed and mediates adherence by binding to chicken plasminogen. *Microb Pathog* **51**: 285–90.

Chen, J.-R., Weng, C.-N., Ho, T.-Y., Cheng, I.-C., and Lai, S.-S. (2000) Identification of the copper-zinc superoxide dismutase activity in *Mycoplasma hyopneumoniae*. *Vet Microbiol* **73**: 301–10.

Chen, L., Keramati, L., and Helmann, J.D. (1995) Coordinate regulation of *Bacillus subtilis* peroxide stress genes by hydrogen peroxide and metal ions. *Proc Natl Acad Sci U S A* **92**: 8190–4.

Chen, L., Li, X., Zhou, X., Zeng, J., Ren, Z., Lei, L., *et al.* (2018c) Inhibition of *Enterococcus faecalis* Growth and Biofilm Formation by Molecule Targeting Cyclic di-AMP Synthetase Activity. *J Endod* **44**: 1381–88.

Chen, L.-S., Li, C., You, X.-X., Lin, Y.-W., and Wu, Y.-M. (2018a) The *mpn668* gene of *Mycoplasma pneumoniae* encodes a novel organic hydroperoxide resistance protein. *Int J Med Microbiol* **308**: 776–83.

Chen, S., Hao, H., Zhao, P., Ji, W., Li, M., Liu, Y., and Chu, Y. (2018b) Differential Immunoreactivity to Bovine Convalescent Serum Between *Mycoplasma bovis* Biofilms and Planktonic Cells Revealed by Comparative Immunoproteomic Analysis. *Front Microbiol* **9**.

Chen, W.-H., Noort, V. van, Lluch-Senar, M., Hennrich, M.L., Wodke, J.A.H., Yus, E., *et al.* (2016) Integration of multi-omics data of a genome-reduced bacterium: Prevalence of post-transcriptional regulation and its correlation with protein abundances. *Nucleic Acids Res* **44**: 1192–1202.

Chiu, K.-H., Wang, L.-H., Tsai, T.-T., Lei, H.-Y., and Liao, P.-C. (2017) Secretomic Analysis of Host-Pathogen Interactions Reveals That Elongation Factor-Tu Is a Potential Adherence Factor of *Helicobacter pylori* during Pathogenesis. *J Proteome Res* **16**: 264–273.

Choi, I.-G., Shin, D.H., Brandsen, J., Jancarik, J., Busso, D., Yokota, H., *et al.* (2003) Crystal structure of a stress inducible protein from *Mycoplasma pneumoniae* at 2.85 A resolution. *J Struct Funct Genomics* **4**: 31–4.

Choi, P.H., Vu, T.M.N., Pham, H.T., Woodward, J.J., Turner, M.S., and Tong, L. (2017) Structural and functional studies of pyruvate carboxylase regulation by cyclic di-AMP in lactic acid bacteria. *Proc Natl Acad Sci* **114**: E7226–E7235.

Chopra-Dewasthaly, R., Citti, C., Glew, M.D., Zimmermann, M., Rosengarten, R., and Jechlinger, W. (2008) Phase-locked mutants of *Mycoplasma agalactiae*: defining the molecular switch of high-frequency Vpma antigenic variation. *Mol Microbiol* **67**: 1196–210.

Chopra-Dewasthaly, R., Marenda, M., Rosengarten, R., Jechlinger, W., and Citti, C. (2005) Construction of the first shuttle vectors for gene cloning and homologous recombination in *Mycoplasma agalactiae*. *FEMS Microbiol Lett* **253**: 89–94.

Chourasia, B.K., Chaudhry, R., and Malhotra, P. (2014) Delineation of immunodominant and cytadherence segment(s) of *Mycoplasma pneumoniae* P1 gene. *BMC Microbiol* **14**: 108.

Christen B., Abeliuk E., Collier J.M., Kalogeraki V.S., Passarelli B., Coller J.A., *et al.* (2011) The essential genome of a bacterium. *Mol Syst Biol* **7**: 528.

Christensen, P., and Oxelius, V.A. (2009) A reaction between some *Streptococci* and Iga myeloma proteins. *Acta Pathol Microbiol Scand Sect C Immunol* **83C**: 184–188.

Christman, M.F., Morgan, R.W., Jacobson, F.S., and Ames, B.N. (1985) Positive control of a regulon for defenses against oxidative stress and some heat-shock proteins in *Salmonella typhimurium*. *Cell* **41**: 753–62.

Chuba, J. V. (1994) Susceptibility of monoclonal IgG paraproteins to plasmic cleavage using glycerin-stabilized human plasmin. *Biochem Biophys Res Commun* **202**: 367–73.

Chuchue, T., Tanboon, W., Prapagdee, B., Dubbs, J.M., Vattanaviboon, P., and Mongkolsuk, S. (2006) *ohrR* and *ohr* are the primary sensor/regulator and protective genes against organic hydroperoxide stress in *Agrobacterium tumefaciens*. *J Bacteriol* **188**: 842–51.

Citti, C., and Blanchard, A. (2013) *Mycoplasmas* and their host: Emerging and re-emerging minimal pathogens. *Trends Microbiol* **21**: 196–203.

Citti, C., and Rosengarten, R. (1997) *Mycoplasma* genetic variation and its implication for pathogenesis. *Wien Klin Wochenschr* **109**: 562–8.

Citti, C., Nouvel, L.-X., and Baranowski, E. (2010) Phase and antigenic variation in *Mycoplasmas*. *Future Microbiol* **5**: 1073–85.

Cizelj, I., Bercic, R.L., Dusanic, D., Narat, M., Kos, J., Dovc, P., and Bencina, D. (2011) *Mycoplasma gallisepticum* and *Mycoplasma synoviae* express a cysteine protease CysP, which can cleave chicken IgG into Fab and Fc. *Microbiology* **157**: 362–72.

Collin, M., and Kilian, M. (2014) Bacterial Modulation of Fc Effector Functions. In *Antibody Fc*. *Elsevier*, **pp:** 317–32.

Commichau, F. M., Dickmanns, A., Gundlach, J., Ficner, R., and Stülke, J. (2015). A jack of all trades: the multiple roles of the unique essential second messenger cyclic di-AMP. *Mol. Microbiol.* **97**: 189–204.

Commichau, F.M., and Stülke, J. (2008) Trigger enzymes: bifunctional proteins active in metabolism and in controlling gene expression. *Mol Microbiol* **67**: 692–702.

Commichau, F.M., Gunka, K., Landmann, J.J., and Stülke, J. (2008) Glutamate metabolism in *Bacillus subtilis*: gene expression and enzyme activities evolved to avoid futile cycles and to allow rapid responses to perturbations of the system. *J Bacteriol* **190**: 3557–64.

Commichau, F.M., Heidemann, J.L., Ficner, R., and Stülke, J. (2019) Making and Breaking of an Essential Poison: the Cyclases and Phosphodiesterases That Produce and Degrade the Essential Second Messenger Cyclic di-AMP in Bacteria. *J Bacteriol* **201**: 1–14.

Cordova, C.M.M., Lartigue, C., Sirand-Pugnet, P., Renaudin, J., Cunha, R.A.F., and Blanchard, A. (2002) Identification of the origin of replication of the *Mycoplasma pulmonis* chromosome and its use in *oriC* replicative plasmids. *J Bacteriol* **184**: 5426–35.

Cordwell, S.J., Basseal, D.J., Pollack, J.D., Humphery, Smith, I. (1997) Malate/lactate dehydrogenase in mollicutes: evidence for a multienzyme protein. *Gene* **195**: 113–20.

Cornelis, P., Wei, Q., Andrews, S.C., and Vinckx, T. (2011) Iron homeostasis and management of oxidative stress response in bacteria. *Metallomics* **3**: 540–49.

Corrigan, R. M., Abbott, J. C., Burhenne, H., Kaever, V., and Gründling, A. (2011). c-di-AMP is a new second messenger in *Staphylococcus aureus* with a role in controlling cell size and envelope stress. *PLoS Pathog.* **7**:e1002217.

Corrigan, R. M., and Gründling, A. (2013). Cyclic di-AMP: another second messenger enters the fray. *Nat. Rev. Microbiol.* **11**: 513–524.

Corrigan, R. M., Campeotto, I., Jeganathan, T., Roelofs, K. G., Lee, V. T., and Gründling, A. (2013). Systematic identification of conserved bacterial c-di-AMP receptor proteins. *Proc. Natl. Acad. Sci. U.S.A.* **110**: 9084–89.

Corrigan, R.M., Bowman, L., Willis, A.R., Kaever, V., and Gründling, A. (2015) Cross-talk between two nucleotide-signaling pathways in *Staphylococcus aureus*. *J Biol Chem* **290**: 5826–39.

Cserzö, M., Wallin, E., Simon, I., Heijne, G. von, and Elofsson, A. (1997) Prediction of transmembrane alpha-helices in prokaryotic membrane proteins: the dense alignment surface method. *Protein Eng* **10**: 673–76.

Cussiol, J.R.R., Alegria, T.G.P., Szweda, L.I., and Netto, L.E.S. (2010) Ohr (organic hydroperoxide resistance protein) possesses a previously undescribed activity, lipoyl-dependent peroxidase. *J Biol Chem* **285**: 21943–50.

Cussiol, J.R.R., Alves, S.V., Oliveira, M.A. de, and Netto, L.E.S. (2003) Organic hydroperoxide resistance gene encodes a thiol-dependent peroxidase. *J Biol Chem* **278**: 11570–8.

Dallo, S.F., and Baseman, J.B. (2000) Intracellular DNA replication and long-term survival of pathogenic *Mycoplasmas*. *Microb Pathog* **29**: 301–9.

Dandekar, T., Huynen, M., Regula, J.T., Ueberle, B., Zimmermann, C.U., Andrade, M.A., *et al.* (2000) Re-annotating the *Mycoplasma pneumoniae* genome sequence: adding value, function and reading frames. *Nucleic Acids Res* **28**: 3278–88.

Dandekar, T., Snel, B., Schmidt, S., Lathe, W., Suyama, M., Huynen, M. and Bork, P. (2002) Comparative genome analysis of the Mollicutes. *Molecular Biology and Pathogenicity of Mycoplasmas*, Edited by S. Razin & R. Herrmann. New York:Kluwer; **pp**: 255–279.

Desmet, C.J., and Ishii, K.J. (2012) Nucleic acid sensing at the interface between innate and adaptive immunity in vaccination. *Nat Rev Immunol* **12**: 479–91.

Devaux, L., Kaminski, P.-A., Trieu-Cuot, P., and Firon, A. (2018) Cyclic di-AMP in host-pathogen interactions. *Curr Opin Microbiol* **41**: 21–28.

Dey, R.J., Dey, B., Zheng, Y., Cheung, L.S., Zhou, J., Sayre, D., *et al.* (2017) Inhibition of innate immune cytosolic surveillance by an *M. tuberculosis* phosphodiesterase. *Nat Chem Biol* **13**: 210–17.

Dhandayuthapani, S., Rasmussen, W.G., Baseman, J.B., (1999) Disruption of gene *mg218* of *Mycoplasma genitalium* through homologous recombination leads to an adherence-deficient phenotype. *Proc. Natl. Acad. Sci. USA* **96**: 5227–32.

Diethmaier, C., Newman, J. A., Kovács,ÁT., Kaever, V., Herzberg, C., Rodrigues, C., *et al.* (2014). The YmdB phosphodiesterase is a global regulator of late adaptive responses in *Bacillus subtilis*. *J. Bacteriol* **196:** 265–75.

Diethmaier, C., Pietack, N., Gunka, K., Wrede, C., Lehnik-Habrink, M., Herzberg, C., *et al.* (2011) A novel factor controlling bistability in *Bacillus subtilis*: the YmdB protein affects flagellin expression and biofilm formation. *J Bacteriol* **193**: 5997–6007.

Dietrich, L.E.P., Teal, T.K., Price-Whelan, A., and Newman, D.K. (2008) Redox-Active Antibiotics Control Gene Expression and Community Behavior in Divergent Bacteria. *Science* **321**: 1203-6.

Dowds, B.C.A. (1994) The oxidative stress response in *Bacillus subtilis*. *FEMS Microbiol Lett* **124**: 255–63.

Du, B., Ji, W., An, H., Shi, Y., Huang, Q., Cheng, Y., *et al.* (2014) Functional analysis of c-di-AMP phosphodiesterase, GdpP, in *Streptococcus suis* serotype 2. *Microbiol Res* **169**: 749–58.

Dubnau, D. (1991). Genetic competence in *Bacillus subtilis*. *Microbiol. Rev*. **55**:395–424.

Dyballa, N., and Metzger, S. (2009) Fast and sensitive colloidal coomassie G-250 staining for proteins in polyacrylamide gels. *J Vis Exp*.

Dybvig, K. (1990) Mycoplasmal Genetics. *Annu Rev Microbiol* **44**: 81–104.

Dybvig, K., and Khaled, M. (1990) Isolation of a second cryptic plasmid from *Mycoplasma mycoides* subsp. *mycoides*. *Plasmid* **24**: 153–5.

Dybvig, K., and Voelker, L.L. (1996) MOLECULAR BIOLOGY OF *MYCOPLASMAS*. *Annu Rev Microbiol* **50**: 25–57.

Ebensen, T., Libanova, R., Schulze, K., Yevsa, T., Morr, M., and Guzmán, C.A. (2011) Bis-(3',5')-cyclic dimeric adenosine monophosphate: strong Th1/Th2/Th17 promoting mucosal adjuvant. *Vaccine* **29**: 5210–20.

Eilers, H. (2010). *Transcription in Mycoplasma pneumoniae.* PhD thesis. University of Göttingen, Göttingen, Germany.

Engelmann, S., and Hecker, M. (1996) Impaired oxidative stress resistance of *Bacillus subtilis sigB* mutants and the role of *katA* and *katE*. *FEMS Microbiol Lett* **145**: 63–9.

Faulkner, M.J., Ma, Z., Fuangthong, M., and Helmann, J.D. (2012) Derepression of the *Bacillus subtilis perR* peroxide stress response leads to iron deficiency. *J Bacteriol* **194**: 1226–35.

Feng, M., Schaff, A.C., Cuadra Aruguete, S.A., Riggs, H.E., Distelhorst, S.L., and Balish, M.F. (2018) Development of *Mycoplasma pneumoniae* biofilms in vitro and the limited role of motility. *Int J Med Microbiol* **308**: 324–34.

Fillat, M.F. (2014) The FUR (ferric uptake regulator) superfamily: Diversity and versatility of key transcriptional regulators. *Arch Biochem Biophys* **546**: 41–52.

Fischetti, V.A. (1989) *Streptococcal* M protein: molecular design and biological behavior. *Clin Microbiol Rev* **2**: 285–314.

Fleischmann, R.D., Adams, M.D., White, O., Clayton, R.A., Kirkness, E.F., Kerlavage, A.R., *et al.* (1995) Whole-genome random sequencing and assembly of *Haemophilus influenzae* Rd. *Science* **269**: 496–512.

Foley, J.H., Walton, B.L., Aleman, M.M., O'Byrne, A.M., Lei, V., Harrasser, M., *et al.* (2016) Complement Activation in Arterial and Venous Thrombosis is Mediated by Plasmin. *EBioMedicine* **5**: 175–182.

Fraser, C.M., Gocayne, J.D., White, O., Adams, M.D., Clayton, R.A., Fleischmann, R.D., *et al.* (1995) The Minimal Gene Complement of *Mycoplasma genitalium Science* **270**: 397-403.

Frick, I.M., Wikström, M., Forsén, S., Drakenberg, T., Gomi, H., Sjöbring, U., and Björck, L. (1992) Convergent evolution among immunoglobulin G-binding bacterial proteins. *Proc Natl Acad Sci U S A* **89**: 8532–6.

Fuangthong, M., Atichartpongkul, S., Mongkolsuk, S., and Helmann, J.D. (2001) OhrR is a repressor of *ohrA*, a key organic hydroperoxide resistance determinant in *Bacillus subtilis*. *J Bacteriol* **183**: 4134–41.

Gallagher, L.A., Ramage, E., Jacobs, M.A., Kaul, R., Brittnacher, M., and Manoil, C. (2007) A comprehensive transposon mutant library of *Francisella novicida*, a bioweapon surrogate. *Proc Natl Acad Sci U S A* **104**: 1009–14.

Galvão, L.C.C., Miller, J.H., Kajfasz, J.K., Scott-Anne, K., Freires, I.A., Franco, G.C.N., *et al.* (2015) Transcriptional and Phenotypic Characterization of Novel Spx-Regulated Genes in *Streptococcus mutans*. *PLoS One* **10**: e0124969.

Gao, F., and Zhang, C.-T. (2008) Ori-Finder: a web-based system for finding *oriCs* in unannotated bacterial genomes. *BMC Bioinformatics* **9**: 79.

Gerdes, S.Y., Scholle, M.D., Campbell, J.W., Balázsi, G., Ravasz, E., Daugherty, M.D., *et al.* (2003) Experimental determination and system level analysis of essential genes in *Escherichia coli* MG1655. *J Bacteriol* **185**: 5673–84.

Giaever, G., Chu, A.M., Ni, L., Connelly, C., Riles, L., Véronneau, S., *et al.* (2002) Functional profiling of the *Saccharomyces cerevisiae* genome. *Nature* **418**: 387–91.

Gibson, D.G., Benders, G.A., Andrews-Pfannkoch, C., Denisova, E.A., Baden-Tillson, H., Zaveri, J., *et al.* (2008) Complete chemical synthesis, assembly, and cloning of a *Mycoplasma genitalium* genome. *Science* **319**: 1215–20.

Gibson, D.G., Glass, J.I., Lartigue, C., Noskov, V.N., Chuang, R.-Y., Algire, M.A., *et al.* (2010) Creation of a bacterial cell controlled by a chemically synthesized genome. *Science* **329**: 52–6.

Giovannoni, S.J., Tripp, H.J., Givan, S., Podar, M., Vergin, K.L., Baptista, D., *et al.* (2005) Genome streamlining in a cosmopolitan oceanic bacterium. *Science* **309**: 1242–5.

Glass, J.I., Assad-Garcia, N., Alperovich, N., Yooseph, S., Lewis, M.R., Maruf, M., *et al.* (2006) Essential genes of a minimal bacterium. *Proc Natl Acad Sci U S A* **103**: 425–30.

Glass, J.I., Merryman, C., Wise, K.S., Hutchison, C.A., and Smith, H.O. (2017) Minimal Cells-Real and Imagined. *Cold Spring Harb Perspect Biol* **9**: 1–12.

Goldberg AP, Szigeti B, Chew YH, Sekar JA, Roth YD *et al.* (2018) Emerging whole-cell modeling principles and methods. *Curr Opin Biotechnol* **51**:97–102.

Gomelsky, M. (2011). cAMP, c-di-GMP, c-di-AMP and now cGMP: bacteria use them all! *Mol. Microbiol.* **79**: 562–565.

Gonchoroski, T., Virginio, V.G., Thompson, C.E., Paes, J.A., Machado, C.X., and Ferreira, H.B. (2017) Evolution and function of the *Mycoplasma hyopneumoniae* peroxiredoxin, a 2-Cys-like enzyme with a single Cys residue. *Mol Genet Genomics* **292**: 297–305.

Goodyear, C.S., and Silverman, G.J. (2004) *Staphylococcal* toxin induced preferential and prolonged in vivo deletion of innate-like B lymphocytes. *Proc Natl Acad Sci* **101**: 11392–97.

Goret, J., Roy, C. Le, Touati, A., Mesureur, J., Renaudin, H., Claverol, S., *et al.* (2016) Surface lipoproteome of *Mycoplasma hominis* PG21 and differential expression after contact with human dendritic cells. *Future Microbiol* **11**: 179–94.

Görke, B., and Stülke, J. (2008). Carbon catabolite repression in bacteria: many ways to make most out of nutrients. *Nat. Rev. Microbiol.* **6**: 613–24.

Graille, M., Harrison, S., Crump, M.P., Findlow, S.C., Housden, N.G., Muller, B.H., *et al.* (2002) Evidence for plasticity and structural mimicry at the immunoglobulin light chain-protein L interface. *J Biol Chem* **277**: 47500–6.

Graille, M., Stura, E.A., Corper, A.L., Sutton, B.J., Taussig, M.J., Charbonnier, J.-B., and Silverman, G.J. (2000) Crystal structure of a *Staphylococcus aureus* protein A domain complexed with the Fab fragment of a human IgM antibody: Structural basis for recognition of B-cell receptors and superantigen activity. *Proc Natl Acad Sci* **97**: 5399–5404.

Grant, S.G., Jessee, J., Bloom, F.R., and Hanahan, D. (1990) Differential plasmid rescue from transgenic mouse DNAs into *Escherichia coli* methylation-restriction mutants. *Proc Natl Acad Sci U S A* **87**: 4645–9.

Gries, C.M., Bruger, E.L., Moormeier, D.E., Scherr, T.D., Waters, C.M., and Kielian, T. (2016) Cyclic di-AMP Released from *Staphylococcus aureus* Biofilm Induces a Macrophage Type I Interferon Response. *Infect Immun* **84**: 3564–74.

Grimmer, J., and Dumke, R. (2019) Organization of multi-binding to host proteins: The glyceraldehyde-3-phosphate dehydrogenase (GAPDH) of *Mycoplasma pneumoniae*. *Microbiol Res* **218**: 22–31.

Grosjean, H., Breton, M., Sirand-Pugnet, P., Tardy, F., Thiaucourt, F., Citti, C., *et al.* (2014) Predicting the minimal translation apparatus: lessons from the reductive evolution of mollicutes. *PLoS Genet* **10**: e1004363.

Großhennig, S., Ischebeck, T., Gibhardt, J., Busse, J., Feussner, I., and Stülke, J. (2016) Hydrogen sulfide is a novel potential virulence factor of *Mycoplasma pneumoniae*: Characterization of the unusual cysteine desulfurase/desulfhydrase HapE. *Mol Microbiol* **100**: 42–54.

Großhennig, S., Schmidl, S.R., Schmeisky, G., Busse, J., and Stülke, J. (2013) Implication of glycerol and phospholipid transporters in *Mycoplasma pneumoniae* growth and virulence. *Infect Immun* **81**: 896–904.

Grover, R.K., Zhu, X., Nieusma, T., Jones, T., Boero, I., MacLeod, A.S., *et al.* (2014) A structurally distinct human *Mycoplasma* protein that generically blocks antigen-antibody union. *Science* **343**: 656–61.

Gründel, A., Jacobs, E., and Dumke, R. (2016a) Interactions of surface-displayed glycolytic enzymes of Mycoplasma pneumoniae with components of the human extracellular matrix. *Int J Med Microbiol* **306**: 675–85.

Gründel, A., Pfeiffer, M., Jacobs, E., and Dumke, R. (2015) The network of surface-displayed glycolytic enzymes in *Mycoplasma pneumoniae* and their interactions with human plasminogen. *Infect Immun* **84**: 1071-15.

Gründel, A., Pfeiffer, M., Jacobs, E., and Dumke, R. (2016) Network of Surface-Displayed Glycolytic Enzymes in *Mycoplasma pneumoniae* and Their Interactions with Human Plasminogen. *Infect Immun* **84**: 666–76.

Güell, M., van Noort, V., Yus, E., Chen, W. H., Leigh-Bell, J., Michalodimitrakis, K., *et al.* (2009). Transcriptome complexity in a genome-reduced bacterium. *Science* **326:** 1268–71.

Guérout-Fleury, A.-M., Shazand, K., Frandsen, N., and Stragier, P. (1995) Antibiotic-resistance cassettes for *Bacillus subtilis*. *Gene* **167**: 335–6.

Guillot, A., Boulay, M., Chambellon, É., Gitton, C., Monnet, V., and Juillard, V. (2016) Mass Spectrometry Analysis of the Extracellular Peptidome of *Lactococcus lactis*: Lines of Evidence for the Coexistence of Extracellular Protein Hydrolysis and Intracellular Peptide Excretion. *J Proteome Res* **15**: 3214–24.

Gundlach, J., Dickmanns, A., Schröder-Tittmann, K., Neumann, P., Kaesler, J., Kampf, J., *et al.* (2015a). Identification, characterization, and structure analysis of the cyclic di-AMP-binding PII-like signal transduction protein DarA. *J. Biol. Chem.* **290:** 3069–80.

Gundlach, J., Herzberg, C., Kaever, V., Gunka, K., Hoffmann, T., Weiß, M., *et al.* (2017). Control of potassium homeostasis is an essential function of the second messenger cyclic di-AMP in *Bacillus subtilis*. *Sci. Signal.* **10**: eaal3011.

Gundlach, J., Mehne, F. M., Herzberg, C., Kampf, J., Valerius, O., Kaever, V., *et al.* (2015b). An essential poison: synthesis and degradation of cyclic di-AMP in *Bacillus subtilis*. *J. Bacteriol.* **197**: 3265–74.

Gunka, K. (2011) Der Einfluss der Glutamatdehydrogenasen auf die Verknüpfung des Kohlenstoff- und Stickstoffstoffwechsels in *Bacillus subtilis*. PhD thesis. University of Göttingen, Göttingen, Germany.

Guo, Y., Zhu, H., Wang, J., Huang, J., Khan, F., Zhang, J., *et al.* (2017) TrmFO, a Fibronectin-Binding Adhesin of *Mycoplasma bovis*. *Int J Mol Sci* **18**: 1732.

Gusarov, I., and Nudler, E. (2005) NO-mediated cytoprotection: Instant adaptation to oxidative stress in bacteria. *Proc Natl Acad Sci* **102**: 13855–60.

Gutierrez, C., and Devedjian, J.C. (1991) Osmotic induction of gene *osmC* expression in *Escherichia coli* K12. *J Mol Biol* **220**: 959–73.

Hagemann, L., Gründel, A., Jacobs, E., and Dumke, R. (2017) The surface-displayed chaperones GroEL and DnaK of *Mycoplasma pneumoniae* interact with human plasminogen and components of the extracellular matrix. *Pathog Dis* **75**: 1–12.

Halbedel, S., and Stülke, J. (2007) Tools for the genetic analysis of *Mycoplasma*. *Int J Med Microbiol* **297**: 37–44.

Halbedel, S., Busse, J., Schmidl, S., and Stülke, J. (2006). Regulatory protein phosphorylation in *Mycoplasma pneumoniae*: a PP2C-type phosphatase serves to dephosphorylate HPr(Ser-P). *J. Biol. Chem.* **281:** 26253–9.

Halbedel, S., Hames, C., and Stülke, J. (2004). *In vivo* activity of enzymatic and regulatory components of the phosphoenolpyruvate:sugar phosphotransferase system in *Mycoplasma pneumoniae*. *J. Bacteriol.* **186**: 7936–43.

Halbedel, S., Hames, C., and Stülke, J. (2007) Regulation of carbon metabolism in the mollicutes and its relation to virulence. *J Mol Microbiol Biotechnol* **12**: 147–54.

Hall, A., Karplus, P.A., and Poole, L.B. (2009) Typical 2-Cys peroxiredoxins - structures, mechanisms and functions. *FEBS J* **276**: 2469–77

Hallamaa, K.M., Tang, S.-L., Ficorilli, N., and Browning, G.F. (2008) Differential expression of lipoprotein genes in *Mycoplasma pneumoniae* after contact with human lung epithelial cells, and under oxidative and acidic stress. *BMC Microbiol* **8**: 124.

Hames C., Halbedel S., Hoppert M., Frey J., Stülke J., (2009) Glycerol metabolism is important for cytotoxicity of *Mycoplasma pneumoniae*. *J Bacteriol*; **191**: 747–753.

Hames, C., Halbedel, S., Schilling, O., and Stülke, J. (2005). MMR: a method for the simultaneous introduction of multiple mutations into the glpK gene of *Mycoplasma pneumoniae*. *Appl. Environ. Microbiol.* **71**: 4097–4100.

Hardy, R.D., Coalson, J.J., Peters, J., Chaparro, A., Techasaensiri, C., Cantwell, A.M., *et al.* (2009) Analysis of pulmonary inflammation and function in the mouse and baboon after exposure to *Mycoplasma pneumoniae* CARDS toxin. *PLoS One* **4**: e7562.

Harpel, P.C., Gordon, B.R., and Parker, T.S. (1989) Plasmin catalyzes binding of lipoprotein (a) to immobilized fibrinogen and fibrin. *Proc Natl Acad Sci U S A* **86**: 3847–51.

Hashimoto, M., Ichimura, T., Mizoguchi, H., Tanaka, K., Fujimitsu, K., Keyamura, K., *et al.* (2005) Cell size and nucleoid organization of engineered *Escherichia coli* cells with a reduced genome. *Mol Microbiol* **55**: 137–49.

Helmann, J.D. (2014) Specificity of metal sensing: iron and manganese homeostasis in *Bacillus subtilis. J Biol Chem* **289**: 28112–20.

Helmann, J.D., Wu, M.F.W., Gaballa, A., Kobel, P. a, Morshedi, M.M., Fawcett, P., and Paddon, C. (2003) The global transcriptional response of *Bacillus subtilis* to peroxide stress is coordinated by three transcription factors. *J Bacteriol* **185**: 243–53.

Henderson, B., and Martin, A. (2011) Bacterial virulence in the moonlight: multitasking bacterial moonlighting proteins are virulence determinants in infectious disease. *Infect Immun* **79**: 3476–91.

Henderson, B., Nair, S., Pallas, J., and Williams, M.A. (2011) Fibronectin: A multidomain host adhesin targeted by bacterial fibronectin-binding proteins. *FEMS Microbiol Rev* **35**: 147–200.

Hengge, R. (2009). Principles of c-di-GMP signaling in bacteria. *Nat. Rev. Microbiol.* **7**: 263–273.

Heo, Y.-J., Chung, I.-Y., Cho, W.-J., Lee, B.-Y., Kim, J.-H., Choi, K.-H., *et al.* (2010) The major catalase gene (*katA*) of *Pseudomonas aeruginosa* PA14 is under both positive and negative control of the global transactivator OxyR in response to hydrogen peroxide. *J Bacteriol* **192**: 381–90.

Herbig, A.F., and Helmann, J.D. (2001) Roles of metal ions and hydrogen peroxide in modulating the interaction of the *Bacillus subtilis* PerR peroxide regulon repressor with operator DNA. *Mol Microbiol* **41**: 849–59.

Hilbert, H., Himmelreich, R., Plagens, H., and Herrmann, R. (1996) Sequence analysis of 56 kb from the genome of the bacterium *Mycoplasma pneumoniae* comprising the *dnaA* region, the *atp* operon and a cluster of ribosomal protein genes. *Nucleic Acids Res* **24**: 628–39.

Himmelreich, R., Hilbert, H., Plagens, H., Pirkl, E., Li, B.C., and Herrmann, R. (1996) Complete sequence analysis of the genome of the bacterium *Mycoplasma pneumoniae*. *Nucleic Acids Res* **24**: 4420–49.

Himmelreich, R., Plagens, H., Hilbert, H., Reiner, B., and Herrmann, R. (1997) Comparative analysis of the genomes of the bacteria *Mycoplasma pneumoniae* and *Mycoplasma genitalium*. *Nucleic Acids Res* **25**: 701–12.

Holtmann, G., Bakker, E. P., Uozumi, N., and Bremer, E. (2003). KtrAB and KtrCD: two K^+ uptake systems in *Bacillus subtilis* and their role in adaptation to hypertonicity. *J. Bacteriol.* **185**: 1289–98.

Horstmann, R.D., Sievertsen, H.J., Knobloch, J., and Fischetti, V.A. (1988) Antiphagocytic activity of streptococcal M protein: selective binding of complement control protein factor H. *Proc Natl Acad Sci U S A* **85**: 1657–61.

Houshaymi, B.M., Miles, R.J., and Nicholas, R.A. (1997) Oxidation of glycerol differentiates African from European isolates of *Mycoplasma mycoides* subspecies *mycoides* SC (small colony). *Vet Rec* **140**: 182–3.

Huberts, D.H.E.W., and Klei, I.J. van der (2010) Moonlighting proteins: An intriguing mode of multitasking. *Biochim Biophys Acta - Mol Cell Res* **1803**: 520–25.

Hutchison III, C.A. (1999) Global Transposon Mutagenesis and a Minimal *Mycoplasma* Genome. *Science* **286**: 2165–69.

Hutchison III, C.A., Chuang, R.-Y., Noskov, V.N., Assad-Garcia, N., Deerinck, T.J., Ellisman, M.H., *et al.* (2016) Design and synthesis of a minimal bacterial genome. *Science* **351**: aad6253.

Huynh, T. N., and Woodward, J. J. (2016). Too much of a good thing: regulated depletion of c-di-AMP in the bacterial cytoplasm. *Curr. Opin. Microbiol.* **30**: 22–29.

Huynh, T. N., Choi, P. H., Sureka, K., Ledvina, H. E., Campillo, J., Tong, L., *et al.* (2016). Cyclic di-AMP targets the cystathionine beta-synthase domain of the osmolyte transporter OpuC. *Mol. Microbiol.* **102**: 233–43.

Huynh, T. N., Luo, S., Pensinger, D., Sauer, J. D., Tong, L., and Woodward, J. J. (2015). An HD-domain phosphodiesterase mediates cooperative hydrolysis of c-di-AMP to affect bacterial growth and virulence. *Proc. Natl. Acad. Sci. U.S.A.* **112:** E747–56.

Imlay, J.A. (2008) Cellular defenses against superoxide and hydrogen peroxide. *Annu Rev Biochem* **77**: 755–76.

Imlay, J.A. (2015) Transcription Factors That Defend Bacteria Against Reactive Oxygen Species. *Annu Rev Microbiol* **69**: 93–108.

Inamine, J.M., Ho, K.C., Loechel, S., and Hu, P.C. (1990) Evidence that UGA is read as a tryptophan codon rather than as a stop codon by Mycoplasma pneumoniae, *Mycoplasma genitalium*, and *Mycoplasma gallisepticum*. *J Bacteriol* **172**: 504–6.

Inaoka, T., Matsumura, Y., and Tsuchido, T. (1999) SodA and manganese are essential for resistance to oxidative stress in growing and sporulating cells of *Bacillus subtilis*. *J Bacteriol* **181**: 1939–43.

Into, T., Dohkan, J.I., Inomata, M., Nakashima, M., Shibata, K.I., and Matsushita, K. (2007) Synthesis and characterization of a dipalmitoylated lipopeptide derived from paralogous lipoproteins of *Mycoplasma pneumoniae*. *Infect Immun* **75**: 2253–9.

Into, T., Kiura, K., Yasuda, M., Kataoka, H., Inoue, N., Hasebe, A., *et al.* (2004) Stimulation of human Toll-like receptor (TLR) 2 and TLR6 with membrane lipoproteins of *Mycoplasma fermentans* induces apoptotic cell death after NF-kappa B activation. *Cell Microbiol* **6**: 187–99.

Ishag, H.Z.A., Liu, M.J., Yang, R.S., Xiong, Q.Y., Feng, Z.X., and Shao, G.Q. (2016) A replicating plasmid-based vector for GFP expression in *Mycoplasma hyopneumoniae*. *Genet Mol Res* **15**: 1-8.

Janis, C., Lartigue, C., Frey, J., Wróblewski, H., Thiaucourt, F., Blanchard, A., and Sirand-Pugnet, P. (2005) Versatile use of *oriC* plasmids for functional genomics of *Mycoplasma capricolum* subsp. *capricolum*. *Appl Environ Microbiol* **71**: 2888–93.

Jeffery, C.J. (1999) Moonlighting proteins. *Trends Biochem Sci* **24**: 8–11.

Jenkins, C., Samudrala, R., Geary, S.J., and Djordjevic, S.P. (2008) Structural and functional characterization of an organic hydroperoxide resistance protein from *Mycoplasma gallisepticum*. *J Bacteriol* **190**: 2206–16.

Jiang, D., Nelson, M.L., Gally, F., Smith, S., Wu, Q., Minor, M., *et al.* (2012) Airway Epithelial NF-κB Activation Promotes *Mycoplasma pneumoniae* Clearance in Mice. *PLoS One* **7**: e52969.

Johansson, J., Mandin, P., Renzoni, A., Chiaruttini, C., Springer, M., and Cossart, P. (2002) An RNA thermosensor controls expression of virulence genes in *Listeria monocytogenes*. *Cell* **110**: 551–61.

Johnson, C., Kannan, T.R., and Baseman, J.B. (2011) Cellular vacuoles induced by *Mycoplasma pneumoniae* CARDS toxin originate from Rab9-associated compartments. *PLoS One* **6**: e22877.

Johnson, D.C., Dean, D.R., Smith, A.D., and Johnson, M.K. (2005) Structure, function, and formation of biological iron-sulfur clusters. *Annu Rev Biochem* **74**: 247–81.

Jores, J., Ma, L., Ssajjakambwe, P., Schieck, E., Liljander, A.M., Chandran, S., *et al.* (2019) Removal of a subset of non-essential genes fully attenuates a highly virulent *Mycoplasma strain*. *bioRxiv* 508978. (in peer-review)

Joseph, P., Fantino, J.R., Herbaud, M.L., and Denizot, F. (2001) Rapid orientated cloning in a shuttle vector allowing modulated gene expression in Bacillus subtilis. *FEMS Microbiol Lett* **205**: 91–7.

Junier, I., Unal, E.B., Yus, E., Lloréns-Rico, V., and Serrano, L. (2016) Insights into the Mechanisms of Basal Coordination of Transcription Using a Genome-Reduced Bacterium. *Cell Syst* **2**: 391–401.

Kadaoui, K.A., and Corthésy, B. (2007) Secretory IgA mediates bacterial translocation to dendritic cells in mouse Peyer's patches with restriction to mucosal compartment. *J Immunol* **179**: 7751–7.

Kannan, T.R., and Baseman, J.B. (2006) ADP-ribosylating and vacuolating cytotoxin of *Mycoplasma pneumoniae* represents unique virulence determinant among bacterial pathogens. *Proc Natl Acad Sci U S A* **103**: 6724–9.

Kannan, T.R., Musatovova, O., Balasubramanian, S., Cagle, M., Jordan, J.L., Krunkosky, T.M., *et al.* (2010) *Mycoplasma pneumoniae* Community Acquired Respiratory Distress Syndrome toxin expression reveals growth phase and infection-dependent regulation. *Mol Microbiol* **76**: 1127–41.

Karas, B.J., Moreau, N., Deernick, T.J., Gibson, D.G., Venter, J.C., Smith, H., and Glass, J. (2019) Direct transfer of a *Mycoplasma mycoides* genome to yeast is enhanced by removal of the mycoides glycerol uptake factor gene glpF. *ACS Synth Biol*. (in press)

Karimova, G., Pidoux, J., Ullmann, A., and Ladant, D. (1998) A bacterial two-hybrid system based on a reconstituted signal transduction pathway. *Proc Natl Acad Sci U S A* **95**: 5752–5756.

Kenri, T., Kawakita, Y., Kudo, H., Matsumoto, U., Mori, S., Furukawa, Y., *et al.* (2018) Production and characterization of recombinant P1 adhesin essential for adhesion, gliding, and antigenic variation in the human pathogenic bacterium, *Mycoplasma pneumoniae*. *Biochem Biophys Res Commun* 6–11.

Kim, H., Youn, S. J., Kim, S. O., Ko, J., Lee, J. O., and Choi, B. S. (2015) Structural studies of potassium transport protein KtrA regulator of conductance of K^+ (RCK) C domain in complex with cyclic diadenosine monophosphate (c-di-AMP). *J. Biol. Chem.* **290:** 16393–402.

Kim, H.K., Thammavongsa, V., Schneewind, O., and Missiakas, D. (2012) Recurrent infections and immune evasion strategies of *Staphylococcus aureus*. *Curr Opin Microbiol* **15**: 92–9.

Kim, J.N., Roth, A., and Breaker, R.R. (2007) Guanine riboswitch variants from *Mesoplasma florum* selectively recognize 2'-deoxyguanosine. *Proc Natl Acad Sci U S A* **104**: 16092–7.

King, K.W., and Dybvig, K. (1991) Plasmid transformation of Mycoplasma mycoides subspecies mycoides is promoted by high concentrations of polyethylene glycol. *Plasmid* **26**: 108–15.

King, K.W., and Dybvig, K. (1994) Mycoplasmal cloning vectors derived from plasmid pKMK1. *Plasmid* **31**: 49–59.

Knoops, B., Goemaere, J., Eecken, V. Van der, and Declercq, J.-P. (2011) Peroxiredoxin 5: Structure, Mechanism, and Function of the Mammalian Atypical 2-Cys Peroxiredoxin. *Antioxid Redox Signal* **15**: 817–829.

Kobayashi, K., Ehrlich, S.D., Albertini, A., Amati, G., Andersen, K.K., Arnaud, M., *et al.* (2003) Essential *Bacillus subtilis* genes. *Proc Natl Acad Sci U S A* **100**: 4678–83.

Krause, D.C., Chen, S., Shi, J., Jensen, A.J., Sheppard, E.S., and Jensen, G.J. (2018) Electron cryotomography of *Mycoplasma pneumoniae* mutants correlates terminal organelle architectural features and function. *Mol Microbiol* **108**: 306–18.

Krishnakumar, R., Assad-Garcia, N., Benders, G.A., Phan, Q., Montague, M.G., and Glass, J.I. (2010) Targeted chromosomal knockouts in *Mycoplasma pneumoniae*. *Appl Environ Microbiol* **76**: 5297–9.

Küh**ner, S., Noort, V. van, Betts, M.J., Leo-Macias, A., Batisse, C., Rode, M., *et al.*** (2009) Proteome Organization in a Genome-Reduced Bacterium. *Science* **326**: 1235–1240.

Kunst, F., and Rapoport, G. (1995) Salt stress is an environmental signal affecting degradative enzyme synthesis in *Bacillus subtilis*. *J Bacteriol* **177**: 2403–7.

Labroussaa, F., Lebaudy, A., Baby, V., Gourgues, G., Matteau, D., Vashee, S., *et al.* (2016) Impact of donor-recipient phylogenetic distance on bacterial genome transplantation. *Nucleic Acids Res* **44**: 8501–11.

Lartigue, C., Blanchard, A., Renaudin, J., Thiaucourt, F., and Sirand-Pugnet, P. (2003) Host specificity of mollicutes *oriC* plasmids: Functional analysis of replication origin. *Nucleic Acids Res* **31**: 6610–8.

Lartigue, C., Glass, J.I., Alperovich, N., Pieper, R., Parmar, P.P., Hutchison, C.A., *et al.* (2007) Genome transplantation in bacteria: changing one species to another. *Science* **317**: 632–8.

Lartigue, C., Vashee, S., Algire, M.A., Chuang, R.-Y., Benders, G.A., Ma, L., *et al.* (2009) Creating bacterial strains from genomes that have been cloned and engineered in yeast. *Science* **325**: 1693–6.

Lauer, P., Rinaudo, C.D., Soriani, M., Margarit, I., Maione, D., Rosini, R., *et al.* (2005) Microbiology: Genome analysis reveals pili in group B streptococcus. *Science* **309**: 105.

Lee, J.-W., and Helmann, J.D. (2006) The PerR transcription factor senses H_2O_2 by metal-catalysed histidine oxidation. *Nature* **440**: 363–7.

Lee, S.-W., Browning, G.F., and Markham, P.F. (2008) Development of a replicable *oriC* plasmid for *Mycoplasma gallisepticum* and *Mycoplasma imitans*, and gene disruption through homologous recombination in *M. gallisepticum*. *Microbiology* **154**: 2571–80.

Lesniak, J., Barton, W. a, and Nikolov, D.B. (2002) Structural and functional characterization of the Pseudomonas hydroperoxide resistance protein Ohr. *EMBO J* **21**: 6649–59.

Lesniak, J., Barton, W.A., and Nikolov, D.B. (2003) Structural and functional features of the *Escherichia coli* hydroperoxide resistance protein OsmC. *Protein Sci* **12**: 2838–43.

Li, S., Xue, G., Zhao, H., Feng, Y., Yan, C., Cui, J., and Sun, H. (2019) The *Mycoplasma pneumoniae* HapE alters the cytokine profile and growth of human bronchial epithelial cells. *Biosci Rep* **39**: BSR20182201.

Lin, C.-J., Sasse, C., Gerke, J., Valerius, O., Irmer, H., Frauendorf, H., *et al.* (2015) Transcription Factor SomA Is Required for Adhesion, Development and Virulence of the Human Pathogen Aspergillus fumigatus. *PLoS Pathog* **11**: e1005205.

Lindahl, G., and Akerström, B. (1989) Receptor for IgA in group A streptococci: cloning of the gene and characterization of the protein expressed in *Escherichia coli*. *Mol Microbiol* **3**: 239–47.

Liu, S., Bayles, D.O., Mason, T.M., and Wilkinson, B.J. (2006) A cold-sensitive *Listeria monocytogenes* mutant has a transposon insertion in a gene encoding a putative membrane protein and shows altered (p)ppGpp levels. *Appl Environ Microbiol* **72**: 3955–9.

Livak, K.J., and Schmittgen, T.D. (2001) Analysis of relative gene expression data using real-time quantitative PCR and the 2(-Delta Delta C(T)) Method. *Methods* **25**: 402–8.

Lluch-Senar, M., Delgado, J., Chen, W. H., Lloréns-Rico, V., O'Reilly, F. J., Wodke, J. A., *et al.* (2015). Defining a minimal cell: essentiality of small ORFs and ncRNAs in a genome-reduced bacterium. *Mol. Syst. Biol.* **11**:780.

Lluch-Senar, M., Luong, K., Lloréns-Rico, V., Delgado, J., Fang, G., Spittle, K., *et al.* (2013) Comprehensive methylome characterization of *Mycoplasma genitalium* and *Mycoplasma pneumoniae* at single-base resolution. *PLoS Genet* **9**: e1003191.

López-García, P., Eme, L., and Moreira, D. (2017) Symbiosis in eukaryotic evolution. *J Theor Biol* **434**: 20–33.

Loprasert, S., Fuangthong, M., Whangsuk, W., Atichartpongkul, S., and Mongkolsuk, S. (2000) Molecular and physiological analysis of an OxyR-regulated *ahpC* promoter in *Xanthomonas campestris* pv. *phaseoli*. *Mol Microbiol* **37**: 1504–14.

Luo, Y., and Helmann, J. D. (2012). Analysis of the role of *Bacillus subtilis* σM in β-lactam resistance reveals an essential role for c-di-AMP in peptidoglycan homeostasis. *Mol. Microbiol.* **83**, 623–39.

Lynch, R.E., and Cole, B.C. (1980) *Mycoplasma pneumoniae*: A prokaryote which consumes oxygen and generates superoxide, but which lacks superoxide dismutase. *Top Catal* **96**: 98–105.

Lysnyansky, I., Ron, Y., Sachse, K., and Yogev, D. (2001) Intrachromosomal recombination within the vsp locus of *Mycoplasma bovis* generates a chimeric variable surface lipoprotein antigen. *Infect Immun* **69**: 3703–12.

Lysnyansky, I., Sachse, K., Rosenbusch, R., Levisohn, S., and Yogev, D. (1999) The *vsp* locus of *Mycoplasma bovis*: gene organization and structural features. *J Bacteriol* **181**: 5734–41.

Ma, L., Jensen, J.S., Myers, L., Burnett, J., Welch, M., Jia, Q., and Martin, D.H. (2007) *Mycoplasma genitalium*: An efficient strategy to generate genetic variation from a minimal genome. *Mol Microbiol* **66**: 220–36.

Ma, Z., Lee, J.W., and Helmann, J.D. (2011) Identification of altered function alleles that affect *Bacillus subtilis* PerR metal ion selectivity. *Nucleic Acids Res* **39**: 5036–44.

Machado, C.X., Pinto, P.M., Zaha, A., and Ferreira, H.B. (2009) A peroxiredoxin from *Mycoplasma hyopneumoniae* with a possible role in H_2O_2 detoxification. Microbiology **155**: 3411–9.

Madsen, M.L., Nettleton, D., Thacker, E.L., Edwards, R., and Minion, F.C. (2006) Transcriptional Profiling of *Mycoplasma hyopneumoniae* during Heat Shock Using Microarrays. *Infect Immun* **74**: 160–6.

Maglennon, G.A., Cook, B.S., Matthews, D., Deeney, A.S., Bossé, J.T., Langford, P.R., *et al.* (2013) Development of a self-replicating plasmid system for *Mycoplasma hyopneumoniae*. *Vet Res* **44**: 63.

Maier, T., Schmidt, A., Güell, M., Kühner, S., Gavin, A.C., Aebersold, R., and Serrano, L. (2011) Quantification of mRNA and protein and integration with protein turnover in a bacterium. *Mol Syst Biol* **7**: 1–12.

Manikandan, K., Sabareesh, V., Singh, N., Saigal, K., Mechold, U., and Sinha, K. M. (2014). Two-step synthesis and hydrolysis of cyclic di-AMP in *Mycobacterium tuberculosis*. *PLoS ONE* **9**:e86096.

Maniloff, J. (1996) The minimal cell genome: "on being the right size". *Proc Natl Acad Sci* **93**: 10004–6

Marinho, H.S., Real, C., Cyrne, L., Soares, H., and Antunes, F. (2014) Hydrogen peroxide sensing, signaling and regulation of transcription factors. *Redox Biol* **2**: 535–62.

Marino, M., Braun, L., Cossart, P., and Ghosh, P. (1999) Structure of the lnlB leucine-rich repeats, a domain that triggers host cell invasion by the bacterial pathogen *L. monocytogenes*. *Mol Cell* **4**: 1063–72.

Mariscal, A.M., González-González, L., Querol, E., and Piñol, J. (2016) All-in-one construct for genome engineering using Cre-lox technology. *DNA Res* **23**: 263–70.

Martin-Verstraete, I., Débarbouillé, M., Klier, A., and Rapoport, G. (1992) Mutagenesis of the *Bacillus subtilis* "−12, −24" promoter of the levanase operon and evidence for the existence of an upstream activating sequence. **J Mol Biol** *226*: 85–99.

Matteau, D., Pepin, M.-E., Baby, V., Gauthier, S., Arango Giraldo, M., Knight, T.F., and Rodrigue, S. (2017) Development of *oriC* -Based Plasmids for *Mesoplasma florum*. *Appl Environ Microbiol* **83**: e03374-16.

Matyushkina, D., Pobeguts, O., Butenko, I., Vanyushkina, A., Anikanov, N., Bukato, O., *et al.* (2016) Phase Transition of the Bacterium upon Invasion of a Host Cell as a Mechanism of Adaptation: a *Mycoplasma gallisepticum* Model. *Sci Rep* **6**: 35959.

McFarland, A.P., Burke, T.P., Carletti, A.A., Glover, R.C., Tabakh, H., Welch, M.D., and Woodward, J.J. (2018) RECON-dependent inflammation in hepatocytes enhances L*isteria monocytogenes* cell-to-cell spread. *MBio* **9**: 1–15.

McFarland, A.P., Luo, S., Ahmed-Qadri, F., Zuck, M., Thayer, E.F., Goo, Y.A., *et al.* (2017) Sensing of Bacterial Cyclic Dinucleotides by the Oxidoreductase RECON Promotes NF-κB Activation and Shapes a Proinflammatory Antibacterial State. *Immunity* **46**: 433–45.

McGillivray, S.M., Ebrahimi, C.M., Fisher, N., Sabet, M., Zhang, D.X., Chen, Y., *et al.* (2009) ClpX contributes to innate defense peptide resistance and virulence phenotypes of *Bacillus anthracis*. *J Innate Immun* **1**: 494–506.

McGowin, C.L., and Totten, P.A. (2017) The Unique Microbiology and Molecular Pathogenesis of *Mycoplasma genitalium*. *J Infect Dis* **216**: S382–8.

Mehne, F. M. P., Gunka, K., Eilers, H., Herzberg, C., Kaever, V., and Stülke, J. (2013). Cyclic-di-AMP homeostasis in *Bacillus subtilis*: both lack and high-level accumulation of the nucleotide are detrimental for cell growth. *J. Biol. Chem.* **288**: 2004–17.

Mehne, F. M., Schröder-Tittmann, K., Eijlander, R. T., Herzberg, C., Hewitt, L., Kaever, V., *et al.* (2014). Control of the diadenylate cyclase CdaS in *Bacillus subtilis*: an autoinhibitory domain limits c-di-AMP production. *J. Biol. Chem.* **289**: 21098–107.

Merzbacher, M., Detsch, C., Hillen, W., and Stulke, J. (2004) *Mycoplasma pneumoniae* HPr kinase/phosphorylase. Assigning functional roles to the P-loop and the HPr kinase/ phosphorylase signature sequence motif. *Eur J Biochem* **271**: 367–74.

Meyer, F. M., Gerwig, J., Hammer, E., Herzberg, C., Commichau, F. M., Völker, U., *et al.* (2011). Physical interactions between tricarboxylic acid cycle enzymes in *Bacillus subtilis*: evidence for a metabolon. *Metab. Eng.* **13**: 18–27.

Mijakovic, I., Grangeasse, C., and Turgay, K. (2016) Exploring the diversity of protein modifications: special bacterial phosphorylation systems. *FEMS Microbiol Rev* **40**: 398–417.

Miles RJ. Catabolism in mollicutes. (1992) *J Gen Microbiol* **138**: 1773–83.

Miravet-Verde, S., Lloréns-Rico, V., and Serrano, L. (2017) Alternative transcriptional regulation in genome-reduced bacteria. *Curr Opin Microbiol* **39**: 89–95.

Mols, M., and Abee, T. (2011) Primary and secondary oxidative stress in *Bacillus*. *Environ Microbiol* **13**: 1387–94.

Mongkolsuk, S., and Helmann, J.D. (2002) Regulation of inducible peroxide stress responses. *Mol Microbiol* **45**: 9–15.

Mongkolsuk, S., Praituan, W., Loprasert, S., Fuangthong, M., and Chamnongpol, S. (1998) Identification and characterization of a new organic hydroperoxide resistance (*ohr*) gene with a novel pattern of oxidative stress regulation from *Xanthomonas campestris* pv. *phaseoli*. *J Bacteriol* **180**: 2636–43.

Monteiro, G., Horta, B.B., Pimenta, D.C., Augusto, O., and Netto, L.E.S. (2007) Reduction of 1-Cys peroxiredoxins by ascorbate changes the thiol-specific antioxidant paradigm, revealing another function of vitamin C. *Proc Natl Acad Sci* **104**: 4886–91.

Moscoso, J. A., Schramke, H., Zhang, Y., Tosi, T., Dehbi, A., Jung, K., *et al.* (2016). Binding of cyclic di-AMP to the *Staphylococcus aureus* sensor kinase KdpD occurs via the universal stress protein domain and downregulates the expression of the Kdp potassium transporter. *J. Bacteriol.* **198**: 98–110.

Mossessova, E., and Lima, C.D. (2000) Ulp1-SUMO Crystal Structure and Genetic Analysis Reveal Conserved Interactions and a Regulatory Element Essential for Cell Growth in Yeast. *Mol Cell* **5**: 865–76.

Mudahi-Orenstein, S., Levisohn, S., Geary, S.J., and Yogev, D. (2003) Cytadherence-Deficient Mutants of *Mycoplasma gallisepticum* Generated by Transposon Mutagenesis. *Infect Immun* **71**: 3812-20.

Mühlradt, P.F., Kiess, M., Meyer, H., Süssmuth, R., and Jung, G. (1997) Isolation, structure elucidation, and synthesis of a macrophage stimulatory lipopeptide from *Mycoplasma fermentans* acting at picomolar concentration. *J Exp Med* **185**: 1951–8.

Nascimento, N.C. do, Guimaraes, A.M.S., Santos, A.P., SanMiguel, P.J., and Messick, J.B. (2012) Complete genome sequence of *Mycoplasma haemocanis* strain Illinois. *J Bacteriol* **194**: 1605–6.

Nelson, J. W., Sudarsan, N., Furukawa, K., Weingerg, Z., Wang, J. X., and Breaker, R. R. (2013). Riboswitches in eubacteria sense the second messenger cyclic di-AMP. *Nat. Chem. Biol.* **9**: 834–9.

Nelson, K.J., and Parsonage, D. (2011) Measurement of peroxiredoxin activity. *Curr Protoc Toxicol* **Chapter 7**: Unit7.10.

Nelson, K.J., Knutson, S.T., Soito, L., Klomsiri, C., Poole, L.B., and Fetrow, J.S. (2011) Analysis of the peroxiredoxin family: Using active-site structure and sequence information for global classification and residue analysis. *Proteins Struct Funct Bioinforma* **79**: 947–964.

Nicolas, P., Mäder, U., Dervyn, E., Rochat, T., Leduc, A., Pigeonneau, N., *et al.* (2012) Condition-dependent transcriptome reveals high-level regulatory architecture in *Bacillus subtilis*. *Science* **335**: 1103–6.

Nilsson, R.P., Beijer, L., and Rutberg, B. (1994) The *glpT* and *glpQ* genes of the glycerol regulon in *Bacillus subtilis*. *Microbiology* **140**: 723–30.

Nissen, P., Hansen, J., Ban, N., Moore, P. B., and Steitz, T. A. (2000). The structural basis of ribosome activity in peptide bond synthesis. *Science* **289**: 920–30.

Nocek, B., Mulligan, R., Kwon, K., Anderson, W.F., and Joachimiak, A. (to be published) High resolution crystal structure of the organic hydroperoxide resistance protein from *Vibrio cholerae* O1 biovar eltor str. N16961.

Noort, V. van, Seebacher, J., Bader, S., Mohammed, S., Vonkova, I., Betts, M.J., *et al.* (2012) Cross-talk between phosphorylation and lysine acetylation in a genome-reduced bacterium. *Mol Syst Biol* **8**: 571.

Nunoshiba, T., Hidalgo, E., Amábile Cuevas, C.F., and Demple, B. (1992) Two-stage control of an oxidative stress regulon: the *Escherichia coli* SoxR protein triggers redox-inducible expression of the *soxS* regulatory gene. *J Bacteriol* **174**: 6054–6060.

Ogasawara, N., and Yoshikawa, H. (1992) Genes and their organization in the replication origin region of the bacterial chromosome. *Mol Microbiol* **6**: 629–34.

Oh, S.-Y., Shin, J.-H., and Roe, J.-H. (2007) Dual role of OhrR as a repressor and an activator in response to organic hydroperoxides in *Streptomyces coelicolor*. *J Bacteriol* **189**: 6284–92.

Okusawa, T., Fujita, M., Nakamura, J.-I., Into, T., Yasuda, M., Yoshimura, A., *et al.* (2004) Relationship between structures and biological activities of mycoplasmal diacylated lipopeptides and their recognition by toll-like receptors 2 and 6. *Infect Immun* **72**: 1657–65.

Omasits, U., Ahrens, C.H., Müller, S., and Wollscheid, B. (2014) Protter: interactive protein feature visualization and integration with experimental proteomic data. *Bioinformatics* **30**: 884–6.

Onono, J.O., Wieland, B., and Rushton, J. (2014) Estimation of impact of contagious bovine pleuropneumonia on pastoralists in Kenya. *Prev Vet Med* **115**: 122–9.

Oppenheimer-Shaanan, Y., Wexselblatt, E., Katzhaendler, J., Yavin, E., and Ben-Yehuda, S. (2011). c-di-AMP reports DNA integrity during sporulation in *Bacillus subtilis*. *EMBO Rep.* **12:** 594–601.

Orué Lucana, D.O. de, Zou, P., Nierhaus, M., and Schrempf, H. (2005) Identification of a novel two-component system SenS/SenR modulating the production of the catalase-peroxidase CpeB and the haem-binding protein HbpS in *Streptomyces reticuli*. *Microbiology* **151**: 3603–14.

Page, C.A., and Krause, D.C. (2013) Protein kinase/phosphatase function correlates with gliding motility in *Mycoplasma pneumoniae*. *J Bacteriol* **195**: 1750–7.

Parent, A., Caux-Thang, C., Signor, L., Clémancey, M., Sethu, R., Blondin, G., *et al.* (2013) Single glutamate to aspartate mutation makes ferric uptake regulator (Fur) as sensitive to H_2O_2 as peroxide resistance regulator (PerR). *Angew Chemie - Int Ed* **52**: 10339–43.

Parrott, G.L., Kinjo, T., and Fujita, J. (2016) A compendium for *Mycoplasma pneumoniae*. *Front Microbiol* **7**.

Patel, A.H., Nowlan, P., Weavers, E.D., and Foster, T. (1987) Virulence of protein A-deficient and alpha-toxin-deficient mutants of *Staphylococcus aureus* isolated by allele replacement. *Infect Immun* **55**: 3103–10.

Perkins, A., Parsonage, D., Nelson, K.J., Ogba, O.M., Cheong, P.H.Y., Poole, L.B., and Karplus, P.A. (2016) Peroxiredoxin Catalysis at Atomic Resolution. *Structure* **24**: 1668–78.

Pi, H., and Helmann, J.D. (2017) Sequential induction of Fur-regulated genes in response to iron limitation in *Bacillus subtilis*. *Proc Natl Acad Sci* **114**: 201713008.

Pich, O.Q., Burgos, R., Planell, R., Querol, E., and Piñol, J. (2006) Comparative analysis of antibiotic resistance gene markers in *Mycoplasma genitalium*: application to studies of the minimal gene complement. *Microbiology* **152**: 519–27.

Pilo, P., Frey, J., and Vilei, E.M. (2007) Molecular mechanisms of pathogenicity of *Mycoplasma mycoides* subsp. *mycoides* SC. *Vet J* **174**: 513–21.

Piñero-Lambea, C., Shaw, D., Lluch-Senar, M., Pinol, J., Serrano, L., (unpublished) GP35-mediated clean deletion in *Mycoplasma pneumoniae*.

Pleass, R.J., Areschoug, T., Lindahl, G., and Woof, J.M. (2001) Streptococcal IgA-binding Proteins Bind in the Cα2-Cα3 Interdomain Region and Inhibit Binding of IgA to Human CD89. *J Biol Chem* **276**: 8197–204.

Pollack, J.D. (2002) The necessity of combining genomic and enzymatic data to infer metabolic function and pathways in the smallest bacteria: amino acid, purine and pyrimidine metabolism in Mollicutes. *Front. Biosci*. **7**:1762–81.

Pollack, J.D., Williams, M. V, and McElhaney, R.N. (1997) The comparative metabolism of the mollicutes (*Mycoplasmas*): the utility for taxonomic classification and the relationship of putative gene annotation and phylogeny to enzymatic function in the smallest free-living cells. *Crit Rev Microbiol* **23**: 269–354.

Porcheron, G., and Dozois, C.M. (2015) Interplay between iron homeostasis and virulence: Fur and RyhB as major regulators of bacterial pathogenicity. *Vet Microbiol* **179**: 2–14.

Postic, G., Danchin, A., and Mechold, U. (2012). Characterization of NrnA homologs from *Mycobacterium tuberculosis* and *Mycoplasma pneumoniae*. *RNA* **18:** 155–165.

Prince, O.A., Krunkosky, T.M., and Krause, D.C. (2014) *In vitro* spatial and temporal analysis of *Mycoplasma pneumoniae* colonization of human airway epithelium. *Infect Immun* **82**: 579–86.

Pritchard, R.E., Prassinos, A.J., Osborne, J.D., Raviv, Z., and Balish, M.F. (2014) Reduction of hydrogen peroxide accumulation and toxicity by a catalase from *Mycoplasma iowae*. *PLoS One* **9**: e105188.

Qi, J., Zhang, F., Wang, Y., Liu, T., Tan, L., Wang, S., *et al.* (2018) Characterization of *Mycoplasma gallisepticum* pyruvate dehydrogenase alpha and beta subunits and their roles in cytoadherence. 1–20.

Quintana, I., Espariz, M., Villar, S.R., González, F.B., Pacini, M.F., Cabrera, G., *et al.* (2018) Genetic Engineering of *Lactococcus lactis* Co-producing Antigen and the Mucosal Adjuvant 3′ 5′- cyclic di Adenosine Monophosphate (c-di-AMP) as a Design Strategy to Develop a Mucosal Vaccine Prototype. *Front Microbiol* **9**.

Raeder, R., Woischnik, M., Podbielski, A., and Boyle, M.D. (1998) A secreted streptococcal cysteine protease can cleave a surface-expressed M1 protein and alter the immunoglobulin binding properties. *Res Microbiol* **149**: 539–48.

Rao, F., See, R. Y., Zhang, D., Toh, D. C., Ji, Q., and Liang, Z. X. (2010). YybT is a signaling protein that contains a cyclic dinucleotide phosphodiesterase domain and a GGDEF domain with ATPase activity. *J. Biol. Chem.* **285**: 473–482.

Raymond, B.B.A., Jenkins, C., Turnbull, L., Whitchurch, C.B., and Djordjevic, S.P. (2018) Extracellular DNA release from the genome-reduced pathogen *Mycoplasma hyopneumoniae* is essential for biofilm formation on abiotic surfaces. *Sci Rep* **8**: 10373.

Reddick, L.E., and Alto, N.M. (2014) Bacteria fighting back: How pathogens target and subvert the host innate immune system. *Mol Cell* **54**: 321–328.

Renaudin, J. (2002) Extrachromosomal elements and gene transfer. In Razin S, Herrmann R. (eds.) Molecular biology and pathogenicity of *Mycoplasmas*. *Kluwer Academic Publishers/ Plenum Press. New York*, **pp**. 347-70.

Reuß, D. (2017) Large-scale genome reduction in bacteria: From *Bacillus subtilis* to Mini*Bacillus*. Ph.D. thesis, Georg-August-University of Göttingen, Göttingen

Reuß, D.R., Altenbuchner, J., Mäder, U., Rath, H., Ischebeck, T., Sappa, P.K., *et al.* (2017) Large-scale reduction of the *Bacillus subtilis* genome: consequences for the transcriptional network, resource allocation, and metabolism. *Genome Res* **27**: 289–99.

Reuß, D.R., Commichau, F.M., Gundlach, J., Zhu, B., and Stülke, J. (2016) The Blueprint of a Minimal Cell: Mini*Bacillus*. *Microbiol Mol Biol Rev* **80**: 955–87.

Rhee, S.G., and Woo, H.A. (2011) Multiple functions of peroxiredoxins: peroxidases, sensors and regulators of the intracellular messenger H_2O_2, and protein chaperones. *Antioxid Redox Signal* **15**: 781–94.

Rhee, S.G., Woo, H.A., Kil, I.S., and Bae, S.H. (2012) Peroxiredoxin functions as a peroxidase and a regulator and sensor of local peroxides. *J Biol Chem* **287**: 4403–10.

Robertson, J.A., Stemler, M.E., and Stemke, G.W. (1984) Immunoglobulin A protease activity of *Ureaplasma urealyticum*. *J Clin Microbiol* **19**: 255–8.

Rodriguez, G.M., Voskuil, M.I., Gold, B., Schoolnik, G.K., and Smith, I. (2002) *ideR*, an Essential Gene in *Mycobacterium tuberculosis*: Role of IdeR in Iron-Dependent Gene Expression, Iron Metabolism, and Oxidative Stress Response. *Infect Immun* **70**: 3371–81.

Rojas-Tapias, D.F., and Helmann, J.D. (2018) Induction of the Spx regulon by cell wall stress reveals novel regulatory mechanisms in Bacillus subtilis. *Mol Microbiol* **107**: 659–674.

Römling, U. (2008). Great times for small molecules: c-di-AMP, a second messenger candidate in bacteria and archaea. *Sci. Signal.* **1**:e39.

Rooijakkers, S.H.M., Kessel, K.P.M. van, and Strijp, J.A.G. van (2005) Staphylococcal innate immune evasion. *Trends Microbiol* **13**: 596–601.

Rosenberg, J., Dickmanns, A., Neumann, P., Gunka, K., Arens, J., Kaever, V., *et al.* (2015). Biochemical and structural analysis of the essential diadenylate cyclase CdaA from *Listeria monocytogenes*. *J. Biol. Chem.* **290:** 6596–606.

Rottem, S. (2003) Interaction of *Mycoplasmas* With Host Cells. *Physiol Rev* **83**: 417–32.

Russell-Jones, G.J., Gotschlich, E.C., and Blake, M.S. (1984) A surface receptor specific for human IgA on group B streptococci possessing the Ibc protein antigen. *J Exp Med* **160**: 1467–75.

Ryan-Payseur, B.K., and Freitag, N.E. (2018) *Bacillus subtilis* Biofilms: a Matter of Individual Choice. *MBio* **9**.

Saikolappan, S., Sasindran, S.J., Yu, H.D., Baseman, J.B., and Dhandayuthapani, S. (2009) The *Mycoplasma genitalium* MG-454 gene product resists killing by organic hydroperoxides. *J Bacteriol* 191: 6675–6682.

Sambrook, J., Fritsch, E. F., and Maniatis, T. (1989). Molecular Cloning: A Laboratory Manual, 2nd Edn. *Cold Spring Harbor*, **NY**: Cold Spring Harbor Laboratory.

Sanderson-Smith, M.L., Oliveira, D.M.P. De, Ranson, M., and McArthur, J.D. (2012) Bacterial plasminogen receptors: mediators of a multifaceted relationship. *J Biomed Biotechnol* **2012**: 272148.

Schafer, E.R., Oneal, M.J., Madsen, M.L., and Minion, F.C. (2007) Global transcriptional analysis of *Mycoplasma hyopneumoniae* following exposure to hydrogen peroxide. *Microbiology* **153**: 3785–90.

Schäfer, H., Heinz, A., Sudzinová, P., Voß, M., Hantke, I., Krásný, L., and Turgay, K. (2019) Spx, the central regulator of the heat and oxidative stress response in *B. subtilis*, can repress transcription of translation-related genes. *Mol Microbiol* **111**: 514–33.

Schär, J., Stoll, R., Schauer, K., Loeffler, D.I.M., Eylert, E., Joseph, B., *et al.* (2010) Pyruvate Carboxylase Plays a Crucial Role in Carbon Metabolism of Extra- and Intracellularly Replicating *Listeria monocytogenes*. *J Bacteriol* **192**: 1774–84.

Schilling, O., Herzberg, C., Hertrich, T., Vörsmann, H., Jessen, D., Hübner, S., *et al.* (2006). Keeping signals straight in transcription regulation: specificity determinants for the interaction of a family of conserved bacterial RNA-protein couples. *Nucleic Acids Res.* **34:** 6102–6115.

Schmalisch, M., Langbein, I., and Stülke, J. (2002) The general stress protein Ctc of *Bacillus subtilis* is a ribosomal protein. *J Mol Microbiol Biotechnol* **4**: 495–501.

Schmeisky, A.G. (2013) Untersuchung zur kohlenstoffabhängigen Wasserstoffperoxidproduktion und Virulenz in *Mycoplasma pneumoniae* und *Mycoplasma genitalium*. PhD thesis. University of Göttingen, Göttingen, Germany.

Schmidl, S. R., Gronau, K., Hames, C., Busse, J., Becher, D., Hecker, M., *et al.* (2010a). The stability of cytadherence proteins in *Mycoplasma pneumoniae* requires activity of the protein kinase PrkC. *Infect. Immun.* **78**: 184–192.

Schmidl, S.R. (2010) Pathogenicity of a minimal organism: Role of protein phosphorylation in *Mycoplasma pneumoniae*. PhD thesis. University of Göttingen, Göttingen, Germany.

Schmidl, S.R., Gronau, K., Pietack, N., Hecker, M., Becher, D., and Stülke, J. (2010b) The Phosphoproteome of the Minimal Bacterium *Mycoplasma pneumoniae*. *Mol Cell Proteomics* **9**: 1228–42.

Schmidl, S.R., Otto, A., Lluch-Senar, M., Piñol, J., Busse, J., Becher, D., and Stülke, J. (2011) A Trigger Enzyme in *Mycoplasma pneumoniae*: Impact of the Glycerophosphodiesterase GlpQ on Virulence and Gene Expression. *PLoS Pathog* **7**: e1002263.

Schmidt, A., Trentini, D.B., Spiess, S., Fuhrmann, J., Ammerer, G., Mechtler, K., and Clausen, T. (2014) Quantitative Phosphoproteomics Reveals the Role of Protein Arginine Phosphorylation in the Bacterial Stress Response. *Mol. Cell Proteomics* **13**: 537 LP-550.

Schmitt, K., Smolinski, N., Neumann, P., Schmaul, S., Hofer-Pretz, V., Braus, G.H., and Valerius, O. (2017) Asc1p/RACK1 Connects Ribosomes to Eukaryotic Phosphosignaling. Mol Cell Biol **37**.

Schreiner, S.A., Sokoli, A., Felder, K.M., Wittenbrink, M.M., Schwarzenbach, S., Guhl, B., *et al.* (2012) The surface-localised α-enolase of *Mycoplasma suis* is an adhesion protein. *Vet Microbiol* **156**: 88–95.

Schurwanz, N., Jacobs, E., and Dumke, R. (2009) Strategy to create chimeric proteins derived from functional adhesin regions of *Mycoplasma pneumoniae* for vaccine development. *Infect Immun* **77**: 5007–15.

Schuster, C. F., Bellows, L. E., Tosi, T., Campeotto, I., Corrigan, R. M., Freemont, P., *et al.* (2016). The second messenger c-di-AMP inhibits the osmolyte uptake system OpuC in *Staphylococcus aureus*. *Sci. Signal.* **9**:ra81.

Schwartz, K.T., Carleton, J.D., Quillin, S.J., Rollins, S.D., Portnoy, D.A., and Leber, J.H. (2012) Hyperinduction of host beta interferon by a *Listeria monocytogenes* strain naturally overexpressing the multidrug efflux pump MdrT. *Infect Immun* **80**: 1537–45.

Seybert, A., Gonzalez-Gonzalez, L., Scheffer, M.P., Lluch-Senar, M., Mariscal, A.M., Querol, E., *et al.* (2018) Cryo-electron tomography analyses of terminal organelle mutants suggest the motility mechanism of *Mycoplasma genitalium*. *Mol Microbiol* **108**: 319–29.

Shahid, M.A., Marenda, M.S., Markham, P.F., and Noormohammadi, A.H. (2014) Development of an oriC vector for use in *Mycoplasma synoviae*. *J Microbiol Methods* **103**: 70–6.

Sharma, S., Citti, C., Sagné, E., Marenda, M.S., Markham, P.F., and Browning, G.F. (2015) Development and host compatibility of plasmids for two important ruminant pathogens, *Mycoplasma bovis* and *Mycoplasma agalactiae*. *PLoS One* **10**: e0119000.

Shen, Y., Naujokas, M., Park, M., and Ireton, K. (2000) InlB-Dependent Internalization of *Listeria* Is Mediated by the Met Receptor Tyrosine Kinase. *Cell* **103**: 501–10.

Shevchenko, A., Wilm, M., Vorm, O., and Mann, M. (1996) Mass spectrometric sequencing of proteins silver-stained polyacrylamide gels. *Anal Chem* **68**: 850–8.

Shifrine, M., Bailey, K.P., and Stone, S.S. (1972) Contagious bovine pleuropneumonia: isolation of *Mycoplasma mycoides* var. *mycoides* from ticks collected from infected cattle and infection attempts using these ticks. *Bull Epizoot Dis Afr* **20**: 43–5.

Shimizu, T. (2016) Inflammation-inducing Factors of *Mycoplasma pneumoniae*. *Front Microbiol* **7**: 414.

Shimizu, T., Kida, Y., and Kuwano, K. (2007) Triacylated lipoproteins derived from Mycoplasma pneumoniae activate nuclear factor-kappaB through toll-like receptors 1 and 2. *Immunology* **121**: 473–83.

Shimizu, T., Kimura, Y., Kida, Y., Kuwano, K., Tachibana, M., Hashino, M., and Watarai, M. (2014) Cytadherence of *Mycoplasma pneumoniae* induces inflammatory responses through autophagy and toll-like receptor 4. *Infect Immun* **82**: 3076–86.

Sidorin, E. V, and Solov'eva, T.F. (2011) IgG-binding proteins of bacteria. *Biochem* **76**: 295–308.

Simonsen, L.O., Harbak, H., and Bennekou, P. (2012) Cobalt metabolism and toxicology-A brief update. *Sci Total Environ* **432**: 210–15.

Sjöbring, U., Björck, L., and Kastern, W. (1991) Streptococcal protein G. Gene structure and protein binding properties. *J Biol Chem* **266**: 399–405.

Sleator, R.D. (2016) JCVI-syn3.0 - A synthetic genome stripped bare! *Bioengineered* **7**: 53–6.

Smith, E.J., Visai, L., Kerrigan, S.W., Speziale, P., and Foster, T.J. (2011) The Sbi protein is a multifunctional immune evasion factor of *Staphylococcus aureus*. *Infect Immun* **79**: 3801–9.

Smith, L.G. (2010) *Mycoplasma pneumoniae* and Its Complications. *Infect Dis Clin North Am* **24**: 57–6.

Somarajan, S.R., Kannan, T.R., and Baseman, J.B. (2010) *Mycoplasma pneumoniae* Mpn133 is a cytotoxic nuclease with a glutamic acid-, lysine- and serine-rich region essential for binding and internalization but not enzymatic activity. *Cell Microbiol* **12**: 1821–31.

Somerson, N.L., Purcell, R.H., Taylor-Robinson, D., And Chanock, R.M. (1965) Hemolysin Of *Mycoplasma pneumoniae*. *J Bacteriol* **89**: 813–8.

Speck, C., Weigel, C., and Messer, W. (1997) From footprint to toeprint: a close-up of the DnaA box, the binding site for the bacterial initiator protein DnaA. *Nucleic Acids Res* **25**: 3242–7.

Spooner, R.K., Russell, W.C., and Thirkell, D. (1992) Characterization of the immunoglobulin A protease of *Ureaplasma urealyticum*. *Infect Immun* **60**: 2544–6.

Steinchen, W., and Bange, G. (2016). The magic dance of the alarmones (p)ppGpp. *Mol. Microbiol.* **101**: 531–44.

Sukchawalit, R., Loprasert, S., Atichartpongkul, S., and Mongkolsuk, S. (2001) Complex regulation of the organic hydroperoxide resistance gene (*ohr*) from *Xanthomonas* involves OhrR, a novel organic peroxide-inducible negative regulator, and posttranscriptional modifications. *J Bacteriol* **183**: 4405–12.

Sun, G., Xu, X., Wang, Y., Shen, X., Chen, Z., and Yang, J. (2008) *Mycoplasma pneumoniae* infection induces reactive oxygen species and DNA damage in A549 human lung carcinoma cells. *Infect Immun* **76**: 4405–13.

Sureka, K., Choi, P. H., Precit, M., Delince, M., Pensinger, D. A., Huynh, T. N., *et al.* (2014). The cyclic dinucleotide c-di-AMP is an allosteric regulator of metabolic enzyme function. *Cell* **158:** 1389–1401.

Tacchi, J.L., Raymond, B.B.A., Haynes, P.A., Berry, I.J., Widjaja, M., Bogema, D.R., *et al.* (2016) Post-translational processing targets functionally diverse proteins in *Mycoplasma hyopneumoniae*. *Open Biol* **6**: 150210.

Tajima, M., Yagihashi, T., and Miki, Y. (1982) Capsular material of *Mycoplasma gallisepticum* and its possible relevance to the pathogenic process. *Infect Immun* **36**: 830–3.

Tambi, N.E., Maina, W.O., and Ndi, C. (2006) An estimation of the economic impact of contagious bovine pleuropneumonia in Africa. *Rev Sci Tech* **25**: 999–1011.

Tan, E., Rao, F., Pasunooti, S., Pham, T.H., Soehano, I., Turner, M.S., *et al.* (2013) Solution structure of the PAS domain of a thermophilic YybT protein homolog reveals a potential ligand-binding site. *J Biol Chem* **288**: 11949–59.

Telford, J.L., Barocchi, M.A., Margarit, I., Rappuoli, R., and Grandi, G. (2006) Pili in Gram-positive pathogens. *Nat Rev Microbiol* **4**: 509–19.

Teramoto, H., Inui, M., and Yukawa, H. (2013) OxyR acts as a transcriptional repressor of hydrogen peroxide-inducible antioxidant genes in *Corynebacterium glutamicum* R. *FEBS J* **280**: 3298–312.

Thomas, C., Jacobs, E., and Dumke, R. (2013) Characterization of pyruvate dehydrogenase subunit B and enolase as plasminogen-binding proteins in *Mycoplasma pneumoniae*. *Microbiol (UK)* **159**: 352–65.

Tonry, J.H., Mcnichol, B.A., Ramarao, N., Chertow, D.S., Kim, K.S., Stibitz, S., *et al.* (2012) *Bacillus anthracis* protease InhA regulates BslA-mediated adhesion in human endothelial cells. *Cell Microbiol* **14**: 1219–1230.

Touati, D. (2000) Iron and Oxidative Stress in Bacteria. *Arch Biochem Biophys* **373**: 1–6.

Townsley, L., Yannarell, S.M., Huynh, T.N., Woodward, J.J., and Shank, E.A. (2018) Cyclic di-AMP Acts as an Extracellular Signal That Impacts *Bacillus subtilis* Biofilm Formation and Plant Attachment. *MBio* **9**: 1–13.

Traoré, D.A.K., Ghazouani, A. El, Jacquamet, L., Borel, F., Ferrer, J.-L., Lascoux, D., *et al.* (2009) Structural and functional characterization of 2-oxo-histidine in oxidized PerR protein. *Nat Chem Biol* **5**: 53–9.

Travers, A., and Muskhelishvili, G. (2005) DNA supercoiling - a global transcriptional regulator for enterobacterial growth? *Nat Rev Microbiol* **3**: 157–69.

Tretyakova, N.Y., Groehler, A., and Ji, S. (2015) DNA-Protein Cross-Links: Formation, Structural Identities, and Biological Outcomes. *Acc Chem Res* **48**: 1631–44.

Troxell, B., and Hassan, H.M. (2013) Transcriptional regulation by Ferric Uptake Regulator (Fur) in pathogenic bacteria. *Front Cell Infect Microbiol* **3**: 1–13.

Tryon, V.V., and Baseman, J.B. (1992) Pathogenic determinants and mechanisms. In Maniloff J (ed.). *Mycoplasmas*: molecular biology and pathogenesis. *American Society for Microbiology, Washington, D.C*. **pp**: 457–71.

Tsarmpopoulos, I., Gourgues, G., Blanchard, A., Vashee, S., Jores, J., Lartigue, C., and Sirand-Pugnet, P. (2016) In-Yeast Engineering of a Bacterial Genome Using CRISPR/Cas9. *ACS Synth Biol* **5**: 104–9.

Tu, W.Y., Pohl, S., Summpunn, P., Hering, S., Kerstan, S., and Harwood, C.R. (2012) Comparative analysis of the responses of related pathogenic and environmental bacteria to oxidative stress. *Microbiology* **158**: 636–47.

Tully, J.G., Taylor-Robinson, D., Cole, R.M. and Rose, D.L. (1981) A newly discovered *Mycoplasma* in the human urogenital tract. *Lancet* **1**:1288-1291.

Tully, J.G., Taylor-Robinson, D., Rose, D.L., Furr, P.M., and Hawkins, D.A. (1983) Evaluation of culture media for the recovery of *Mycoplasma hominis* from the human urogenital tract. *Sex Transm Dis* **10**: 256–60.

Vilei, E.M., Abdo, E.M., Nicolet, J., Botelho, A., Gonçalves, R., and Frey, J. (2000) Genomic and antigenic differences between the European and African/Australian clusters of *Mycoplasma mycoides* subsp. *mycoides* SC. *Microbiology* **146**: 477–86.

Vlamakis, H., Chai, Y., Beauregard, P., Losick, R., and Kolter, R. (2013) Sticking together: building a biofilm the *Bacillus subtilis* way. *Nat Rev Microbiol* **11**: 157–68.

Vliet, A.H. van, Baillon, M.L., Penn, C.W., and Ketley, J.M. (1999) *Campylobacter jejuni* contains two fur homologs: characterization of iron-responsive regulation of peroxide stress defense genes by the PerR repressor. *J Bacteriol* **181**: 6371–6.

Völker, U., Andersen, K.K., Antelmann, H., Devine, K.M., and Hecker, M. (1998) One of two *osmC* homologs in *Bacillus subtilis* is part of the *sigmaB*-dependent general stress regulon. *J Bacteriol* **180**: 4212–8.

Wach, A. (1996) PCR-synthesis of marker cassettes with long flanking homology regions for gene disruptions in *S. cerevisiae*. *Yeast* **12**: 259–65.

Waites, K.B., and Talkington, D.F. (2004) *Mycoplasma pneumoniae* and Its Role as a Human Pathogen. **17**: 697–728.

Waldo, R.H., and Krause, D.C. (2006) Synthesis, stability, and function of cytadhesin P1 and accessory protein B/C complex of *Mycoplasma pneumoniae*. *J Bacteriol* **188**: 569–75.

Waldron, K.J., and Robinson, N.J. (2009) How do bacterial cells ensure that metalloproteins get the correct metal? *Nat Rev Microbiol* **7**: 25.

Wang, H., O'Sullivan, D.J., Baldwin, K.A., and McKay, L.L. (2000) Cloning, sequencing, and expression of the pyruvate carboxylase gene in *Lactococcus lactis* subsp. *lactis* C2. *Appl Environ Microbiol* **66**: 1223–7.

Wang, W., Erbe, A.K., Hank, J.A., Morris, Z.S., and Sondel, P.M. (2015) NK Cell-Mediated Antibody-Dependent Cellular Cytotoxicity in Cancer Immunotherapy. *Front Immunol* **6**: 368.

Watanabe, H., Uruma, T., Nakamura, H., and Aoshiba, K. (2014) The role of *Mycoplasma pneumoniae* infection in the initial onset and exacerbations of asthma. *Allergy Asthma Proc* **35**: 204–210.

Waters, E., Hohn, M.J., Ahel, I., Graham, D.E., Adams, M.D., Barnstead, M., *et al.* (2003) The genome of *Nanoarchaeum equitans*: insights into early archaeal evolution and derived parasitism. *Proc Natl Acad Sci U S A* **100**: 12984–8.

Wei, S., Guo, Z., Li, T., Zhang, T., Li, X., Zhou, Z., *et al.* (2012) Genome sequence of *Mycoplasma iowae* strain 695, an unusual pathogen causing deaths in turkeys. *J Bacteriol* **194**: 547–548.

Whiteley, A.T., Garelis, N.E., Peterson, B.N., Choi, P.H., Tong, L., Woodward, J.J., and Portnoy, D.A. (2017a) c-di-AMP modulates *Listeria monocytogenes* central metabolism to regulate growth, antibiotic resistance and osmoregulation. *Mol Microbiol* **104**: 212–233.

Whiteley, A.T., Pollock, A.J., and Portnoy, D.A. (2015) The PAMP c-di-AMP Is Essential for *Listeria monocytogenes* Growth in Rich but Not Minimal Media due to a Toxic Increase in (p)ppGpp. [corrected]. *Cell Host Microbe* **17**: 788–98.

Whiteley, A.T., Ruhland, B.R., Edrozo, M.B., and Reniere, M.L. (2017b) A Redox-Responsive Transcription Factor Is Critical for Pathogenesis and Aerobic Growth of *Listeria monocytogenes*. *Infect Immun* **85**.

Widjaja, M., Harvey, K.L., Hagemann, L., Berry, I.J., Jarocki, V.M., Raymond, B.B.A., *et al.* (2017) Elongation factor Tu is a multifunctional and processed moonlighting protein. *Sci Rep* **7**: 11227.

Willby, M.J., Balish, M.F., Ross, S.M., Lee, K.K., Jordan, J.L., and Krause, D.C. (2004) HMW1 is required for stability and localization of HMW2 to the attachment organelle of Mycoplasma pneumoniae. *J Bacteriol* **186**: 8221–8.

Witte, C.E., Whiteley, A.T., Burke, T.P., Sauer, J.-D., Portnoy, D.A., and Woodward, J.J. (2013) Cyclic di-AMP Is Critical for *Listeria monocytogenes* Growth, Cell Wall Homeostasis, and Establishment of Infection. *MBio* **4**: 1–10.

Witte, G., Hartung, S., Büttner, K., and Hopfner, K. P. (2008). Structural biochemistry of a bacterial checkpoint protein reveals diadenylate cyclase activity regulated by DNA recombination intermediates. *Mol. Cell* **30:** 167–178.

Wodke, J. A., Alibés, A., Cozzuto, L., Hermoso, A., Yus, E., Lluch-Senar, M., *et al.* (2015). MyMpn: a database for the systems biology model organism *Mycoplasma pneumoniae*. *Nucleic Acids Res.* **43:** D618–D623.

Wolański, M., Donczew, R., Zawilak-Pawlik, A., and Zakrzewska-Czerwińska, J. (2014) *oriC*-encoded instructions for the initiation of bacterial chromosome replication. *Front Microbiol* **5**: 735.

Wolf, M., Müller, T., Dandekar, T., and Pollack, J.D. (2004) Phylogeny of Firmicutes with special reference to *Mycoplasma* (Mollicutes) as inferred from phosphoglycerate kinase amino acid sequence data. *Int J Syst Evol Microbiol* **54**: 871–875

Wood, Z.A., Schröder, E., Harris, J.R., and Poole, L.B. (2003) Structure, mechanism and regulation of peroxiredoxins. *Trends Biochem Sci* **28**: 32–40.

Woodward, J.J., Iavarone, A.T., and Portnoy, D.A. (2010) c-di-AMP secreted by intracellular *Listeria monocytogenes* activates a host type I interferon response. *Science* **328**: 1703–5.

Woude, M.W. van der, and Bäumler, A.J. (2004) Phase and antigenic variation in bacteria. *Clin Microbiol Rev* **17**: 581–611.

Yamamoto, T., Kida, Y., Sakamoto, Y., and Kuwano, K. (2017) Mpn491, a secreted nuclease of *Mycoplasma pneumoniae*, plays a critical role in evading killing by neutrophil extracellular traps. *Cell Microbiol* **19**.

Yavlovich, A., Tarshis, M., and Rottem, S. (2004) Internalization and intracellular survival of *Mycoplasma pneumoniae* by non-phagocytic cells. *FEMS Microbiol Lett* **233**: 241–46.

Ye, M., Zhang, J. J., Fang, X., Lawlis, G. B., Troxell, B., Zhou, Y., *et al.* (2014). DhhP, a cyclic di-AMP phosphodiesterase of *Borrelia burgdorferi*, is essential for cell growth and virulence. *Infect. Immun.* **82:** 1840–49.

You, C., Okano, H., Hui, S., Zhang, Z., Kim, M., Gunderson, C. W., *et al.* (2013). Coordination of bacterial proteome with metabolism by cyclic AMP signaling. *Nature* **500:** 301–6.

Yu, Y., Wang, H., Wang, J., Feng, Z., Wu, M., Liu, B., *et al.* (2018) Elongation Factor Thermo Unstable (EF-Tu) Moonlights as an Adhesin on the Surface of *Mycoplasma hyopneumoniae* by Binding to Fibronectin. *Front Microbiol* **9**: 974.

Yus, E., Güell, M., Vivancos, A.P., Chen, W.-H., Lluch-Senar, M., Delgado, J., *et al.* (2012) Transcription start site associated RNAs in bacteria. *Mol Syst Biol* **8**: 585.

Yus, E., Lloréns-Rico. V., Martínez, S., Gallo, C., Eilers, H., Blötz, C., Stülke, J., Lluch-Senar, M., Serrano, L. (2019; submitted) Reconstruction of regulatory network in a minimal bacterium reveals extensive non-transcription factor dependent regulation.

Yus, E., Maier, T., Michalodimitrakis, K., Noort, V. Van, Yamada, T., Chen, W.H., *et al.* (2009) Impact of genome reduction on bacterial metabolism and its regulation. *Science (80-)* **326**: 1263–8.

Yus, E., Yang, J., Sogues, A., and Serrano, L. (2017) A reporter system coupled with high-throughput sequencing unveils key bacterial transcription and translation determinants. *Nat Commun* **8**: 368.

Zeden, M.S., Schuster, C.F., Bowman, L., Zhong, Q., Williams, H.D., and Gründling, A. (2018) Cyclic di-adenosine monophosphate (c-di-AMP) is required for osmotic regulation in *Staphylococcus aureus* but dispensable for viability in anaerobic conditions. *J Biol Chem* **293**: 3180–200.

Zhang, W., and Baseman, J.B. (2014) Functional characterization of osmotically inducible protein C (MG_427) from *Mycoplasma genitalium*. *J Bacteriol* **196**: 1012–9.

Zhao, X., and Drlica, K. (2014) Reactive oxygen species and the bacterial response to lethal stress. *Curr Opin Microbiol* **21**: 1–6.

Zheng, M., Åslund, F., and Storz, G. (1998) Activation of the OxyR Transcription Factor by Reversible Disulfide Bond Formation. *Science* **279**: 1718-22.

Zheng, Y., Zhou, J., Sayre, D.A., and Sintim, H.O. (2014) Identification of bromophenol thiohydantoin as an inhibitor of DisA, a c-di-AMP synthase, from a 1000 compound library, using the coralyne assay. *Chem Commun* **50**: 11234–7.

Zhou, J., Sayre, D. A., Zheng, Y., Szmacinski, H., and Sintim, H. O. (2014). Unexpected complex formation between coralyne and c-di-AMP provides a simple fluorescent turn-on assay to detect this bacterial second messenger. *Anal. Chem.* **86:** 2412–20.

CHAPTER 10 | Curriculum vitae

Cedric Blötz

Birth 01.02.90, Northeim

Nationality German

Contact Wilhelm-Raabe-Straße 3

37574 Einbeck OT Kreiensen

Mail cbloetz@gmx.de

Doctoral thesis **Identification and characterization of essential and virulence genes of *Mycoplasma pneumoniae***
April 2016 - April 2019

Master thesis **Structural and functional characterization of RNase J2 from *Bacillus subtilis***
October 2013 - September 2015

Bachelor thesis **The influence of cyclic di-guanosine monophosphate on the biofilm-formation of *Bacillus subtilis***
October 2010 - September 2013

Abitur **Professional high school - main focus: economics**

April 2006 - April 2009